Cellular aging in myeloproliferative neoplasms

Von der Fakultät für Mathematik, Informatik und Naturwissenschaften der RWTH Aachen University zur Erlangung des akademischen Grades einer Doktorin der Naturwissenschaften genehmigte Dissertation

vorgelegt von

Vithurithra Tharmapalan, M.Sc.

aus

Puloly North, Sri Lanka

Berichter: Univ.-Prof. Dr. med. Dr. rer. nat. Wolfgang Wagner

Univ.-Prof. Dr. med. Steffen Koschmieder

Priv. -Doz. Dr. rer. nat. Jacopo Di Russo

Tag der mündlichen Prüfung: 19. Februar 2025

Table of Contents

Abstract

Myeloproliferative neoplasms (MPN) are a group of clonal hematological malignancies that are caused by specific driver mutations, such as *JAK2* V617, which stimulate abnormal cell proliferation. These MPN associated mutations are associated with aberrant DNA methylation (DNAm) patterns, although the underlying cause remains unclear. This thesis aims to investigate if cellular aging is accelerated in MPN, which might provide new therapeutic options by senolytic molecules that selectively induce death in senescent cells and possibly eliminate the mutant cell population. Furthermore, we aim to better understand if the *JAK2* V617 mutation directly evokes the MPN-associated aberrant DNAm.

To address these questions, we analyzed three cellular aging parameters, including epigenetic age, telomere length, and cellular senescence in blood samples of healthy donors and MPN patients. Our results indicated that even in healthy donors, the fraction of senescent cells tends to increase with age. Across all MPN entities, we observed a significant acceleration of epigenetic age and senescence associated genes, whereas telomere attrition was particularly observed in primary myelofibrosis. Overall, accelerated cellular aging was correlated with *JAK2* V617F allele burden and was more pronounced in *JAK2* V617F mutated colonies than their wild type counterparts. Treatment with senolytics resulted in a significant reduction in senescent cells and epigenetic age in healthy blood cells treated with RG7112, JQ1, nutlin-3a and AMG232. Whereas MPN cells showed a reduction in the *JAK2* V617F allele burden and an increase in telomere length with JQ1 and piperlongumine. Genome wide methylation analysis of induced pluripotent stem cells (iPSCs) and iPSC-derived hematopoietic progenitor cells with *JAK2* mutation showed no significant methylation differences compared to wild type counterparts. However, we observed a moderate association between shared hypomethylation patterns in patients with the *JAK2* mutation.

Overall, our findings show that cellular aging is accelerated in malignant clones, and these cells can be targeted with senolytics. In iPSCs, the *JAK2* V617 driver mutation alone does not recapitulate the DNAm alterations observed in MPN patients suggesting that epigenetic changes accumulate with disease progression rather than at early disease onset. Our results highlight the complex interplay between cellular aging, epigenetic changes, and the *JAK2* V617F mutation in MPNs and may thereby provide new avenues for targeting both cellular aging and the malignant cell population.

Zusammenfassung

Myeloproliferative Neoplasien (MPN) sind eine Gruppe klonaler hämatologischer Malignome, die durch spezifische Treibermutationen wie *JAK2* V617F verursacht werden und zu abnormalem Zellwachstum führen. Diese Mutationen sind mit abweichenden DNA-Methylierungsmustern (DNAm) assoziiert, obwohl die zugrundeliegenden Ursachen unklar sind. Diese Dissertation untersucht, ob die zelluläre Alterung bei MPN beschleunigt ist, um mögliche therapeutische Optionen durch senolytische Moleküle zu evaluieren, die selektiv seneszente Zellen abtöten und möglicherweise die mutierte Zellpopulation eliminieren könnten. Zudem soll geklärt werden, ob die *JAK2* V617-Mutation direkt die MPN-assoziierte DNAm-Veränderung hervorruft.

Zur Beantwortung dieser Fragen analysierten wir drei Parameter der zellulären Alterung – epigenetisches Alter, Telomerlänge und zelluläre Seneszenz – in Blutproben von gesunden Spendern und MPN-Patienten. Unsere Ergebnisse zeigen, dass die Anzahl seneszenter Zellen bei gesunden Spendern mit dem Alter tendenziell zunimmt. Bei allen MPN-Entitäten wurde eine signifikante Beschleunigung des epigenetischen Alters und der seneszenz-assoziierten Gene beobachtet, während die Telomerverkürzung insbesondere bei primärer Myelofibrose ausgeprägt war. Insgesamt korrelierte die beschleunigte zelluläre Alterung mit der *JAK2* V617F-Allellast und war in mutierten Kolonien stärker ausgeprägt als in Wildtyp-Kolonien. Die Behandlung mit Senolytika wie RG7112, JQ1, Nutlin-3a und AMG232 führte zu einer signifikanten Reduktion seneszenter Zellen und des epigenetischen Alters in gesunden Blutproben. In MPN-Zellen wurden durch JQ1 und Piperlongumin eine Reduktion der *JAK2* V617F-Allellast und eine Verlängerung der Telomere erreicht. Die genomweite Methylierungsanalyse von induzierten pluripotenten Stammzellen (iPSCs) und iPSC-abgeleiteten hämatopoetischen Vorläuferzellen mit *JAK2*-Mutation zeigte keine signifikanten Methylierungsunterschiede im Vergleich zu Wildtyp-Zellen. Dennoch beobachteten wir eine moderate Assoziation zwischen gemeinsamen Hypomethylierungsmustern bei Patienten mit der *JAK2*-Mutation.

Zusammengefasst zeigen unsere Ergebnisse, dass die zelluläre Alterung in malignen Klonen beschleunigt ist und durch Senolytika gezielt behandelt werden kann. In iPSCs allein führt die *JAK2* V617-Mutation nicht zu den bei MPN-Patienten beobachteten DNAm-Veränderungen, was darauf hindeutet, dass epigenetische Änderungen mit dem Fortschreiten der Krankheit akkumulieren und nicht zu Beginn der Krankheit auftreten. Unsere Ergebnisse verdeutlichen das komplexe Zusammenspiel zwischen zellulärer Alterung, epigenetischen Veränderungen und der *JAK2* V617F-Mutation bei MPN und eröffnen neue Ansätze zur gezielten Behandlung sowohl der zellulären Alterung als auch der malignen Zellpopulation.

1. Introduction

1.1 Normal and malignant hematopoiesis

Hematopoiesis is a process of blood cell production by hematopoietic stem cells (HSCs) residing in the bone marrow. The balance of self-renewal and differentiation of the cells needs to be tightly regulated to ensure a functional hematopoietic system without any bias that leads to hematological diseases (Orkin & Zon, 2008).

1.1.1 Normal hematopoiesis

The development of hematopoiesis in the human embryo occurs in three distinct waves. The first wave, which begins at approximately 3 weeks of gestation, leads to the production of three types of blood cells in the yolk sac: primitive erythroid, megakaryocyte, and macrophage progenitors. These cells fulfill the immediate needs of the developing embryo. The second embryonic wave, originating in the yolk sac around 4-5 weeks of gestation, gives rise to multipotent cells, namely lymphoid progenitors and erythromyeloid progenitor cells (EMPs) in the yolk sac blood islands. The third wave leads to the generation of hematopoietic stem/progenitor cells (HSPCs) in the dorsal aorta. During the second and third waves, a highly specialized endothelium known as the hemogenic endothelium (HE) forms, from which hematopoietic progenitor cells arise through a process known as endothelial-to-hematopoietic transition (EHT; Figure 1). Cells from both the second and third waves migrate to the fetal liver, where they mature and expand before taking up residence in the bone marrow just before birth, becoming the main site of hematopoiesis (Gao et al., 2018; Ivanovs et al., 2017). The overlapping and transient nature of these waves makes it difficult to distinguish the contributions of HSC-dependent and HSC-independent hematopoiesis to the adult hematopoietic system (Neo et al., 2021). Studies in human and mouse models have shown that hematopoiesis is a continuous process with significant heterogeneity in lineage commitment. Despite the incomplete understanding of the intrinsic decisions of cellular phenotypes, it is known that transcription factors provide an entry point for how an HSC develops during embryogenesis and in lineage restricted differentiation. Interestingly, most of these transcription factors in the hematopoietic system are involved in chromosomal translocations or somatic mutations in human hematopoietic malignancies. Alterations in these transcriptional regulators are associated with malignant transformation (Orkin & Zon, 2008; Velten et al., 2017).

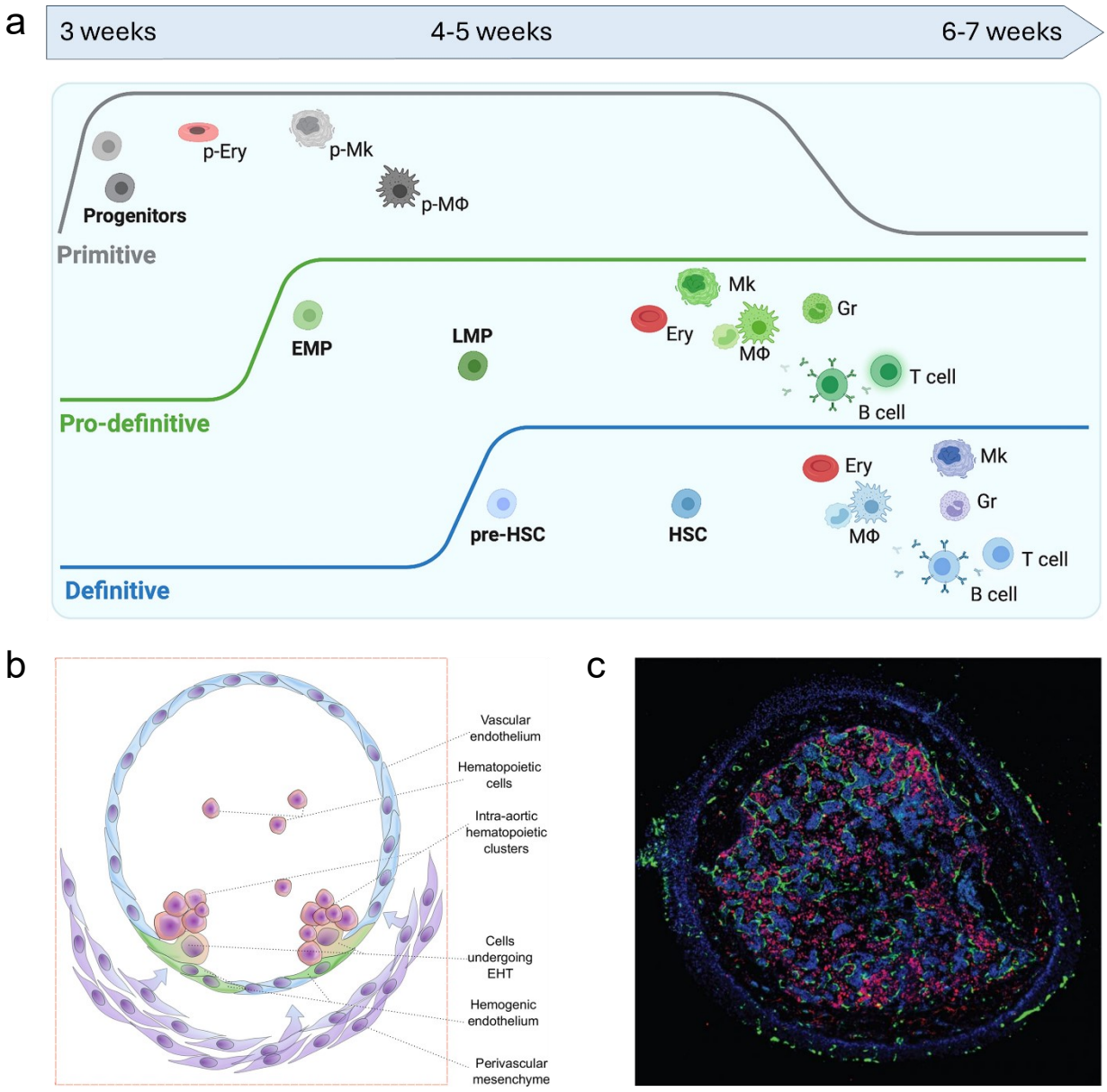

Figure 1. Embryonic hematopoietic development.

a) Hematopoietic development is a process that occurs in three distinct phases, which are collectively referred to as the primitive, pro-definitive, and definitive waves of hematopoiesis. The primitive wave is responsible for the production of erythrocytes (p-Ery), megakaryocytes (p-Mk), and macrophages (p-MΦ). The pro-definitive wave gives rise to erythro-myeloid progenitors (EMPs) and lympho-myeloid progenitors (LMPs). The definitive wave generates pre-HSCs, which mature into HSCs capable of self-renewal. Both the pro-definitive and definitive wave progenitors migrate to the liver, where they produce erythrocytes (Ery), megakaryocytes (Mk), granulocytes (Gr), T cells and B cells, as well as monocyte-derived macrophages (MΦ). b) Hematopoietic cells, including pre-HSCs, arise from hemogenic endothelium (green), organized in intra-aortic hematopoietic clusters. This endothelial-to-hematopoietic transition (EHT) and HSC emergence is regulated and directly or indirectly influenced by signaling and cell-extrinsic factors from the microenvironment, including vascular endothelial cells (light blue) and perivascular mesenchyme (purple). c) Cross section of the bone marrow vascular network showing co-distribution of bone marrow sinusoids (green), along with staining for CD45 hematopoietic cells (red). This figure was adapted from (Canu & Ruhrberg, 2021; Lange et al., 2021; Yvernogeau et al., 2019), used under the terms of the Creative Commons Attribution 4.0 International License and with permission from Springer Nature.

In adults, hematopoiesis primarily occurs in the bone marrow. The hematopoietic system is organized hierarchically, with HSCs giving rise to committed progenitors that further differentiate

into functional blood cells. This process branches into two main lineages: myeloid and lymphoid lineages. Myeloid lineages include erythrocytes, megakaryocytes, and innate immune cells such as monocytes, neutrophils, eosinophils, basophils, and dendritic cells. Lymphoid lineages include B, T and NK cells, which are responsible for adaptive immunity (Figure 2). The classic model of human hematopoiesis suggests that the long-term HSCs remain quiescent to minimize cell cycle associated DNA damage and produce short-term HSCs, followed by progenitors in a lineage restricted manner. In this way, the replicative burden is carried by the differentiated cells, necessary to maintain the steady state of hematopoiesis. Here, the stem cell fate is more a binary fate choice (Haas et al., 2018; Morrison et al., 1997). On the other hand, the continuum model proposes that cell differentiation is not a series of abrupt divisions, but rather a process in which a cell makes multiple decisions and ultimately becomes identical to another cell that has made the same decisions, regardless of their disparate origins. Furthermore, the original state of the cell including the history of the cells, its interaction with the environment and its internal state can influence the decision making of the differentiation trajectory (Liggett & Sankaran, 2020). This hierarchical organization of the hematopoietic system tells us how a small pool of cells is responsible for the continuous generation of large numbers of mature functional cells. As new methods are developed, gene expression alone may oversimplify the model and may not be sufficient to discriminate different cell populations. Single cell genomics has shown the functional and phenotypic variation of cells, which were once thought to be homogeneous (Liggett & Sankaran, 2020).

Hematopoiesis is regulated by a complex interplay of intracellular and extracellular factors. The intracellular factors include transcriptional and epigenetic regulators, as well as metabolic pathways, which control the activity of HSCs. Extracellular factors, particularly long-range humoral and neural signals or local cues from the bone marrow microenvironment, play a crucial role in the shaping of HSC fate (Pinho & Frenette, 2019). In 1978, Schofield first introduced the concept of the hematopoietic stem cell niche as a regulator which maintains the HSC function (Schofield, 1978). The bone marrow niche is perivascular and is created partly by mesenchymal stromal cells (MSCs), endothelial cells, osteoblasts, adipocytes, and hematopoietic cells. Over time, studies have found that the crosstalk between the multiple cell types within the niche and HSCs plays a crucial role in maintaining the stem cell renewal potential (Morrison & Scadden, 2014; Pinho & Frenette, 2019). Understanding this complex interplay in normal hematopoiesis and its potential dysregulation in pathological conditions may provide insights into hematopoietic disorders and provide crucial information about the development of novel therapeutic strategies.

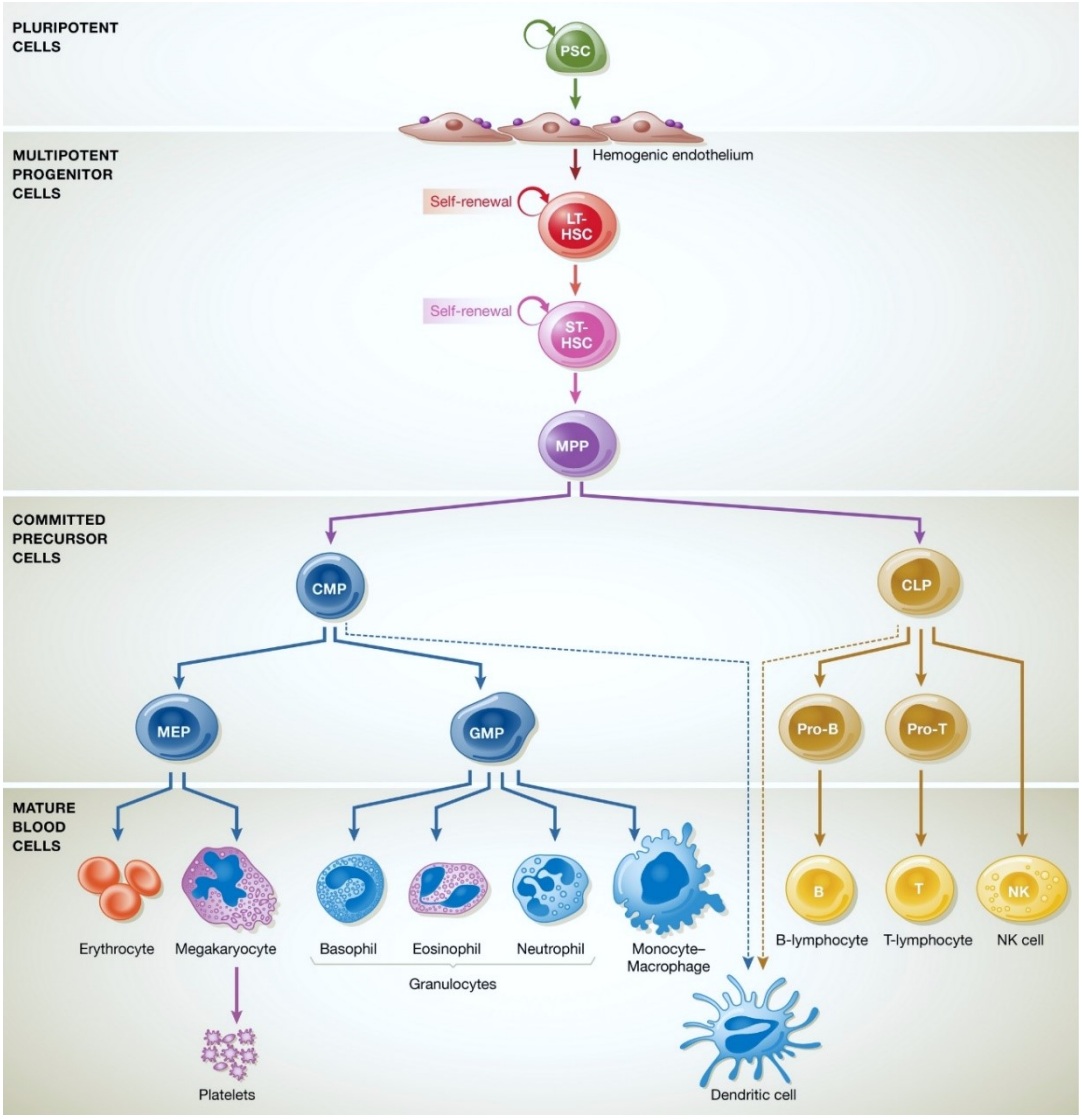

Figure 2. Hierarchy model of hematopoietic development.
Multipotent long term hematopoietic stem cells (LT-HSCs) possess the capacity for long-term reconstitution potential and can undergo further differentiation towards short term HSCs (ST-HSCs) and also multipotent progenitors (MPPs) within the bone marrow. Subsequent differentiation of MPPs results in the generation of either common myeloid progenitor (CMPs), which possess the capacity to differentiate into the myeloid lineage, or common lymphoid progenitor (CLPs), which are capable of generating the lymphoid lineage. Subsequently, both megakaryocyte erythroid progenitor (MEPs) and granulocyte macrophage progenitor (GMPs) are capable of forming all differentiated cells of the myeloid lineage within the bone marrow. In contrast, CLPs undergo further differentiation into pro-T cells and T cells through a process of positive and negative selection within the thymus. Additionally, CLPs in the bone marrow are responsible for the generation of B cells following the B-cell transition. This figure was reprinted from (Ackermann et al., 2015) with the permission from Springer Nature.

1.1.2 Clonal hematopoiesis

Clonal hematopoiesis refers to the expansion of a single hematopoietic cell due to genetic changes, leading to the formation of a distinct population of blood cells. This process is closely related to aging and is increasingly recognized as a critical risk factor for hematological malignancies and cardiovascular disease. As vertebrates including humans age, they accumulate somatic mutations in their hematopoietic cells. These mutations can be broadly

classified into driver mutations, which provide a fitness advantage to the cells, and the passenger mutations, which do not have direct advantage but can still impact clonal evolution by altering the genetic landscape of the cells. When these mutations lead to insufficient differentiation or unrestricted self-renewal of hematopoietic cells, they can result in a higher risk of developing malignancies (Ahmad et al., 2023). The concept of clonal hematopoiesis was initially introduced in the context of hematopoietic stem cell transplantation, where it was observed that a single donor-derived hematopoietic stem cell could repopulate the entire hematopoietic system of the recipient. With the advent of next generation sequencing technologies, it has become evident that clonal hematopoiesis is a common occurrence in healthy individuals, particularly with advancing age (Genovese et al., 2014; Jaiswal et al., 2014; Xie et al., 2014). While clonal hematopoiesis also exists in non-malignant state or pre-malignant condition, it is classified into clonal hematopoiesis of indeterminate potential (CHIP), this refers to a presence of somatic mutations in hematopoietic cells without overt hematological malignancy (Kovtonyuk et al., 2016; Li et al., 2020). The prevalence of CHIP increases with age, being detectable in less than 1 % of individuals under 40 years old, but rising to 10-20 % of individuals over 70 years (Jaiswal et al., 2014).

The most common mutated genes in clonal hematopoiesis are loss-of-function mutations in enzymes involves in epigenetic regulation *DNMT3A* (encoding DNA (cytosine-5-)-methyltransferase 3α), *TET2* (encoding tet methylcytosine dioxygenase 2), *ASXL1* (encoding additional sex combs–like transcriptional regulator 1), splicing factors such as *SF3B1* (encoding splicing factor 3b, subunit 1), *SRSF2* (encoding serine and arginine rich splicing factor 2), *PRPF8* (encoding pre-mRNA processing factor 8), *U2AF1* (encoding U2 small nuclear RNA auxiliary factor 1), and key regulatory genes such as *JAK2* (encoding Janus kinase 2) and *TP53* (encoding tumor protein p53; Figure 3) (Jaiswal & Ebert, 2019). These somatic mutations can be found not only in HSCs but also in circulating immune cells, potentially resulting in altered immune responses that contribute to various age-related, and cancer associated diseases. The detection of CHIP with increased risk for hematologic malignancies and some other adverse outcomes are defined to be >2 % of sequenced alleles carrying a specific mutation, or 4 % of cells for heterozygous mutations. For example, the *JAK2* mutation is frequently found in healthy people without clinical manifestations, yet it is also associated with the development of myeloid malignancies, particularly MPN (Jaiswal, 2020). However, the underlying mechanisms that regulate the growth of specific clones remain poorly understood.

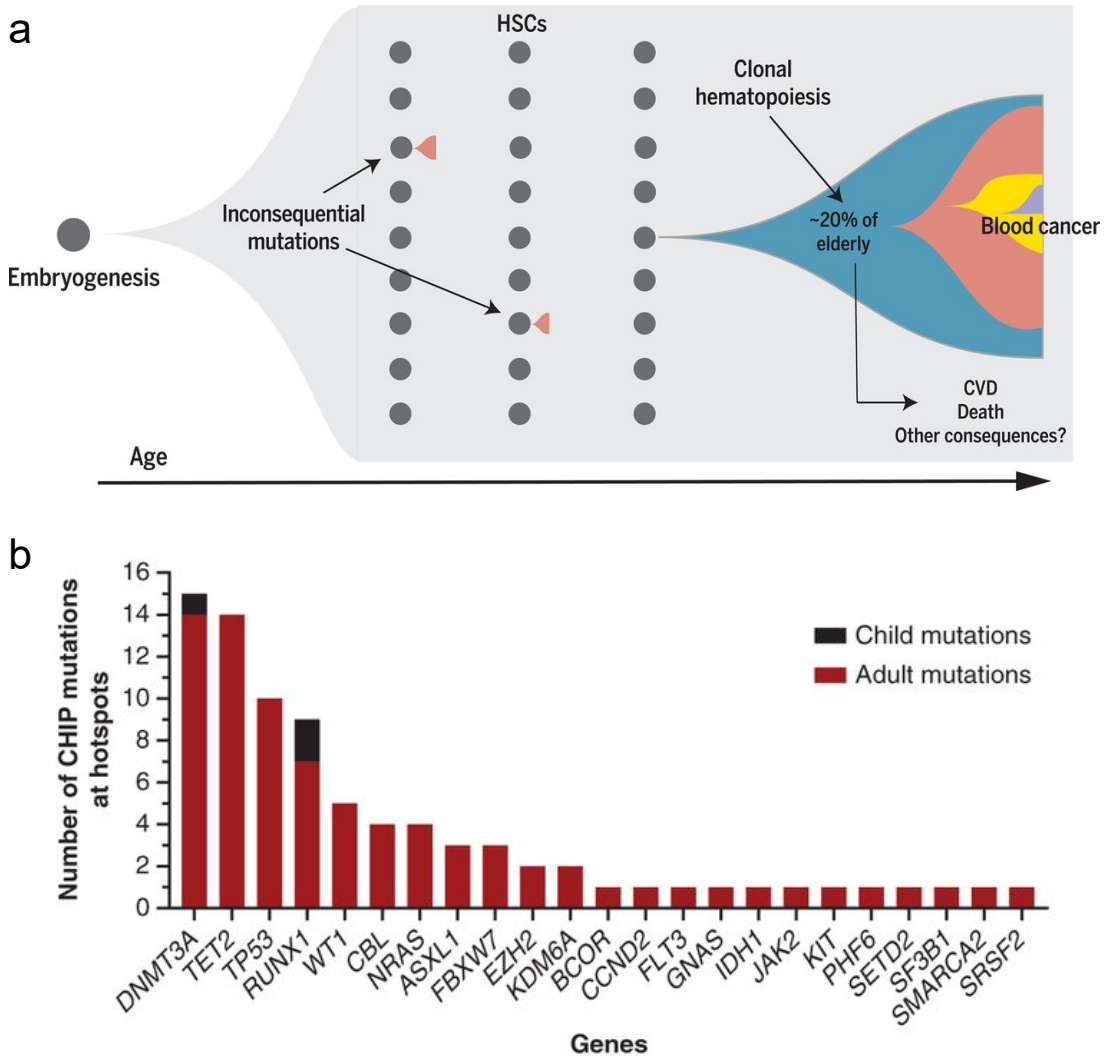

Figure 3. Clonal hematopoiesis and aging.
a) In the normal process of hematopoiesis, an unaffected hematopoietic stem cell (HSC) differentiates into various blood cells. In contrast, in clonal hematopoiesis, a somatic mutation in an HSC leads to increased renewal and clonal expansion of mutated HSCs, a condition termed clonal hematopoiesis of indeterminate potential (CHIP). This can result in myeloid bias, and potentially malignant transformation. b) Genes with CHIP mutations identical to mutations reported at hotspots from 4,530 individuals. Black color indicates the mutations identified in a child sample. The figure was adapted from (Feusier et al., 2021; Jaiswal & Ebert, 2019) with the permission from American Association for Cancer Research and the American Association for the Advancement of Science.

Clonal hematopoiesis is an age-related phenomenon. Aging is associated with several changes in the HSC function, including decline in regenerative capacity, reduced lymphoid potential, increased myeloid differentiation, and modified homing/mobilization efficiency. There is also an increase in platelet production, with a specific HSC subset favoring platelet production expanding over time. Recent studies in mice have shown that inhibiting platelet programming by targeting the transcription factor FOG-1 results in expansion of the lymphoid compartment, indicating that the age-related shift in platelet differentiation may contribute to reduced lymphopoiesis (Belyavsky et al., 2021). Despite the previous assumption that CHIP was only relevant to adults, recent findings have identified clonal mutations in both leukemic hotspots and non-hotspots in

children without blood disorders (Figure 3) (Feusier et al., 2021). This highlights the necessity for further investigation into CHIP across all age groups.

The bone marrow microenvironment also plays a crucial role in the development of clonal hematopoiesis. With age, the differentiation balance of MSCs shifts towards adipogenesis over osteogenesis, which can also influence hematopoiesis and HSC niches (Zhang et al., 2020). Despite the expansion of HSCs and megakaryocytes, HSCs tend to move away from the megakaryocytes perivascular niche with age. In addition, the reduced capacity of megakaryocytes to stimulate osteoblast expansion with aging leads to degeneration or loss of bone (Ghosh et al., 2021). These age-related changes collectively contribute to the decreased HSC quiescence, alterations in immune responses, and an increased incidence of various cancer types. Alterations in the bone marrow microenvironment can promote cancer development, and malignant cells can further produce factors that can alter stromal cell function, potentially leading to metastasis with increasing age (Anderson & Simon, 2020; Calvi & Link, 2015; Sadighi Akha, 2018).

More than 70 genes have been identified as recurrently mutated in myeloid malignancies, including acute myeloid leukemia (AML), myelodysplastic syndrome (MDS), and myeloproliferative neoplasms (MPN) (Goldman et al., 2023). In particular, mutations commonly associated with CHIP, such as those in the genes *DNMT3A*, *TET2*, and *ASXL1*, have also been identified in MPNs (Bartels et al., 2020), which is the primary focus of this thesis. Although CHIP does not exhibit abnormal blood counts or other symptoms of hematological disease, it represents a state in which hematopoietic stem cells have acquired mutations that provide a selective advantage. MPNs are more prevalent in the elderly population, and the latency period for the acquisition of the mutation and the diagnosis is several decades, suggesting that it takes a longer time to generate a proliferation advantage. A mere one in ten individuals with CHIP will eventually receive an associated cancer diagnosis, but the consequences of a prognosis that either overlooks premalignant disease or results in unnecessary treatment are significant (Goldman et al., 2023; Maslah et al., 2023). As these diseases are heterogeneous, an understanding of the complex relationship between aging, somatic mutations, and clonal dynamics in the hematopoietic system could offer valuable insights into the pathogenesis of MPNs and facilitate the development of more targeted and effective therapies.

1.2 Myeloproliferative neoplasms

Myeloproliferative neoplasms are a group of clonal hematopoietic disorders, where the clonal expansion of a transformed hematopoietic stem cell compartment occurs due to specific driver mutations. The classical Philadelphia-chromosome negative MPN, also known as BCR-ABL negative MPN, include essential thrombocythemia (ET), polycythemia vera (PV) and primary myelofibrosis (PMF). Somatic mutations dysregulate the Janus kinase/signal transduction and activation of transcription (JAK/STAT) pathway, leading to a constitutive activation of JAK2 kinase and the other downstream regulatory pathways, including STATs, resulting in an abnormal proliferation of blood cells (Barbui et al., 2018). On the other hand, there are BCR-ABL positive MPNs. *BCR-ABL* oncogene is a fusion gene where a recombination of the chromosome 9 in *ABL* gene and chromosome 22 in *BCR* gene occurs in the hematopoietic stem cell compartment. This fusion of the chromosomes leads to both elongated chromosome 9q+ and truncated chromosome 22 called Philadelphia chromosome. This fusion gene BCR-ABL1 activates tyrosine kinase enzyme and leads to abnormal proliferation of the leukemic stem cells, results in chronic myeloid leukemia (CML) (Cross et al., 2023; Melo et al., 1993). Due to its unique pathogenesis and treatment options, CML is separated from the rest of the MPNs. In this thesis, the main focus is on BCR-ABL negative MPN, which is also mentioned as MPN throughout the thesis.

MPN groups are classified based on the proliferation and change of the different hematopoietic compartments. Essential thrombocythemia (ET) is categorized by thrombocytosis, as risk of clotting and megakaryocytic hyperplasia in the bone marrow. ET is one of the last classical MPNs to be described by Emil Epstein and Alfred Goedel in 1934 (Fabris & Randi, 2009). It is the most common type of MPN with a prevalence of 1.0 to 2.5 individuals per 100,000 in the population and it occurs more frequently in women. The age of the disease onset typically between the age of 50 to 60 years (Gangat et al., 2024). It is diagnosed by 4 major criteria: an increase in platelet count > 450 × 10^9/L, abnormal proliferation of megakaryocyte progenitors in the bone marrow with the hyperlobulated nuclei, the presence of a MPN driver mutation and not meeting the criteria of other MPN subtypes (Arber et al., 2016; Thiele et al., 2023). The chance of ET directly progressing to post-ET myelofibrosis (MF) or blast phase is quite rare (Carobbio et al., 2023), but differentiation between ET and pre-PMF is still challenging as there are no clear measurements to differentiate between these two groups (Tefferi, 2011).

Polycythemia vera (PV) is characterized by clonal erythrocytosis. It is one of the early described groups in MPN called “maladie de Vaquez,” in 1892 by Louis Henri Vaquez and later systematically reviewed by William Osler in 1903 (Tefferi et al., 2021). The incidence of PV is approximately 0.4 to 2.8 per 100,000 population, and it is slightly more common in men

compared to women (Moulard et al., 2014). The average age of diagnosis is around 60 to 65 years (Szuber et al., 2019) and there is a significant risk of progression to AML. It is diagnosed by 3 main criteria: increased amount of hemoglobin, hematocrit, and red cell mass, and a bone marrow biopsy showing hypercellularity for age with trilineage growth of erythroid, granulocyte and megakaryocyte proliferation. Further, there is a presence of one of the MPN driver mutations *JAK2* V617F or *JAK2* exon 12 (Arber et al., 2016; Thiele et al., 2023). Regular phlebotomies combined with low-dose aspirin is considered first-line treatment for low-risk PV patients. Further, patients can be treated with cytoreductive drugs such as hydroxyurea, IFN-alpha or with JAK2 inhibitors leading to the specific inhibition of highly proliferating cells (Tefferi et al., 2021). It is challenging to treat PV patients as the twenty year risk for thrombosis or post-PV MF or AML are 26 %, 16 % and 4 %, respectively (Tefferi & Barbui, 2023).

Primary myelofibrosis (PMF) is a more advanced disease phenotype in the MPN subgroup in which megakaryocytic proliferation and atypia are accompanied by the reticulin and/or collagen fibrosis in the bone marrow with grade 2 or 3 on a scale of 0 to 3. In addition, the presence of MPN somatic mutations and not meeting the criteria for other MPN subtypes are important diagnostic criteria. More recently, PMF has been subclassified into pre-PMF and overt/post-PMF regarding the quantity and quality of fibrosis (Arber et al., 2016; Thiele et al., 2023). Allogeneic hematopoietic stem cell transplantation is the only curative treatment option for PMF (Passamonti & Mora, 2023). There is a risk of leukemic transformation, and the acquisition of additional mutations is associated with poor prognosis and survival (Tefferi, 2023; Yan et al., 2023).

It is important to note that all MPN entities can transform into another type and progress to more severe hematological malignancies including AML. For example, PV and ET can progress to secondary myelofibrosis, and all of the above have a chance of transformation to leukemia. The likelihood that MPN will progress differs between subtypes and it remains a challenge to understand and predict the progression at an early stage.

1.2.1 Mutations in MPN

The three driver mutations initiating MPN are Janus Kinase 2 gene (*JAK2*), myeloproliferative leukemic gene (*MPL*), and calreticulin (*CALR*). They are mutually exclusive, mostly prevail alone, and occur in almost 95 % of MPN cases. The remaining patients who do not exhibit any of these mutations are classified as triple negative, showing a similar MPN phenotype.
One of the earliest mutations discovered in 2005 is *JAK2* V617F (Baxter et al., 2005; James et al., 2005; Kralovics et al., 2005; Levine et al., 2005), a tyrosine kinase gain of function in the *JAK2* gene in exon 14 on chromosome 9. This results from the exchange of guanine (G) to thymine (T), which leads to the change of valine to phenylalanine at the position 617 of the amino

acid sequence. About 95 % of patients with PV, and 50-60 % with ET and PMF carry this mutation. Other mutations in the *JAK2* gene, which are less common can be found in exon 12 and are present in around 2-5 % of PV patients who are negative for *JAK2* V617F (Vainchenker & Kralovics, 2017).

Healthy JAK2 signaling can be activated by different cytokines binding to their corresponding receptor including the erythropoietin receptor (EPOR), thrombopoietin receptor (TPOR or MPL), and granulocyte/macrophage colony-stimulating factor receptor (GM-CSFR). When the cytokines bind to transmembrane receptors, the receptor associated JAKs are activated, which leads to phosphorylation of STAT proteins and formation of homo or heterodimers. The dimerized STATs translocate to the nucleus and by binding to the transcription sites, they regulate the gene transcription (Figure 4). Different signaling proteins such as JAK, interferon (IFN), interleukin-6 (IL-6), and interleukin-3 (IL-3) activate different STATs and induce the transcription and expression of genes for various cellular functions, including cell cycle, apoptosis, cell proliferation, epithelial-mesenchymal transition (EMT), angiogenesis, and the production of inflammatory factors. These functions are involved in various cellular processes and may play a role in the development of various diseases (Bader & Meyer, 2022). The presence of *JAK2* V617F mutation impairs the pseudo-kinase domain and increases JAK2 kinase activity, which leads to constitutive activation of JAK/STAT signaling and resultant cytokine-independent growth, leading to excessive proliferation and survival of myeloid progenitor cells. The downstream activation of intracellular signaling occurs via STAT protein signaling, activation of mitogen-activated protein kinase (MAPK) signaling, and phosphoinositide 3-kinase (PI3K) signaling, which collectively support the proliferation of malignant cells (Vainchenker & Kralovics, 2017). Studies show that the impact of the *JAK2* mutation alone would not be sufficient for the self-renewal of the myeloid lineage cells or the hematopoietic stem cells to initiate the MPN disease (Lanikova et al., 2019). Instead, the *JAK2* V617F mutation often occurs in combination with other mutations. In some cases, *JAK2* V617F can be an initial mutation (“first hit”), setting the stage for MPN development, alternatively, it can occur as a subsequent (“second hit”) event in cells that have already acquired other genetic mutations (Kralovics, 2008). *JAK2* V617F allele burden is a commonly used measurement to check the severity and progression of the disease, and over time it is shown that heterozygous mutations have a potential to change to homozygous mutations. This occurs in about 30 % of patients with PV and PMF and only 2-4 % with ET (Vannucchi et al., 2008). The most prevalent transition to homozygosity is a consequence of partial uniparental disomy (UPD), where due to chromosomal abnormality in the short arm of chromosome 9p leads to loss of one copy also known as loss of heterogeneity (LOH) and duplicate the remaining copy by mitotic recombination (Kralovics et al., 2005).

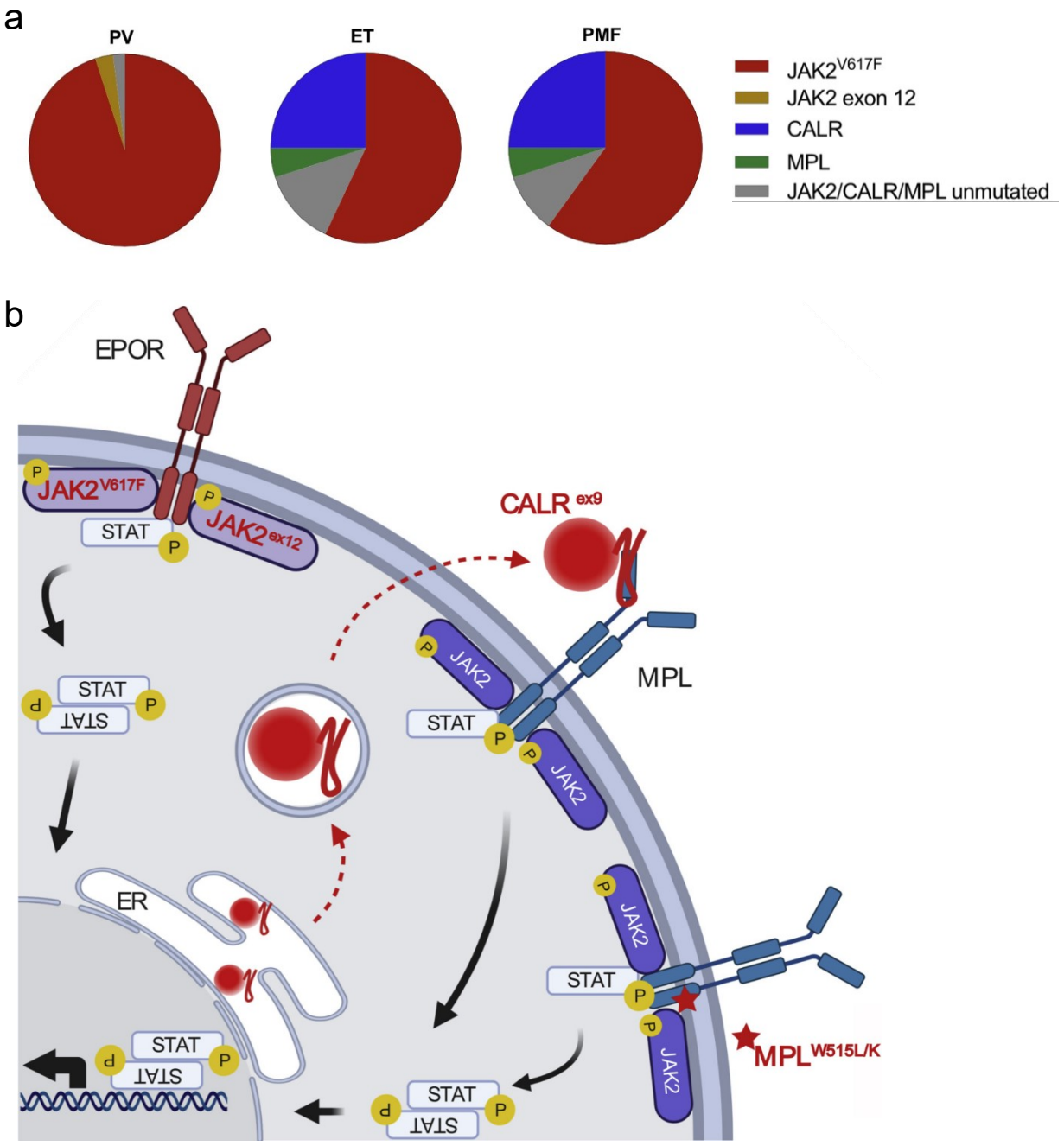

Figure 4. The JAK-STAT signaling pathway in MPN.

a) The approximate frequencies of somatic driver mutations in MPN are as follows: *JAK2* V617F, *JAK2* exon 12, *CALR*, and *MPL* mutations in PV, ET, and PMF. *JAK2/CALR/MPL* unmutated cases are referred to as triple negative MPN. b) The JAK/STAT signaling pathway is initiated when a specific ligand binds to a receptor on the cell surface. This triggers the activation of Janus kinases (JAKs) associated with the receptor. The activated JAKs phosphorylate tyrosine residues on the receptor, creating docking sites for signal transducer and activator of transcription (STAT) proteins. These STAT proteins bind to the receptor, are phosphorylated by the JAKs, and form dimers. Subsequently, the STAT dimers migrate into the cell nucleus, where they bind to specific DNA sequences and regulate the transcription of target genes. This process enables the cell to respond to extracellular signals by altering gene expression. Somatic driver mutations in *JAK2*, *CALR*, and *MPL* converge on constitutively activated JAK2-STAT signaling. EPOR, erythropoietin receptor; ER, endoplasmic reticulum; MPL, thrombopoietin receptor. The figure was adapted from (Szybinski & Meyer, 2021), used under the terms of the Creative Commons Attribution 4.0 International License.

Calreticulin (*CALR*) mutation, which was discovered in 2013 (Klampfl et al., 2013; Nangalia et al., 2013), has significantly advanced the diagnostic gaps for the remaining MPN patients. This mutation is present in 30 % of ET and 30 % of PMF patients who do not carry a *JAK2* or *MPL* mutation (Vainchenker & Kralovics, 2017). The two most prevalent types of *CALR* mutations in MPN are 52 bp deletion and 5 bp insertion of the amino acids, respectively known as type 1 and 2. Both of these mutations result in a frameshift in exon 9, leading to the generation of a positively charged C-terminus of the protein (Pietra et al., 2016). These mutations cause the CALR protein to be secreted outside the cell, instead of being retained within the endoplasmic reticulum. The mutated protein binds to the thrombopoietin receptor (MPL/TpoR), and acts as rogue chaperones, ensuring that TpoR reaches the cell surface and activates JAK/STAT signaling, specifically driving the expansion of the megakaryocytic lineage (Merlinsky et al., 2019; Pecquet et al., 2019). As the protein is located outside of the cells, it is recognized by other immune cells and this led to the development of a treatment option using monoclonal antibodies or vaccines (Kramer & Mullally, 2023).

Thrombopoietin receptor or myeloproliferative leukemia protein (*MPL*) mutations were first identified as a result of their constitutive activation of the downstream signaling pathway in *JAK2* V617F mediated transformation of myeloprogenitor cells, leading to cytokine independent growth (Pikman et al., 2006). Overall, the presence of the mutation is in 3 % of ET and 5 % of PMF (Vainchenker & Kralovics, 2017). The gain of function mutation MPLW515L, was identified in a murine bone marrow transplant assay (Pikman et al., 2006), as a result of G to T transition at codon 515 with the substitution of tryptophan to leucine. MPL receptors are selectively expressed on the HSCs and cells in the megakaryocyte differentiation pathway. Activation of the MPL receptor by its ligand TPO leads to activation of JAK/STAT, which triggers the downstream signaling pathways and promotes megakaryopoiesis and thrombopoiesis (Plo et al., 2017). The loss of MPL has been shown to significantly reduce the MPN development in *JAK2* V617F transgenic mice, suggesting that MPL expression is important for the development and severity of MPN (Sangkhae et al., 2014). Despite the fact that all MPN drivers act through constitutive activation of MPL, they exhibit markedly different clinical phenotypes (Constantinescu et al., 2021).

A prevailing question in the field is how a single mutation can give rise to different cell phenotypes. The phenotypic diversity observed in *JAK2* mutated MPNs, particularly between ET and PV has been previously attributed to the mutation load, with higher *JAK2* burden in PV patients than in ET patients. Additionally, the presence of homozygous clones is more prominent in PV phenotypes than in ET phenotypes (Rumi et al., 2014). Nevertheless, recent studies have shown that the presence and the order of mutations can affect the outcome of MPN disease and influence the disease progression. Additional bystander mutations in MPN are observed in genes

encoding epigenetic modifiers such as *DNMT3A, TET2* and *IDH1/2,* splicing factors such as *SF3B1*, *U2AF1* and *SRSF2* or transcription factors like *TP53*, *RUNX1* and *IKZF1* (Greenfield et al., 2021). The interplay between the additional mutations and the MPN driver mutation can alter gene expression and influence the disease outcome. For example, *JAK2* is recognized as the initial mutation in PV, but a prior mutation of TET2 alters the transcriptional consequences of *JAK2* V617F and is more likely to lead to ET (Ortmann et al., 2015). Also, the accumulation of the mutation within the same clone originated from a single mutated cell or across different clones can result in a different likelihood of disease progression. A mouse model with Jak2 V617F and Tet2 loss resulted in a rapid progression to myelofibrosis and a decreased overall survival (Lanikova et al., 2019). *TET2* is a demethylating enzyme, and when it is mutated, it enhances the self-renewal capacity of HSCs. Furthermore, a mouse model in which Jak2 is mutated with loss of EZH2 results in a more aggressive MPN phenotype with an overall expansion of the LSK stem/ progenitor compartment (Shimizu et al., 2016). EZH2 is a member of the repressive Polycomb complex (PRC2) and plays a role in epigenetic repression of gene expression by trimethylation of the histone H3K27 marks. Loss of function mutation in EZH2 have been observed in MPN and has been shown to be associated with leukemic transmission and worsened overall survival. Recently, it has been hypothesized that the phenotypic differences between MPN subunits may arise from the variations in the specific cytokine receptors activated by the respective driver mutations, their interaction with other co-occurring mutations, and the order of acquisition (Vainchenker & Kralovics, 2017).

1.2.2 Therapy options in MPN

The current treatment strategies for MPNs are primarily aimed to control symptoms, reduce spleen size, and manage thrombosis as well as prevent progression to secondary MF and AML. First line of therapy includes aspirin and phlebotomy to decrease the risk of thrombotic events and rebalance the hemostasis. Additionally, hydroxyurea and interferon-alpha (IFN-alpha) are used to normalize blood counts (Moliterno et al., 2023). Second line of treatment involves JAK inhibitors, such as ruxolitinib, fedratinib, and baricitinib. These JAK1/JAK2 inhibitors function by blocking the activity of the JAK2 enzyme and the overactive JAK-STAT signaling pathway, which helps to control blood counts, reduce spleen size and inflammation, and improve symptoms. However, these drugs can cause adverse effects such as cytopenia, thrombocytopenia, and anemia, which may necessitate adjustments to the treatment regimen. Furthermore, drug resistance, particularly towards ruxolitinib, is a common challenge, highlighting the need for the development of new therapeutic approaches (Pandey et al., 2022; Vannucchi et al., 2017).
Moreover, targets other than JAK2 are being investigated to treat MPN clones that are not dependent on JAK2. These include MDM2 inhibitors, BCL2 inhibitors, BET inhibitors, telomerase inhibitors, and cell cycle regulators, which have shown promise in preclinical and clinical studies (How et al., 2023). CALR-specific monoclonal antibodies effectively bind to CALR-mutant

proteins outside of the cells, offering a treatment option for patients with *CALR* mutations (Kramer & Mullally, 2023). Allogeneic stem cell transplantation remains the only curative option for myelofibrosis, but the timing of this intervention is critical for optimal outcomes. Leukemic transformation, specifically blast phase MPN, represents a significant concern in the context of disease progression. Studies have shown that combination treatment with hypomethylating agents and the BCL-2 inhibitor venetoclax or ruxolitinib with hypomethylating agents could improve the overall response rates. Furthermore, drugs that inhibit IDH1/2 have shown favorable outcomes in advanced MPN cases, where IDH2 mutation is a risk factor for leukemic transformation in PMF patients (Tefferi et al., 2023).

Long term use of medications can influence clonal selection, a crucial aspect to consider as patients often require lifelong treatment. Patients with ET and PV are generally associated with a life expectancy of 20-30 years. Therefore, disease progression is a significant concern, particularly in younger patients. The objective of treatment is to improve the molecular response and achieve removal of mutated cells. However, it is crucial to understand the molecular response beyond simply reducing *JAK2* allele burden, as some treatments can potentially select for more aggressive subclones. During treatment, clonal selection can lead to the expansion of additional mutations such as TP53 and DNMT3A, which requires careful monitoring. For example, IFN-alpha treatment has been shown to negatively affect *DNMT3A* mutant MPNs (Usart et al., 2024), and MDM2 inhibition has selected for the emergence of TP53 clones (Maslah et al., 2022). Implementing early intervention strategies for high-risk patients may assist in postponing or even interfering the leukemic transformation by selectively removing inflammatory cytokines that could influence disease progression. These strategies should focus on targeting the most malignant stem-cell-like clones, rather than just reducing the allele burden (How et al., 2023).

Genetic and molecular profiling of patients is of great significance for the selection of optimal drug options. This knowledge could be used to treat patients with combination treatments for multiple mutations and may even contribute to the prediction of drug resistance in the future (Goyal et al., 2023). This personalized approach can facilitate the identification of the most appropriate treatment strategies for individual patients, taking into account the specific genetic and molecular characteristics of their disease.

1.3 Cellular aging

Longevity research is a rapidly growing field aiming to understand the fundamental biological mechanisms of aging and develop new interventions to promote healthy aging and extend life span. The aging process is heterogeneous and continuous, with different organisms, body parts, and individual cells aging at different rates (Carmona & Michan, 2016). The understanding of an individual's age based on biological age rather than chronological age was a crucial step in aging research. While chronological age simply denotes the number of years an individual has been alive, biological age is more accurate reflection of the individuals health status (Jylhava et al., 2017). Studying aging has not only enabled a better understanding of aging-related diseases such as premature aging or neurodegenerative diseases, but has also allowed for overall prediction of survival and risk factors for other diseases (Fransquet et al., 2019). It has been questioned philosophically whether aging should be classified as a disease to be treated, given that it is the primary cause of death for living organisms. In 1881, August Weismann published the first evolutionary theory of aging, proposing that aging is determined by the needs of the species, which are determined through natural selection. This theory proposes that aging results from the progressive accumulation of cellular damage leading to the dysfunction of specific systems or cells. Since then, numerous theories have been proposed, focusing on the aspects that were beneficial in early life but detrimental in late life. These include the accumulation of mutations, the allocation of resources between reproduction and somatic maintenance, and the limited number of cell divisions (Arnold & Rose, 2023). A more recent hypothesis, the hyperfunction theory, suggests that the continued activation of certain signaling pathways that initially drive developmental growth and reproduction in early life and fails to switch off properly in later life, contributing to aging (Blagosklonny, 2022).

The concept of **'hallmarks of aging'** was first introduced by López-Otín and colleagues in 2013, discussing nine key molecular, cellular, and systemic changes associated with the aging process. These include genomic instability, telomere attrition, epigenetic alteration, loss of proteostasis, mitochondrial dysfunction, cellular senescence, stem cell exhaustion, deregulated nutrient sensing, and altered intracellular communication (Lopez-Otin et al., 2013). In subsequent years, these hallmarks were expanded to additional causes including dysbiosis, disabled macroautophagy, and chronic inflammation (Lopez-Otin, Blasco, et al., 2023). Interestingly, several hallmarks of aging are shared with those of cancer, including genomic instability, epigenomic alterations, chronic inflammation, dysbiosis and cellular senescence (Falandry et al., 2014; Gems & de Magalhaes, 2021; Lopez-Otin, Pietrocola, et al., 2023). In the 2000s, Hanahan and Weinberg first described the six hallmarks of cancer and subsequently in 2011, expanded them to ten hallmarks (Hanahan & Weinberg, 2000, 2011). The primary cause of cancer is the accumulation of somatic driver mutations in oncogenes or tumor suppressor

genes, particularly as individuals age and surpass the mutational threshold required for cancer initiation. Studies have shown that several aging related factors such as changes in DNA methylation (Klutstein et al., 2016; Lin & Wagner, 2015) and telomere length (Kim Sh et al., 2002; Shammas, 2011), exhibit an association with both aging and malignancy. These shared aspects of aging in healthy adults and in malignancies are the main focus of this thesis. Studying these aspects may offer insights into the development of preventive and therapeutic strategies.

1.3.1 Epigenetics and DNA methylation

Epigenetics refers to the mechanism which contribute to changes in gene expression without changing the underlying DNA sequence. The epigenome is defined as the entire collection of epigenetic modifications and mechanisms. These changes can occur at various levels, including DNA methylation (DNAm), histone modifications and chromatin remodeling. Within the cell nucleus, DNA is tightly wrapped around histone proteins, forming fundamental units called nucleosomes. These nucleosomes are further compacted into chromatin, which is ultimately organized into distinct chromosomes (Alberts et al., 2002). The structural organization of the chromatin plays a role in regulating gene expression. Chromatin primarily exists in two states: heterochromatin and euchromatin. Heterochromatin also known as the dense and compact "closed" form of chromatin, limits the accessibility of the machinery required for gene expression through interaction with DNAm and specific histone modifications. On the other hand, euchromatin, a less compact "open" form of chromatin, is associated with active gene transcription and is typically linked to unmethylated DNA and a distinct set of histone modifications (Nothof et al., 2022). This dichotomy between heterochromatin and euchromatin is fundamental to the dynamic regulation of gene expression within the cell (shown in Figure 5).

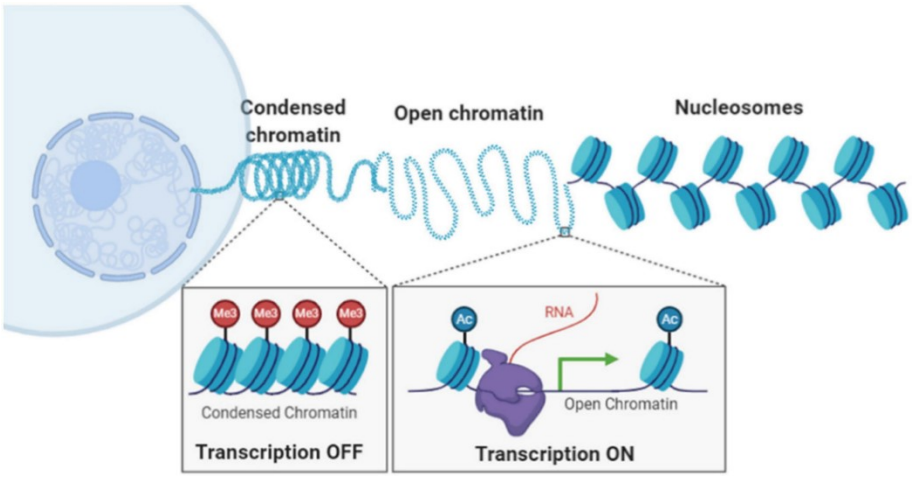

Figure 5. The interplay between chromatin organization and DNA methylation.
The dense, “closed” heterochromatin is associated with DNA methylation, which limits gene expression. In contrast, the less compact, “open” euchromatin is associated with unmethylated DNA, which promotes gene transcription. Therefore, chromatin packaging regulates gene expression by controlling DNA accessibility. The figure was adapted from (Xu & Liu, 2021), used under the terms of the Creative Commons Attribution License.

DNA methylation is an epigenetic modification, that involves the addition of a methyl group (-CH3) to the DNA, commonly at cytosine-guanine dinucleotides, also known as CpG sites. This leads to changes in gene state without altering the underlying nucleotide bases. In mammals, methylation occurs predominantly at the 5' position of cytosine (5mC). However, there is also non-CG methylation, whereby methyl groups are added to cytosines in CHG or CHH sites with H representing any nucleotide except guanine (He & Ecker, 2015). The specific location at which the methyl group is added is important for gene function and regulation of transcription. Regions with low CpG density typically exhibit high levels of methylation, while GC-rich regions called 'CpG islands', which are predominantly located in promoter regions, are usually less methylated (Deaton & Bird, 2011; Teschendorff et al., 2013). Methylation of CpG sites in close proximity to transcription start sites has been shown to repress gene transcription, whereas methylation within the gene bodies has been associated with increased gene expression and the protection against intragenic transcription initiation. In this thesis, the term DNA methylation refers to the 5mC methylation. The first identification of 5mC methylation in bacteria was in 1925, nearly a century later, numerous discoveries have facilitated the understanding of the mechanism behind DNA methylation, and several new sequencing techniques have been developed to elucidate its dynamic role in development and disease (Mattei et al., 2022).

The majority of mammalian DNA methylation patterns are generated by *de novo* DNA methyltransferases (DNMTs). DNMT3A and DNMT3B are a group of enzymes primarily responsible for the addition and maintenance of methyl groups to establish new DNA methylation patterns. Whereas DNMT1 binds to hemimethylated DNA strands and maintains methylation patterns during DNA replication, ensuring the inheritance of the epigenetic marks. DNMTs recognize specific DNA sequences based on specific motifs or structures to mediate methylation, although the underlying mechanism is not yet clearly understood. This process is initiated by a co factor called S-adenyl methionine (SAM), which serves as a methyl donor under the enzymatic reaction. This transfers the methyl group to the fifth carbon of cytosine residue, forming 5-methylcytosine through covalent binding. These modifications alter the structure and function of the underlying DNA. In contrast, DNA demethylation is a process that involves the removal of methyl groups from DNA and can occur by either active or passive mechanisms. Passive demethylation is due to a lack of functional methylation maintenance. During DNA replication, DNMT1 fails to methylate the newly synthesized DNA strand, resulting in a gradual loss of DNA methylation during multiple replication cycles. Active demethylation is mediated by the ten-eleven translocation (TET) family of enzymes which oxidizes 5mC to 5-hydroxymethylcytosine (5hmC) by adding a hydroxy group. TET can further oxidize 5hmC to additional oxidized forms of cytosine. This is then recognized by the base excision repair (BER) machinery, which removes the modified cytosine and replaces it with the unmethylated cytosines (Moore et al., 2013) (Figure 6).

Maintaining a balance between DNA methylation and demethylation is crucial for normal cell function and preventing the development of age-related hematological malignancies. For instance, mutations in *DNMT3A* and *TET2* are frequently observed in CHIP and are associated with impaired hematopoietic stem cell function. Especially, DNMT3As are highly mutated in AML patients and have been shown to impair differentiation capacity, favoring self-renewal (Buscarlet et al., 2017). Similarly, TET2 deficiency in mice has been shown to increase self-renewal potential (Cimmino et al., 2017).

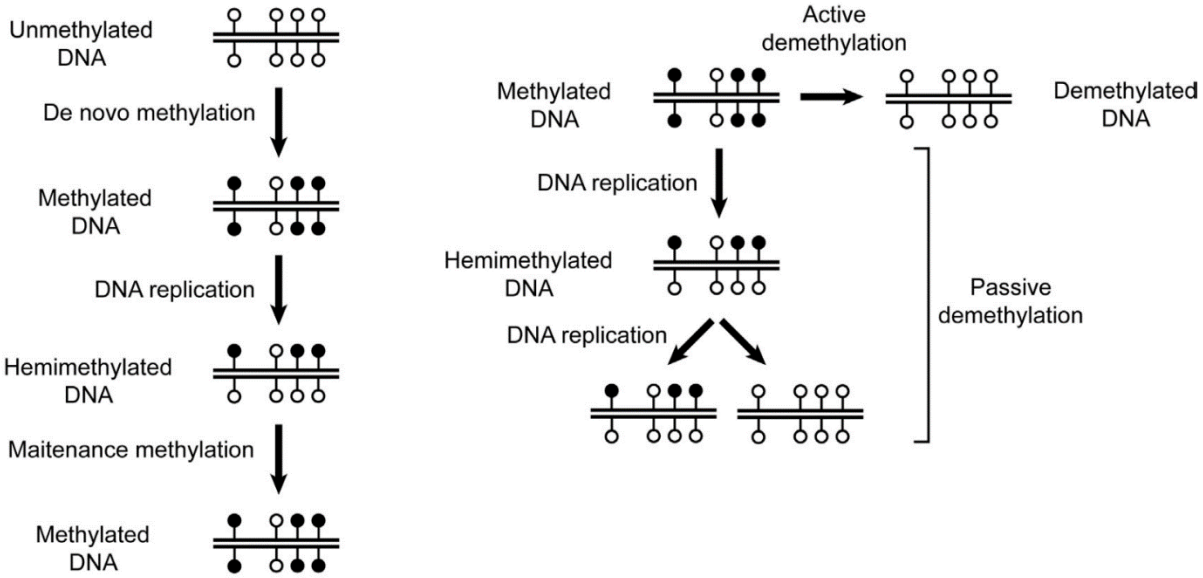

Figure 6. Mechanisms of DNA methylation and demethylation.
During the initial stages of development, *de novo* methylation adds methyl groups to specific CpG sites on both DNA strands. Following each replication cycle, the methylated CpGs become hemimethylated, whereby the newly synthesized daughter strand is unmethylated. The maintenance of these methylation patterns copies the original DNA methylation pattern. In the event of DNMT1 inhibition or absence, passive demethylation occurs over successive cell divisions as a consequence of the absence of methylation in the new DNA strand. In contrast, active demethylation is defined as the enzymatic replacement of 5-methylcytosine with cytosine. This figure was adapted from (Veland & Chen, 2017) with permission from Elsevier.

DNA methylation is a dynamic process. Even though the methylation patterns are largely specific in differentiated cells, which could be altered by both intrinsic and extrinsic factors including diet, exercise and stress (Barres & Zierath, 2016). These changes in methylation patterns are studied during development, aging, and disease progression. With increasing age, a general trend towards global hypomethylation is observed, particularly in repetitive sequences like transposable elements. This phenomenon is also observed in cancer compared to normal tissues. The loss of methylation in repetitive regions may lead to genomic instability and the development of aging-related pathologies. On the other hand, hypermethylation in promoter regions can silence genes involved in DNA repair, cell cycle regulation, and tumor suppression, contributing to age-related diseases including cancer (Ahuja & Issa, 2000; Luo et al., 2018).

During aging, stochastic methylation errors accumulate in the genome, a phenomenon known as epigenetic drift, which contributes to age-related diseases (Teschendorff et al., 2013). These aberrant DNA methylation patterns have been associated with carcinogenesis, as they affect the accessibility of regulatory elements in the genome. This ultimately results in the unexpected silencing or activation of genes, which can contribute to disease onset (Issa, 2014).

Certain epigenetic modifications are highly reproducible in specific DNAm sites and correlate with age. This could be utilized to underpin the concept of 'epigenetic clock'. Since 2011, researchers have successfully established DNAm clocks based on a few CpG sites to predict an individual's epigenetic age, which is widely used to estimate chronological age in various applications, including forensics (Bell et al., 2019; Bocklandt et al., 2011; Koch & Wagner, 2011). The evolution of epigenetic clocks has been marked by significant advances in technology, including the development of Illumina BeadChip technology, newer technologies for DNAm profiling, an increase in available datasets, and improvements in algorithms for integrating age-related DNAm changes. Notable examples include the Hannum clock for leukocytes and the multi-tissue clock by Horvath (Hannum et al., 2013; Horvath, 2013). Since then, it has evolved into a new generation of clocks to understand mortality risks and to predict individuals biological age (Horvath & Raj, 2018). Studies in a large cohort of old adults have shown that epigenetic age in the blood can be used as a prognostic marker for cardiovascular disease, cancer and all-cause mortality (Perna et al., 2016). Epigenetic reprogramming is shown to reverse the adult cells into pluripotent cells and has shed new light on aging research, as this process can effectively reset the aging clock, with partial reprogramming promising rejuvenating cells while maintaining their identity (Puri & Wagner, 2023; Takahashi & Yamanaka, 2006). This has led to the development of promising chemical based rejuvenation strategies, including small molecules such as DNA methyltransferase and histone acetylase inhibitors (Pereira et al., 2024).

1.3.2 Telomeres

The ends of chromosomes are protected by telomere caps with repetitive nucleotide sequence 'TTAGGG' and a set of special proteins called shelterin form a nucleoprotein complex. This keeps the ability of the cell to divide in every cell replication and protects the chromosomes from degradation (Greider, 1996; Vieri et al., 2021). The shelterin complex is composed of six proteins that maintain telomeres by preventing DNA repair proteins from accessing them. Telomeres consist of repetitive sequences, and if this has been mistaken for DNA damage, it could potentially lead to chromosome fusions. Additionally, these shelterin proteins regulate telomerase access and activity at telomeres, contributing to the formation of a high order of telomere structure (Palm & de Lange, 2008). Furthermore, Blackburn et al. discussed the capping status of telomeres (by the shelterin complex) as being more important than telomere length (TL) in determining cellular functionality. Even if the TL is short, it might still be capped

and functional, whereas a long TL might be uncapped and dysfunctional. This is due to the fact that the protective function of telomeres depends not only on their length, but also on the integrity of the shelterin complex that binds them (Blackburn, 2001). Furthermore. mutations or destabilization in these proteins can impair telomere protection, resulting in genomic instability and influencing telomere related diseases (Palm & de Lange, 2008).

During cell division, the inability of DNA polymerase to fully replicate DNA results in a gradual shortening of telomeres. Therefore, the maintenance of TL is regulated by the enzyme telomerase, a reverse transcriptase consisting of two enzymes, telomerase reverse transcriptase (TERT) and telomerase RNA component (TERC). TERT is a catalytic subunit that adds guanine rich repetitive sequences to the 3' ends of chromosomes using an RNA template provided by TERC, thereby counteracting the progressive shortening that occurs with each replication cycle (Greider, 1996; Vieri et al., 2021)(Chan & Blackburn, 2004). Telomerase is tightly regulated and is active in germ cells and some adult stem cells but is repressed in most somatic cells. When telomere activity is repressed, it leads to a progressive and cumulative loss of the protective telomeric caps, which eventually results in cellular senescence or apoptosis and contributes to the aging mechanism (Trybek et al., 2020). This phenomenon termed replicative senescence was first explained by Hayflick in 1961 that cultured fibroblast cells have a limited proliferation capacity and stop dividing after several passages (Hayflick & Moorhead, 1961). This finding was later confirmed in different cell types. A comparison between adult bone marrow-derived MSC and umbilical cord-derived MSC shows clear differences in multipotential capacity, as well as an increase in pluripotent factor expression and telomerase activity in neonatal MSC (Blasco, 2005). Notably, a study has shown that telomerase positive clones with elongated telomeres showed reduced expression of the senescence marker β-galactosidase (Bodnar et al., 1998), supporting the association between TL and senescence. As an example, human stem cells have a restricted number of cell divisions, with approximately 50 to 70 before reaching replicative senescence (Boyle et al., 2023; Zvereva et al., 2010), and approximately 50 bp lost per cell division (Werner et al., 2015). The age associated accelerated rate of telomere attrition is commonly regarded as a contributor to the organismal aging, and this phenomenon can be exploited as a biomarker for predicting biological age.

Diseases associated with aging or cancers often show shortened telomeres and dysregulated telomerase activity. In fact, telomerase activity is present in approximately 85 % of malignant tumors in comparison to normal cells and its activity is higher in advanced and metastatic tumors, making it a viable cancer biomarker and therapeutic target. The unlimited proliferation of cancer cells is frequently attributed to increased telomerase reactivation, which compensates for shortening of telomeres that occurs during each cell division (Ivancich et al., 2017; Razgonova et al., 2020). Studies on mice lacking telomerase activity have shown accelerated aging and

increased resistance to cancer (Blasco, 2005). However, the initial generation of telomerase-knockout mice does not demonstrate significant telomere shortening or any discernible phenotypic abnormalities. Abnormalities in tissue development are typically observed from the fifth generation onward. By the sixth generation, mice exhibit infertility and defective hematopoietic progenitor function (Calado & Young, 2009). Reintroducing telomerase activity in aged telomerase-deficient mice has demonstrated a rejuvenating effect by restoring telomere length and improving cellular function (Jaskelioff et al., 2011). Telomerase inhibitors are being explored as potential cancer therapies to halt excessive cell division and tumor growth. Although telomerase activators are proposed to counteract aging by delaying telomere attrition, they remain a potential target, given their opposite role in aging and cancer (Shay, 2016). Imetelstat, a telomerase inhibitor, has shown efficacy in the treatment of myelofibrosis and thrombocytopenia by attenuating the removal of DNA damage signals from telomeres in telomerase-positive cancer cells (Fragkiadaki et al., 2022; Tefferi et al., 2015). Understanding and influencing telomerase activity and telomere dynamics offers promising opportunities for both cancer therapies and anti-aging strategies.

1.3.3 Senescence

Cellular senescence is a permanent cell arrest phase where cells remain metabolically active but cease to proliferate or enter apoptosis. This process can be induced by various factors, including DNA damage, telomere shortening, epigenetic deregulation, induction of oncogenes, mitotic dysfunction, and metabolic and oxidative stress (Hernandez-Segura et al., 2018; Kumari & Jat, 2021). With increasing age, the efficiency of the immune system decreases, leading to the accumulation of senescent cells, where the paracrine effect of these cells leads to the release of inflammatory cytokines and chemokines, including senescence-associated secretory phenotype (SASP). SASP activates pro-inflammatory signals to signal immune cells to remove senescent cells but with age, there is a link between the elevated levels of senescence associated markers and inflammation, fibrosis, and other age-related pathologies, which contribute to an increased risk of death (Salech et al., 2022; St Sauver et al., 2023; Tripathi et al., 2021). Another phenomenon is known as replicative senescence, in which cells undergo senescence due to the shortening of telomeres caused by the limited number of cell cycle divisions. Accumulation of senescent cells increases with age and also contribute to age-related pathologies (Zvereva et al., 2010).

Two pathways contribute to cellular senescence: p53/p21 pathway and p16INK4a/pRB pathway. When cells encounter genomic or epigenomic damage leading to DNA damage response (DDR), the tumor suppressor protein p53 and its downstream p21, an inhibitor of cyclin-dependent kinase (CDK) are activated. This blocks the activity of several CDK complexes and eventually leads to the repression of genes associated with cell cycle progression, resulting in cell cycle

arrest (Amaya-Montoya et al., 2020; Kumari & Jat, 2021). The second pathway is p16INK4a/pRB. Here, p16INK4a, a tumor suppressor and CDK/cell cycle inhibitor, is activated by senescence-induced stress. This leads to the binding of CDK4/6 and prevents them from phosphorylating the tumor suppressor and transcriptional regulator protein pRB. This results in the stabilized and active form of pRB with a hypophosphorylated state, which in turn binds to the transcription factor E2F, inhibiting cell cycle progression at the transition from G1 to S phase. This leads to cell cycle exit and inducing cellular senescence (Amaya-Montoya et al., 2020; Kumari & Jat, 2021) (Figure 7). The duration of cells in each phase of the cell cycle is associated with the state of cellular senescence. Senescent cells exhibit shortened G1 and G2 phases and an extended S phase. For instance, embryonic stem cells are capable of prolonged undifferentiated proliferation, which has been hypothesized to be due to their rapid cell division, which occurs at an average rate of 15 hours in humans and 10 hours in mice, in comparison to somatic cells, which typically take 25-32 hours. This allows the embryonic cells to remain in a state of proliferation without undergoing the processes of senescence or quiescence (Becker et al., 2006; Padgett & Santos, 2020).

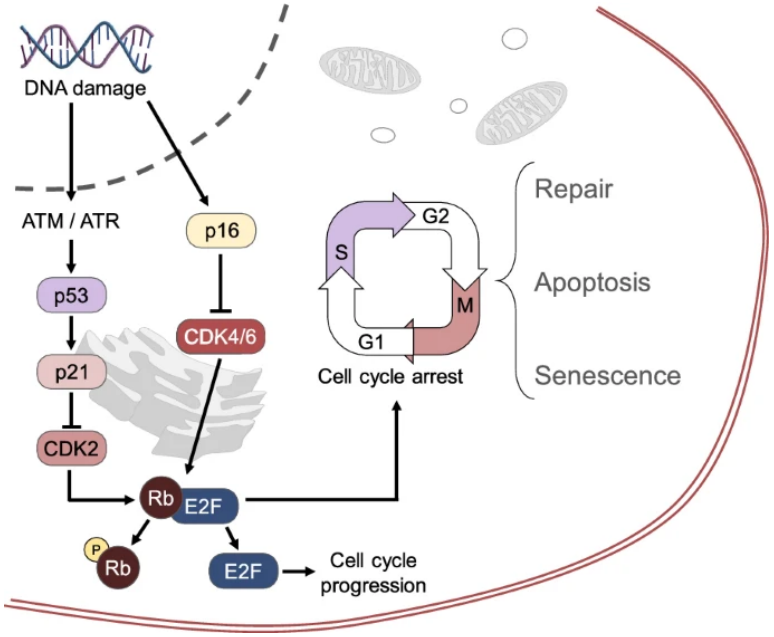

Figure 7. Senescence associated pathways.
In response to DNA damage, the DNA damage response (DDR) pathway activates ATM/ATR kinases, which stabilize p53. This leads to increased p21 expression, inhibiting CDK2 and keeping retinoblastoma protein (Rb) complexed with E2F, leading to cell senescence or apoptosis. Additionally, DDR enhances p16 expression, inactivating CDK4/6, further preventing cell cycle progression. In short, DDR activation halts cell division and promotes cell senescence or apoptosis in response to DNA damage. This figure was adapted from (Amaya-Montoya et al., 2020), used under the terms of the Creative Commons Attribution 4.0 International License.

Cellular senescence plays a dual role. The complex nature of senescence is referred to as a “two-edged sword”, with a distinction between helper senescence (promotes tissue regeneration) and deleterious senescence (causes tissue damage), which are depending on the

early and late phases of senescence (Tripathi et al., 2021). Short-term senescence can promote tissue repair and regeneration during early embryonic development and upon tissue damage. To achieve this, senescent cells arrest their own proliferation, recruit phagocytic immune cells and promote tissue renewal (Munoz-Espin & Serrano, 2014). The early or pre-senescent cells are more receptive to reversal than fully senescent cells (Reimann et al., 2024). While persistent senescent cells can lead to chronic inflammation and fibrosis, which in turn destroys the tissue (Paramos-de-Carvalho et al., 2021). Interestingly, programmed developmental senescence has been found to depend on the p21 signaling pathway rather than p53 or DNA damage (Storer et al., 2013). Senescence may serve as a potential biomarker for the study of aging and disease progression. Previous studies have shown that the expression of senescence-associated markers such as p21, p53, p16, reactive oxygen species (ROS), and nuclear factor-kappa B (NF-kB), increases with the chronological age of patient-derived MSCs. In addition, a specific cellular senescence marker SA-β-galactosidase (SA-β-gal) shows an age-related increase (Gil, 2023; Kapetanos et al., 2021). Furthermore, the absence of p21 has been associated with developmental abnormalities (Munoz-Espin et al., 2013). Proteins and genes associated with the senescence signaling pathway have been detected in age-related diseases such as dementia-related neurodegeneration and Alzheimer's disease (Saez-Atienzar & Masliah, 2020). A recent study demonstrated the impact of the coronavirus disease (COVID-19) on the elderly population and its association with virus-induced senescence (Lee et al., 2021). Studies have shown that the continuous removal of senescent cells in mouse models leads to an increase in lifespan (Karin et al., 2019). Timely clearance of senescence is important for maintaining tissue homeostasis and preventing age related pathogenesis.

The role of senescence in cancer is quite complex. On the one hand, senescence plays a role in tumor suppression by limiting the proliferation of premalignant cells that could potentially transform into malignant cells. When cells are exposed to mutations, uncontrolled replication results in a large number of mutated cells. However, senescence induces growth arrest in these cells, preventing the damage from being passed on to daughter cells (Shay & Roninson, 2004). The activation of certain oncogenes, such as RAS and BRAF, can trigger oncogene-induced senescence, a phenomenon that has been observed in various cancers (X. L. Liu et al., 2018). On the other hand, excessive and prolonged senescence may promote malignancies, chronic inflammation, immune deficit and stem cell exhaustion as individuals age (Huang et al., 2022). Reprogramming of senescent cells leads to spontaneous re-entry into the cell cycle, and promotion of tumor progression through self-renewal capacity (Milanovic et al., 2018). Notably, the phase of senescence, whether it is in the early or late stage, may play a critical role in determining whether it is beneficial or detrimental to the cell (Herranz & Gil, 2018).

1.3.3.1 Senolytic drug treatment

The elimination of senescent cells has been considered as a potential therapeutic target for age related phenotypes and diseases, including cancer. Senolytics are a group of small molecules that specifically target senescent cells by interfering with their anti-apoptotic pathways and triggering apoptosis. Researchers including Kirkland J. and colleagues have made a significant contribution to the study of senolytics and their effects on the disease. These compounds have been tested *in vivo*, *in vitro*, and xenograft models, with some of them currently undergoing early clinical trials for age related diseases (Wyles et al., 2022). Studies have demonstrated that senolytic treatments can selectively remove senescent cells, reduce proinflammatory cytokines, and extend survival in mice with the administration of senolytic cocktail of dasatinib plus quercetin (Xu et al., 2018). In human trials, senolytics have shown improvement in physical function for patients with idiopathic pulmonary fibrosis (Justice et al., 2019) and removal of senescent cells in diabetic chronic kidney disease (Hickson et al., 2019). The therapeutic potential of senolytics extends to improving organ quality of elderly patients prior to transplantation. This could facilitate the use of organs from elderly patients for transplantation in the future (Matsunaga et al., 2021). Additionally, combination treatment of senolytics with anti-cancer treatment has shown great potential (Chaib et al., 2022; Kirkland & Tchkonia, 2020), by potentially removing therapy-induced senescent cells, which is associated with relapse, drug resistance and immunosuppression (Lelarge et al., 2024).

Various senolytic drugs have been designed to target different mechanisms of anti-apoptotic pathways. This is achieved by inducing DNA damage and impairing the DNA repair mechanism in the senescent cells (Figure 8). These include BET inhibitors, such as JQ1, which targets the non-homologous end joining DNA repair pathway, thereby eliminating senescent cells. This is relevant for repairing double stand DNA breaks and activating autophagy pathway (Wakita et al., 2020). The BH3-only proteins of the BCL-2 family function as pro-apoptotic effectors, triggering the canonical mitochondrial apoptosis pathway. These proteins mediate their pro-apoptotic functions through BH1-3 pro-apoptotic proteins, such as BAX and BAK, while their activity is suppressed by the BCL-2 family members, BH1-4 (Lomonosova & Chinnadurai, 2008). The first BH3-mimetic to receive clinical approval is ABT263 (Navitoclax), which targets multiple BCL-2 proteins, including BCL-2, BCL-xL and BCL-w (Kuykendall et al., 2020). Another BH3 mimetic, S63845, is a selective inhibitor of the anti-apoptotic protein MCL-1 (Ewald et al., 2019). Dasatinib is a tyrosine kinase inhibitor that has been demonstrated to interfere with the EFNB-dependent suppression of apoptosis in senescent cells. Quercetin is a naturally occurring flavonoid that has been shown to interfere the activity of several anti-apoptotic pathways (Zhu et al., 2015). The combination treatment with dasatinib and quercetin showed a reduction in markers of senescence, such as p16 and p21, as well as SA-β-gal positive cells (Hickson et al.,

2019). MDM2 inhibitors, which target the interaction between MDM2 and p53, result in the reactivation of functional p53 and the death of senescent cells (Konopleva et al., 2020). With regard to the p53-MDM2 binding site, different structurally unique small inhibitors have been developed. These include AMG232, which is being tested in clinical trials for use in MPN patients who have failed treatment with JAK inhibitors (NCT03662126), and RG7112, which is also being tested in clinical trials in leukemia patients (NCT01970930); whereas, nutlin-3a has been shown to increase the degree of apoptosis in MPN by increasing p53 and p21 protein levels (Lu et al., 2012). Piperlongumine is an amide alkaloid derived from the fruit of long pepper that exhibits selective cytotoxicity towards cancer cells. This is achieved through the inhibition of oxidative stress response proteins, which are important for the survival of senescent cells with elevated levels of reactive oxygen species (X. Liu et al., 2018). Additionally, innovative approaches, including antibody-drug conjugates and chimeric antigen receptor T-cell (CAR-T) therapies are being developed to specifically target and eliminate senescent cells (Lelarge et al., 2024). Furthermore, the development of broad-spectrum of senolytic drugs remains a challenge, as current options show variable efficacy across different types of senescent cells. Overall, to date, senolytics have shown promising results in clinical trials and need to be studied in various diseases to be used as different therapeutic approaches.

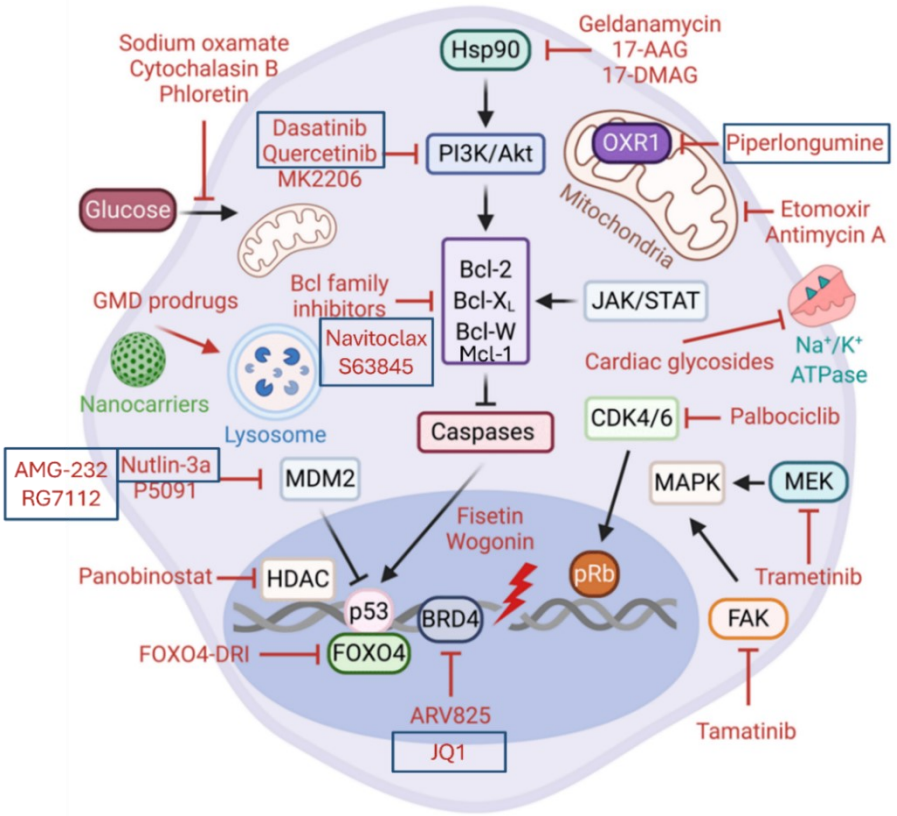

Figure 8. Senolytics mechanism of action.
Senolytics are a class of drugs that primarily target senescent cells through various mechanisms of action, ultimately leading to apoptosis. These anti-apoptotic pathways include Bcl-2 family proteins, p53, and the PI3K/Akt/mTOR pathway. This Figure was adapted from (Demirci et al., 2021), used under the terms of the Creative Commons Attribution.

1.4 Induced pluripotent stem cells

The discovery of induced pluripotent stem cells (iPSCs) by Yamanaka and Takahashi in 2006 pioneered the field of stem cell research. iPSCs have the capacity to proliferate indefinitely without losing their pluripotency and the ability to differentiate into the three germ layers, ectoderm, endoderm, and mesoderm. This groundbreaking work demonstrated that somatic cells could be reprogrammed into a pluripotent state, a characteristic previously observed only in embryonic stem cells (ESC) derived from the inner cell mass of the blastocysts (Hassani et al., 2019). A systematic screening of 24 genes associated with pluripotency led to the identification of four transcription factors that were necessary to induce pluripotency in mouse fibroblasts: octamer binding transcription factor 3/4 (OCT3/4), sex-determining region y-box 2 transcription factor (SOX2), kruppel-like factor 4 (KLF4), and the cellular myelocytomatosis oncogene (C-MYC), abbreviated as the OSKM factors or also known as the Yamanaka factors (Takahashi & Yamanaka, 2006). This discovery paved the way for the successful reprogramming of human cells into iPSCs in 2007, independently reported by Yamanaka (Takahashi et al., 2007) and Thomson; whereas Thomson used a different combination of factors consisting of: OCT4, SOX2, NANOG, and cell lineage abnormal 28 (LIN28) also known as the Thomson factors (Yu et al., 2007).

The concept of cellular reprogramming builds on earlier studies in developmental biology using the technique somatic cell nuclear transfer. This showed that somatic cells contain the genetic code of the zygote and can be manipulated to become totipotent cells. Additionally, fusing the ESCs with somatic cells showed that the resulting ESCs exhibit the inherited developmental capacity of the original embryonic cells. (Tada et al., 2003), leading to the expression of pluripotency associated genes, including OCT 3/4 (Tada et al., 2001). OCT3/4 is a key transcription factor that binds to DNA and regulates the expression of pluripotency associated genes that are important for embryonic development. When OCT3/4 expression is lost, the cells begin to differentiate (Zeineddine et al., 2014). The OSKM transcription factors drive the establishment of the pluripotency network during reprogramming. This involves two major steps: the silencing of somatic gene expression by the ectopic expression of OSKM factors and the activation of the pluripotency (Papp & Plath, 2011). C-MYC induces chromatin remodeling that allows exogenous OCT4 to bind to its target genes. OCT4 then cooperates with SOX2 and KLF4 to activate the expression of the target genes encoding transcription factors such as OCT4, SOX2 and NANOG. This forms the endogenous transcription factor network that maintains the pluripotency state of iPSCs (Buganim et al., 2013). Subsequent studies have shown that the use of alternative combinations of minimal pluripotency factors, by omitting C-MYC or KLF4 can also be effective in reprogramming. Furthermore, the use of additional genes and chemicals known

as enhancers, can promote the reprogramming and enhance its efficiency (Takahashi & Yamanaka, 2016).

There have been several methods developed to express the reprogramming transcription factors into the host cell. The efficiency of reprogramming is highly dependent on the method used. Viral transduction via integrative lentivirus or retrovirus is viewed as the classical method to deliver the transcription factors into the cell. However, this can lead to genomic alterations in the host genome. In contrast, Sendai virus, a negative sense single stranded RNA (ssRNA) that replicates in the cytoplasm without integrating into the host genome, appears to avoid genomic alterations to the host genome (Fusaki et al., 2009). Non-viral methods that can replicate independently without integrating into the host genome, such as chemical compounds, episomal plasmids, recombinant proteins, and DNA-free small molecules, have been shown to be less efficient in successful reprogramming. Synthetic mRNA delivery methods, which use molecules to influence signaling pathways involved in the pluripotency network without introducing exogenous DNA into host cells, are seen as an alternative approach (Cerneckis et al., 2024; Takahashi & Yamanaka, 2016). Quality control of iPSCs has been an important aspect due to the variability in reprogramming efficiency. The gold standard method to evaluate the pluripotency of iPSCs is the formation of teratomas in immune compromised mice, which should contain all three germ layers. Recent studies have shown that epigenetic markers such as changes in the DNA methylation levels on specific genes can also be used to validate the pluripotent state of the cell (Schmidt et al., 2023).

1.4.1 Induced pluripotent stem cells as a disease model

iPSC technology has significantly advanced the modeling of human diseases. Traditional methods often relied on mouse models, but the fundamental inter-species differences have been challenging to mirror human clinical pathophysiology. When it comes to blood diseases, it is crucial to study human primary cells, as well as disease specific model systems such as immortalized cell lines to investigate disease associated pathways. The emergence of iPSC models has sought to bridge the gap between the two systems, by enabling the derivation of patient-specific diseased cells and facilitating scalable experiments. Reprogramming patient-specific cells into a pluripotent state allows for the generation of various somatic cell types that display disease phenotypes. Furthermore, iPSC technology has been employed in 3D culture and most interestingly in the generation of organoids to mimic the human organ and its microenvironment (Alle et al., 2021; Rowe & Daley, 2019).

A key advantage, but also a limitation of this method is that it is highly patient-specific. On a positive note, this enables autologous transplantation using the patient's own cells and allows the development of personalized medicine. Conversely, variations in epigenetics and genetics

among patients can result in differences in iPSC characteristics, thereby making comparisons between different studies for a specific disease or mutation challenging. Utilizing multiple patient derived iPSC lines and controls would facilitate the understanding of disease mechanisms and pathways. Although the reprogramming of somatic cells into multiple iPSCs remains challenging, significant improvements have been made to increase the efficiency and reproducibility. Despite these challenges, iPSC technology has been rapidly evolving, specifically in the areas of drug discovery, personalized medicine, and regenerative cellular therapies (Doss & Sachinidis, 2019).

The introduction of genetic modifications in iPSCs is a valuable technique to study specific genetic mutations and diseases, through the insertion or deletion of genes or small single nucleotide sequences. This technique employs engineered nucleases, which contain sequence specific DNA binding domains fused to a non-specific DNA cleavage module. These nucleases induce DNA double stranded breaks (DSB) at specific genomic sites, thereby activating the DNA repair machinery. Two distinct repair mechanisms can occur: non-homologous end joining (NHEJ), or homology directed repair (HDR). Zinc-finger nucleases and transcription activator like effector nucleases (TALENs) were used for genetic modifications until the discovery of clustered regularly interspaced short palindromic repeats guided Cas9 nucleases (CRISPR/Cas9) (Gaj et al., 2013). In 2012, Jennifer Doudna and Emmanuelle Charpentier discovered the Cas9 protein from *Streptococcus pyogenes* (Jinek et al., 2012). Cas9 is an RNA guided nuclease and is not dependent on protein-DNA interaction (Swartjes et al., 2020). The gene editing system consists of two parts, the Cas9 nuclease and the single guide RNA (sgRNA), which contains a protospacer adjacent motif (PAM) sequence specific for the Cas9 protein. When introducing the mutation, the sgRNA is designed to target the genomic location where the mutation needs to be introduced. Upon introduction into iPSCs, they combine and target the DNA complementary to the sgRNA, resulting in a DSB a couple of base pairs down the PAM sequence. Once the cell detects this DSB, the DNA repair machinery is activated. NHEJ typically introduces small insertions or deletions at the cleavage site and ligates the broken DNA ends without the need for a template. In HDR, the cell finds homologous regions adjacent to the DSB, either from the other chromosome or provided exogenously as a plasmid or single-stranded oligodeoxynucleotides along with the Cas9/sgRNA. The donor DNA template with the correct sequence e.g. wild type sequence or with a new sequence e.g. generation of reporter cell lines, is used as a repair template (Figure 9) (Pinjala et al., 2023; Sander & Joung, 2014). Even though the sgRNA has a high specificity owing to the 18-20 base pair length, it is crucial to consider off-target effects to minimize the risk of genomic instability and tumorigenic potential (Manghwar et al., 2020).

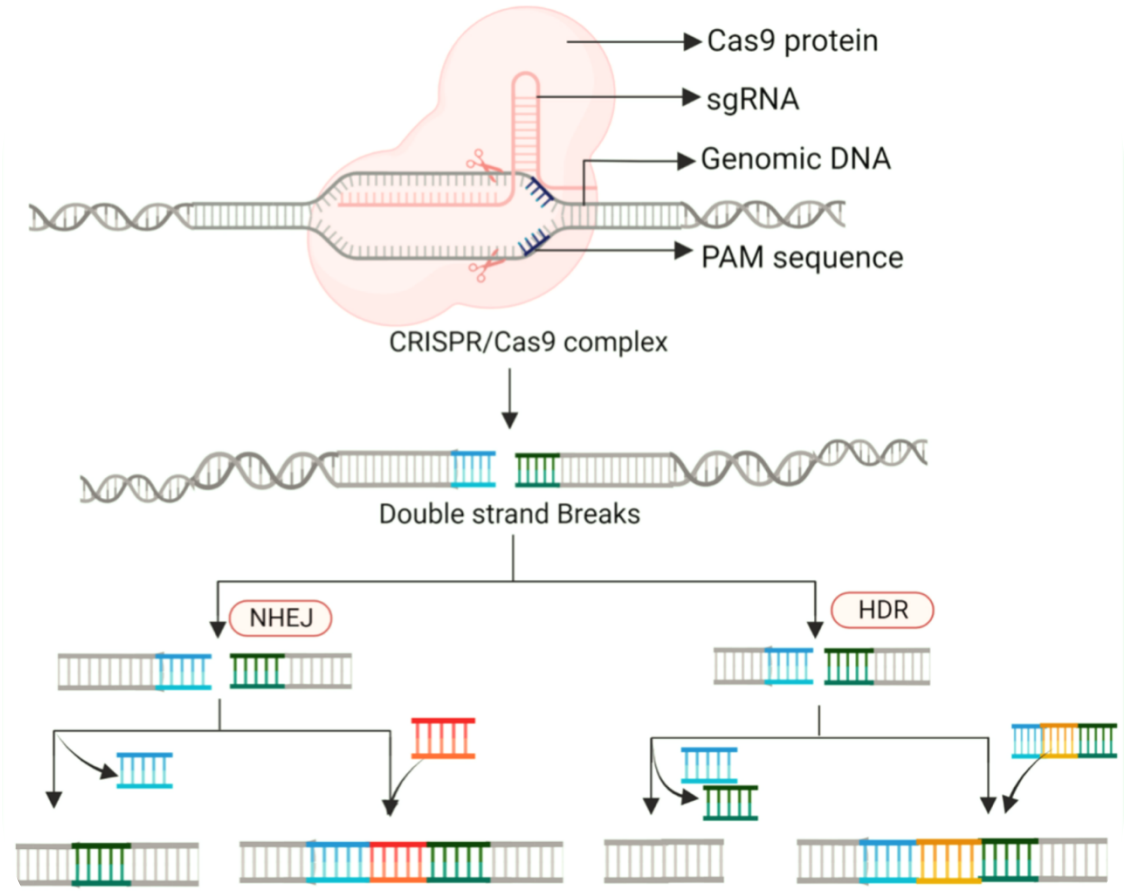

Figure 9. Schematic view of CRISPR/Cas9 genome editing.
Cas9 recognizes the target sequence with gRNA, and guide Cas9 endonuclease to cut the upstream of PAM, resulting in the double-strand break (DSB) of the target site DNA. The DSBs can be repaired by two distinct pathways: nonhomologous end joining (NHEJ) and homology-directed repair (HDR). NHEJ-mediated repair can introduce random insertion and/or deletion of variable lengths of DNA at the site of a DSB, while HDR-mediated repair can introduce precise point mutations or insertions from a single-stranded or double-stranded DNA donor template. The figure was adapted from (Pinjala et al., 2023), used under the terms of the Creative Commons Attribution 4.0 International License.

1.4.2 Hematopoietic differentiation of iPSCs

Since the identification of ESC and iPSCs, studies have been conducted to differentiate these cells into specific cell lineages. Genetic manipulation of iPSCs has led to the introduction of disease specific molecular defects which have been instrumental in capturing specific disease models. In this thesis, we focus on studying MPN, a hematological malignancy. Therefore, studying the iPSC-derived hematopoietic stem and progenitor cells (iHPCs) using directed differentiation is valuable to recapitulate the malignant phenotype *in vivo* (Papapetrou, 2019). Initially, efforts were made to generate primitive progenitor cells resembling the early yolk sac, mainly focusing on the erythroid and myeloid lineages. More recently, protocols have been developed to achieve progenitors that resemble definitive-like hematopoiesis. Despite recent modifications to the method, it remains challenging to resemble bona fide HSCs with the capacity for long term engraftment. iPSCs are differentiated in a stepwise manner by inducing

transcription factors that lead to differentiation of specific lineages and removing factors related to pluripotency (Figure 10) (Rowe & Daley, 2019). The differentiation process is achieved through a 2D culture based on an extracellular matrix or by embryoid body formation in a 3D culture. In order to mimic the embryogenesis, iPSCs are directed to transition from the endothelial to hematopoietic lineage. This transition is then directed towards the mesoderm lineage, where the cells further specified towards hematopoietic progenitor cells such as megakaryocytes and platelets. This is achieved by the addition of cytokines or growth factors including bone morphogenetic protein 4 (BMP4), vascular endothelial growth factor A (VEGF), fibroblast growth factor 2 (FGF2, also known as basic FGF) and stem cell factor (SCF) (Rowe & Daley, 2019). BMP4 and FGF2 play a crucial role in the initial specification process of hematopoiesis. BMP4 expression is observed in the early human yolk sac, where it induces the mesodermal lineage. The formation and patterning of the mesoderm is controlled by BMP, WNT, and Nodal signaling (Shen et al., 2019), which activate downstream Hox genes involved in hematopoietic specification (Alsayegh et al., 2019). This is followed by hematoendothelial specification via FGF2 and VEGF signaling. FGF2 signaling contributes to the maintenance of pluripotency and induces the expression of a multitude of target genes including those involved in cell survival, proliferation, and differentiation (Mossahebi-Mohammadi et al., 2020). VEGF play an important role in maintaining the hematopoietic microenvironment by regulating angiogenesis and vascular development (Shibuya, 2011). VEGF and FGF2 facilitate the homing and engraftment of HSCs within the bone marrow like niche (Mesnieres et al., 2021; Yin et al., 2020). SCF is also known as a receptor for tyrosine kinase (KIT). SCF binds to the KIT receptor, thereby activating the EPOR, which induces cell proliferation and maturation (Lee et al., 2023).

In addition, feeder cells derived from mouse bone marrow stromal cells have been demonstrated to stimulate the differentiation of human iPSCs (Lee et al., 2023). It remains challenging to mimic the homing capabilities and niche factors observed in bone marrow, as they provide crucial signals and factors that support the self-renewal, maintenance, and differentiation of the blood cells (Rao et al., 2022). Although there are still challenges to overcome for clinical applications, it is a valuable tool for disease modeling and studying a specific mutation.

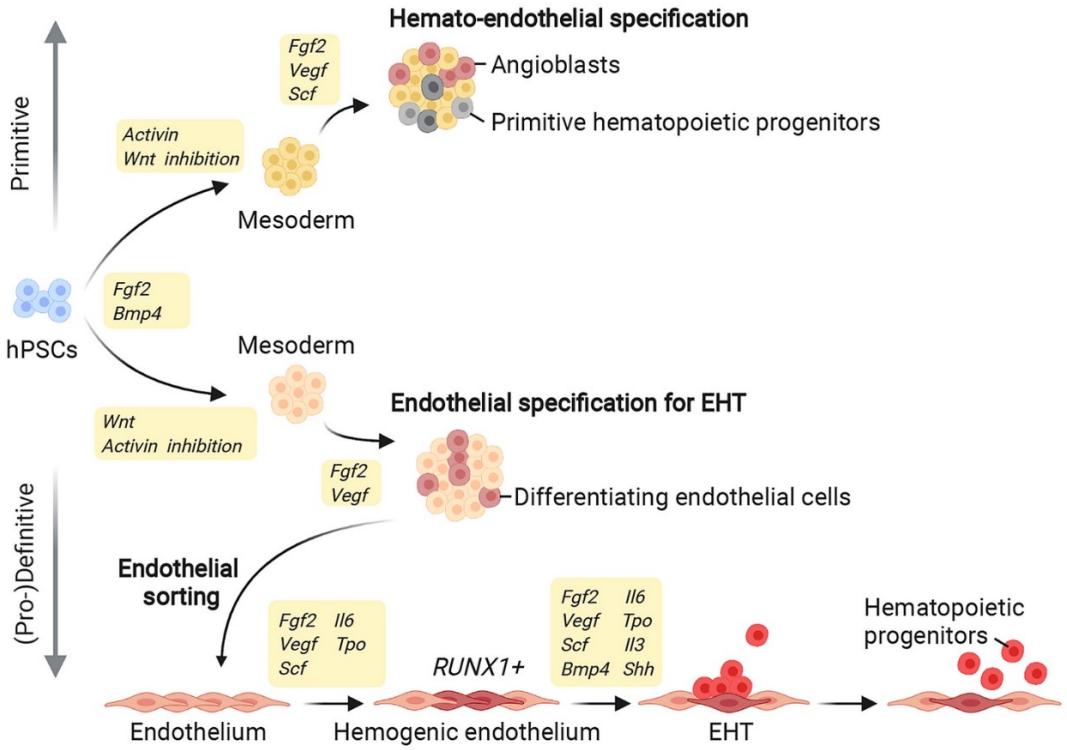

Figure 10. Differentiating human pluripotent stem cells towards a hematopoietic fate.
FGF and BMP have been shown to induce differentiation of hPSCs towards a mesodermal lineage. The combination of activin activation and WNT inhibition facilitates the differentiation of mesodermal cells into primitive hematopoietic cells. Alternatively, the activation of the WNT pathway in conjunction with the inhibition of activin induces the differentiation of mesodermal cells into endothelial cells, including hemogenic endothelial cells that express RUNX1 and undergo endothelial to hematopoietic transition (EHT) to yield (pro-)definitive hematopoietic cells. This figure was reprinted from (Canu & Ruhrberg, 2021), used under the terms of the Creative Commons Attribution 4.0 International License.

1.4.3 DNA methylation changes in iPSC derived cells

DNA methylation plays a crucial role in cellular differentiation and development. During the early embryonic development, DNA methylation is largely removed except for a few imprinted genes to establish a pluripotent state. These imprinted genes represent a subset of genes where one allele is silenced through random DNA methylation. This remains inactive throughout the life of the cell, maintaining the cellular identity (Law & Jacobsen, 2010). The development of the embryo is a highly orchestrated event which leads to global *de novo* methylation and establish gene-specific demethylation patterns, that activate the onset of specific genes that are required for self-renewal and cell differentiation. DNA methylation patterns undergo changes during the process of lineage commitment, whereby specific genes become either methylated or demethylated, while other genes associated with alternative lineages are silenced by DNA methylation. During hematopoiesis, DNA methylation is essential for maintaining HSCs. Through the mediation of epigenetic modification, DNA methylation facilitates the generation of HSPCs through the repression of Notch signaling. The loss of DNMT1 has been shown to induce hypomethylation in genes associated with Notch signaling, which subsequently elevates Notch

activity in hemogenic endothelial cell, thereby repressing the generation of HSPCs (Li et al., 2022).

Similarly, the reprogramming of a somatic cell into a pluripotent cell is accompanied by a reset of the global epigenome to resemble the ESCs. This occurs through active demethylation, which not only facilitates the expression of pluripotency associated genes but also drives other events, such as the mesenchymal-to-epithelial transition. This transition is another critical event that needs to occur during the reprogramming process. Overall, remodeling of chromatin accessibility and DNA methylation erases somatic cell identity and resulting in the formation of a new signature and a change in chromatin state (Cerneckis et al., 2024). A multitude of studies have been conducted to study DNA methylation changes in iPSCs and their directed differentiated counterparts. The DNA methylation profiles of 22 iPSC lines derived from five different cell types and five ESCs showed that iPSCs have a distinct methylation profile. At the early passages, iPSCs showed an aberrant methylation pattern compared to ESCs. However, the continuous culturing of iPSCs led to reduced differences between iPSCs and ESCs, both on the whole genome and on the X chromosome. This suggests that iPSCs gradually lose the traits inherited from their parental cell type during reprogramming and long term culture (Nishino et al., 2011). Similarly, a recent study has shown that iPSC-derived neurons have a similar epigenetic and gene expression patterns to neurons derived from non-reprogrammed human ESCs. This suggests a similarity in the epigenetic state of iPSC and ESC differentiated cells (de Boni et al., 2018). However, more studies are needed to fully understand how closely iPSC derived neurons mimic native brain neurons at both molecular and functional levels. An unpublished work showed that during the differentiation of cardiomyocytes from iPSCs, DNA methylation levels decreased in specific promoter regions associated with cell cycle genes, and potentially leading to cell cycle arrest (N. Li et al., 2024). Additionally, iPSC-derived HSCs exhibit both epigenetic and transcriptional distinctions from cord blood-derived HSCs or adult HSCs. Further, additional coculture with MSCs did not significantly increase the epigenetic similarities to primary HSCs (Cypris et al., 2019). Overall, DNA methylation plays a crucial role in reprogramming and differentiation of iPSCs, however, there are still challenges in fully recapitulating the epigenetic profiles of primary cell types in iPSC-derived cells.

While there is evidence indicating that iPSC reprogramming removes most epigenetic marks, studies have shown that there could be potential residual somatic cell specific epigenetic signatures which remain in these iPSCs. Despite iPSCs closely resembling primary ESC, it has been observed that the partial removal of somatic cell specific epigenetic signatures can influence the differentiation potential of iPSCs (Ohi et al., 2011). The cell type used for reprogramming has been shown to have an impact on hematopoietic differentiation due to its residual epigenetic memory (Kim et al., 2010). Interestingly, this epigenetic memory can also be

used to exploit the enhancement of the desired cell type differentiation. Studies have shown that iPSCs reprogrammed from hematopoietic cells or human umbilical cord vein endothelial cells (HUVECs) are more suitable for iHPCs differentiation (Phetfong et al., 2016) than iPSCs derived from fibroblasts (Kim et al., 2010).

When considering the disease-derived iPSCs, it is important to note that residual epigenetic memory may still exhibit features of oncogenic potential due to the aberrant DNA methylation patterns. Hypermethylation of different gene sets in CpG islands is a prominent feature of malignancies and could influence the phenotype of iPSCs (Shamsian et al., 2022). However, some studies have shown that the oncogenic potential of the cell may not be expressed in the pluripotent state of the cells. For example, *DNMT3A* knockouts in iPSCs, targeting exon 19 or exon 23 were found to significantly impair *de novo* DNA methylation during hematopoietic differentiation of iPSCs. Nevertheless, differentiation efficiency was only slightly reduced in exon 19 knockouts and increased in exon 23 knockouts, but both were partially able to recapitulate the DNA methylation patterns observed in AML (Cypris et al., 2022). Additionally, iPSCs derived from AML patients showed a reset in DNA methylation and gene expression profiles after reprogramming (Chao et al., 2017). Therefore, such research is important for understanding the intricate epigenetic changes that occur during the reprogramming and differentiation of specific disease derived iPSCs in disease modeling.

1.5 Aim of the thesis

In this thesis, we first sought to study the potential rejuvenating effect of senolytics on healthy aged human blood samples. Utilizing cellular aging parameters such as epigenetic age and cellular senescence, we aimed to understand the age-related changes and heterogeneity in peripheral blood mononuclear cells (PBMC) from young and old individuals. In addition, we aimed to determine whether the treatment of PBMCs with different senolytics could remove senescent cells, reduce epigenetic aging, and remodel lymphocyte composition. The rationale for this approach is that blood samples are easily clinically accessible and that the majority of previous senolytic studies have focused on mouse models or artificially induced senescence, rather than naturally occurring senescent cells in human samples.

Secondly, we aimed to understand cellular aging aspects in MPN, which is more prevalent in the elderly. It has been speculated that driver mutations may accelerate senescence and genetic instability, potentially leading to disease progression, requiring the development of new diagnostic tools. To address this, we analyzed cellular aging parameters to distinguish mutant cells exhibiting signs of aging compared to healthy controls. Utilizing colony forming unit assays, we sought to capture aging associated changes that occur predominantly in the mutation clones

compared to wild type colonies. Our aim was to systematically correlate these aging markers with specific mutations and their disease burden across different MPN subtypes. In addition, we hypothesized that eliminating these senescent cells using senolytic drugs could potentially target the mutant clones carrying driver mutations associated with MPN.

Lastly, we aimed to analyze the DNA methylation changes in the iPSCs model carrying *JAK2* V617F mutation, which is a key driver mutation in MPN. DNA methylation changes are an important factor in cellular aging and can alter gene expression changes in MPN. This led us to question whether the aberrant DNA methylation patterns influence specifically the mutant *JAK2* clones compared to their synergistic wild type counterparts. While previous studies have compared DNA methylation changes in MPN patients *versus* healthy individuals and across MPN subgroups, however, to date, no experiment has been performed to study the global methylation changes in an iPSC model of MPN. For this purpose, we intend to utilize three established iPSC clones carrying the *JAK2* V617F mutation and their WT clones and perform hematopoietic differentiation (iHPCs) to capture the mutant phenotypic cells. By comparing the DNA methylation profiles of iHPCs with those of patients carrying the *JAK2* V617F mutation, we aim to gain insights into whether the iPSC model can recapitulate the global DNA methylation changes observed in patients. Furthermore, we wanted to find out whether the driver mutation alone is enough to recapitulate the MPN phenotype and the aberrant DNA methylation patterns.

2. Methods and Materials

2.1 Cell culture-based experiments

2.1.1 Human blood samples

We used peripheral blood of 148 patients diagnosed with different sub entities of MPN. Samples were taken after informed and written consent according to the guidelines approved by the local ethics committees of RWTH Aachen University (EK 127/12). As a reference, blood samples of 134 healthy donors (EK 206/09) were used for age-adaptation of TL measured via flow-FISH as described previously (Ferreira et al., 2020; Rufer et al., 1999). Furthermore, a separate cohort of 128 healthy controls was used for the measurement of epigenetic age deviation. In addition, some more healthy samples were used for the senolytic treatment. These samples were obtained after informed and written consent according to guidelines approved by the local ethics committees of RWTH Aachen University (EK 041/15 and EK 099/14).

2.1.2 Mouse blood samples

We received samples from different mouse models regarding MPN to further understand the cellular aging in mouse models with specific knockouts.

1. Vav-*iCre*$^{tg/+}$-*Jak2*$^{V617F/+}$ mouse model: to study *Jak2 V617F* driver mutation in MPN
The Vav-Cre-lox system was used to induce the Jak2 V617F mutation in the C57BL/6 mouse model, as described previously (Dagher et al., 2021). Six wild type (WT) and three heterozygous Jak2 V617F (VF) mice at 20 weeks of age and 3 WT and 1 VF mice at 30 weeks of age were used for epigenetic age prediction and telomere length measurements. The genotype of the mouse was confirmed by PCR, and massive splenomegaly and elevated myeloid and erythroid markers were observed in VF mice compared with WT mice. Bone marrow cells were collected for analysis by flushing tibiae and femurs, and red blood cells were lysed. The samples were collected by Julian Baumeister (Department of Hematology, Oncology, Hemostaseology and Stem Cell Transplantation, Faculty of Medicine, RWTH Aachen University, 52074 Aachen, Germany).

2. SCLtTA/ BCR-ABL mouse model: to study chronic phase of CML
The expression of BCR-ABL is restricted to hematopoietic stem- and progenitor cells (Koschmieder et al., 2005). The regulation of the BCR-ABL expression system by the 3'-enhancer of the murine SCL gene (stem cell leukemia) and the tetracycline expression system in the FVB\N mouse model. BCR-ABL expression is therefore restricted to double transgenic (DTG) mice, which have both the SCLtTA construct and the BCR-ABL construct and can be

regulated by adding tetracycline to the drinking water (tet-off system). In the absence of tetracycline, the tetracycline transactivator (tTA) binds to the tetracycline-responsive element (TRE) and activates BCR-ABL expression. When tetracycline is present, it binds to tTA and prevents it from activating BCR-ABL expression. Bone marrow samples of six WT and six which express BCR-ABL is collected and were used to measure epigenetic age prediction. The samples were collected by Marlena Bütow (Department of Hematology, Oncology, Hemostaseology and Stem Cell Transplantation, Faculty of Medicine, RWTH Aachen University, 52074 Aachen, Germany).

3. Vav-Cre PDGFRβ mutant mouse model: to study the expression of PDGFRβ in MPN
Cre transgenic mice can be used to delete gene sequences flanked by loxP sites in specific somatic tissues (Buhl et al., 2020). Prior to Cre recombination exposure, no expression of the constitutively active βJ mutant isoform is observed, and the mutant alleles function as a knockout. Homozygous for the PDGFRβ allele are neonatal fatal, only heterozygous mice are viable. Peripheral blood samples of fifty three WT and nine which express PDGFRβ were collected and used to measure epigenetic age prediction (one outlier has been removed from each group). The samples were collected by Dickson W L Wong (Institute of Pathology, RWTH Aachen University Hospital, 52074 Aachen, Germany).

2.1.3 Isolation of peripheral blood mononuclear cells

The isolation of blood cells is performed from peripheral blood, followed by density gradient centrifugation. For this purpose, the synthetic polysaccharide Ficoll is used which has a density of about 1.078 g/mL. Thus, Ficoll has a higher density than lymphocytes, monocytes, and platelets, but a lower density than erythrocytes and most granulocytes. The blood was passed through a 100 µm cell strainer and diluted 1:1 with cold PBS containing 2 % FCS. 20 mL of the Ficoll (Panbiotech, Aidenbach, Germany) was transferred to a 50 mL falcon tube and 30 mL of sample was carefully added on top without mixing of the two phases. Cells were centrifuged for 30 min at 1200 rpm without brakes. Afterwards, the milky interface phase contained the PBMC which is carefully transferred to a new Falcon containing PBS using the plastic-Pasteur pipettes. The PBMC were washed twice with PBS containing 2 % FCS. The cells were washed once, centrifugated at 1200 rpm for 10 min. The cells were counted using hematocytometer Neubauer chamber, for that 10 µL of cells was mixed with 10 µL of trypan blue and 10 µL of the mixture was used in the chamber and counted only the cells which translucent light. 2 x10^6 cells per well to a 6- well plate was subjected to culture for three days. PBMCs were cultured in StemSpan Serum-Free Expansion Medium (Stemcell Technologies, Vancouver, Canada), supplemented with 10 ng/mL SCF, 20 ng/mL TPO, 10 ng/mL FGF-1 (all PeproTech, Hamburg, Germany), 10 µg/mL heparin (Ratiopharm, Ulm, Germany), and 100 U/mL penicillin/streptomycin (Lonza, Basel, Switzerland). The rest of the cells were frozen in a freezing medium consisting of DMEM

medium supplemented with 40 % of FCS and 10 % of DMSO, in a cryotube in a Mr. Frosty at -80 °C, and after 3 days cells were transferred to a -140 °C freezer.

2.1.4 Magnetic separation of CD34+ cells

PBMCs of MPN patients were isolated by gradient centrifugation and enriched for CD34+ cells by magnetic-activated cell sorting (MACS) with microbeads (Miltenyi Biotech, Germany). DNA was isolated before and after CD34+ enrichment with the Monarch® PCR & DNA Cleanup Kit (New England Biolabs, Frankfurt, Germany) and then used for TL measurements.

2.1.5 Colony forming unit assay

The colony-forming unit (CFU) assay allows to evaluate the proliferation and differentiation capacity of hematopoietic cells. For that, peripheral blood mononuclear cells (PBMCs) were isolated by gradient centrifugation with Pancoll (Pan Biotech) and 1 x10^6 cells per condition were transferred on a 1 mL semisolid medium StemMACS HSC-CFU Media lite with Epo (Miltenyi). Stem MACS HSC-CFU Media based on methylcellulose in IMDM and supplemented with fetal bovine serum (FBS) and different growth factor, these medium mimics the effect of stromal cells and provide optimal growth conditions for CD34+ cells. Colony forming unit (CFU) assays were plated in triplicates in 35 mm cell culture dishes (with grid, Thermo Fisher®, Waltham, MA, USA). Hematopoietic differentiated iPSCs after 16 days, 5,000 cells per genotype were transferred a semisolid medium to perform CFU (Kalmer et al., 2022). After 14 days, distinct colonies were counted and classified (Figure 11). Some of the MPN patient derived CFUs were cultured and genotyped by Milena Kalmer (Department of Hematology, Oncology, Hemostaseology and Stem Cell Transplantation, Faculty of Medicine, RWTH Aachen University, 52074 Aachen, Germany).

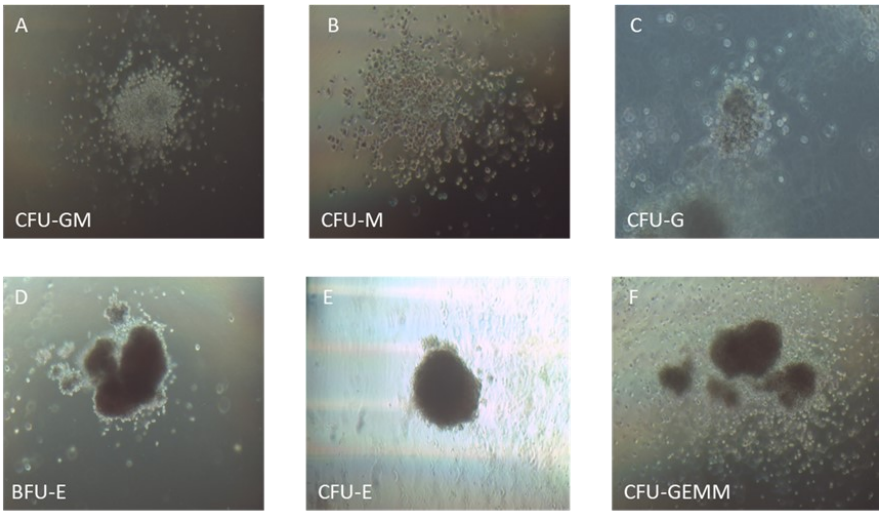

Figure 11. Classification of single colonies from colony forming assay.
Abbreviations: CFU-GM (colony-forming unit – granulocyte, macrophage), CFU-M (colony-forming unit – macrophage), CFU-G (colony-forming unit – granulocyte), BFU-E (burst-forming unit – erythroid), CFU-E (colony-forming unit – erythroid), and CFU-GEMM (colony-forming unit – granulocyte, erythrocyte, macrophage, megakaryocyte). The figure was adapted from Miltenyi manual.

2.1.6 Generation of *JAK2* V617F iPSC

Induced pluripotent stem cells (iPSC) from three PV patients were generated by reprogramming PBMCs with OCT4, SOX2, c-MYC and KLF4 in CytoTune Sendai virus vectors as described before (Boehnke et al., 2021; Flosdorf et al., 2024; Satoh et al., 2021). Briefly, the CRISPR/Cas9 complex (Alt-R HiFi Cas9 nuclease plus gRNA), single-stranded donor template and electroporation enhancer were delivered to cells using the Neon Transfection System and the 100 µL kit (Thermo Fisher Scientific). Before electroporation, iPSCs were treated for 1 h with HDR enhancer (5 µM; IDT, Coralville, United States) and 10 µM Rho kinase (ROCK) inhibitor (Y-27632, Abcam, Cambridge, UK). Electroporated cells were seeded on Laminin 521 (Biolamina, Sundbyberg, Sweden) coated plates in StemMACS iPS-Brew XF (Miltenyi Biotec) supplemented with 1× CloneR (Stemcell Technologies, Vancouver, Canada). Genotyping of CRISPR-repaired iPS cell lines was performed by allele-specific PCR targeting the *JAK2* V617F mutation.

In patient 1 with 37 % *JAK2* V617F allele burden in the PBMCs, only WT (Human Pluripotent Stem Cell Registry; UKAi002-A) and heterozygous (UKAi002-B) iPSC clones were obtained after reprogramming. Therefore, CRISPR/Cas9 genome engineering was used to introduce the *JAK2* V617F mutation generating a homozygous *JAK2* V617F iPSC clone (UKAi002-B3). Similarly, in patient 2 with 96 % *JAK2* V617F allele burden in the PBMCs gave rise to only homozygous iPSC clones (UKAi003-A), and the heterozygous (UKAi003-A2) and wild type ones (UKAi003-A1) were generated by CRISPR/Cas9 repair. In patient 3 with 25 % *JAK2* V617F allele burden in the PBMCs, only WT (UKAi013-A) and heterozygous (UKAi013-B) clones were obtained, and CRISPR/Cas9 was used to generate homozygous clones (UKAi013-B1; Supplement Table S1). Those iPSCs used in this study were kindly provided by Niclas Flosdorf (Department of Cell Biology, Institute for Biomedical Engineering, RWTH Aachen University Medical School, 52074 Aachen, Germany; Institute for Cell and Tumor Biology, RWTH Aachen University Medical School, 52074 Aachen, Germany) and generated in the group of Prof. Martin Zenke (Department of Cell Biology, Institute for Biomedical Engineering, RWTH Aachen University Medical School, Aachen, Germany; Department of Hematology, Oncology, Hemostaseology and Stem Cell Transplantation, Faculty of Medicine, RWTH Aachen University, 52074 Aachen, Germany).

iPSCs were cultured on tissue culture plastic (TCP) coated with vitronectin (0.5 mg/cm^2; Stemcell Technologies, Vancouver, Canada; this coating was used as standard coating) in StemMACS iPS-Brew XF (Miltenyi Biotec, Bergisch Gladbach, Germany) with 100 U/mL penicillin and 100 µg/mL streptomycin (both from Thermo Fisher Scientific), in the following referred to as iPSC medium. Cells were passaged at a confluency of about 70 % every three to four days by aspiration of the old medium, washing with PBS and dissociation with 0.5 mM EDTA. As soon

as iPSC colonies started to show fragmentation, EDTA was aspirated from cells and fresh medium was used to detach them from the plate with as little pipetting as possible to keep colony pieces as big as possible. The cell solution was then distributed with fresh iPSC medium onto freshly coated TCP plates in a ratio of 1:6 to 1:12 depending on the growth rate of different iPSC clones.

For cryopreservation of iPSCs, medium was aspirated, cells were washed with PBS and treated with Accutase (Stemcell technologies, Vancouver, Canada) for three to five minutes until cells started to detach from vitronectin coated TCP. Accutase treatment was stopped by addition of KnockOut-DMEM (KO-DMEM; Thermo Fisher Scientific) in a ratio of 1:2, all cells were washed from the well and centrifuged at 220 rcf for four minutes. The pellet was then carefully resuspended in Cryo-SFM (PromoCell, Heidelberg, Germany) supplemented with 10 µM ROCK inhibitor and cells were transferred to cryo vials. Cells were then frozen in a Mr. Frosty container and stored at -80°C for two days until they were transferred to liquid nitrogen for long-term storage. For usage of stored iPSCs, cryo vials were removed from the liquid nitrogen tank, the lid was slightly unscrewed to allow nitrogen to evaporate, and vials were then thawed at 37°C in a water bath until only a small ice cube was still visible. Then, cells were transferred to 10 mL of pre-warmed KO-DMEM and centrifuged at 220 rcf for four minutes. Afterwards, cells were resuspended in iPSC medium supplemented with 10 µM ROCK inhibitor and transferred onto freshly coated TCP. After 24 h medium was exchanged to iPSC medium without ROCK inhibitor.

2.1.7 Differentiation of *JAK2* V617F iPSC into hematopoietic lineage

Hematopoietic differentiation of iPSC clones was performed as described previously (Cypris et al., 2022). First, embryonic bodies (EBs) were generated in an alternative method and not in the classical ‘spin EB formation’ using microcontact printed vitronectin patches, as iPSCs should be formed via gradual self-assembly within iPSC colonies and at their transition into EBs. To print these patches onto 6-well plates, polydimethylsiloxane (PDMS) pillars with a diameter of 600 µm were generated according to a protocol established by Mohamed Elsafi Mabrouk (Stem Cell Biology, Helmholtz Institute for Biomedical Engineering, RWTH Aachen Medical School, Aachen, Germany) (Elsafi Mabrouk et al., 2022). For this, 6-well plates underwent air plasma treatment at 50 W for 30 seconds. 10 µg/mL vitronectin was pipetted on top of the PDMS pillars and incubated for 30 minutes at room temperature. The coated PDMS pillars were then used to print round vitronectin patches onto the plasma treated 6-wells for at least one minute. On these patterned coatings, iPSCs can grow and self-organize to embryoid body structures. iPSCs were cultured for at least two passages on matrigel, harvested as single cells with Accutase and 100,000 cells were seeded into each well of a microcontact printed 6-well plate (around 300-400 vitronectin spots per well) with StemMACS iPS Brew XF medium (Miltenyi Biotec) and 10 µM

ROCK inhibitor to form EBs. Self-detachment of EBs was observed after 6 to 9 days, depending on the clone.

EBs were slowly centrifuged at 15 rcf for three minutes and carefully resuspended in serum-free medium containing 50 % IMDM, 50 % Ham's F12, 1 % chemically defined lipid concentrate, 2 mM GlutaMAX (all Thermo Fisher Scientific), 0.5 % Albiomin (Unifols), 400 µM 1-thioglycerol, 50 µg/mL L-ascorbic acid, and 6 µg/mL holo transferrin (all Sigma Aldrich, St. Louis, MO, USA) supplemented with 10 ng/mL FGF-2 (Peprotech, Hamburg, Germany) and 10 ng/mL BMP-4 (Miltenyi Biotec). Approximately 30 to 50 EBs were distributed per well on a gelatin coated 6-well plate. From day 2 to day 7, cells were cultured in serum-free medium supplemented with 10 ng/mL FGF 2, 10 ng/mL BMP-4, 50 ng/mL SCF, 10 ng/mL VEGF-A (all Peprotech), and 10 U/mL penicillin/streptomycin (Thermo Fisher Scientific). From day 8 to day 16, serum-free medium was supplemented with 10 ng/mL FGF-2 and 50 ng/mL SCF only, Figure 12. Cells were harvested on day 16 and their immunophenotype was analyzed by flow cytometry, and stem cell potential with colony forming unit assays. Further cells were collected for DNA methylation analysis.

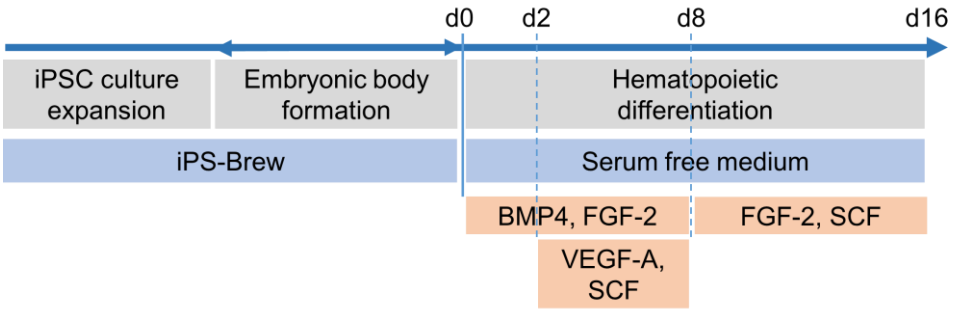

Figure 12. Scheme for hematopoietic differentiation of iPSCs.
Hematopoietic differentiation protocol. EBs were formed from iPSCs and differentiated toward the hematopoietic lineage.

2.2 Treatment with senolytic drug and telomerase inhibitor

To estimate the senolytic activity of the senolytic compounds on cellular subsets of healthy and MPN patients with *JAK2* V617F mutation, we cultured cells for three days at different concentrations and analyzed proliferation and viability. PBMCs were cultured in StemSpan Serum-Free Expansion Medium (Stemcell Technologies, Vancouver, Canada), supplemented with 10 ng/mL SCF, 20 ng/mL TPO, 10 ng/mL FGF-1 (all PeproTech, Hamburg, Germany), 10 µg/mL heparin (Ratiopharm, Ulm, Germany), and 100 U/mL penicillin/streptomycin (Lonza, Basel, Switzerland) for three days. Selected nine drugs (nine senolytic compounds and the telomerase inhibitor BIBR 1532) were tested for their impacts on cell viability. Senolytics treatment of blood samples of healthy individuals was supported by Michael Bleichert (Stem Cell

Biology, Helmholtz Institute for Biomedical Engineering, RWTH Aachen Medical School, Aachen, Germany).

For a comparative approach of these compounds, we estimated the half-maximal inhibitory concentration (IC50) in our culture setting and used one concentration above and one below IC50 (diluted water or DMSO, according to the manufacturer's instructions): nutlin-3a (10 μM (Hasegawa et al., 2009) and 50 μM, Selleck Chemicals LLC, Munich, Germany), JQ1 (10 μM (Miller et al., 2019), 20μM, Sigma-Aldrich), ABT263 (100 nM, 200 nM (Chen et al., 2015), Selleck Chem), piperlongumine (10 μM (Wang et al., 2016), 50 μM, Selleck Chem), S63845 (500 nM, 1μM (Li et al., 2019), Selleck Chem), RG7112 (10 μM (Makii et al., 2016), 50 μM, Selleck Chem), dasatinib combined with quercetin (20 μM (Zoico et al., 2021), 50 μM, both), AMG232 (1 μM (Sahin et al., 2020), 10 μM, Axon medchem, Groningen, Netherlands), and the telomerase inhibitor BIBR 1532 (50 μM (El-Daly et al., 2005), 100 μM, Selleck Chem). Alternatively, cells were cultured in a 24-well plate seeded with 250,000 cells/well (2 wells per condition) for DNA isolation. The effect of senolytics on the clonogenic potential was tested in the CFU medium during 14 days of culture.

While the drug concentrations used in this study may appear relatively high, particularly with regard to long-term treatment or *in vivo* applications, they were at a similar range as described by other studies (nutlin-3a, 10 μM (Hasegawa et al., 2009); JQ1, 1-10 μM (Miller et al., 2019); ABT263, < 1 μM (Chen et al., 2015); piperlongumine, 10 μM (Wang et al., 2016); S63845, 5 nM -1 μM (Li et al., 2019); RG7112, 2.5- 5 μM (Makii et al., 2016); dasatinib (D) + quercetin (Q), 20 μM D + 15 μM Q, (Schafer et al., 2017); AMG232, 1 μM (Sahin et al., 2020); and BIBR 1532, 50 μM (El-Daly et al., 2005)). However, at these concentrations some of the compounds may have other effects beyond senolytics.

2.3 Cell phenotyping

2.3.1 Senescence associated beta-galactosidase (SA-β-gal) assay

As a surrogate marker for senescence, we stained PBMCs and CFUs for β-galactosidase (Senescence Detection Kit; Abcam, Cambridge, UK). PBMCs and CFUs were centrifuged and washed once with PBS, stained with β-gal, and incubated 37 °C at least overnight. Cells were then observed under a microscope (Leica DMRX microscope, Leica Microsystems, Wetzlar, Germany).

As a surrogate marker for senescence, we used fluorescent based assays for quantification of the senescence phenotype in both MPN patients (n = 7) and healthy donors (n = 6; one outlier was removed). For that, PBMCs were pre-treated with 100 nM bafilomycin A1

(Medchemexpress, New Jersey, USA) for one hour and subsequently treated with 33 µM 5-dodecanoylaminofluorescein di-β-D-galactopyranoside (C12FDG, Abcam) for two hours at 37°C. C12FDG is a substrate for β-gal enzyme. Any normal cell that is treated with the C12FDG substrate will exhibit green fluorescence due to the high activity of β-gal in the lysosome at pH 4.0. To distinguish senescent cells, which have a higher concentration of β-gal enzyme, the initial pH within the cell was increased to 6.0 by the addition of bafilomycin A, after which C12FDG was added (Debacq-Chainiaux et al., 2009). The substrate emits bright fluorescence after cleavage by the enzyme, which enabled the detection of senescent cells. Following this, PBMCs were further collected, washed with PBS, and stained with anti-CD34-APC (BD Biosciences) at a dilution of 1:100 for 30 minutes at 4°C. Subsequently, cells were washed with PBS containing 2 % FCS and measured by flow cytometry using a FACS Canto II (BD Biosciences, New Jersey, USA). PBMCs were selected based on their size and granularity by setting the gates for forward scatter (FSC) versus side scatter (SSC), excluding dead cells and cellular debris. Further doublets were excluded by gating FSC-H vs. FSC-A, and β-gal activity was estimated using FITC gate for the green fluorescent signal. The senescent cell population was analyzed using FlowJo software, version 10.4.2 (FlowJo LLC).

2.3.2 Immunophenotypic analysis

Flow cytometric analysis was performed on a FACS Canto II (BD Biosciences) and analyzed with FlowJo software. Antibody staining was performed in MACS-buffer solution (PBS with 2 % FCS and 2 mM EDTA). Incubations were performed on ice for at least 30 min. The following antibodies were used for hematopoietic differentiated cells from iPSCs: CD31-PE (clone WM59), CD34-APC (clone 581), CD43-FITC (clone 1G10) (all BD Biosciences), CD235a-PE (1:1,000; clone HIR2/GA-R2), CD117-cKIT-PE-Cy7 (clone 104D2), (all Thermo Fisher Scientific), CD45-APC-Vio770 (clone 5B1), CD33-APC (clone AC104.3E3) (all Miltenyi Biotec), and CD61-FITC (clone VI-PL2, Biolegend). All antibodies were used in a dilution of 1:100 if not stated otherwise. The following antibodies were used for PBMC from healthy samples: CD34-APC (clone 581), CD45-APC-Vio770 (clone 5B1), CD45-V500 (clone HI30), CD3-FITC (clone SK7), CD14-APC-Cy7 (MφP9), CD56-PE-Cy7 (B159) and CD19-PE (4G7) (all BD Biosciences). After staining, cells were washed with MACS buffer and centrifuged. Pellets were resuspended in 200 µL MACS buffer and measured at the flow cytometer. Compensation was performed with beads (Thermo Fisher Scientific) which were treated with antibodies equivalent to cells but with only one antibody per tube. Gates were set to identify cells as follows: (FSC-A/SSC-A), forward scatter singlets (FSC-H/FSC-A), and the antibody of interest.

2.3.3 Genotyping of single CFU colonies

DNA was extracted from individual colonies using the Monarch® PCR & DNA Cleanup Kit (New England Biolabs, Frankfurt, Germany) according to the manufacturer's instructions. To

determine the mutation status of *JAK2* and *CALR*, allele specific PCRs were performed for *JAK2* V617F and CALRins5 (Table 1), as previously described (Kalmer et al., 2022). Genotyping of the CFU colonies were supported by Milena Kalmer and Margherita Vieri (Department of Hematology, Oncology, Hemostaseology and Stem Cell Transplantation, Faculty of Medicine, RWTH Aachen University, 52074 Aachen, Germany).

Table 1. Primer list for the genotyping of single CFU colonies.

Primer	Sequence
CALRdel52 Frw	ACAACTTCCTCATCACCAACG
CALRdel31 Rev	GGCCTCAGTCCAGCCCTG
CALRins5 common Frw	TAACTGCAGTGTCAGCGGTG
CALRins5 non-mutated allele Rev	TGTCCTCATCATCCTCCTTG
CALRins5 mutant Rev	TGTCCTCATCATCCTCCGAC
JAK2 V617F Frw	TCCTCAGAACGTTGATGGCAG
JAK2 V617F Rev	GTTTTACTTACTCTCGTCTCCACAAAA
JAK2 WT Frw	GCATTTGGTTTTAAATTATGGAGTATATG
JAK2 Rev	ATTGCTTTCCTTTTTCACAAGAT

Abbreviations: Frw: forward; Rev: reverse

2.3.4 Cytospin and Diff-Quik staining of single CFU colonies

Characterization of CFU colonies after cytospinning was performed using a Diff-Quik staining. Diff-Quik staining is a variant of the Romanowsky stain that allows the distinction of hematopoietic cell types. The solutions contain acidic and basic dyes that stain different cellular compartments based on their ionic charge. In this work, cells were additionally stained for benzidine that allows the visualization of hemoglobin in erythrocytes (Radke et al., 1982). Suspension cells were applied on objective slides by a special centrifugation technique called cytospin. The cytospin chamber consists of a funnel, a filter card and a glass slide that are clamped together. The filter card was wetted with PBS attached to the chamber and subsequently centrifuged at 270 rpm for 5 minutes in a Cytospin™ 4 cytocentrifuge (Thermo Fisher Scientific). Cell suspensions (500 cells/µL) were applied to the funnel and centrifuged. The objective slide with cells were air-dried and fixed in methanol (VWR, Radnor, Pennsylvania, United States) for 4 minutes, before incubating in 1 % benzidine solution (Merck-Millipore, Massachusetts, USA) for 2 minutes. Slides were then incubated in 30 % H_2O_2 solution (Merck-Millipore) for 90 seconds, followed by washing in H_2O for 30 seconds and air drying. Slides were then dipped 5× in Diff-Quik solution I for 5 seconds followed by 30 seconds incubation in Diff-Quik solution II (both Merck-Millipore). After final washing of the slides in H_2O and air-drying, stained slide was sealed with Entallan (Merck-Millipore) and a cover slip. Images were captured with Leica DMRX microscope using the Leica application software suite v3.1.10 (both Leica).

2.3.5 Viability assay

Cell viability of PBMCs was analyzed after three days of culture in SFM medium supplemented with drugs in 24 well plates. Cells were incubated for 4 - 5 minutes with 10 µg/mL fluorescein diacetate (FDA; Sigma Aldrich, St. Louis, USA) and 20 µg/mL propidium iodide (PI*; Life Technologies, Carlsbad, USA), in culture medium, and immediately imaged with an EVOS FL microscope. Viable cells were stained with FDA due to esterase activity hydrolyzing the diacetate group, while propidium iodide intercalated in double stranded DNA of dead cells as a result of the porous membrane.

In addition, cell viability of senolytic treated PBMCs was measured with Cell Titer-Glo 2.0 luminescent cell viability assay (Promega, Wisconsin, USA), according to the manufacturer's protocol. In brief, cells were seeded in 96-well plates with 10,000 cells/well (3 wells per condition) for three days. After that, 100 µl of substrate was added to the cells (1:1). The cells were then transferred to white 96-well plates for luminescence measurement. The assay allows the determination of viable cells in culture based on the presence of ATP in the cells. Following cell lysis, the released ATP drives the catalysis of luciferin to oxyluciferin by luciferase. This reaction releases a luminescence signal that was measured using BioTek Synergy 2 plate reader and Gen5 software (Agilent Technologies, California, USA).

2.4 DNA analysis

2.4.1 Epigenetic age prediction with targeted bisulfite amplicon sequencing

Genomic DNA was isolated from cryopreserved whole blood cells after red blood cells depletion with the QIAamp DNA Mini Kit (Qiagen, Hilden, Germany), or for colonies in the CFU assay with NucleoSpin XS Tissue Kit (Macherey-Nagel, Düren, Germany). DNA was quantified with a Nanodrop 2000 Spectrophotometer (Thermo Scientific, Wilmington, USA) and bisulfite converted with the EZ DNA Methylation Kit (Zymo Research, Irvine, USA). For targeted bisulfite amplicon sequencing (BA-seq) three age-associated CG dinucleotides (CpG sites) that are associated with the coiled-coil domain-containing protein 102B (*CCDC102B*), four and a half LIM domains protein 2 (*FHL2*), and phosphodiesterase 4C (*PDE4C*) were amplified using the PyroMark PCR kit (Qiagen) with primers with handle sequences for the subsequent barcoding step (Table 2), as described in detail before (Han et al., 2020). PCR conditions are summarized in Table 3. The three amplicons of each donor were pooled at equal concentrations, quantified with the Qubit (Invitrogen, Massachusetts, USA), and cleaned up with paramagnetic beads (Agencourt AMPure PCR Purification system; Beckman Coulter, California, USA). Four microliters of PCR products were subsequently added to 21 µL PyroMark Master Mix (Qiagen) containing 0.4 µM of barcoded primers (adapted from NEXTflexTM 16S V1-V3 Amplicon Seq

Kit, Bioo Scientific, Austin, USA) for a second PCR. PCR products were again quantified with the Qubit, combined in equimolar ratios, and cleaned by Select-a-Size DNA Clean & Concentrator Kit (Zymo Research). A 12-pM DNA library was diluted with 15 % PhiX spike-in control and eventually subjected to 250 bp pair-end sequencing on a MiSeq lane using the Miseq reagent V2 Nanokit (both from Illumina).

Table 2. Primer sequence for BA-seq for PCR1 with handle sequence.

Primer Name	Target site	Sequence 5' → 3'
CCDC102B For	cg19283806	CTCTTTCCCTACACGACGCTCTTCCGATCTAGTGGGGTAAGTATATGATATAAGGGAGGAAATA
CCDC102B Rev		CTGGAGTTCAGACGTGTGCTCTTCCGATCTCAAACCAATAATATCTATATCATCAACATTTCT
FHL2 For	NA	CTCTTTCCCTACACGACGCTCTTCCGATCTTTTAGTGTTTTTAGGGTTTTGGGAGTATAGTAGTT
FHL2 Rev		CTGGAGTTCAGACGTGTGCTCTTCCGATCTCCTCCTAAAAAATAACCCCCTCCTCCCT
PDE4C For	NA	CTCTTTCCCTACACGACGCTCTTCCGATCTTATGGAGAATTTGGGG
PDE4C Rev		CTGGAGTTCAGACGTGTGCTCTTCCGATCTCTACAAAAAACCCCTACC

NA: neighboring CpG was used, which is not included on the Illumina BeadChip. for – forward, rev. – reverse

Table 3. PCR conditions for bisulfite barcoded amplicon sequencing.

Step	PCR1 (CCDC102B and FHL2)			PCR1 (PDE4C)			PCR2		
	Temp.	Time	Cycles	Temp.	Time	Cycles	Temp.	Time	Cycles
Enzyme activation	95 °C	15 min		95 °C	15 min		95 °C	15 min	
Denaturation	95 °C	30 sec		95 °C	35 sec		95 °C	30 sec	
Annealing	56 °C	30 sec	40x	53 °C	35 sec	35x	60 °C	30 sec	16x
Extension	72 °C	30 sec		72 °C	35 sec		72 °C	30 sec	
Final extension	72 °C	10 min		72 °C	10 min		72 °C	10 min	
Hold	4 °C	∞		4 °C	∞		4 °C	∞	

For PCR1, 1.5 mM MgCl2 was used for CCDC102B, 0.5 mM for PDE4C and no MgCl2 for FHL2. In PCR2, 1.5mM of MgCl2 was used.

FastQ files from MiSeq analysis were aligned to the reference genome hg19 using the Bismark tool (Krueger & Andrews, 2011) and DNA methylation values determined with the Bismark methylation extractor. For heatmaps, the frequencies of DNA methylation patterns in individual reads were calculated by the number of reads containing the pattern divided by the total number of reads of the target region per sample. The most abundant reads of similar patterns within neighboring CpGs were grouped for visualization with Python's package seaborn (Michael Waskom, 2016). Epigenetic age was calculated as follows:

$$\textit{Predicted age (in years)} = 3.86 + 0.825\ DNAm^{FHL2} - 0.342\ DNAm^{CCDC102B} + 1.177\ DNAm^{PDE4C}$$

Alternatively, epigenetic age predictions were based on the binary sequel of methylated and non-methylated CpGs within individual reads of BA-seq data, as described in our previous study (Han et al., 2020). The analysis of Miseq data was performed by Miloš Nikolić (Stem Cell Biology, Helmholtz Institute for Biomedical Engineering, RWTH Aachen Medical School, Aachen, Germany).

2.4.2 Epigenetic age prediction with pyrosequencing

Pyrosequencing was used for fast and robust epigenetic age predictions of mouse bone marrow cell pellets and peripheral blood mononuclear cells (PBMCs) from patients and healthy donors after senolytic drug treatment *in vitro*. For mouse epigenetic age, DNA methylation was measured at the three age-associated CpG sites in Proline rich membrane anchor 1 (*Prima1*), Heat shock transcription factor 4 (*Hsf4*) and Potassium voltage-gated channel modifier subfamily S member 1 (*Kcns1*), using primers mentioned in Table 5, as described in our previous work (Han et al., 2018) and updated by selecting neighboring CpGs for the Prima1 region. PCR was performed using the PyroMark PCR kit (Qiagen), conditions are summarized in Table 4. Pyrosequencing was then performed on the PyroMark Q48 Autoprep system (Qiagen) using the PyroMark Q48 Advanced Reagent Kit. The results were analyzed using PyroMark Q48 Advanced software. Epigenetic age was calculated as follows:

$$Predicted\ age\ (in\ weeks) = -6.325 - 0.308\ DNAm^{Prima1} + 2.588\ DNAm^{Hsf4} + 1.003\ DNAm^{Kcns1}$$

Matthis Schnitker, Michael Bleichert and Miriam DM Sarvaas (Stem Cell Biology, Helmholtz Institute for Biomedical Engineering, RWTH Aachen Medical School, Aachen, Germany) supported the pyrosequencing measurements by helping with DNA isolation, bisulfite conversion, PCR or Q48 measurements.

Table 4. PCR conditions for pyrosequencing for age-associated regions for human and mouse.

Step	PCR (*CCDC102B* and *FHL2*)			PCR (*PDE4C*)			PCR (*Kcns1, Hsf4* and *Prima1*)		
	Temp.	Time	Cycles	Temp.	Time	Cycles	Temp.	Time	Cycles
Enzyme activation	95 °C	15 min		95 °C	15 min		95 °C	15 min	
Denaturation	95 °C	30 sec		95 °C	3 sec		95 °C	30 sec	
Annealing	56 °C	30 sec	50x	52.9 °C	35 sec	50x	58 °C	30 sec	50x
Extension	72 °C	30 sec		72 °C	35 sec		72 °C	30 sec	
Final extension	72 °C	10 min		72 °C	10 min		72 °C	10 min	
Hold	4 °C	∞		4 °C	∞		4 °C	∞	

1.5 mM $MgCl_2$ was used for mouse age specific primers *Kcns1*, *Hsf4* and *Prima1*.

For human samples that were treated with senolytic compounds, we analyzed for DNAm changes at the same age-associated CpGs of *PDE4C*, *CCDC102B*, and *FHL2*, using primers

mentioned in Table 5 and PCR conditions summarized in Table 4, as described in detail before (Han et al., 2020). Epigenetic age was calculated as follows:

Predicted age (in years) = 8.21 + 0.91 $DNAm^{FHL2}$ – 0.68 $DNAm^{CCDC102B}$ + 0.78 $DNAm^{PDE4C}$

Table 5. Primer sequence for pyrosequencing assays for human and mouse aging.

Primer Name	Target site	Sequence 5' → 3'
CCDC102B For	cg19283806	TGTTGAGGGAGGGGAATGTTTGTATTTAT
CCDC102B Rev		Biotin-CCAATAATATCTATATCATCAACATTTCTACAACTT
CCDC102B Seq		GGAGGGGAATGTTTG
FHL2 For	cg22454769	GTGTTTTTAGGGTTTTGGGAGTATAGTAGT
FHL2 Rev		Biotin-CACCTCCTAAAACTTCTCCAATCTCC
FHL2 Seq		GGTTTTGGGAGTATAGTAGTT
PDE4C For	NA	AGGTTTGTAGTAGGTTGAG
PDE4C Rev		Biotin-AACTCAAATCCCTCTC
PDE4C Seq		GTTATAGTATGATTAGAGTTT
Prima1 For		TTGTGTTTAATTAGGAGAGGTAAATTATGAATTAGGTTTATA
Prima1 Rev		Biotin-CAAAATTAATTACACCAACTTATAACCTACTATTC
Prima1 Seq		AATTATGAATTAGGTTTATATTT
Hsf4 For		GTGAGTAGTAAGGTGGGATAAATTGTAGAAAAAATG
Hsf4 Rev		Biotin-TCCCTACTCTCCTACACTCCTCTCAAAACTTA
Hsf4 Seq		ATTGTAGAAAAAATGGGAA
Kcns1 For		GGTTGAGAGGGTGGTAGAAGAAGTTG
Kcns1 Rev		Biotin-ACTCCCCTCCATCCCTACCATATACATCCA
Kcns1 Seq		GAAGATATTTAGAAGTTGAATT

NA: neighboring CpG was used, which is not included on the Illumina BeadChip. for – forward, rev. – reverse

2.4.3 DNA methylation analysis using BeadChip data

For iPSC and iPSC-derived hematopoietic cells the above-mentioned targeted signatures for epigenetic age-prediction could not be applied, because they were specifically trained for primary hematopoietic cells. Also, to further study the global comparison of DNA methylation the Illumina human EPIC methylation microarray at Life and Brain (Life and Brain GmbH, Bonn, Germany) was used. For that purpose, genomic DNA was isolated from nine iPSC clones and their iPSC-derived hematopoietic differentiated cells and also from the peripheral blood of ten PMF patients and ten healthy donors with the QIAamp DNA Mini Kit (Qiagen, Hilden, Germany), and bisulfite converted and hybridized with the Illumina human EPIC methylation microarray. iPSC and iPSC-derived DNA methylation profiles were generated on EPICv1 and patient derived samples using EPICv2 platforms. EPICv1 provides methylation values at more than 850,000 CpG sites, and EPICv2 with over 935,000 CpG sites and sharing between both about 722,000 CPGs. The analysis of DNA methylation data from Illumina BeadChip was performed in R (4.3.0) (R Core Team, 2022). Raw data (.IDAT files) of both datasets were independently preprocessed using the SeSAMe package for R v1.18.4 (Zhou et al., 2018), in the following order: quality masking the probes with poor design, reset the color channel for Type-I probes inference, non-linear dye

bias correction, detection of p-value using out-of-band (OOB) array hybridization, and background correction. Additionally, CpGs at the X and Y chromosomes were removed and also the probes with failed detection P values in three or more samples, with resulting in 630,700 CpGs. Furthermore, we only considered CpGs that were represented by the EPICv1 and EPICv2 BeadChip platforms for the comparison analysis of patient derived samples and iPSC derived samples, with resulting in 590,349 CpGs. The limma R package (3.56.2) was used for calculation of Benjamini-Hochberg adjusted p values and the multidimensional scaling plots (MDS plot). Relevant DNAm changes were defined as showing at least 10-20 % difference in mean beta values and an adjusted p value ≤ 0.05. For gene ontology (GO) analysis the R package missMethyl (1.34.0) was used. The R packages: watermelon, ggplot2, ggrepel, ggbeeswarm, reshape2, ggExtra, gprofiler2, ComplexHeatmap, and VennDiagram were used for graphical presentation.

2.4.4 Telomere length measurements

Telomere lengths were determined via two methods: Flow-fluorescent in situ hybridization (flow-FISH) (Ferreira et al., 2020; Rufer et al., 1999): and Telomere PCR (TEL-PCR) (Rolles et al., 2021).

Cryopreserved whole blood cells after red blood cell depletion were used for the flow-FISH analysis of telomere length (TL) in lymphocytes and granulocytes, as previously described (Ferreira et al., 2020). Briefly, samples were prepared for cell denaturation and mixed with a telomere-specific (CCCTAA)3-peptide nucleic acid FISH probe labeled with FITC (Eurogentec, Liège, Belgium) for DNA hybridization. DNA counterstaining was performed with LDS 751 (Sigma-Aldrich, Missouri, USA). Granulocytes and lymphocytes were stained by LDS 751 and can be distinguished by signal intensities in both the FL-3 channel as well as in the forward scatter (FSC). TL of bovine thymocytes were determined by Western blot (19.515 kb) and used as a reference to convert the TL of granulocytes and lymphocytes into kb. An FC 500 flow cytometer (Becton Dickinson, East Rutherford, USA) was used for data acquisition. All measurements were carried out in triplicates. Healthy controls (n = 134) were used for age adaptation of TL.

TEL-PCR was used for TL measurement in colony forming units (CFUs), iPSCs before and after hematopoietic differentiation and in mouse bone marrow-derived cells. 1.4 ng of genomic DNA per reaction was used in the Absolute Human TL Quantification qPCR Assay Kit (ScienCell, Carlsbad, USA) and FastStart Essential DNA Green Master (Roche, Basel, Switzerland). TL measurements are given in T/S ratios. A T/S ratio is calculated by dividing the number of copies of the telomere template (T) by the single copy reference (SCR) template (S), which is an amplified 100 bp region on human chromosome 17. The TL q-RT-PCR was performed according

to the manufacturer's instructions. Telomere length experiment and the analysis was performed by Margherita Vieri.

2.4.5 Analysis of mutational burden

A clinically validated amplicon-based next-generation sequencing (NGS) panel (Truseq Custom Amplicon Kit, Illumina, San Diego, USA) was used to analyze the coding region of 32 genes that typically harbor mutations associated with hematologic malignancies, as described previously (Kirschner et al., 2018; Olschok et al., 2021). Variants were reviewed manually, using a bidirectional frequency of >1 % for driver mutations and > 5 % for additional mutations as cutoffs. This was done by the genomic facility of Uniklinik Aachen, while receiving the patient samples.

Alternatively, the *JAK2* V617F allele burden was analyzed with digital droplet PCR (ddPCR) using the mutation assay dHsaMDV27944642 from Bio-Rad, according to the manufacturer's instructions. This could be used as an alternative method where the unparalleled accuracy and precision of the result, the specificity of an information make it an effective tool. In brief, each PCR reaction sample is partitioned into 20,000 nanoliter sized droplets and each of the droplets is measured as a single PCR reaction that leads to an increased precision for rare mutation detection with less the 1 % changes. Quantification of the mutation burden was performed on a QX200 ddPCR (Bio-Rad Laboratories, Inc., Hercules, CA, USA) by 25 ng of DNA was added per reaction with the 2x ddPCR supermix for probes (no dUTP) containing a hot start polymerase. 20 µL ddPCR reaction mix was loaded inside the middle well of the disposable eight channel droplet generator DG8 cartridge of the QX200 (Bio-Rad). 70 µL of the droplet generation oil for probes containing the emulsion stabilizing surfactant was then loaded to the bottom wells. The loaded cartridge was covered with the gasket and the droplet was generated in the upper well using the QX200 droplet generator (Bio-Rad). 40 µL of the droplet suspension from the upper well of the cartridge were transferred to the ddPCR deep-well 96-well plates. The plate was sealed with the heat seal foil at 180°C for 5 seconds in the PX1 PCR plate sealer and further processed with the C1000TM Touch 96-Deep Well thermal cycler (Bio-Rad).

2.5 RNA analysis

2.5.1 Senescence associated gene expression analysis using RT-qPCR

To estimate gene expression of three senescence-associated genes (p16, p21, and p53) RNA was isolated from 500,000 cells/well (two 12-wells per condition) with the NucleoSpin RNA, Mini Kit (Macherey-Nagel, Düren, Germany) according to manufacturer's protocol. RNA was quantified with a Nanodrop 2000 Spectrophotometer (Thermo Scientific, Wilmington, USA). 250 ng of RNA was used for cDNA synthesis using the High-Capacity cDNA Reverse Transcription Kit (Applied Biosystems™, Waltham, USA). Quantitative real time (qRT)-PCR was carried out

using TaqMan™ gene expression master mix (Applied Biosystems™, Waltham, USA) and gene-specific TaqMan assays (all from Applied Biosystem, Waltham, USA) in a StepOnePlus™ machine (Applied Biosystems™, Waltham, USA). The PCR conditions were 50°C for 2 min, 95°C for 10 min, followed by 40 cycles at 95°C for 15 sec and 60°C for 1 min. TaqMan assays for p16 (HS_00923894_m1), p21 (HS_00355782_m1) and p53 (HS_01034249_m1) were analyzed. The mRNA expression level of the target gene was normalized using GAPDH (Hs02758991_g1) as housekeeping gene.

2.5.2 Analysis of genes associated with senescence in the microarray data

Gene expression profiles from 6 healthy donors, 6 ET, 11 PV and 9 PMF patients were published by Baumeister, J et al. in GSE174060 (Baumeister, Maie, et al., 2021) and used for senescence pathway analysis (Saul et al., 2022). Significantly differentially regulated genes were selected by a Benjamini–Hochberg adjusted p value <0.05 and log2-fold changes above 0.5 or below −0.5. Enrichment of senescence-associated genes was estimated with hyper geometric distribution analysis.

2.5.3 Statistics

Linear regressions, mean absolute deviation (MAD), and mean absolute error (MAE) of age-predictions were calculated with Excel. Statistical analysis was performed with GraphPad Prism using one sample t-test, unpaired t-test, paired t-test, or one-way ANOVA. P values ≤0.05 were considered as indicative of statistical significance. IC50 values were calculated by nonlinear regression analysis using GraphPad Prism, version 6.

3. Results

3.1 Cellular age in healthy individuals

The aim of this study was to compare the epigenetic age of healthy young and old individuals using different age-associated biomarkers, including epigenetic age, and senescence by analyzing PBMC samples. Furthermore, we aimed to determine if a three-day treatment of human blood samples *in vitro* would reduce these age-associated biomarkers.

3.1.1 Epigenetic age and telomere length in healthy samples

To further explore the healthy human aging, epigenetic age predictions were measured using DNAm patterns with BA-seq at three age-associated genomic regions in the *CCDC102B*, *FHL2* and *PDE4C* genes. We have recently described BA-seq for nine CpGs that provide robust and reliable age predictions (Han et al., 2020). To further ease applicability of the method, we have meanwhile refined the signature to focus on the three regions with the highest correlation with chronological age and on a combination of hyper- and hypo methylated CpGs to reduce the PCR bias. Epigenetic age predictions were measured with blood samples of 128 healthy donors (74 males and 54 females) aged 18-74 years, showing a mean age deviation (MAD) of only 0.8 years, and a correlation with chronological age of R^2 = 0.86 (Figure 13a). This correlation is relatively high compared to our previous models (Han et al., 2020) and with a very low mean age deviation. In addition, flow-FISH analysis of telomere length (TL) in granulocytes revealed a clear association with chronological age in 134 healthy donors, albeit the correlation was lower than for epigenetic age predictions (R^2 = 0.18; Figure 13b). TL measurement was performed by Margherita Vieri (Vieri et al., 2023).

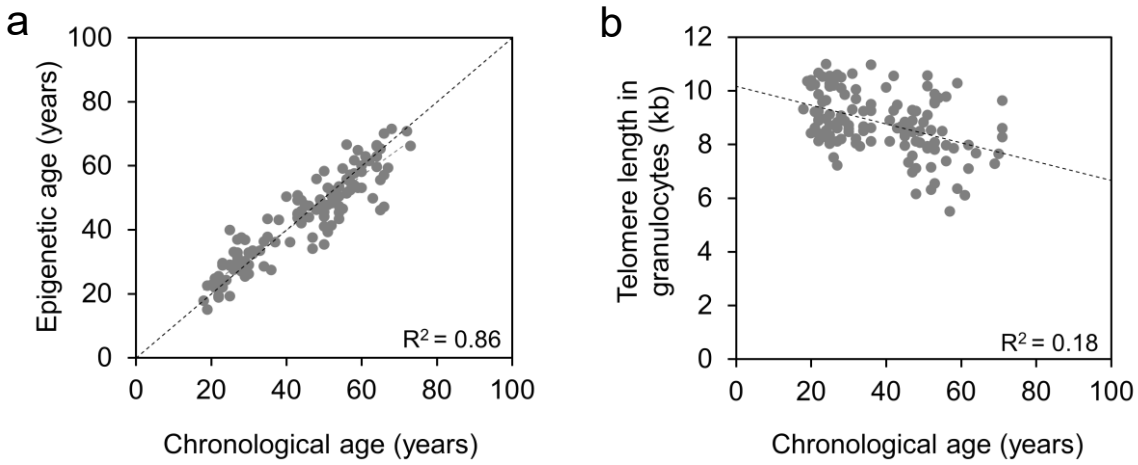

Figure 13. Cellular aging prediction model for healthy blood samples.
a) Correlation of chronological age and epigenetic age predictions by bisulfite barcoded amplicon sequencing (BA-seq) of three CpGs in healthy donors (n = 128) was shown. b) Telomere length (TL, in kb) was measured in granulocytes via flow-FISH in healthy donors, as described before (n = 134) (Vieri et al., 2023).

3.1.2 Heterogeneity of aging in old versus young

The epigenetic age clock has been shown to predict a person's age across all age groups. It is a well-known phenomenon that cellular aging exhibits heterogeneity, meaning that a given sample consists of epigenetically younger and older cells.

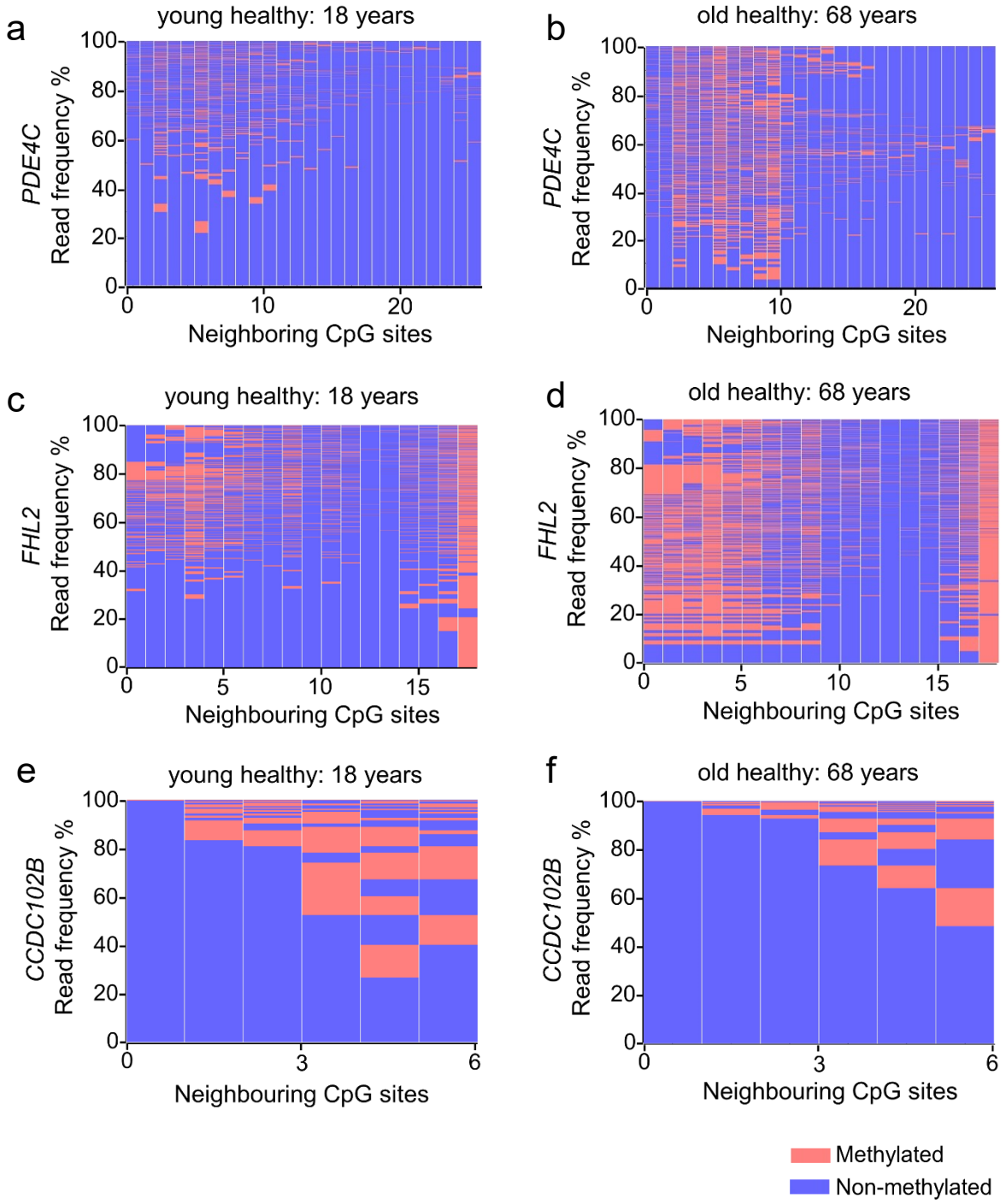

Figure 14. Heterogeneity of age-associated DNA methylation in healthy samples.
Heat map depicts exemplarily the frequencies of DNAm patterns within the neighboring CpGs of the *PDE4C* amplicon in BA-seq data of a) a healthy donor of young age (18 years) and b) a healthy donor of old age (68 years). Furthermore, exemplary heatmaps were also shown for the *FHL2* (c, d) and *CCDC102B* amplicon (e, f).

To better understand the discrepancies in age, we analyzed the DNAm patterns of age-related regions using BA-seq method. This approach was used to consider not only the average DNAm level in a CpG site of interest, but also the DNA methylation state of each individual DNA strand and all neighboring CpGs of the target assay, thereby mimicking single cell resolution. We observed differences between young and old individuals (exemplified for one donor in Figure 14), with the pattern becoming more heterogeneous with increasing age. *FHL2* and *PDE4C* exhibited a gain of methylation with age and showed aberrant methylation in many CpGs in old adults. In contrast, at least 20 % of the regions remained homogeneously unmethylated at younger ages. *CCDC102B*, which loses methylation with age, also does not completely lose methylation at one site, but gradually loses all neighboring CpGs and retains heterogeneity. Nevertheless, the patterns of neighboring CpGs are quite heterogeneous and no obvious clonal DNAm pattern was observed among old or young. This analysis of BA-seq data was supported by Miloš Nikolić.

Cellular aging becomes more complex and heterogeneous as cells accumulate DNA repair errors with age. In order to more accurately quantify the heterogeneous DNA methylation patterns, the n-score was calculated. This score indicates the absolute discrepancy within the target of interest, calculated by the sum of absolute difference between neighboring CpG sites, reflecting how much the DNAm levels change within the amplicons (Eipel et al., 2019). The n-scores for *PDE4C* and *FHL2* were significantly increased with age in healthy samples, which is due to the fact that these regions become more methylated with increasing age. On the other hand, the n-score for *CCDC102B* decreased with age, indicating that this region becomes less methylated with age (Figure 15).

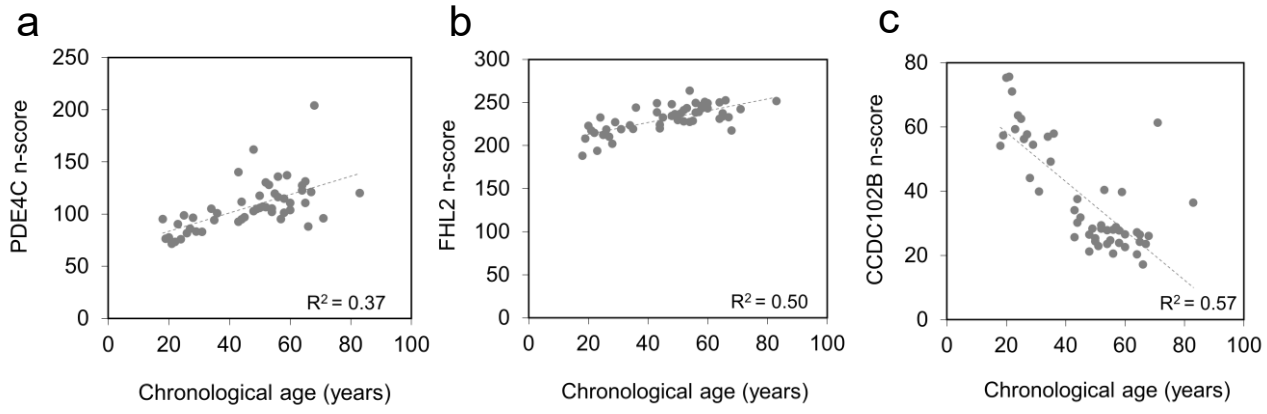

Figure 15. n-score for three age-associated region in healthy samples.
Aberrant DNAm at age-associated CpGs often shows non-coherent DNAm levels at neighboring CpGs sites. This was exemplified by the n-score (Eipel et al., 2019) for the a) *PDE4C*, b) *FHL2,* and c) *CCDC102B* amplicons, which showed a correlation with the chronological age of healthy controls.

3.1.3 Senescence in healthy samples

Cellular senescence is another factor contributing to the process of aging. It has been known that the accumulation of senescent cells increases with age (Di Micco et al., 2021). We used 5-dodecanoylaminofluorescein di-β-D-galactopyranoside (C12FDG), a substrate for the β-Gal enzyme, to measure senescent cells in healthy PBMC cells (n = 9 young ≤45 years and n = 10 old > 45 years). This β-Gal staining was quantified by the green fluorescent signal using flow cytometry. There was an increased tendency towards senescent cells with age in both PBMCs and specifically, lymphocytes (Figure 16a and b, respectively). Nevertheless, the observed differences were not statistically significant. Furthermore, the analysis of senescent cells with a higher intensity for C12FDG fluorescence, as illustrated in Supplemental Figure 1a and as previously described (Arora et al., 2021; Hambright et al., 2024), showed a similar trend with age to that observed in the C12FDG percentage (Figure 16d, e, and f). Exemplarily, the percentage of C12FDG in samples from individuals aged 29 and 61 years was shown to have distinct differences in the percentage of C12FDG cells, although this was not a consistent trend for all samples (Supplemental Figure 1b).

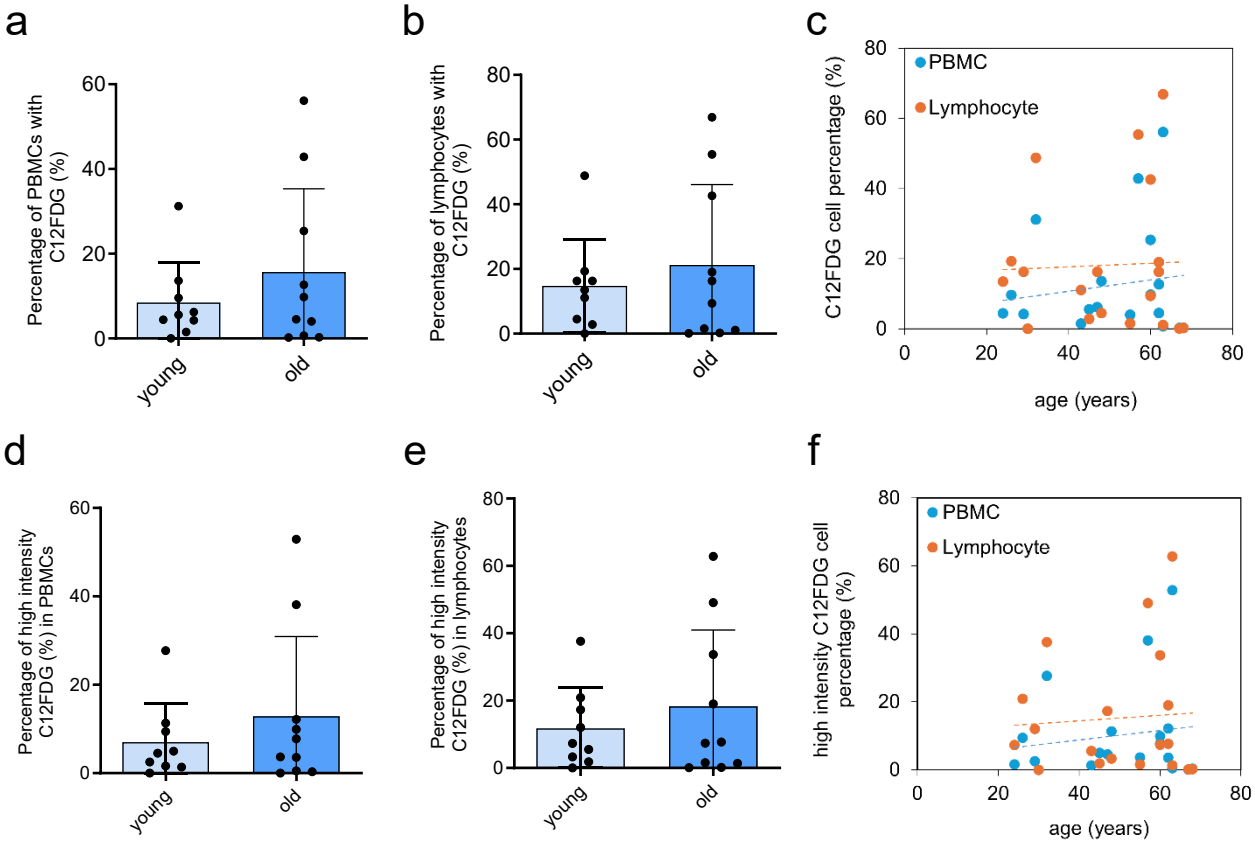

Figure 16. Senescence expression was slightly higher in older adults compared to younger adults. The percentage of senescent cells with C12FDG staining showed a trend towards older adult derived a) PBMCs and b) lymphocytes. c) In addition, the correlation between C12FDG percentage and chronological age was shown. Further, the percentage of high intensity C12 FDG percentage in both d) PBMCs and e) lymphocytes showed a similar trend with older individuals above 45 years. f) The correlation between high intensity C12FDG percentage and chronological age was shown.

3.1.4 Senolytic treatment in healthy samples *in vitro*

The hypothesis of using senolytic drugs to eliminate unwanted senescent cells by various anti-aging mechanism has been primarily studied in mice and cultured cells exposed to specific factors that induce senescence, including irradiated with UV or ionizing radiation or other substances (Di Micco et al., 2021). However, our focus was to study the naturally accumulated senescent cells in healthy young and old blood. To address this question, we cultured PBMCs for three days with nine different senolytic drugs that are thought to specifically target senescent cells: piperlongumine, ABT263, RG7112, nutlin-3a, dasatinib in combination with quercetin (D+Q), AMG232, JQ1 and S63845. A concentration-dependent cell viability assay was performed to determine the IC50 (Figure 17). PBMCs from healthy samples with different ages of 24, 31, 48 and 68 years were treated with each drug, and two concentrations were selected: one below and one above the IC50 (indicated as low and high concentration). The inclusion of two concentrations around IC50 facilitated an expansion of the effective concentration window and enhanced the probability of capturing a diverse range of donors with inherent variability.

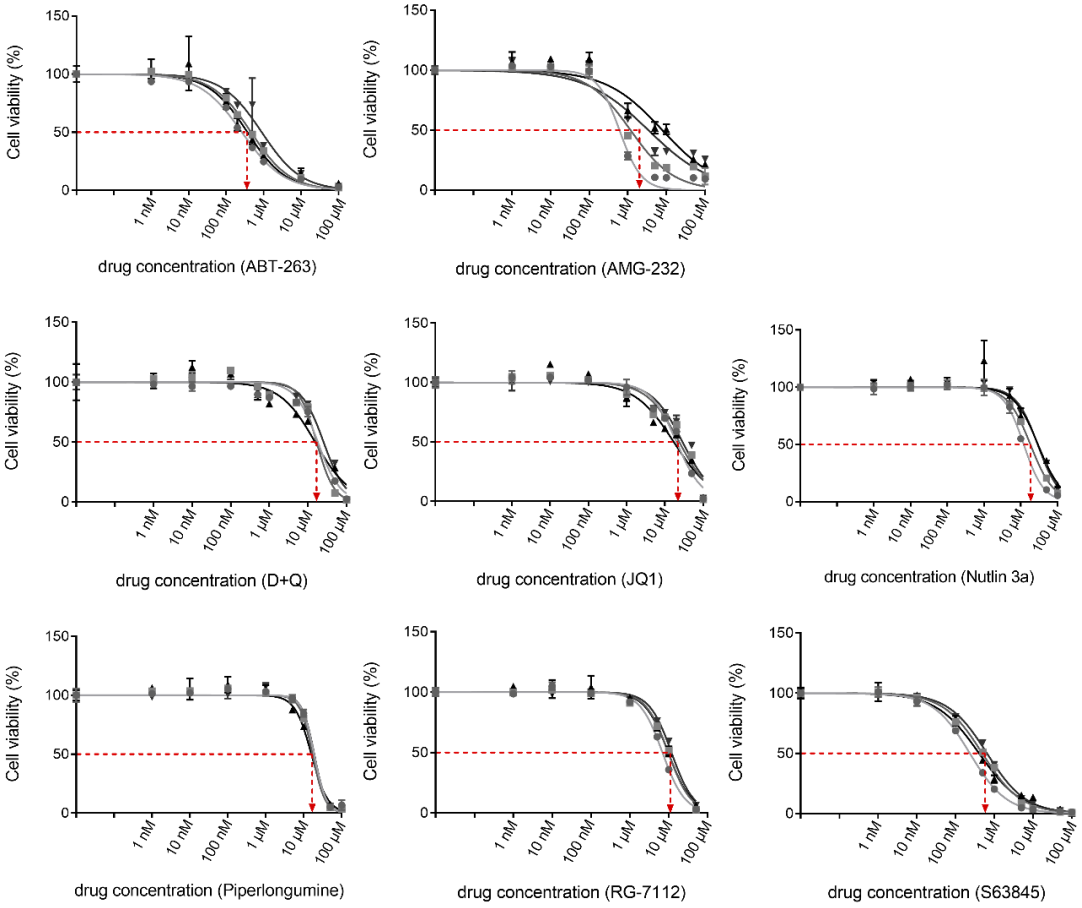

Figure 17. Concentration dependent viability upon senolytic drug treatment in healthy samples. To determine the dose range for subsequent analysis of senolytic compounds, PBMCs from healthy samples with different ages (24, 31, 48 and 68 years) were cultured for three days in 96-well plates at different concentrations as indicated. Each curve represents a healthy donor sample, which was performed in triplicate. Viability was then determined using CellTiter Glo assay and median IC50 values were calculated for each drug; ABT263: 417.7 nM, AMG232: 3.26 µM, D+Q: 17.4 µM, JQ1: 21.75 µM, nutlin-3a: 23.5 µM, piperlongumine: 17.8 µM, RG7112: 9.67 µM, S63845: 446.9 nM.

3.1.4.2 Reversal of epigenetic aging after senolytic treatment *in vitro*

Epigenetic age prediction for the senolytic drug-treated and untreated cells was measured by three age-related CpGs located at the *PDE4C*, *FHL2* and *CCDC102B* gene using pyrosequencing method. The untreated PBMCs showed a particularly good correlation between predicted age and chronological age with a mean age deviation of 0.34 years among all age groups (R^2= 0.95; n = 18; Figure 18a; supported by Michael Bleichert and Miriam DM Sarvaas).

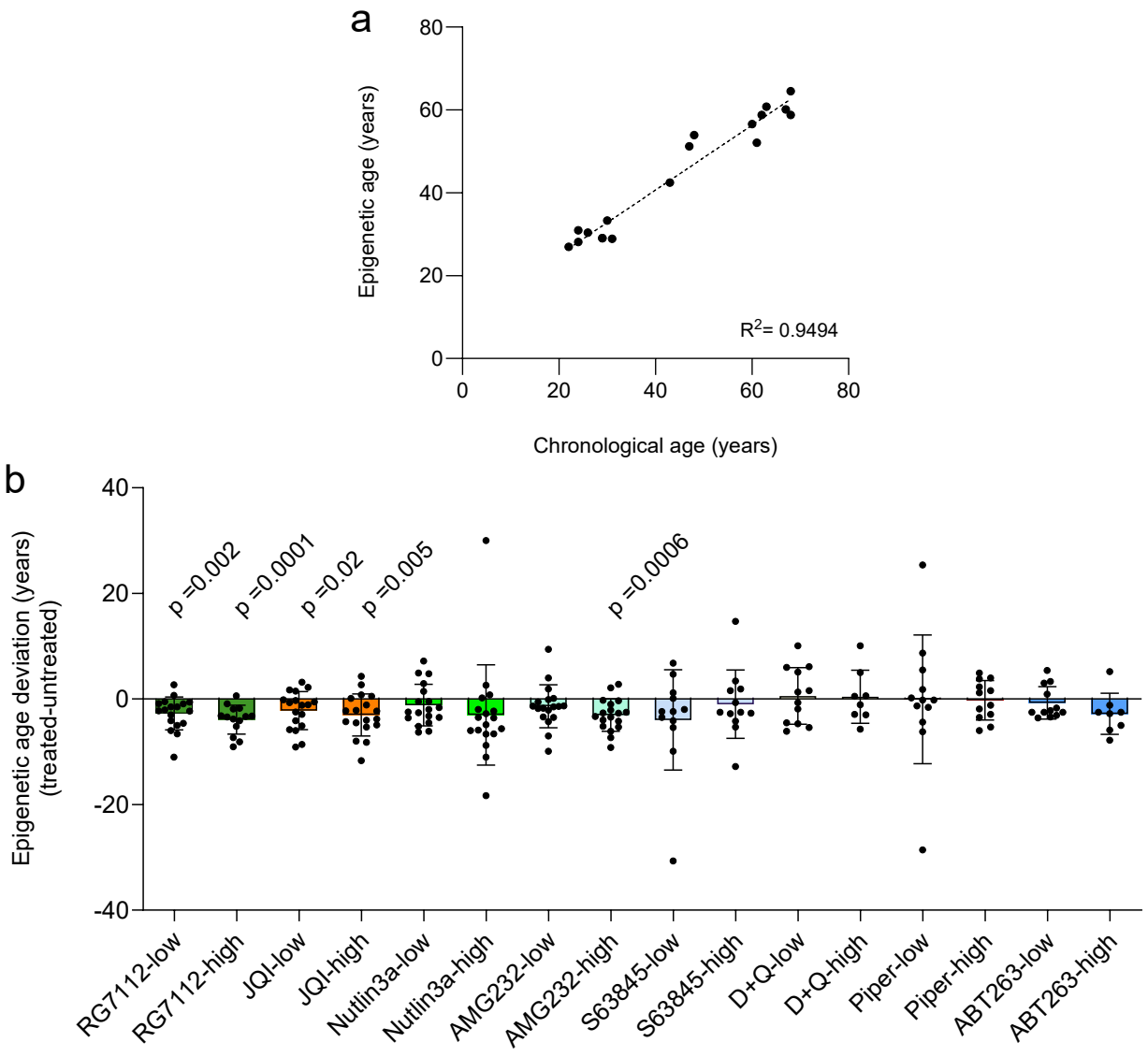

Figure 18. Epigenetic age deviation in young and old samples after senolytics treatment.
a) Correlation of predicted and chronological age of untreated samples was shown. b) Peripheral blood mononuclear cells of healthy donors were cultured for three days with nine different compounds at either high or low concentration: JQ1 (10μM, 20μM), S63845 (500nM, 1μM), ABT263 (200nM,500nM), piperlongumine (10μM, 50μM), dasatinib in combination with quercetin (D+Q; 20nM+ 50nM, 20μM+ 50μM), AMG232 (1μM, 10μM), nutlin-3a (10μM, 50μM), and RG7112 (10μM, 50μM). Epigenetic age deviations in treated vs. untreated (n = 12 to 18) was predicted. Statistics was performed with one sample t-test.

Following the three day senolytic treatment with each component at concentrations below and above the IC50 (indicated as low and high concentration), we observed a general reduction in epigenetic age in all samples. Notably, a significant decrease in epigenetic age predictions was observed for four compounds: RG7112 (average deviations of -2.7 and -3.9 year for low and high concentrations, respectively; p = 0.002 and 0.0001), JQ1 (average deviations of -2.2 and -3.0 years; p = 0.02 and 0.005), and AMG232 (average deviation for high = -3.0 years; p = 0.0006). In addition, a clear trend was observed for nutlin-3a (average deviations of -1.2 and -3.0 years), but this did not reach statistical significance. For the other drugs, we did not observe a clear effect on epigenetic age predictions (Figure 18b).

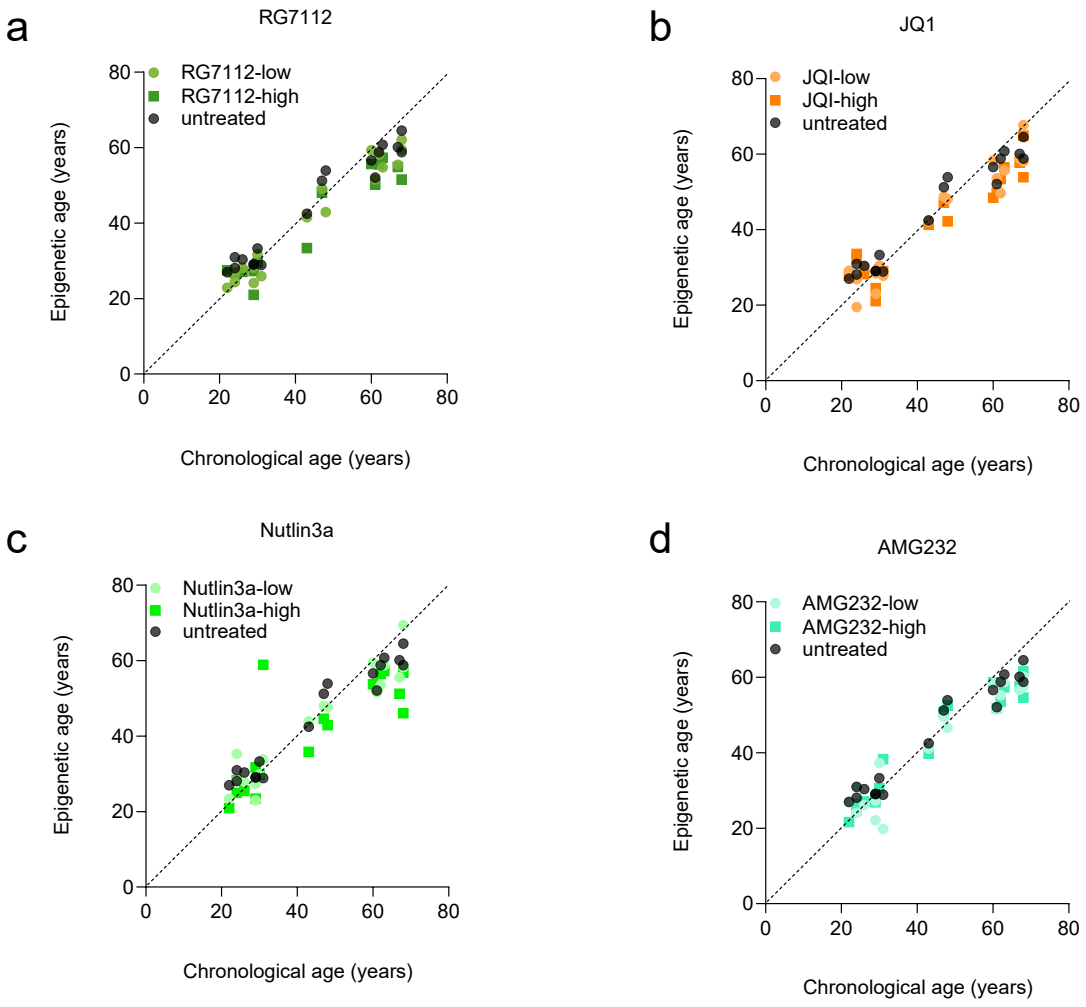

Figure 19. Correlation of chronological age and epigenetic age predictions after senolytic treatment.
Correlation between chronological age and epigenetic age predictions after three-day treatment with a) RG7112, b) JQ1, c) nutlin-3a, and d) AMG232 was demonstrated by comparing the predicted age from both concentrations with that of the untreated cells.

Additionally, we sought to determine whether epigenetic age deviations are age-dependent and also dependent on the drug concentration, as it is possible that each individual derived sample

may require a specific dosage to be effective. For the four selected drugs, an overall reduction in age was observed after treatment. However, in a few donors only one of the concentrations resulted in age reduction (Figure 19a-d). This must be taken into account when choosing the concentration for an individual and should be verified with a larger number of samples to exclude experimental variations.

3.1.4.1 Removal of senescence associated markers after senolytics treatment *in vitro*

Following three days of senolytic treatment, the remaining cells were analyzed by flow cytometry with C12FDG staining. Overall, senolytic drugs had a moderate specific effect on all drugs including both old and young samples (n = 5) in both PBMC and lymphocyte population (Figure 20a and b, respectively). The number of samples was quite small to draw any definitive conclusions. To this end, a larger number of samples (total n = 11) was analysed with the selected four senolytic drugs RG7112, JQ1, AMG232, and nutlin-3a, with only one concentration. These were selected based on their effective outcomes when all following experiments were considered. A significant decline of C12FDG positive cells was observed for both PBMC and lymphocytes (Figure 20a and b) in treatment with RG7112 ($p = 0.02$ and $p = 0.005$, respectively) and nutlin-3a ($p = 0.03$, for both cell types). Furthermore, a significant reduction of senescence in PBMCs was observed for JQ1 ($p = 0.018$).

Furthermore, similar significant changes were observed when we looked at high-density C12FDG cells in both PBMCs and lymphocytes (Figure 20c and d, respectively). The high-density C12FDG subset was cleared by treatment with JQ1 in a 61-year-old female donor in lymphocyte (Figure 20f) and also in PBMCs, as an example (Supplemental Figure 1c and d; for both JQ1 and RG7112). Additionally, phase contrast microscopy revealed that JQ1 senolytic treatment preferentially removes larger plastic adherent cells with irregular shape in a 47-year-old individual PBMC sample, as an example (Figure 20e). Anyhow, we observed a prominent population of β-Gal-positive cells in some patients, regardless of their age.

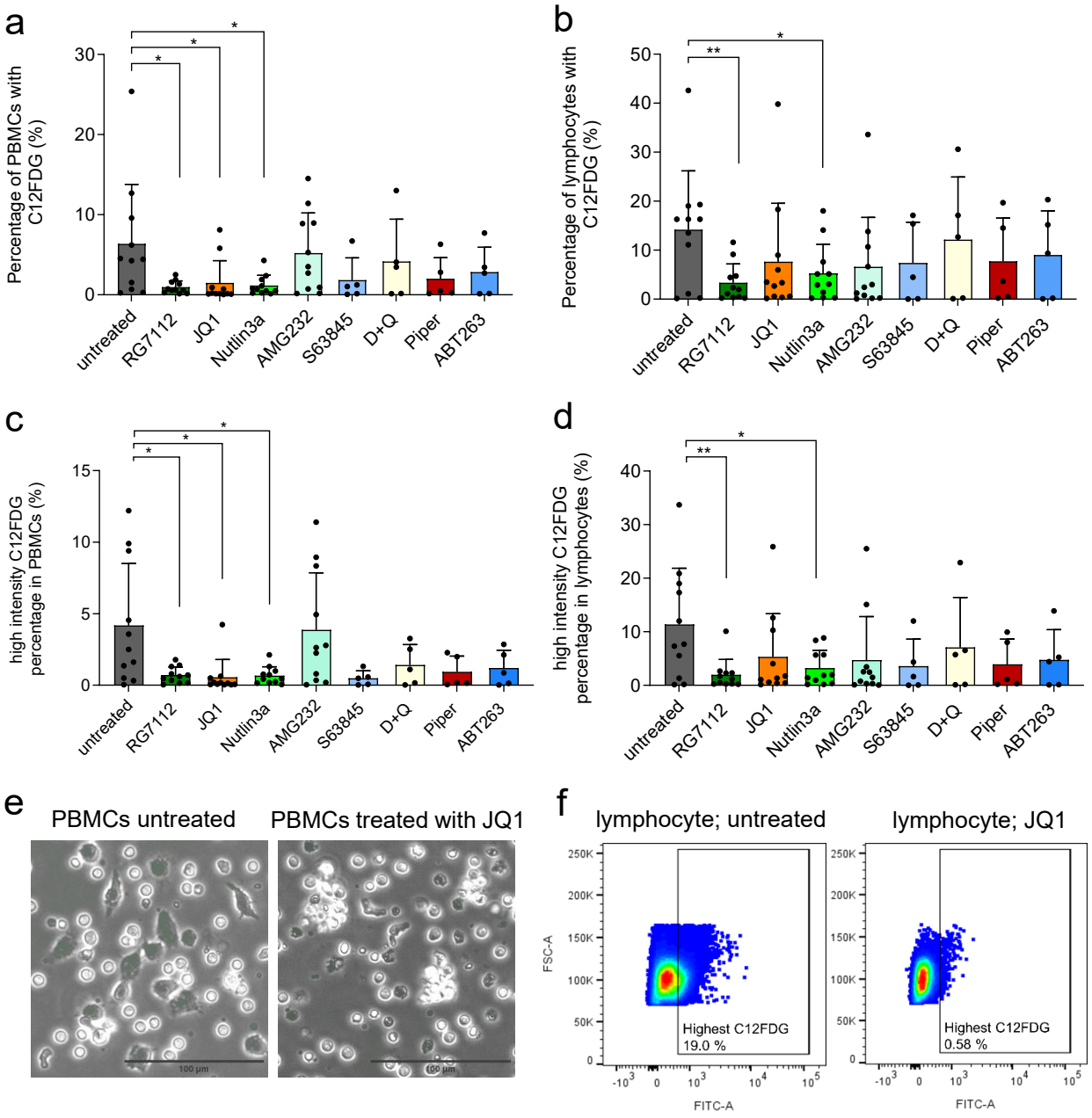

Figure 20. Percentage of senescent cells after senolytics treatment.

Peripheral blood mononuclear cells of healthy donors were cultured for three days with nine different compounds: JQ1 (10μM), S63845 (1μM), ABT263 (200nM), piperlongumine (10μM), dasatinib in combination with quercetin (D+Q; 20nM + 20μM), AMG232 (1μM), nutlin-3a (10μM), and RG7112 (10μM). Percentage of senescent cells stained with C12FDG staining after senolytics treatment was shown for a) PBMCs and b) lymphocytes. Selected senolytics with 6 more healthy adults (n = 11) showed a significant decrease in senescent cells after treatment with RG7112, nutlin-3a and JQ1. c) Additionally, a percentage of high intensity C12FDG percentage in PBMCs and d) lymphocytes showed a reduction in RG7112, JQ1 and nutlin-3a. e) Phase contrast microscopy image of the C12FDG staining of a 47year old PBMC sample was shown for both untreated and treated with JQ1 for 3 days. f) Exemplarily lymphocyte derived from a 61-year aged sample showed a high number of senescent cells in the untreated cells and after treatment with JQ1 for 3 days, the population of senescent cells was successfully removed. Two-way ANOVA with multiple comparison was performed to assess statistical significance; * represents P ≤0.1 and ** represents P ≤0.01.

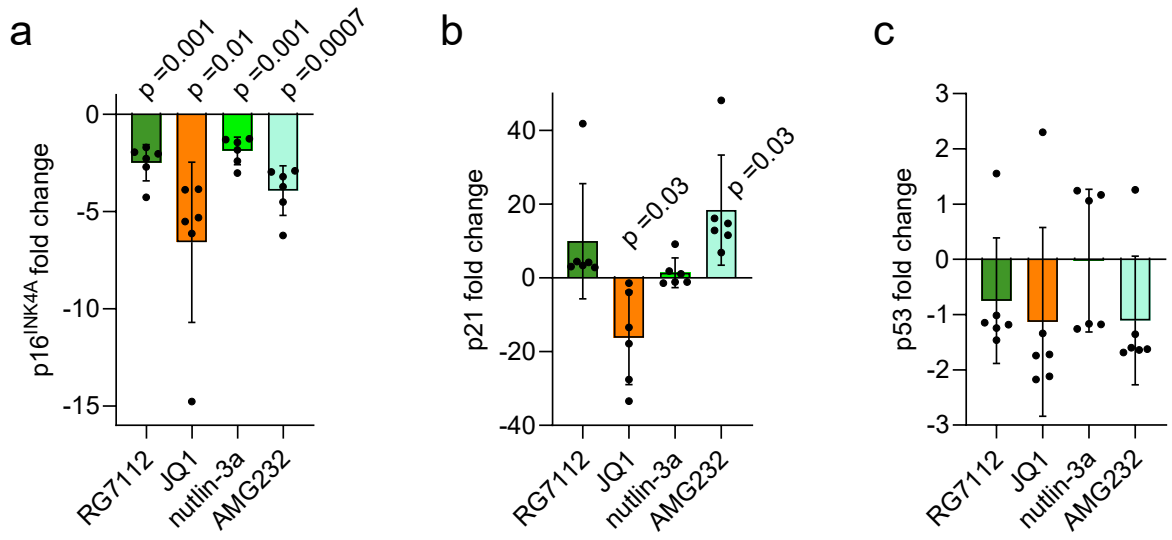

Figure 21. Percentage senescence markers with chosen senolytic drugs.
RT-qPCR for senescence associated markers a) p16 (INK4a), p12 and p53 for selected senolytic drugs including RG7112, JQ1, AMG232 and Nutin3a. One sample t-test was used to assess statistical significance.

Subsequently, we analyzed how gene expression of CDKN2A (p16INK4a), CDKN1A (p21), and TP53 (p53) was affected by the four senolytic compounds that affected epigenetic age predictions. In particular, p16INK4a showed a significant decrease upon treatment with all four compounds, while p53 showed a moderate reduction whereas this was less consistent for p21 (Figure 21). Taken together, our results support the notion that particularly RG7112, JQ1, AMG232, and nutlin-3a preferentially clear the senescent subset of PBMCs *in vitro*.

3.1.4.3 Changes in blood composition after senolytic treatment *in vitro*

Since a reduction in epigenetic age and the removal of senescent cells have been observed in individuals with senolytic treatment, we sought to determine the changes in blood composition as a result of the treatment. Studies have shown that aging results in alterations in the function and proportion of blood cells, including a bias in specific lineages (Baylis et al., 2013). Flowcytometric analysis of the lymphocyte compartment of NK cells, B cells and T cells was measured as shown in Supplemental Figure 1e. Despite the few numbers of samples, a significant reduction in T cell count ($p = 0.02$) and an increase in NK cells ($p = 0.05$) were observed in PBMCs from old donors ($n = 8$) compared to young donors ($n = 3$). There was no significant difference observed for B cells (Figure 22a). Following the senolytic treatment of PBMCs after three days ($n = 5$ to 11), a significant increase in T cells was observed with RG7112 ($p = 0.0037$), JQ1 ($p = 0.0002$), nutlin-3a ($p = 0.0012$), and AMG232 ($p = 0.017$). In contrast, B cells showed a significant reduction with JQ1 ($p = 0.0002$), RG7112 ($p = 0.0386$), and S63845 ($p = 0.045$). In addition, a significant reduction in NK cells was observed with RG7112 ($p =$

0.0175), JQ1 (p = 0.0089), nutlin-3a (p = 0.0063), and AMG232 (p = 0.028) (Figure 22b and c), specifically in old samples.

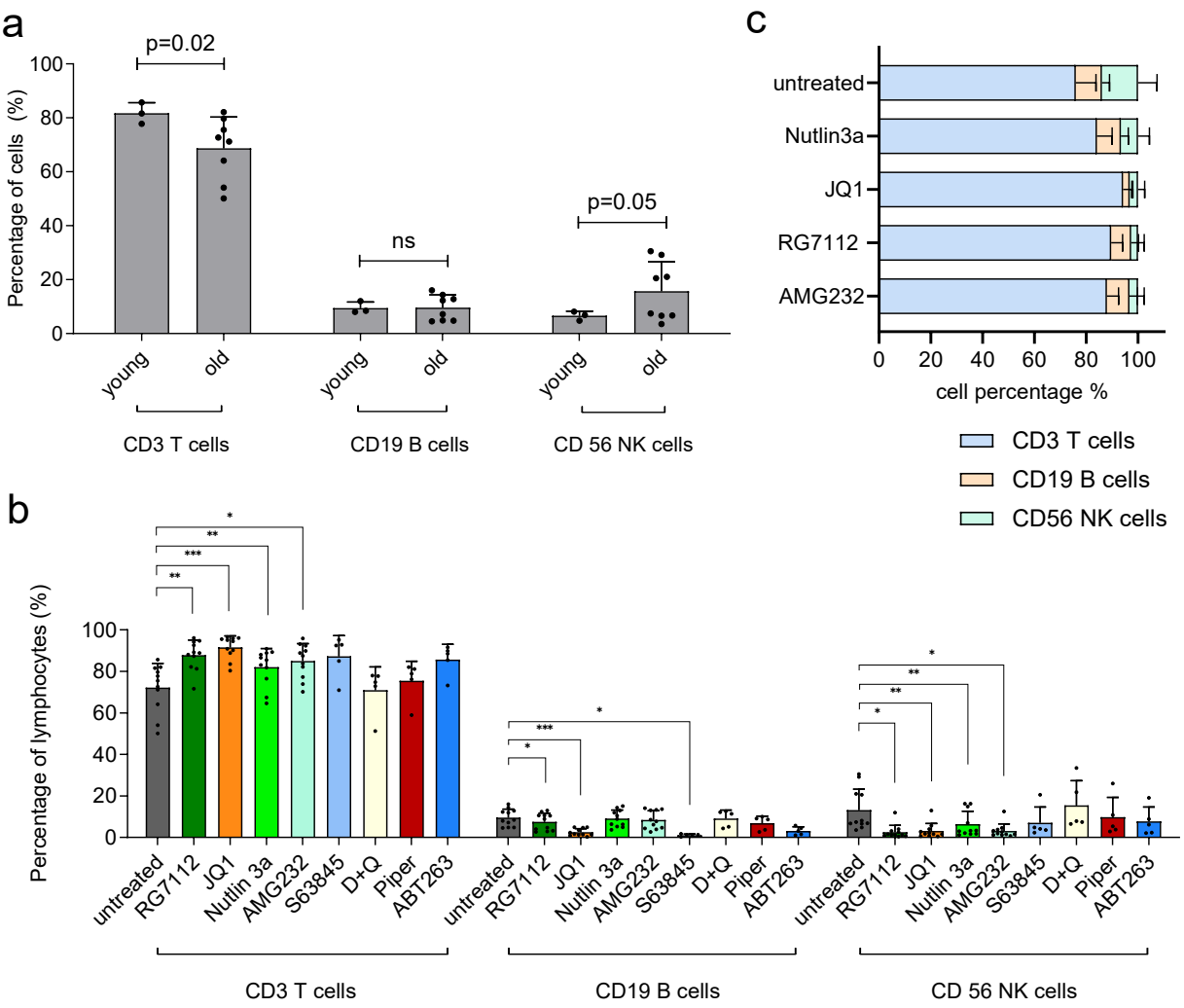

Figure 22. Percentage blood cell compositions after senolytic treatment.
a) Percentage of blood cell composition of T, B, and NK cells in the untreated samples of healthy young (n = 3) old (n = 5) cells were shown. b) Peripheral blood mononuclear cells of healthy donors were cultured for three days with nine different compounds: JQ1 (10μM), S63845 (1μM), ABT263 (200nM), piperlongumine (10μM), dasatinib in combination with quercetin (D+Q; 20nM + 20μM), AMG232 (1μM), nutlin-3a (10μM), and RG7112 (10μM). Percentage of PBMCs was measured after the senolytic treatment in the samples for different lymphocyte population (n = 5 to 11). Statistics was performed with 2- way ANOVA with multiple comparison; * represents P ≤0.1, ** represents P ≤0.01, and *** represents P ≤0.001. c) The treatment specific changes in blood compositions were observed in all 4 drug treated cells compared to untreated cells.

Overall, the results showed that treatment with senolytics, particularly with RG7112, JQ1 nutlin-3a and AMG232 was effective in decreasing epigenetic age and removing the senescent cells from the blood *in vitro*. In addition, changes in blood cell compositions were observed, this might potentially contribute to the selective advantage of the drug on certain aged cell types.

3.2 Cellular age in myeloproliferative neoplasms

3.2.1 Cellular age is accelerated in patients with MPN

Myeloproliferative neoplasms are caused by somatic driver mutations that not only drive sustained cellular proliferation but also contribute to accelerated cellular aging, this could provide a new therapeutic approach to eliminate malignant cells. Therefore, we wanted to study whether MPN patients with specific mutations show signs of accelerated aging using aging parameters such as epigenetic age, telomere length and senescence, and whether these aged cells can be targeted with senolytics and telomerase inhibition.

3.2.1.1 Epigenetic age in MPNs

To explore how MPN affects epigenetic age predictions, we analyzed DNAm with targeted bisulfite amplicon sequencing (BA-seq) at three age-associated genomic regions in the *CCDC102B*, *FHL2* and *PDE4C* genes. Epigenetic age predictions were initially validated with blood samples of 128 healthy donors (74 males and 54 females) aged 18-74 years (as shown previously in Figure 13a) and showed a mean age deviation (MAD) of 0.8 years, and a correlation with chronological age of $R^2 = 0.86$. In contrast, epigenetic age-predictions of 129 MPN patients showed much higher deviations, especially in the advanced MPN entity myelofibrosis (ET: n = 43, MAD = 6.9 years; PV: n = 39, MAD = 9.8 years; PMF: n = 35, MAD = 12.9 years; post-ET/PV MF: n = 12, MAD = 0.3 years; Figure 23a). Overall, epigenetic aging was rather increased, resulting in a positive epigenetic age deviation (predicted age – chronological age; Figure 23b).

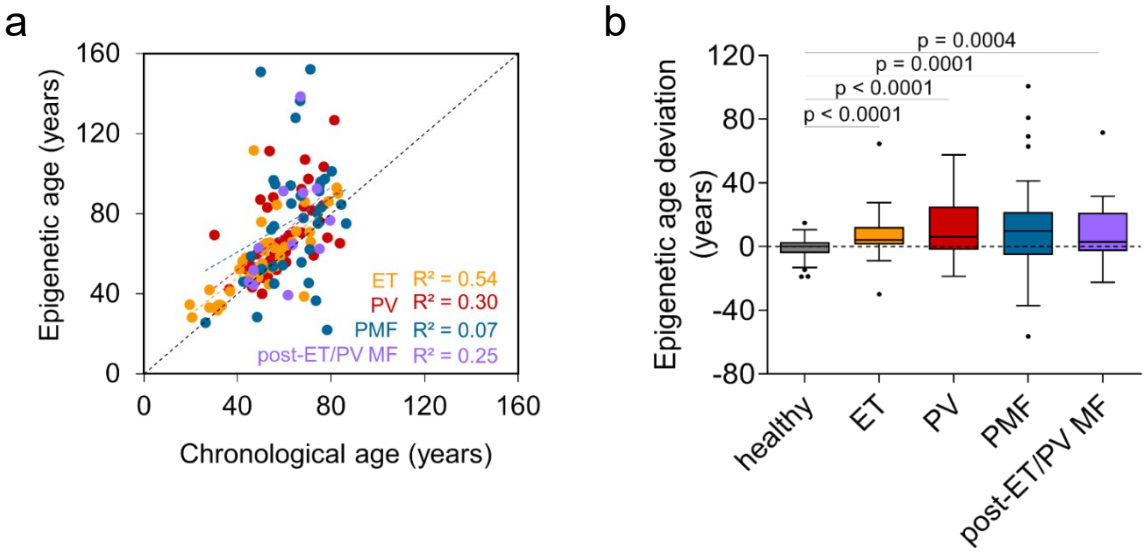

Figure 23. Epigenetic aging is progressively accelerated in MPN entities.
a) Correlation of chronological age and epigenetic age predictions by bisulfite barcoded amplicon sequencing (BA-seq) of three CpGs in MPN patients (n = 129; PV = polycythemia vera, ET = essential thrombocythemia, PMF = primary myelofibrosis). b) Epigenetic age deviation in different MPN entities compared to healthy donors. Unpaired t-test was used to assess statistical significance. This figure was adapted from (Vieri et al., 2023).

3.2.1.2 Telomere length in MPNs

In addition, telomere length (TL) was measured by flow-FISH analysis in granulocytes and lymphocytes as previously described (Ferreira et al., 2020). Granulocytes and lymphocytes are stained with a dye (LDS 751), that can penetrate the cell membrane and bind to nucleic acids and can be distinguished by signal intensities in both the FL-3 channel as well as in the forward scatter (FSC). As mentioned in the section above (3.1.1, Figure 13b), healthy controls (n = 134) were used for age adaptation of TL. This experiment was performed by Margherita Vieri and the data was used to compare the changes between epigenetic age and telomere length.

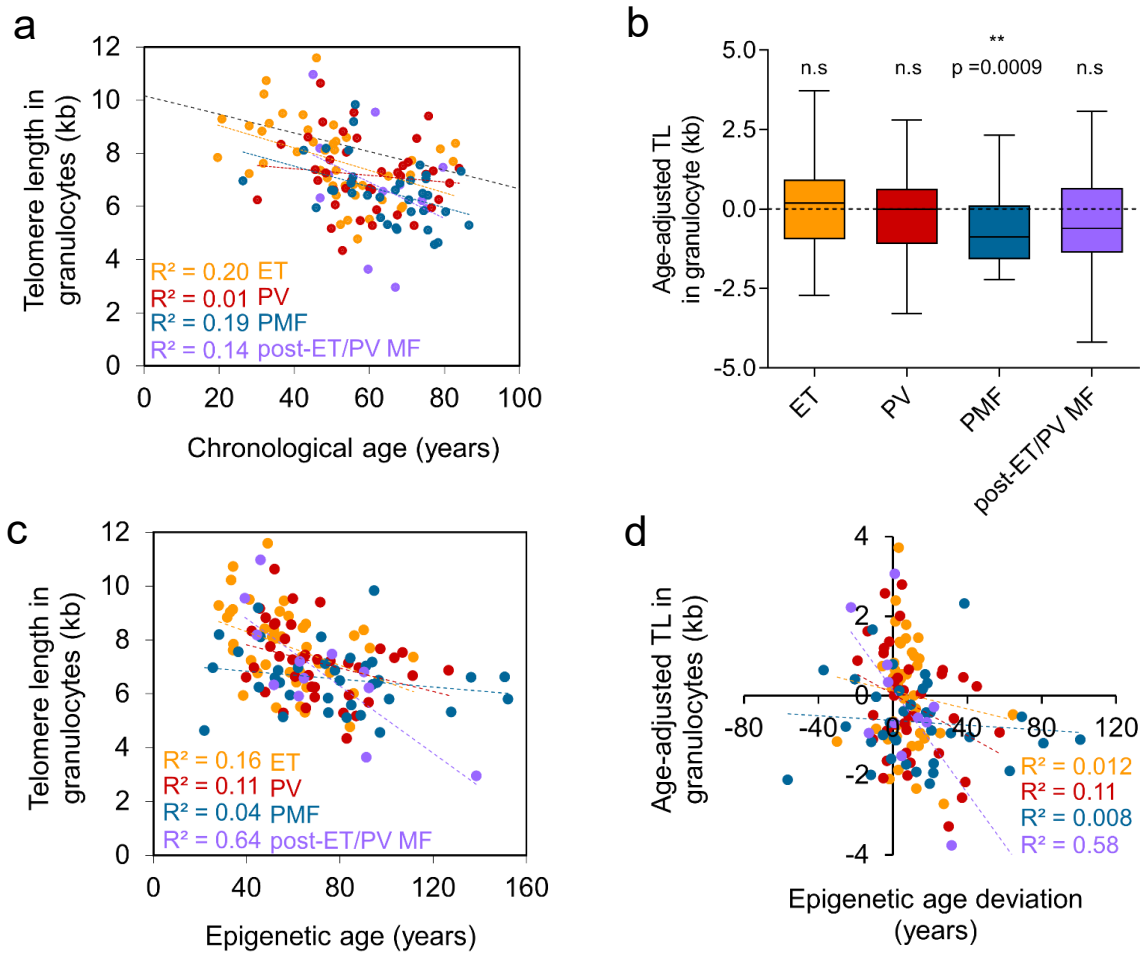

Figure 24. Premature telomere attrition in some MPN entities.
Telomere length (TL, in kb) was measured in granulocytes via flow-FISH in MPN patients, as described before (n = 129; PV = polycythemia vera, ET = essential thrombocythemia, PMF = primary myelofibrosis). b) Age-adapted TL in granulocytes in different MPN entities. One-sample t-test was used to calculate statistical significance. c) Correlation of TL and epigenetic age in different MPN entities. e) Correlation of epigenetic age deviation with age-adjusted TL in granulocytes in MPN entities. This figure was in parts adapted from (Vieri et al., 2023).

In the 129 MPN samples, TL distribution in the granulocytes showed a clear association with chronological age (Figure 24a), while a significant telomere attrition was only observed for the PMF samples (p = 0.0009; Figure 24b). Interestingly, this is in line with higher epigenetic age-predictions in PMF. As expected, no relevant deviation of TL from healthy controls was observed

in the lymphocyte compartment of all three MPN subgroups (Supplemental Figure S2). As TL in granulocytes representing the myeloid compartment revealed a better association than lymphocytes. Overall, there was only a moderate correlation between absolute TL and epigenetic age predictions (Figure 24c) and also between epigenetic age-deviation and age-adjusted TL (Figure 24d), suggesting that both parameters for cellular aging reflect independent biological features of cellular aging.

3.2.1.3 Senescence in MPNs

Cellular senescence is one of the factors contributing to the aging process. With age, the accumulation of senescent cells increases, and the paracrine effect of these cells leads to the release of senescence-associated secretory phenotype (SASP) and inflammation in the surrounding area (Cuollo et al., 2020). Measuring senescence in MPN patients could provide insights into whether the mutations induce senescence.

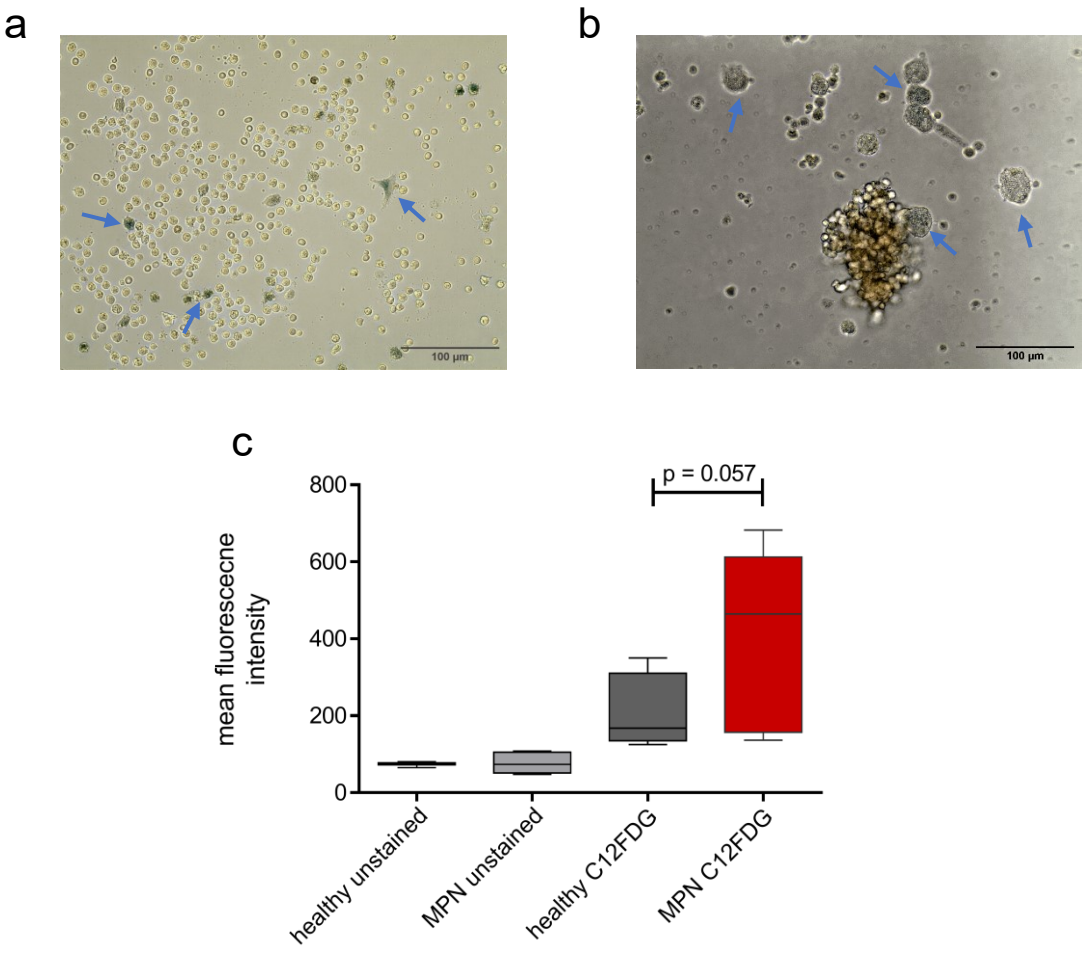

Figure 25. Presence of senescent cells in MPN samples.
β-galactosidase staining in PBMC derived cells show senescence population (blue stained cells) b) β-galactosidase staining within individual colonies depict senescence subsets c) PBMC of MPN patients (n = 7) and healthy donors (n = 6; one outlier was removed) were stained with C12FDG and analyzed by flow cytometry. The mean fluorescence intensity was in tendency higher in MPN samples, indicating that they possess higher β-galactosidase activity.

To this end, we measured senescence using two methods, one is β-gal staining with image-based analysis, which showed the presence of senescent cells in PBMC and also in the CFUs (Figure 25a-b). To further quantify this finding, we utilized C12FDG via flow cytometry to determine the mean fluorescent intensity. In comparison to healthy controls (n = 6), β-gal staining in PBMCs of MPN patients (n = 7) showed a more pronounced trend (p = 0.051; Figure 25c). Overall, these results reinforce the conclusion that aspects of cellular aging including cellular senescence are more prevalent in MPN.

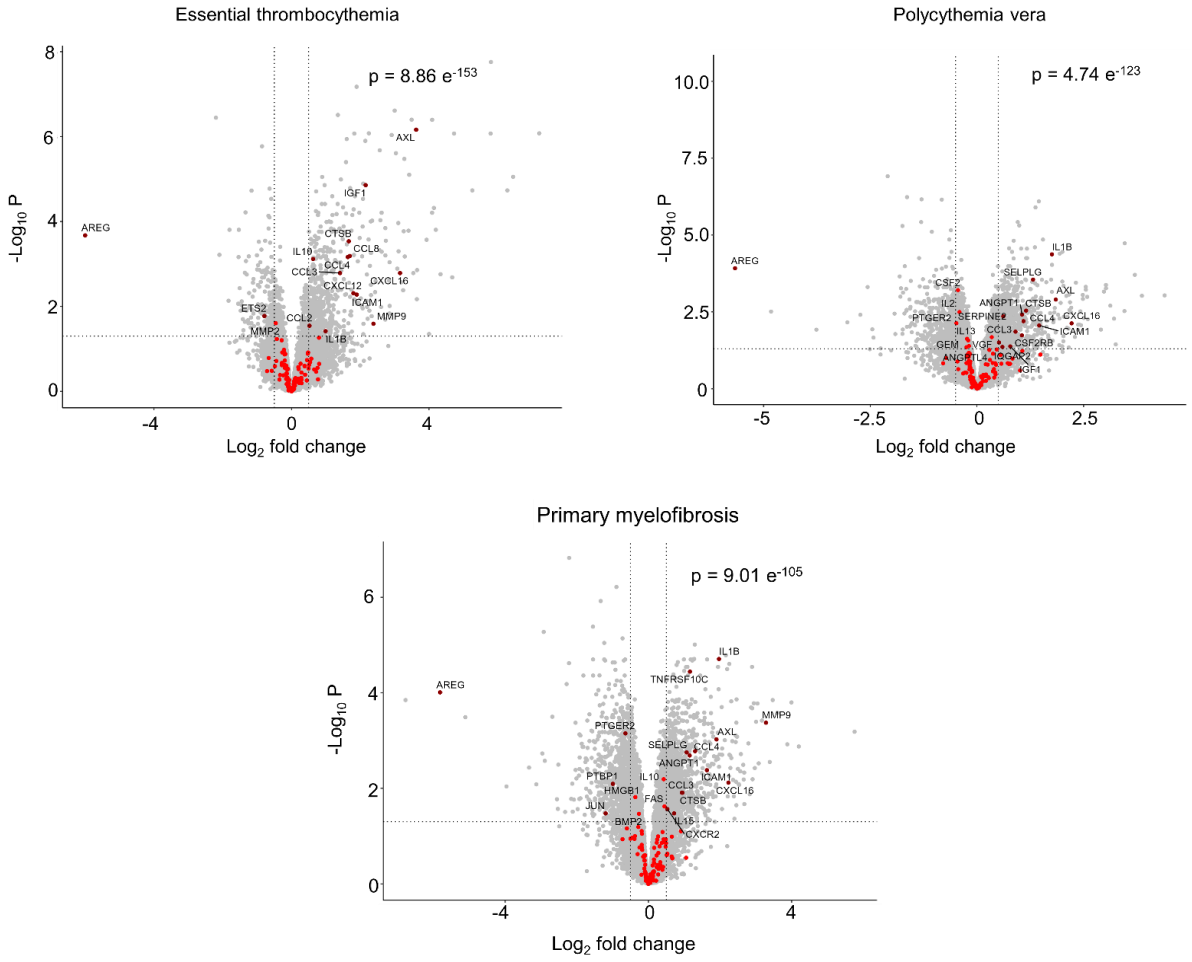

Figure 26. Presence of senescence associated signature in MPN samples.
Gene expression profiles of 6 ET, 11 PV and 9 PMF patients, each compared with 6 healthy donors (Baumeister, Maie, et al., 2021) (GEO submission number GSE174060) and were analyzed for senescence-associated gene expression signatures. To this end, we focused on a set of 125 genes (SenMayo; highlighted in red) that are differentially expressed during senescence (Saul et al., 2022). Significantly differentially regulated genes were selected by a Benjamini–Hochberg adjusted p value <0.05 and log2-fold changes above 0.5 or below −0.5. In fact, differential gene expression in MPN samples versus healthy donors revealed significant enrichment of this senescence-associated gene set for all MPN entities (p-value estimated by hyper geometric distribution). This figure was adapted from (Vieri et al., 2023).

Subsequently, we analyzed whether cellular senescence in MPN is also reflected in changes in senescence-associated gene expression. This was explored using the available gene

expression profiles of CD34+ cells derived from MPN patients (Baumeister et al., 2021). A well-established set of 125 senescence-associated genes, as identified in a recent SenMayo study (Saul et al., 2022), revealed highly significant enrichment in each of the MPN subtypes when compared to healthy controls (Figure 26). The expression of interleukin-1 beta (*IL-1β*) was significantly upregulated in all MPN groups, especially in PMF and PV (both $p < 0.001$). In addition, upregulation of metalloproteinase *MMP9* in ET ($p = 0.026$) and PMF ($p < 0.001$) and downregulation of *AREG* were found in all MPN subtypes (all $p < 0.001$).

3.2.2 Malignant clones show prominent age association in MPN

We then analyzed if these measures for cellular aging were associated with specific somatic mutations, and if they were exclusive to the malignant clone. Given that PBMCs are a mixed population of mutant and wildtype cells, we analyzed PBMCs carrying a specific mutation for their association with the mutant allele frequency, and furthermore single cell derived CFUs to elucidate the association with the malignant clones.

3.2.2.1 Epigenetic age deviation showed a significant increase in patients with *JAK2* V617F in MPNs

Using a next-generation sequencing panel of 32 genes associated with hematological malignancies, we analyzed whether these measures of cellular aging were associated with specific somatic mutations. Epigenetic age deviation showed a significant increase in patients with *JAK2* V617F ($p < 0.001$) and *CALR* mutations ($p = 0.01$; Figure 27a). In particular, patients with the *JAK2* V617F mutation showed a significant association between epigenetic age acceleration ($p = 0.0031$; Figure 27b) and mutation burden when all MPN subgroups were combined. Despite the smaller sample size, the results were also significant for epigenetic age acceleration in PV ($p = 0.0060$). When comparing the *CALR* allele burden with the MPN entities (Figure 27c), PMF showed a similar trend of age acceleration, but for the changes in ET, where we do not see a clear correlation, this could also be due to a very small number of samples with low allele burden. Overall, there is a clear association between the increasing *JAK2* V617F mutation burden and accelerated epigenetic aging in MPNs.

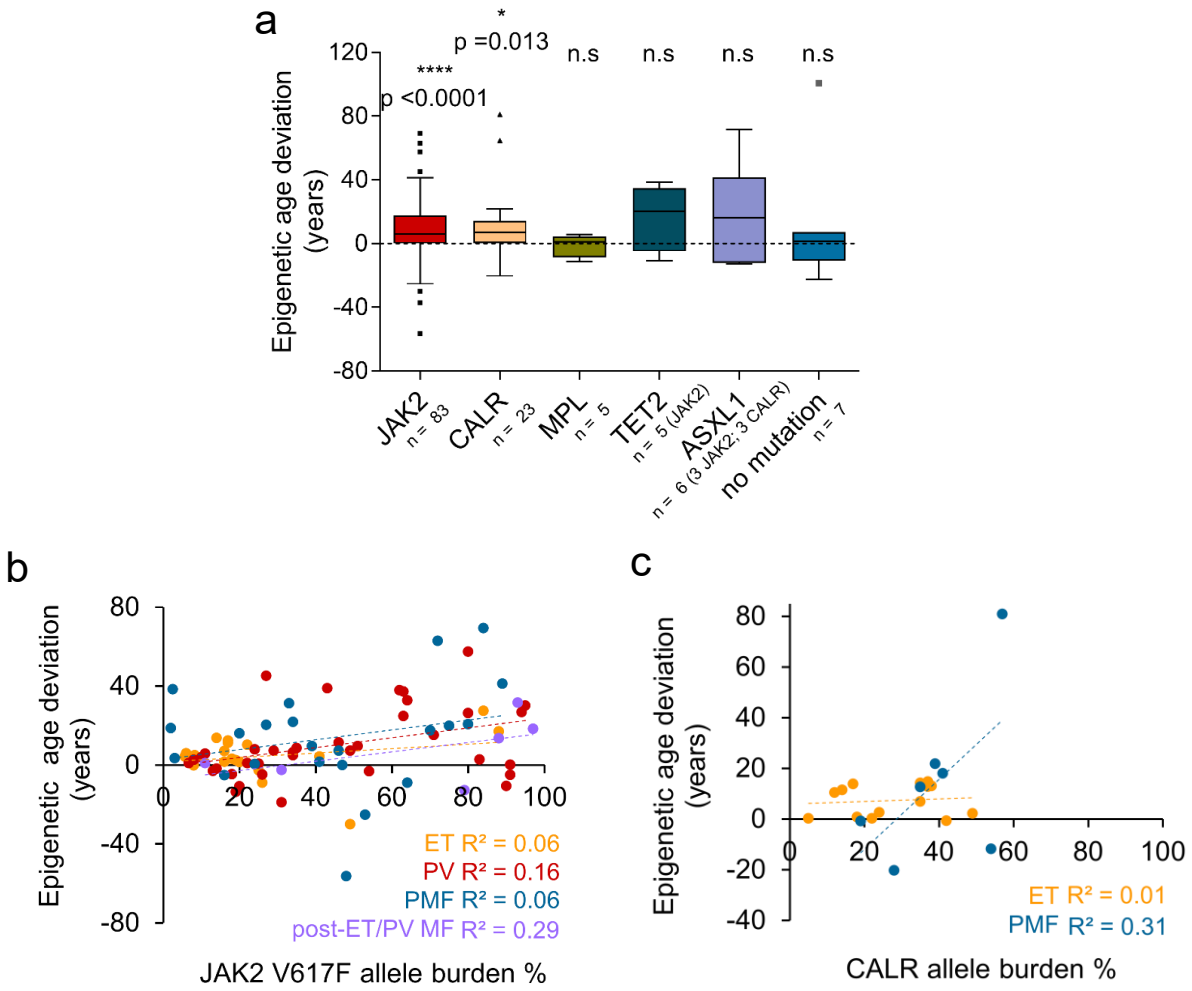

Figure 27. Epigenetic aging by mutations and correlations with *JAK2* V617F burden.
a) Epigenetic age deviation in MPN carrying different driver mutations. Unpaired Welch's t-test was used to assess statistical significance. b) Correlation of epigenetic age deviation and *JAK2* V617F allele burden in different MPN entities. c) Correlation of epigenetic age deviation and *CALR* allele burden in different MPN entities. This figure was adapted from (Vieri et al., 2023).

To further elucidate whether the observed increase in epigenetic age in bulk PBMCs could be recapitulated in a single cell harboring a mutation, we analyzed the malignant clones of patients with MPN and analyzed single cell derived colony forming units (CFUs). Epigenetic age predictions were performed exemplarily for five wild type (WT) and five *JAK2* V617F colonies for an individual patient per MPN sub entity, regardless of their CFU subtypes. As an example, no significant difference was observed in one of the age-associated regions between the subgroups of CFUs in the methylation levels (Supplemental Figure S3). There was some variation between individual colonies, but overall, the epigenetic age predictions were consistently higher for the mutated clones (Figure 28; Supplemental Figure S4). This is in line with the correlation between epigenetic age acceleration and the *JAK2* V617F mutation observed in the PBMC measurement.

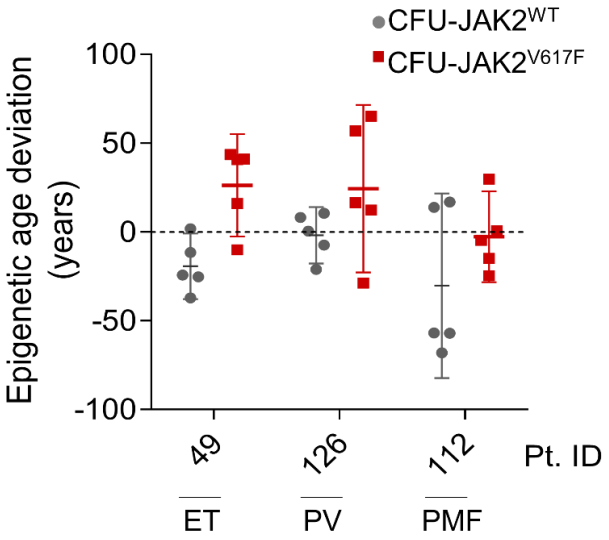

Figure 28. Epigenetic aging is accelerated in colony forming units with *JAK2* V617F.
a) Epigenetic age predictions were performed in CFUs without (n = 5) and with *JAK2* V617F (n = 5) in three different patients affected by either ET, PV, or PMF. This figure was adapted from (Vieri et al., 2023).

3.2.2.1 Telomere length showed a significant decrease in patients with *JAK2* V617F in MPNs

Further analysis of age-adjusted TL in granulocytes showed significantly accelerated telomere shortening in samples with mutations in *CALR* (p = 0.025) and *ASXL1* (p = 0.004; Figure 29a). Notably, patients carrying the *JAK2* V617F mutation showed a significant association of telomere attrition with mutational burden (p < 0.0001; Figure 29b) when all MPN subgroups were combined. Despite the smaller sample size, an association was also observed in TL for PV (p = 0.0144), ET (p = 0.0257) and post ET/PV -MF (p = 0.0418). In ET, TL showed a moderate association with an increasing *CALR* mutation burden (Figure 29c), but due to the limited number of samples and the small range of mutational allele burden, it is difficult to draw any definitive conclusions. In summary, the results suggest that cellular aging in patients with MPN seems to be both particularly accelerated in the malignant clone and correlated with its clone size.

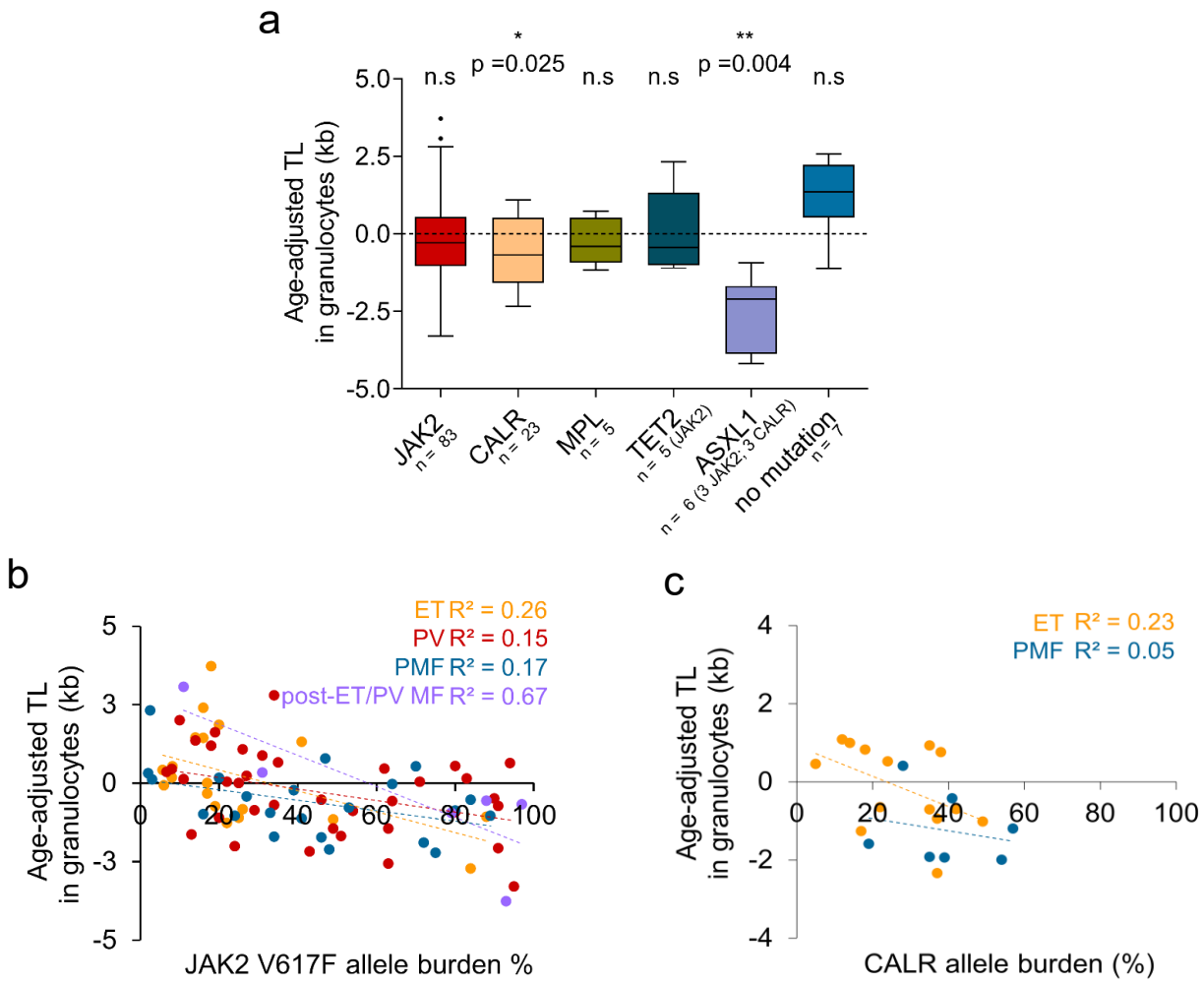

Figure 29. Telomere length by mutations and correlations with *JAK2* V617F burden.
a) Age-adapted TL in granulocytes in MPN carrying different driver mutations. One-sample t-test was used to calculate statistical significance. b) Correlation of age-adjusted TL and *JAK2* V617F allele burden. c) Correlation of age-adjusted TL and *CALR* allele burden. This figure was adapted from (Vieri et al., 2023).

In analogy, we analyzed TL in individual CFU derived *JAK2* V617F and *JAK2* WT colonies with telomere PCR (TEL-PCR) in 10 PV patients and 7 healthy donors (Figure 30a). Overall, the mean TL of colonies with *JAK2* V617F mutation was significantly shorter than in WT colonies ($p = 0.0075$). The degree of telomere shortening in *JAK2* V617F colonies (ΔTLmut-WT) was found to correlate significantly with the patient´s allele burden (Figure 30c). However, these associations were not observed in 7 PMF patients (Figure 30b and d). Telomere length measurements were performed by Margherita Vieri.

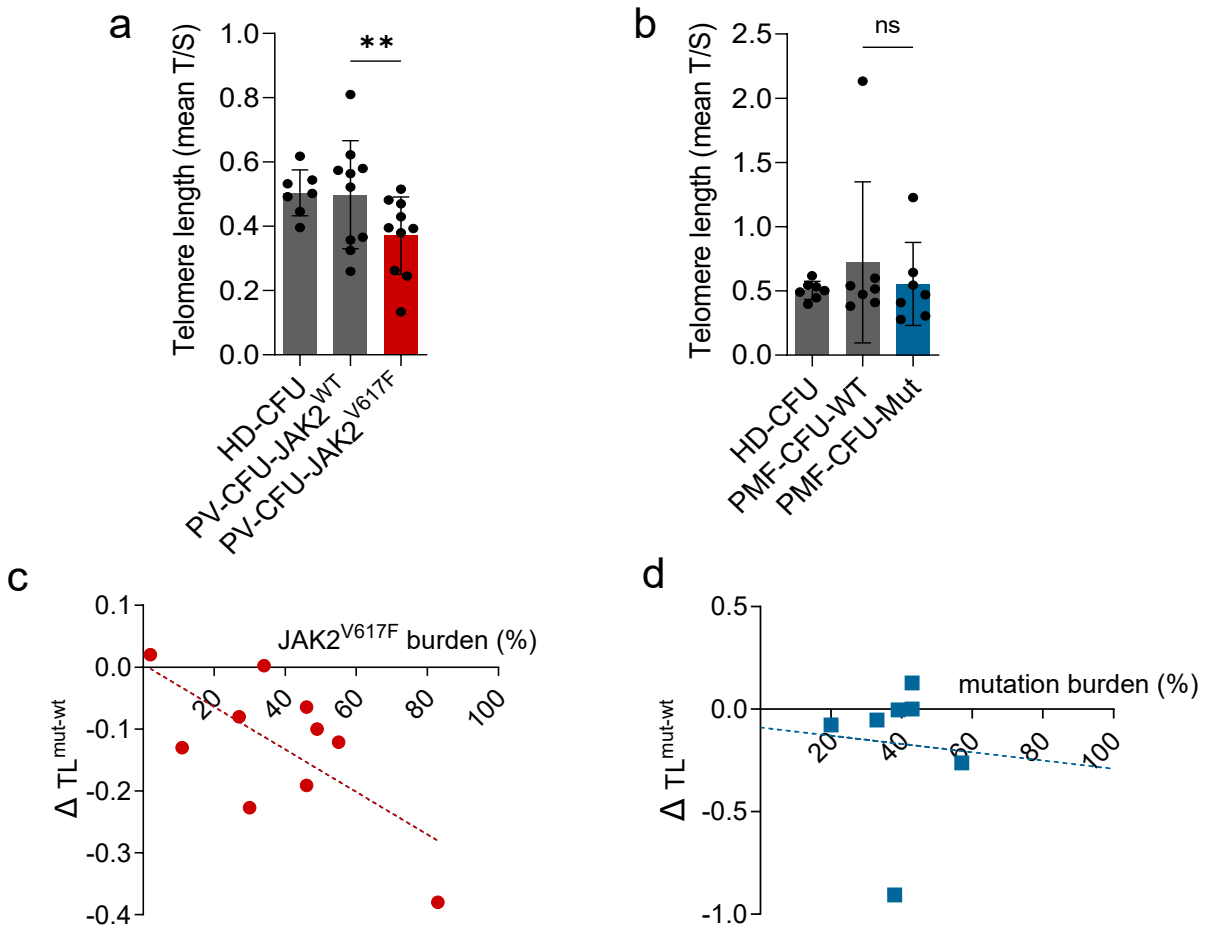

Figure 30. Presence of telomere length attrition in colony forming units with *JAK2* V617F.
a) Telomere length analysis (TEL-PCR) in single colonies derived from ten PV patients (all positive for *JAK2* V617F) and seven healthy donors (HD). For each patient, up to ten colonies were analyzed also for *JAK2* V617F genotype and the mean difference in TL between WT and *JAK2* V617F colonies of each individual PV patient was calculated (paired t-student test). b) In analogy, TL was analyzed in up to ten single colonies derived from seven PMF patients and the same seven healthy donors. c) Correlation between this mean difference in TL with the initial *JAK2* V617F allele burden of the PV patient d) In the PMF patients, there was no clear correlation between the initial *JAK2* V617F allele burden and the discrepancy in TL between mutated and non-mutated colonies. This figure was adapted from (Vieri et al., 2023).

3.2.3 Heterogeneity of epigenetic age based on single-read predictions

It has been speculated that epigenetic age deviations in malignancies are due to altered DNA methylation patterns of the malignant clone, rather than the residual compartment of non-mutated cells. To address this question, we analyzed the individual BA-seq reads. The analysis of BA-seq data was done by Miloš Nikolić.

3.2.3.1 The single read association in the bulk samples of MPN

Each of the three age-associated regions captures several neighboring CpG sites (*PDE4C*, n = 26; *FHL2*, n = 18; and *CCDC102B*, n = 6). We anticipated that these neighboring sites are coherently modified, at least showing a prominent pattern in the malignant clone. In contrast, the

neighboring CpGs seem to be regulated independently (Figure 31). Nevertheless, we observed an aberrant DNA methylation pattern in the *FHL2* and *PDE4C* regions in the MPN sample compared to healthy adults of the same age.

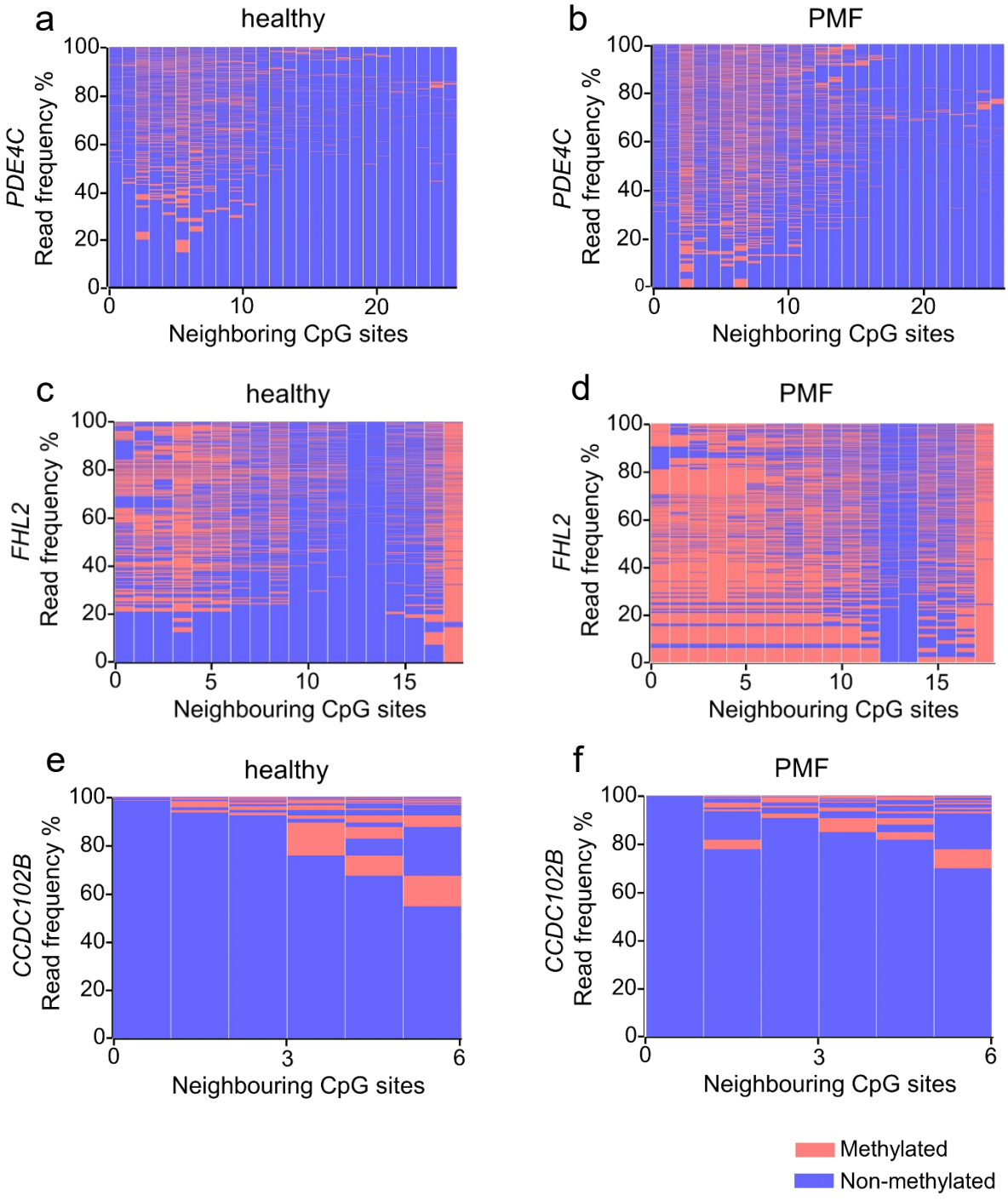

Figure 31. Heterogeneity of age-associated DNA methylation in MPN.
Heat map depicts exemplarily the frequencies of DNAm patterns within the neighboring CpGs of the *PDE4C* amplicon in BA-seq data of a) a healthy donor, and b) a PMF patient of the same age Furthermore, exemplary heatmaps are also shown for the c, d) *FHL2* and e, f) *CCDC102B* amplicon. In healthy and MPN samples the patterns of neighboring CpGs are quite heterogeneous and there is no obvious clonal DNAm pattern in the patient samples.

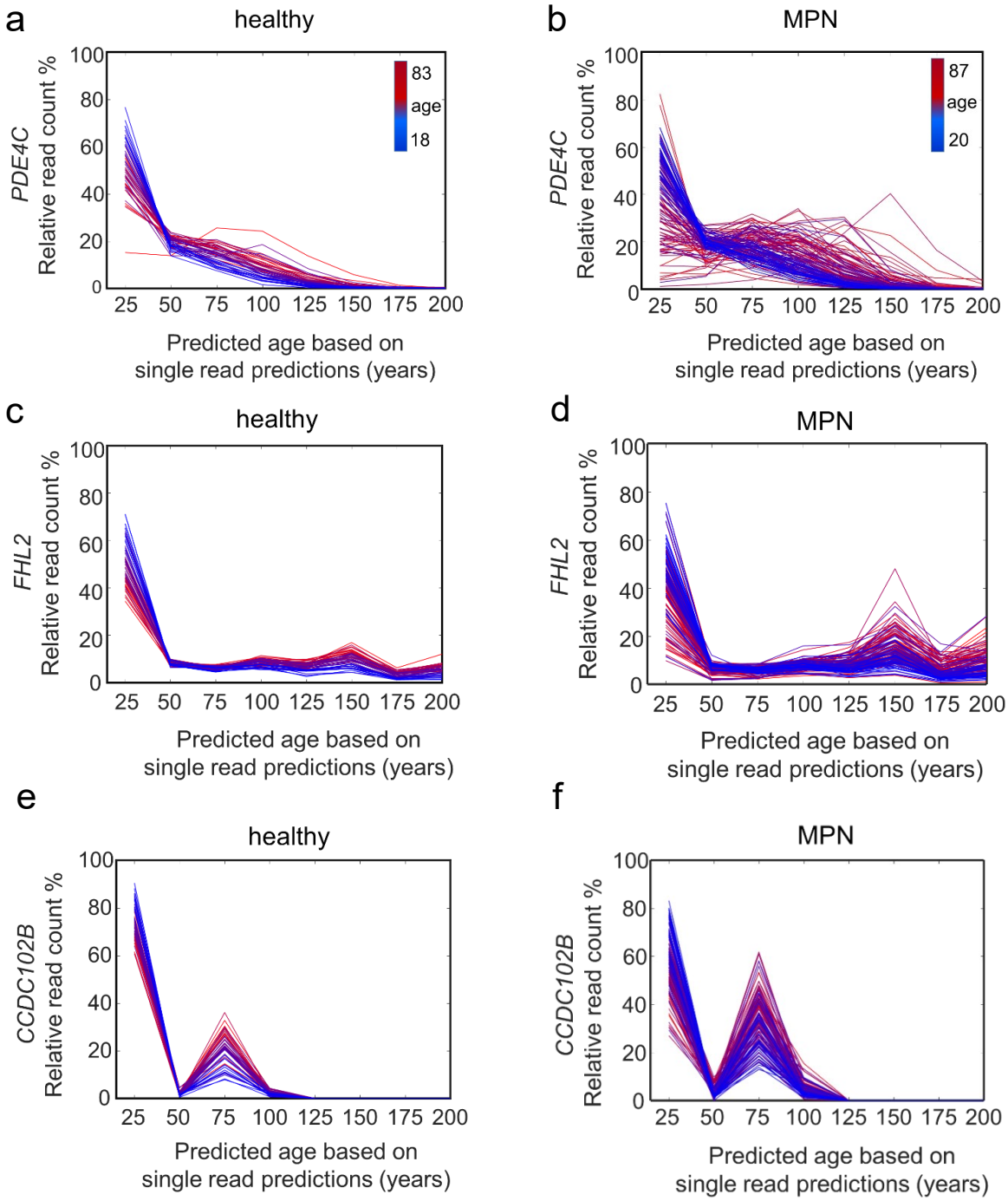

Figure 32. Single read age prediction in healthy and MPN.
The binary code of methylated and non-methylated CpGs of each amplicon was then used for single read prediction for *PDE4C* (a, b), *FHL2* amplicon (c, d), and the *CCDC102B* amplicon (e, f). The histograms demonstrate the heterogeneity of single read predictions (ranging from 0 to 200 years), and their relative frequency are provided for all healthy donors (18 to 83 years old; n = 128; color code depicts donor age) and MPN patients (20 to 87 years old; n = 129). As expected, the higher predictions increase in elderly donors. Notably, the heterogeneity of epigenetic age predictions increases particularly in elderly MPN patients.

The probabilistic method was used to predict epigenetic age for each individual DNA strand. For healthy samples, such single read-predictions followed a more homogeneous pattern than in MPN patients, suggesting that epigenetic aging is more heterogeneous in MPN samples (Figure

32). Notably, *FHL2* and *PDE4C* showed overall good correlation, and less age deviation in healthy samples, whereas MPN showed accelerated aging. Although *CCDC102B* wasn't able to capture the single read prediction in healthy compared to chronological age, overall, we observed a clear difference in MPN compared to healthy (Figure 33).

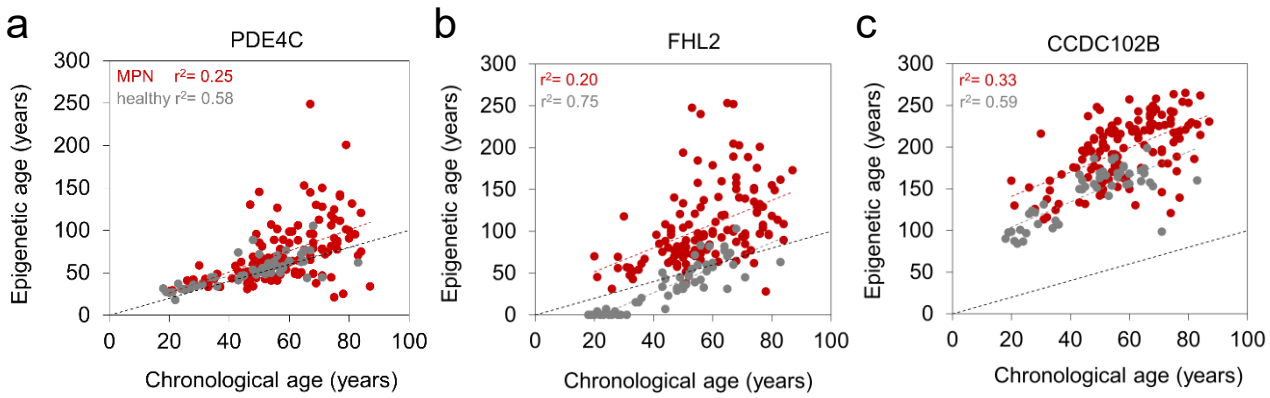

Figure 33. Single-read epigenetic aging is accelerated in MPN compared to healthy patients. Correlation of chronological age and single read epigenetic age prediction of three CpGs a) *PDE4C*, b) *FHL2* and c) *CCDC102B* in MPN patients.

To better understand the variations in DNA methylation levels at neighboring CpGs, we utilized two alternative scoring systems, as described in a previous work (Eipel et al., 2019): the d-score and the n-score. The d-score is the sum of the absolute difference of DNAm values compared with those of age-adjusted controls. It thereby reflects how much a DNAm level in an MPN sample varies from a normal donor, taking all neighboring sites into account. For the 26 CpGs of *PDE4C* the d-score was significantly higher in all MPN entities as compared to healthy controls (Figure 34a). The n-score reflects the absolute difference between neighboring CpG sites and thereby indicates the extent of DNAm level changes within the *PDE4C* amplicons. The n-scores were also significantly higher in MPN samples, especially in PMF (Figure 34b). We observed similar patterns in the other age-associated CpGs, of *FHL2* and *CCDC102B* (results not shown here). Overall, these data demonstrate that age-associated DNAm at neighboring CpGs is heterogeneous particularly within the malignant clone.

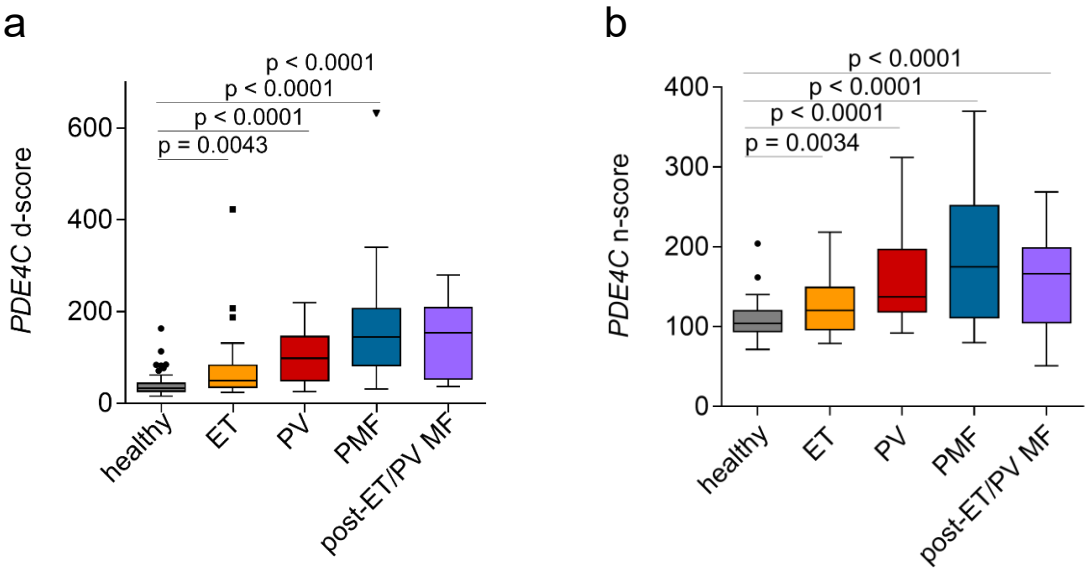

Figure 34. DNA methylation variability in MPN.
a) The DNAm at the neighboring CpGs within the *PDE4C* amplicon was compared to age-adjusted levels in healthy blood samples. The d-score demonstrates clear demarcation of MPN and control samples. b) Aberrant DNAm at age-associated CpGs often shows non-coherent DNAm levels at neighboring CpGs. This is exemplified by the n-score (Eipel et al., 2019) for the *PDE4C* amplicon, which is consistently higher in MPN as compared to healthy controls. Unpaired t-test was used to assess statistical significance.

3.2.3.2 The single read prediction in single cell derived CFUs of MPN

Notably, in contrast to the BA-seq DNA methylation patterns observed in the bulk PBMC analysis, the individual colonies revealed colony-specific prevalent DNAm patterns in all three age-associated regions (Figure 35). This demonstrates that the clonal CFUs capture a specific DNAm pattern, which is at least partly conserved during the 14-day expansion towards a colony. The DNAm patterns differed between CFU colonies carrying the *JAK2* V617F mutation and their WT counterparts were evident. It is interesting to observe that even with the gain of DNA methylation in mutant clones, the patterns were more organized when compared to bulk PBMC samples.

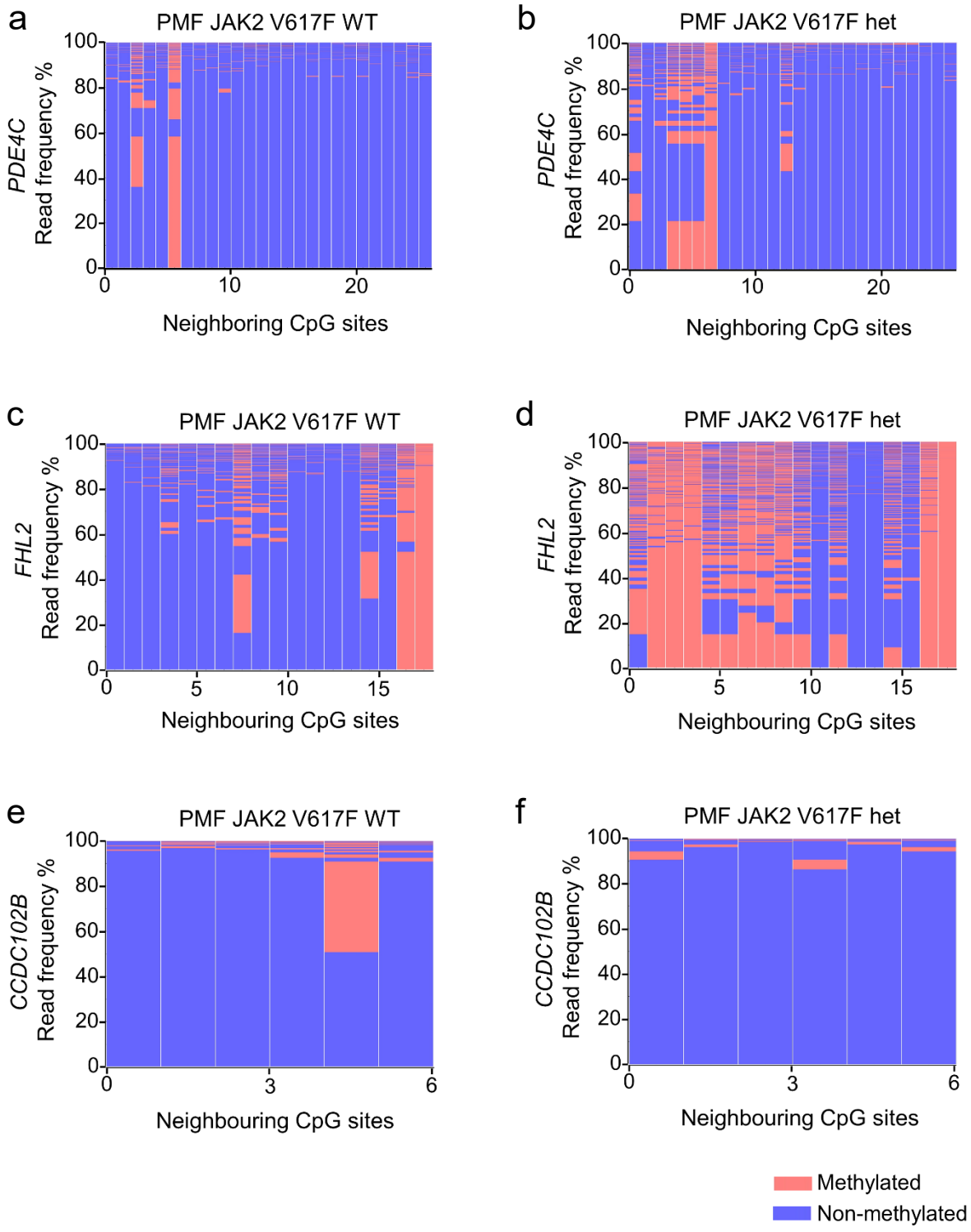

Figure 35. Age-associated DNA methylation is more homogenous in colony forming units.
Individual colony forming units (CFUs) were analyzed after 14 days (in analogy to Figure 28). a, b) The heat maps exemplarily depict frequencies of DNAm patterns within the neighboring CpGs of the *FHL2* amplicon in BA-seq data of a) WT, and b) *JAK2* V617F mutated colonies from the same patient. c, d) In analogy, we analyzed the amplicons of *CCDC102B* for c) WT, and d) *JAK2* V617F colonies from the same patient. In comparison to the corresponding heatmaps of blood (Figure 31) there are consistently more prominent patterns in individual colonies, which might reflect the pattern of the initial colony forming unit.

3.2.4 Senolytic treatment of MPN blood samples *in vitro*

So far, this study has shown that cellular senescence and accelerated cellular aging are enhanced in MPN, particularly in the malignant clones. This suggests that senolytic drugs may be more effective in targeting these cells, which show accelerated aging and mutation than the remaining non-mutant cells. To address this question, we cultured PBMCs for three days with nine different drugs that have been suggested to specifically target senescent cells: piperlongumine, ABT263, RG7112, nutlin-3a, dasatinib in combination with quercetin (D+Q), AMG232, JQ1, and S63845. Furthermore, we tested the telomerase inhibitor BIBR 1532. After performing a concentration dependent cell viability assay to determine the IC50 (Figure 36) using four MPN samples, with each drug and selecting two concentrations, one below and one above the IC50 (indicated as low and high concentration).

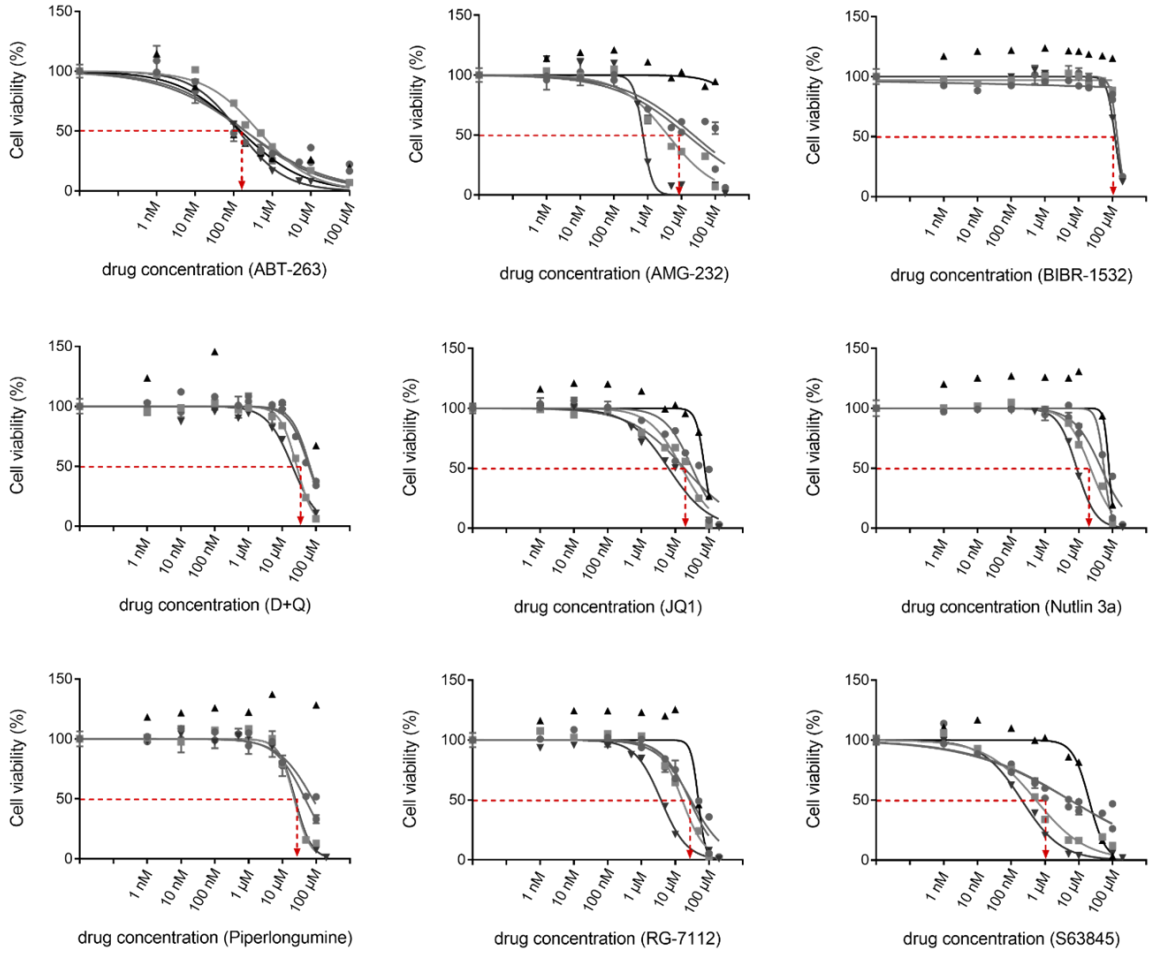

Figure 36. Concentration dependent viability upon senolytic drug treatment in MPN.
To determine the dose range for subsequent analysis of senolytic compounds, PBMCs from MPN patients (79, 132, 135, 146 and 147) were cultured for three days in 96-well plates at different concentrations as indicated. Each curve represents a patient sample, which was performed in triplicate. Viability was then determined using CellTiter Glo assay and median IC50 values were calculated for each drug; ABT263: 196.9 nM, AMG232: 9.2 µM, BIBR 1532 128.3 µM, dasatinib in combination with quercetin (D+Q): 44.15 µM, JQ1: 18.6 µM, nutlin-3a: 46.4 µM, piperlongumine: 35.5 µM, RG7112: 26.7 µM, S63845: 5.5 µM.

PBMCs of 9 MPN patients with *JAK2* V617F mutation were treated using two concentrations of each senolytics. After three days, the remaining *JAK2* V617F mutation burden was analyzed using digital droplet PCR (ddPCR). The ddPCR method revealed a good correlation of *JAK2* V617F allele burden with NGS data in MPN patient samples (R^2 = 0.97) and therefore appeared to be reliable for further measurements (Figure 37a). Overall, the senolytic drugs had only a moderate specific effect on the mutant subsets. Two compounds, JQ1 and piperlongumine showed a moderate but significant reduction in *JAK2* V617F allele burden. Piperlongumine showed an effect only at low concentrations (Figure 37b).

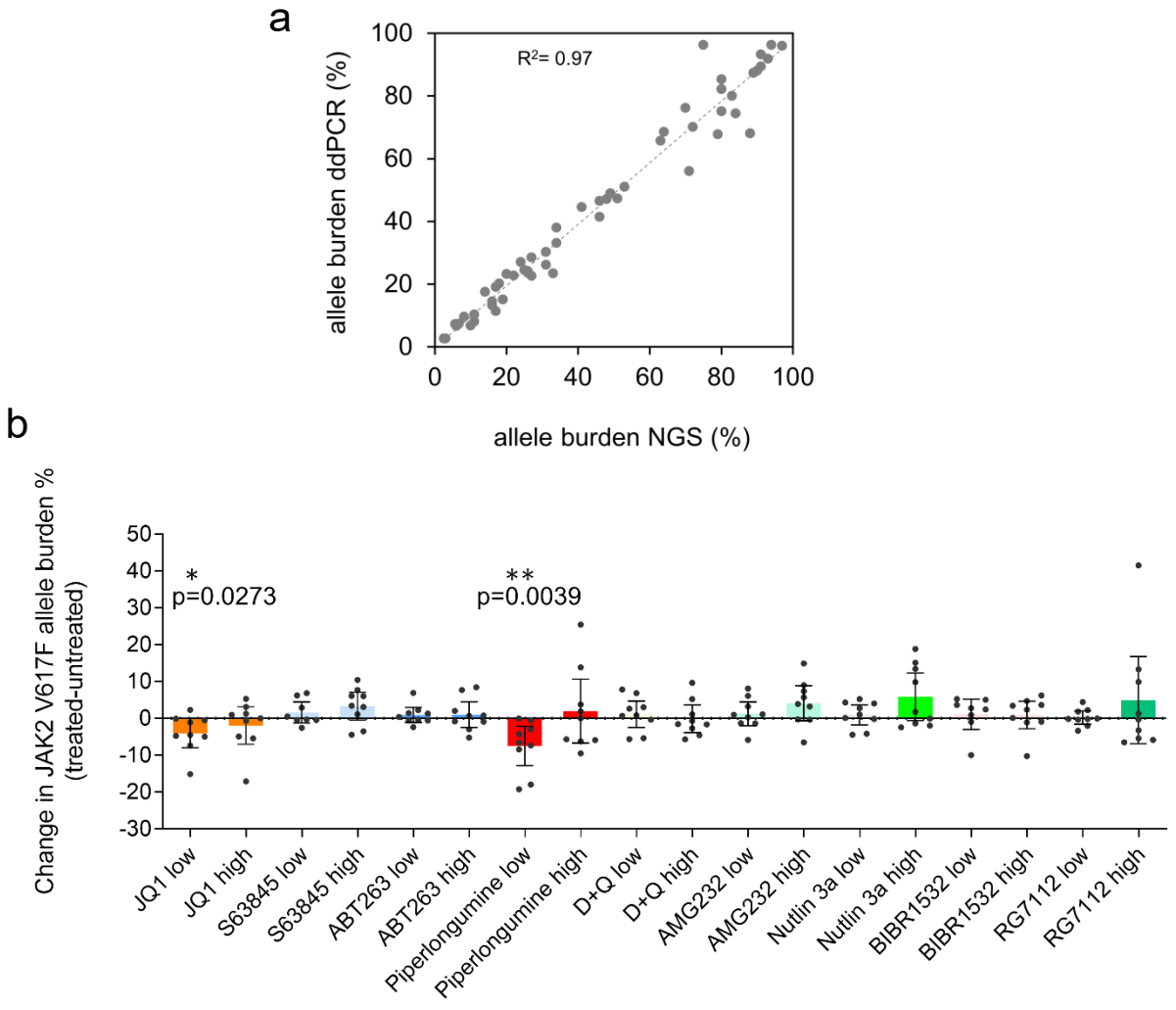

Figure 37. Change in *JAK2* V617F allele burden after senolytic treatment *in vitro*.
a) Analysis of *JAK2* V617F mutation burden with digital droplet PCR versus deep sequencing. The fraction of *JAK2* V617F mutations was analyzed in PBMCs of 50 MPN patients. b) PBMCs of MPN patients were cultured for three days with nine different compounds at either high or low concentration: JQ1 (10μM, 20μM), S63845 (500nM, 1μM), ABT263 (100nM, 200nM), piperlongumine (10μM, 50μM), dasatinib in combination with quercetin (D+Q; 20μM, 50μM), AMG232 (1μM, 10μM), nutlin-3a (10μM, 50μM), BIBR 1532 (50μM, 100μM), and RG7112 (10μM, 50μM). *JAK2* V617F allele burden measured by ddPCR in untreated versus treated cells (n = 9; one-sample t-test). This figure was in parts adapted from (Vieri et al., 2023).

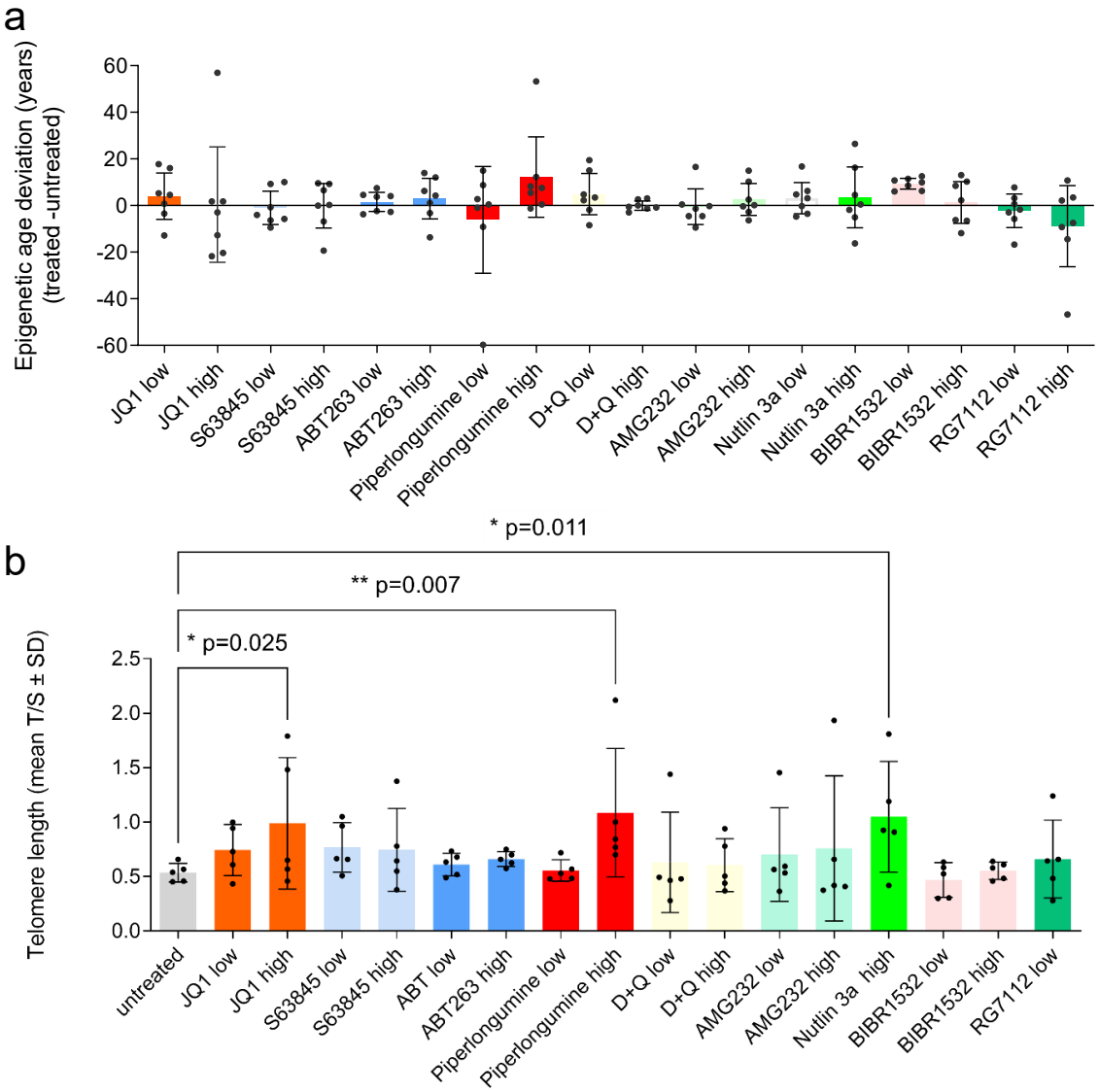

Figure 38. Impact on cellular aging after senolytic treatment *in vitro*.
a) Epigenetic age changes in treated versus untreated cells (n = 7; measured by pyrosequencing; one-sample t-test). b) Changes in telomere length in treated versus untreated cells (n = 5; measured by TEL-PCR; one-way ANOVA). TL in nutlin-3a 10 µM and RG7112 50 µM was not measurable due to a low concentration of DNA in the samples. This figure was adapted from (Vieri et al., 2023).

In analogy, we analyzed if the treatment would have an impact on epigenetic age predictions (n = 7 for each compound; supported by Matthis Schnitker). Our results showed a moderate, non-significant reduction in epigenetic age predictions for both RG7112 and piperlongumine (Figure 38a), which may be due to depletion of clonal cells with premature epigenetic age. Furthermore, we measured TL with TEL-PCR (n = 5 for each compound; performed by Margherita Vieri). A significant increase in telomere length was again observed with JQ1, piperlongumine and nutlin-3a (Figure 38b). These results indicate that at least JQ1 and piperlongumine might have a selective effect on malignant cells with accelerated cellular aging. Overall, our results suggest that cellular aging is accelerated in malignant MPN clones, and this may provide a target for treatment with senolytic drugs.

3.2.5 Mouse models associated with MPN

3.2.5.1 Epigenetic age acceleration in *JAK2* V617F mouse model

Epigenetic age prediction was analysed in vav-cre driven Jak2 V617F transgenic mice after development of an MPN-like phenotype using unfractionated bone marrow cells (Figure 39a). The Jak2 V617F mutant mice (n = 4) exhibited a significant acceleration of epigenetic age compared to WT Jak2 (n = 9; Figure 39b, p = 0.02). TL did not differ between Jak2 WT and Jak2 V617F (Figure 39c), which may be due to differential telomerase expression and TL regulation in mice compared to humans (Calado & Dumitriu, 2013; Tharmapalan & Wagner, 2024).

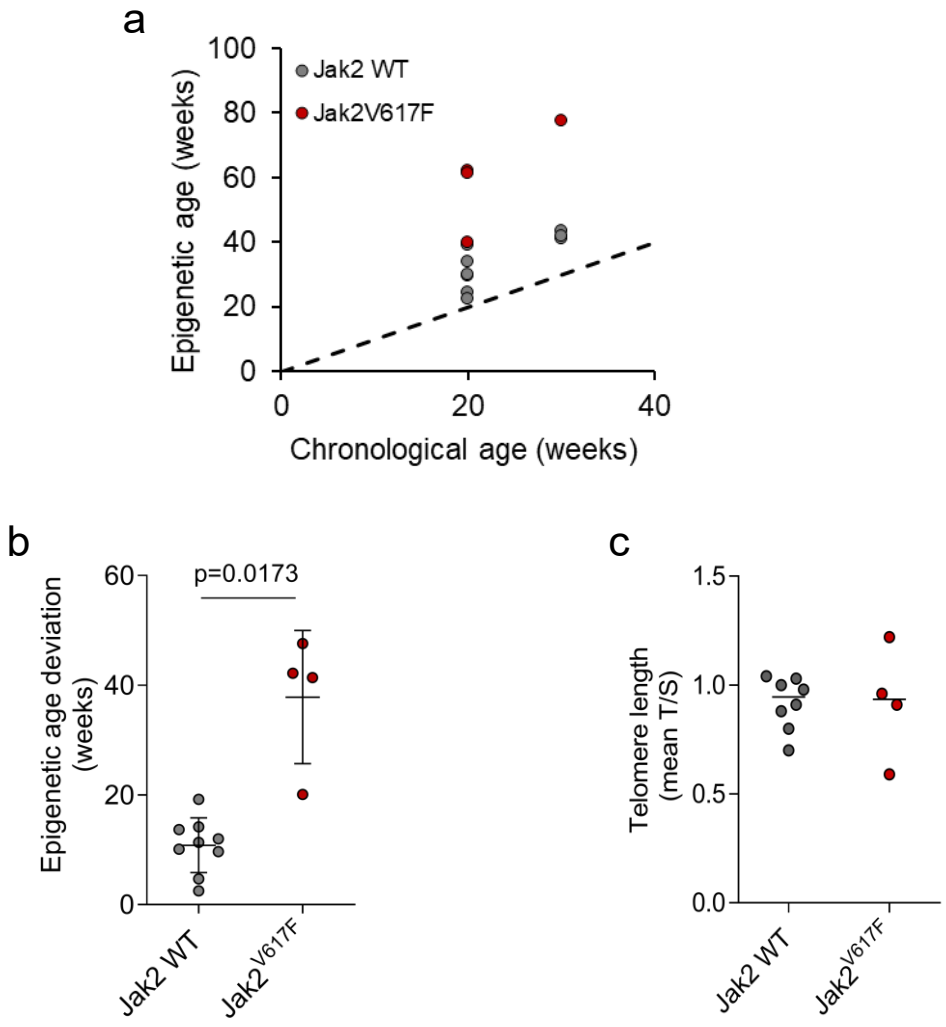

Figure 39. Mouse model to investigate the effect of Jak2 V617F mutation on cellular aging.
a) Epigenetic age in bone marrow derived cells from WT mice (grey) and Jak2 V617F mice (red) is plotted against their chronological age. b) The epigenetic age deviation was compared between both groups. Unpaired Welch's t-test was performed for statistical analysis. c) Telomere length of WT versus Jak2 V617F mice. This figure was in parts adapted from (Vieri et al., 2023).

3.2.5.2 Epigenetic age acceleration in CML mouse model

Chronic myeloid leukemia (CML), a Philadelphia-chromosome positive MPN, causes the fusion of the breakpoint cluster region (BCR) and the gene that encodes for the tyrosine kinase (Abelson murine leukemia; ABL), resulting in a gene encoding the BCR-ABL oncoprotein, which is associated with different types of leukemia (Koschmieder et al., 2005). Bone marrow cells from WT (n = 6) and diseased (n = 6) FVB\N SCLtTA/ Bcr-Abl mice were used to predict epigenetic age. The mean age prediction for WT is 43.9 weeks and for the mutant is 44.6 weeks, and the epigenetic age deviation is slightly higher for the disease phenotype but not significant (WT = 10.7 weeks, mutant = 12.4 weeks; Figure 40b). The age prediction measurements were supported by Juan Perez-Correa.

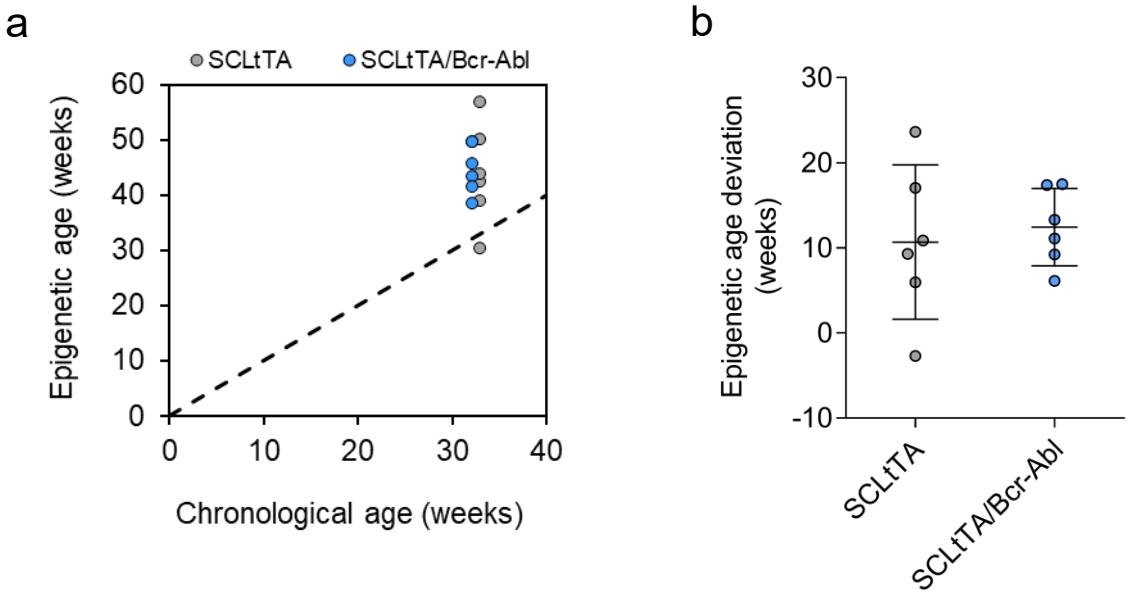

Figure 40. Epigenetic age changes in CML mouse model.
a) Epigenetic age in bone marrow derived cells from WT mice (grey) and CML mice (blue) is plotted against their chronological age. b) The epigenetic age deviation was compared between both groups. Unpaired Welch's t-test was performed for statistical analysis, no statistical significance.

3.2.5.3 Epigenetic age acceleration in PDGFRB mouse model

Platelet-derived growth factor receptor beta (PDGFRB) is a tyrosine kinase receptor that activates the signaling pathway involved in cell growth and differentiation. Chromosomal rearrangement of PDGFRB is associated with hematologic malignancies, including MPN with eosinophilia (Di Giacomo et al., 2022). The Cre+ and +/d mouse models express the mutant form of Pdgfrb, specifically in the HSC. Cre- mice do not express the mutant Pdgfrb and serve as a non-transgenic control. Similarly, Cre+ and +/+ mice represent the WT with normal Pdgfrb expression. Peripheral blood samples were collected from fifty-three WT mice and nine mice expressing Pdgfrb, which were subsequently measured for epigenetic age prediction. The

mutant mice showed an acceleration of epigenetic age compared to the control mice (Figure 41c).

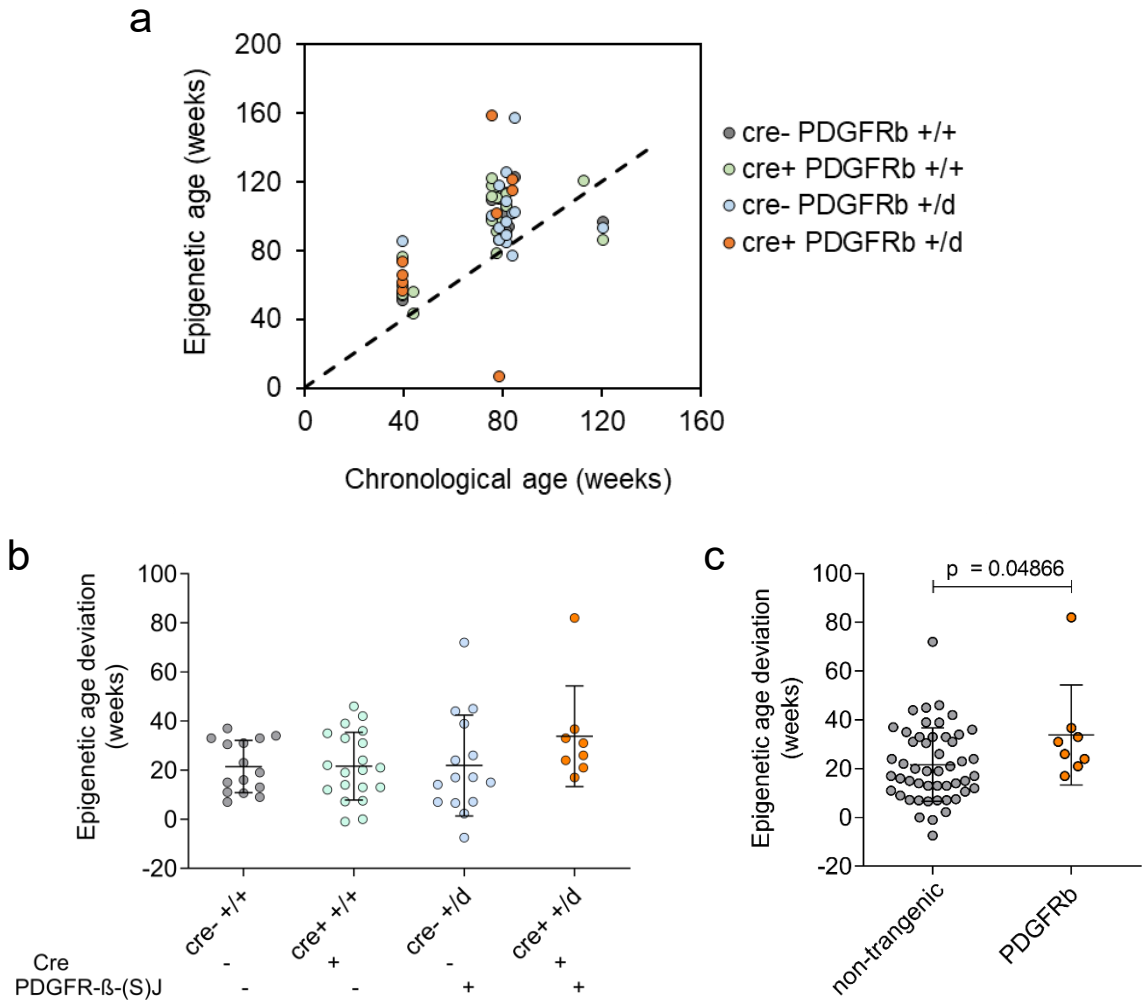

Figure 41. Epigenetic age changes in Pdgfrb mouse model.
a) Epigenetic age in blood cells from WT mice (cre- & +/+ in grey, cre+ & +/+ in green, cre- & +/d in blue) and mutant for Pdgfrb mice (cre+ & +/- in orange) is plotted against their chronological age. b) The epigenetic age deviation was compared between all the groups and c) in both groups of mutant and non-mutant mice. One outlier has been removed from each group and an unpaired Welch's t-test was performed for statistical analysis.

Overall, all disease mouse models showed a tendency towards accelerated epigenetic aging. It is remarkable to observe this difference even within a few samples with different mutations, indicating that age associated DNAm patterns may be a relevant aspect in the pathophysiology of MPN.

3.3 DNA methylation changes in MPN with *JAK2* V617F mutation

There is clear evidence that MPN is associated with aberrant DNA methylations. However, the specific causes of these epigenetic modifications remain unclear. To understand the impact of driver mutations such as *JAK2* V617F on DNA methylation changes, we aimed to systematically analyze DNA methylation profiles in a patient-derived iPSC model. To this end, we used iPSC-derived cells from PV patients with the *JAK2* mutation and directed their differentiation towards hematopoietic progenitor cells.

3.3.1 *JAK2* V617F iPSC differentiated towards to hematopoietic differentiated cells

We used previously established syngeneic induced pluripotent stem cell (iPSC) models from the group of Prof. Martin Zenke (Flosdorf et al., 2024; Satoh et al., 2021). Corresponding iPSC lines were generated from three PV patients with wild type (WT) *JAK2*, heterozygous (het), and homozygous (hom) *JAK2* V617F mutations. Embryonic bodies (EB) were generated from the iPSCs by self-organization using microcontact printing (Elsafi Mabrouk et al., 2022).

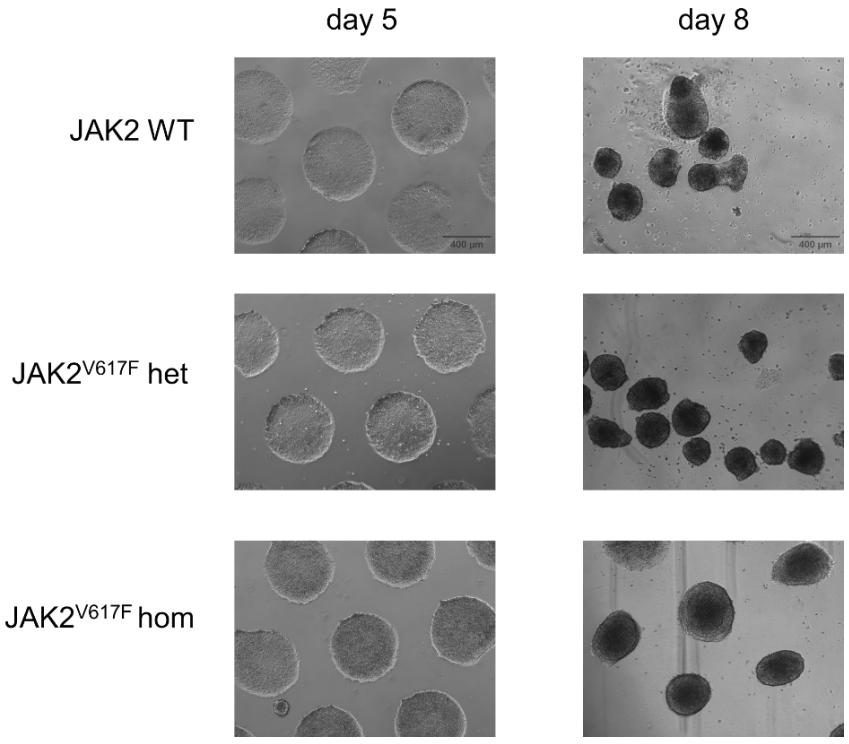

Figure 42. Embryonic body formation of iPSC derived cells.
Exemplary microscopy images of EB generation from all three genotypes: WT, heterozygous (het) *JAK2* mutant, and homozygous (hom) *JAK2* mutant. No clear differences between the clones were observed.

There were no prominent differences in the morphology of the WT and malignant clones in the EB generation (Figure 42). Some clones required a longer period of time to detach from the cell culture plate than others, but this was not exclusive to a specific mutation type. The EBs from PV1 homozygous clone were more dissociated during self-detachment, even when the

experiment was repeated, so we ended up with a lower total number of EBs for this specific clone.

Generated EBs were collected and cultured for 16 days in a gelatine coated plate for hematopoietic cell differentiation. During this period, the endothelial-like morphology observed showed adherence to the plate surface. Additionally, non-adherent cells with a rounded nucleus HSC progenitor phenotype were observed on the cell monolayer. The morphological characteristics of the hemogenic endothelial niche-derived hematopoietic stem cells exhibited a more pronounced phenotype in malignant clones, with patient 2 displaying a particularly distinctive cobblestone-like structure (Figure 43b). Furthermore, the number of cells produced per well on day 16 was found to be higher in mutant clones compared to wild-type clones (data not shown).

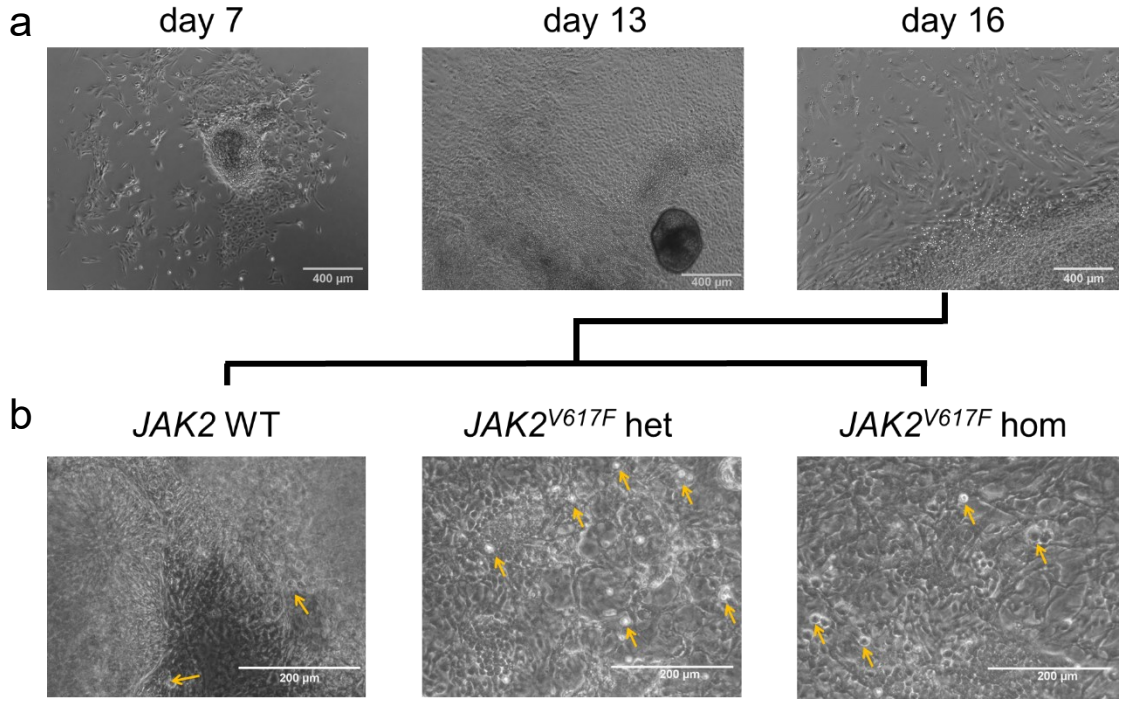

Figure 43. Hematopoietic differentiated cells from EBs.
a) Exemplary microscopic image of one patient derived hematopoietic differentiated cells (iHPCs) from *JAK2* V617F het clone during different days of differentiation. b) Exemplary microscopic image of one patient derived hematopoietic differentiated cells (iHPCs) at day 16 from all three genotypes: WT, het *JAK2* V617F mutant and hom *JAK2* V617F mutant. The hematopoietic stem cells emerged from the hemogenic endothelium niche which formed a typical cobblestone structure (yellow arrows).

3.3.2 Erythroid bias in hematopoietic derived *JAK2* V617F iPSC cells

The iPSCs derived hematopoietic stem and progenitor cells (iHPCs) were collected after 16 days of differentiation and subsequently analyzed for the expression of specific surface markers in order to identify the influence of the mutation on the cell lineages. The mutant iHPCs showed an increase in most hematopoietic markers compared to WT cells, including endothelial marker

CD31, myelomonocytic marker CD33, megakaryocyte marker CD61, erythrocyte marker CD235a, and common leukocyte marker CD45. In contrast, the early hematopoietic progenitor markers such as CD34 and CD117 (c-kit) were not altered (Figure 44a). This difference was further exemplified in a CFU assay, where mutant clones exhibited a bias for erythrocyte and macrophage, and a higher number of CFU colonies compared to the WT cells (Figure 44b). These clones have been previously used in other studies and have been shown to recapitulate the pathognomonic bias toward megakaryocytic and erythroid differentiation of MPN patients (Flosdorf et al., 2024), consistent with our findings.

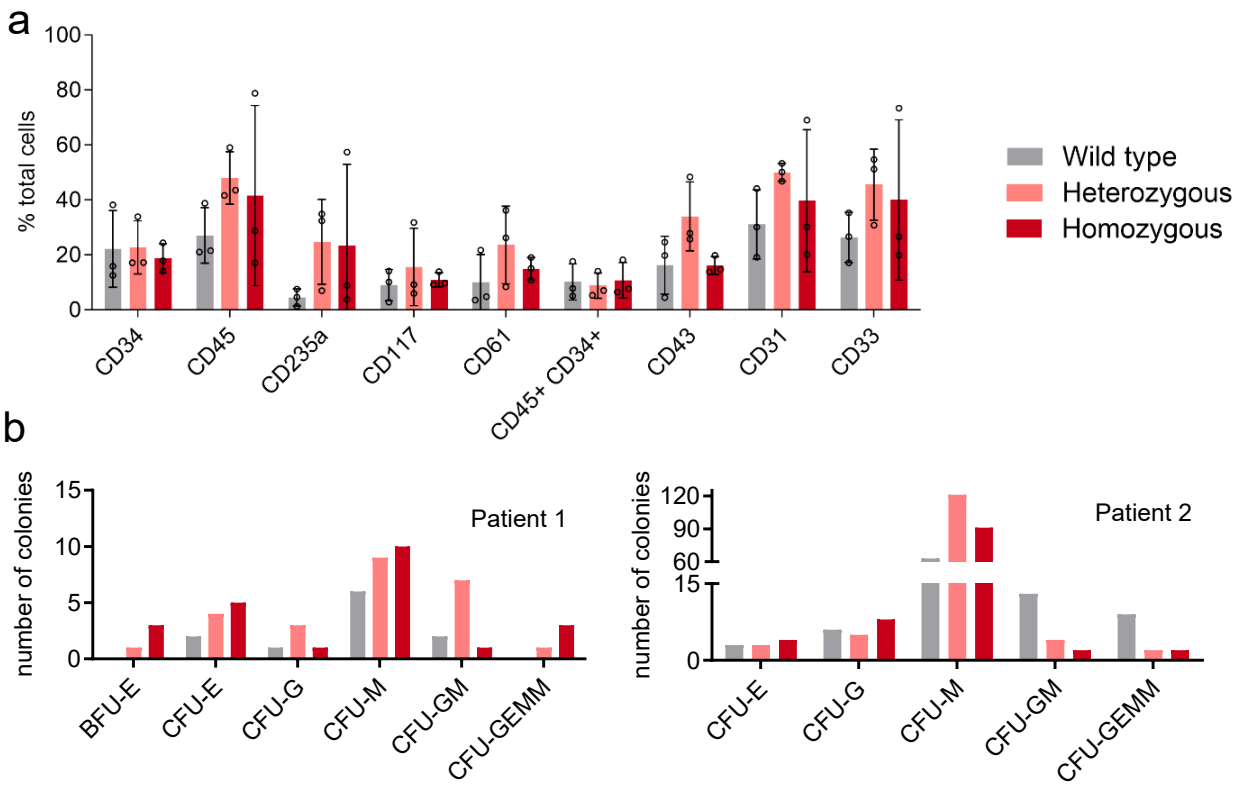

Figure 44. Myeloid bias in the mutant clones derived from hematopoietic differentiated cells.
a) Flow cytometric analysis of hematopoietic surface markers on harvested iHPCs at day 16 of differentiation (n = 3 for each genotype). b) Number of colonies counted for individual colony types after 14 days of colony forming unit (CFU) assays for patient 1 (n = 1) and patient 2 (n = 1) derived iHPCs. CFU-E = CFU erythrocyte; BFU-E = CFU burst forming unit erythrocyte; CFU-M = CFU macrophage; CFU-G = CFU granulocyte; CFU-GM = CFU granulocyte, macrophage; CFU-GEMM = CFU granulocyte, erythrocyte, macrophage, megakaryocyte. *JAK2* WT (grey), *JAK2* V617F het (pink), and *JAK2* V617F hom (red).

We then analyzed the DNAm profiles of all nine iPSCs and their iHPCs after 16 days of differentiation using the Illumina Infinium MethylationEPIC BeadChip. To validate the successful hematopoietic differentiation of iPSCs, the iPSCs and iHPCs were compared. iPSCs are characterized by the expression of pluripotency, for this purpose we utilized two epigenetic signatures such as the Epi-Pluri-Score (Lenz et al., 2015) and the Pluripotency Score (Schmidt et al., 2023).

All iPSCs maintained pluripotency by overlapping with a dataset of other pluripotent cell lines, while iHPCs overall matched the dataset of somatic cell lines (Figure 45a). In addition, the pluripotency score was significantly decreased in iHPCs compared to iPSCs (Figure 45b). The characterization of the three germ layers towards endoderm, ectoderm, and mesoderm markers was deconvoluted using germ layer specific methylation. As expected, iPSCs did not reveal any germ layer specific markers and while iHPCs exhibited mainly the mesoderm markers, they also exhibited other lineages. Furthermore, we observed differences in germ layer markers between the clones (Figure 45c).

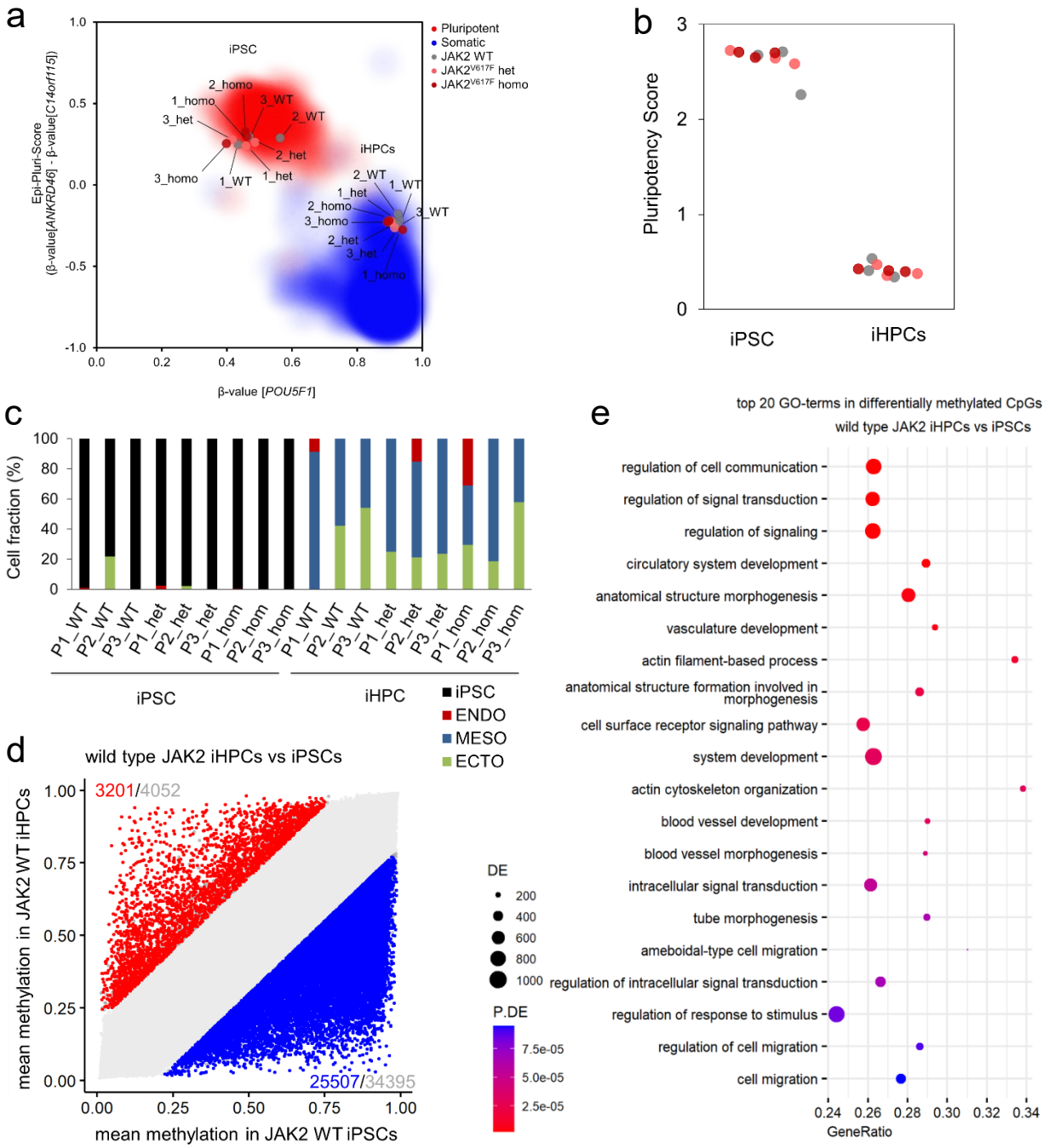

Figure 45. Pluripotency markers of iPSCs and iHPCs by DNA methylation predictions.
iPSCs and iHPCs were compared for a) Epi-pluri score: which analyzed DNA-methylation at three specific CpG sites. One of these CpGs was localized within the pluripotency-associated gene POU5F1 (also known as OCT4). Furthermore, the difference in DNAm levels (β-values) of CpGs in ANKRD46 and C14orf115 was determined and combined as Epi-Pluri-Score. The red and blue clouds refer to DNAm profiles (all Illumina HumanMethylation27 BeadChip platform) of 264 pluripotent and 1,951 non-pluripotent cell preparations, respectively, b) Pluripotency score: DNA-methylation was analyzed at three specific CpG sites. The first CpG is associated with palladin (PALLD, cg00661673), the second with no specific gene (cg21699252) and the third with MYCN opposite strand (MYCNOS, cg21699252) to predict a score, and c) Germ layer tracker: where the differentiation scores were calculated separately for every CpG and represent the difference to the mean methylation values of reference stem cells (Schmidt et al., 2023). d) DNA methylation profiles of WT iPSCs and iHPCs were compared to identify differentially expressed CpGs. The numbers indicate the difference in mean methylation of the cut-off 0.2 in grey and those that are significant in color, with blue indicating hypomethylation and red indicating hypermethylation. e) Gene ontology term analysis of the top statistically significant CpGs that were differentially methylated in both hypo- and hypermethylated genes when comparing WT iHPCs with iPSCs. Biological process terms were considered, and terms with a false discovery rate (FDR) of less than 0.05 were analyzed using the R package missMethyl. Gene ratio is defined as the number of differentially expressed genes (DE genes) divided by the total number of genes in the set. DE is the number of differentially methylated genes. P.DE is the p-value for overrepresentation of the GO term. This figure was in parts adapted from (Flosdorf et al., 2024).

To gain a better understanding of the epigenetic changes that occur during the differentiation to iHPCs in WT, we performed differential DNA methylation analysis with at least a 20 % difference in mean methylation and p-values < 0.05. Comparison of iHPCs with iPSCs resulted in 3,201 hypermethylated and 25,507 hypomethylated significant CpGs (Figure 45d). Gene ontology (GO) analysis of these differentially methylated CpGs showed enrichment of genes associated with the development of anatomical structures, including blood vessels, circulatory systems, and vasculature, as well as cell communication, signal transduction, and cell migration (Figure 45e). This finding is consistent with the endothelial to hematopoietic transition observed during the 3D iPSC hematopoietic differentiation model (Ackermann et al., 2021).

3.3.3 DNA methylation changes in iPSC with *JAK2* V617F

It is known that specific CpG sites gain or lose DNA methylation due to genetic mutations that result in aberrant methylation patterns, a hallmark of cancer (Chen et al., 2017; Esteller, 2005). Therefore, we wanted to see if reprogramming PV cells into iPSCs could potentially reverse these mutation-specific changes in the DNA methylation landscape. To this end, we analyzed the multidimensional scaling plots (MDS plot) of the 10,000 most variable CpG sites and found that the iPSCs tended to cluster based on donor rather than mutation genotype (Figure 46a). This indicates that the iPSCs were still able to capture patient-specific differences. Upon analyzing the mean differentially methylated regions between the WT and mutant iPSCs, no significant CpGs were found and very few differentially methylated sites were present with more than 20 % mean differential methylation (Figure 46b-d). This suggests that both WT and mutant iPSCs show similar patterns of DNA methylation changes and leads to the interpretation that mutation specific methylation changes could be reversed in these clones.

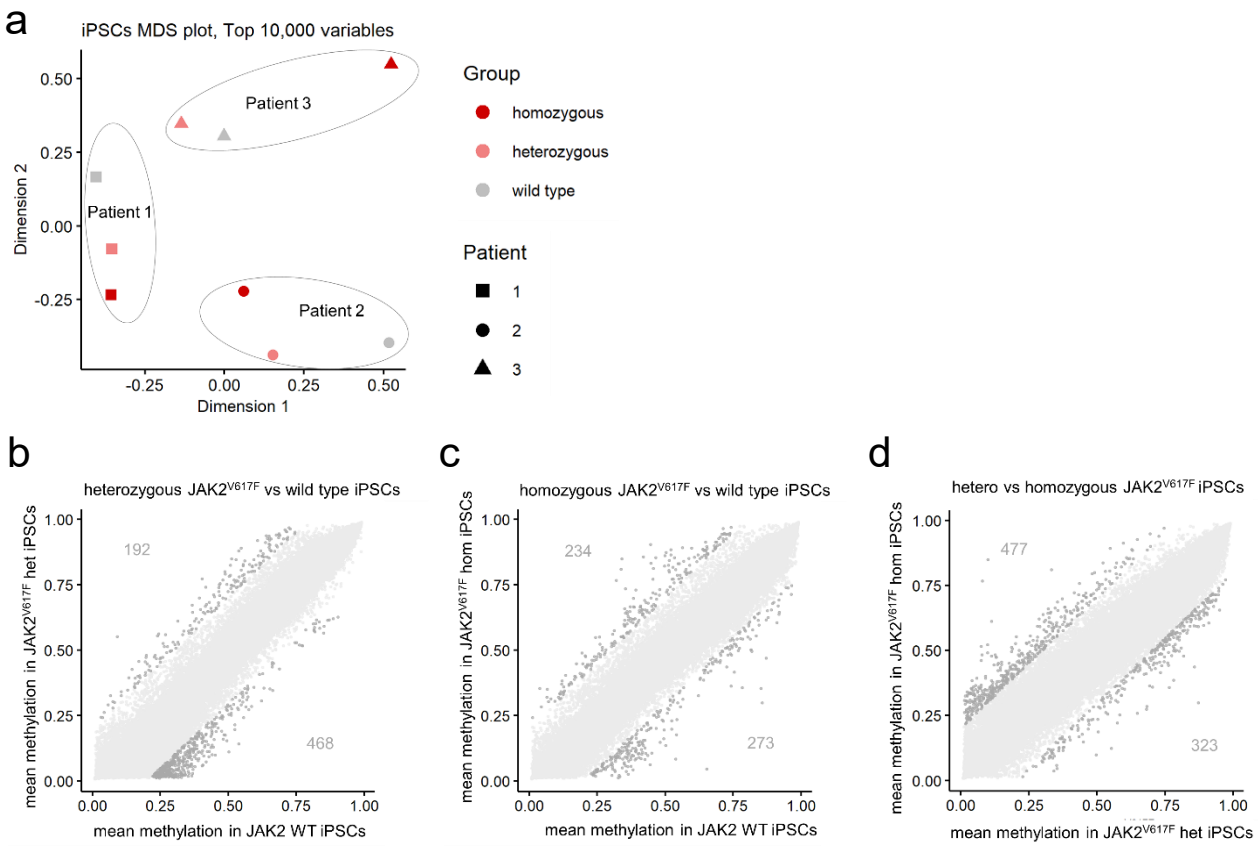

Figure 46. Differentially methylated regions in iPSCs.
a) MDS plot with top 10,000 variables in the iPSC samples alone show differences between the clones. Scatter plot of the mean methylation beta values from b) wild type (WT) iPSCs and *JAK2* V617F heterozygous iPSCs, c) WT iPSCs vs. *JAK2* V617F homozygous iPSCs and d) *JAK2* V617F heterozygous versus homozygous iPSCs are shown. The numbers indicate the difference in mean methylation with a cut-off of 0.2 in grey, at which no CpGs exhibited statistical significance.

3.3.4 DNA methylation changes in hematopoietic cell with *JAK2* V617F

The DNA methylation profiles of iHPCs from WT and mutant clones were compared in order to explore the potential contribution of residual epigenetic memory to the reacquisition of the MPN phenotypic and pathological changes in the differentiated cells. The top 10,000 variable CpG sites were plotted for multidimensional scaling, showed that the iHPCs cluster based on their mutation genotype rather than the donors (Figure 47a), in contrast to what was observed in iPSCs. There were outliers among the 9 clones, such as homozygous iHPCs from patient 3 and WT iHPCs from patient 1. Upon analyzing the mean differentially methylated regions between the WT and mutant iHPCs, no significant CpGs were found (Figure 47b-c). Nevertheless, the distribution of the CpGs among the plots (Figure 47b and c) showed that the CpGs were more clustered around the upper right region, suggesting a higher methylation level in WT iHPCs, while the heterozygous and homozygous iHPCs consistently showed lower methylation levels. The mutant iHPCs exhibited a higher number of hypomethylated CpGs compared to WT, with 6,006 CpGs in heterozygous and 4,612 CpGs in homozygous iHPCs, as well as 3,564 CpGs

shared between both groups. This suggests that certain regions in WT might be associated with gene silencing or regulation due to its hypermethylation, while mutant cells might be transcriptionally active or accessible in those regions due to hypomethylation. Notably, no differences were observed between heterozygous and homozygous iHPCs (Figure 47d). The GO term analysis of the common 3,564 hypomethylated CpGs among heterozygous vs. WT and homozygous vs. WT iHPCs showed an enrichment of genes that were associated with immune system activation, immune response, and cytokine production (Figure 47e). This observation was consistent when considering each individual mutant genotype alone compared to WT iHPCs (Supplemental Figure S5). In contrast, the common 1189 hypermethylated CpGs among heterozygous vs. WT and homozygous vs. WT iHPCs showed no GO term associated genes with FDR less than 0.1.

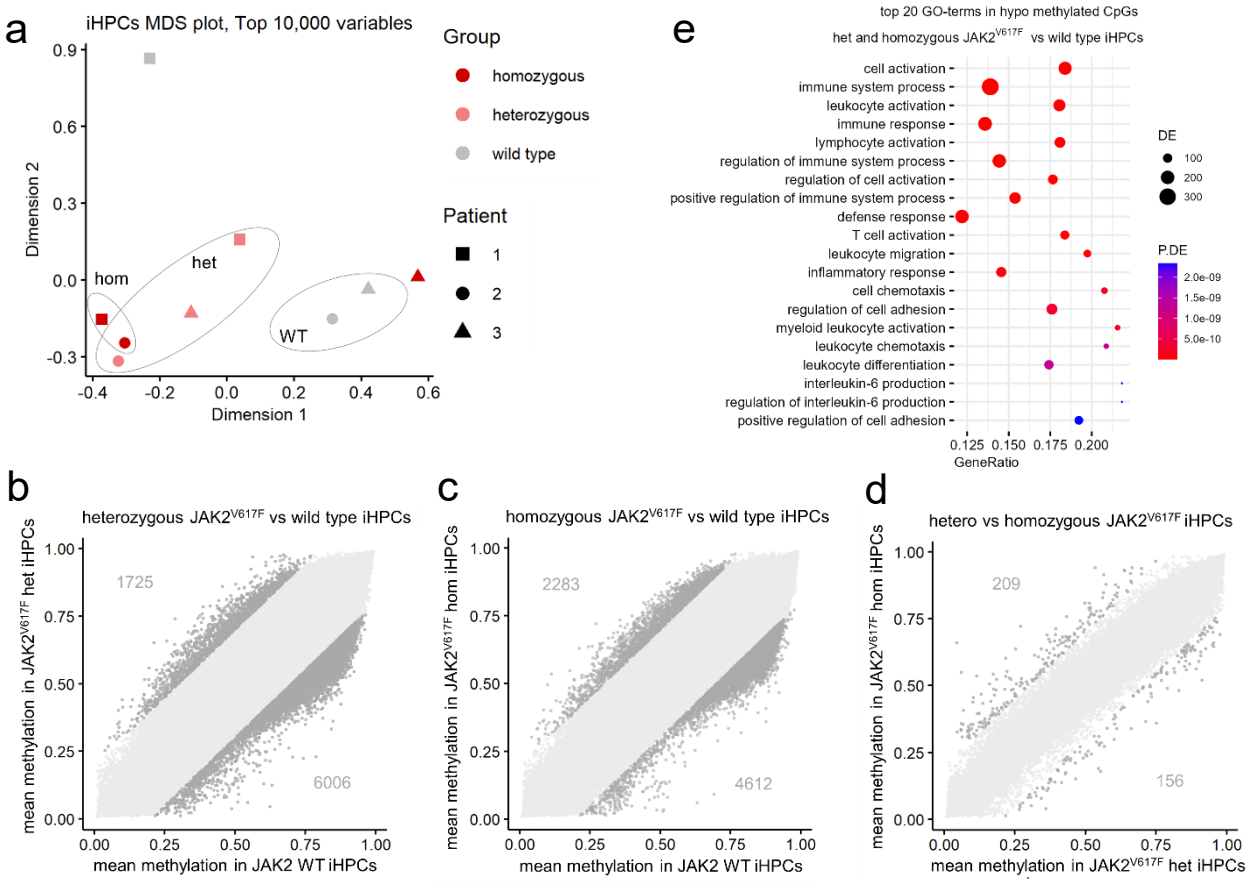

Figure 47. Differentially methylated regions in iHPCs.
a) MDS plot with top 10,000 variables in the iHPCs samples show differences between genotypes rather than between patients. Furthermore, mean methylation values of CpGs when compared between b) wild type (WT) iHPCs vs. *JAK2* V617F heterozygous iHPCs, c) WT iHPCs vs. *JAK2* V617F homozygous iHPCs, and d) *JAK2* V617F heterozygous vs. homozygous iHPCs are shown. The numbers in grey indicate the difference in mean methylation at a cut off of 0.2, at which no CpGs exhibited statistical significance. e) GO term analysis of the top hypomethylated 3564 CpGs that are common between heterozygous and homozygous iHPCs compared to WT iHPCs. Biological process terms were considered, and terms with a false discovery rate (FDR) of less than 0.1 were analyzed using the R package missMethyl. GeneRatio is defined as the number of differentially expressed genes (DE genes) divided by the total number of genes in the set. DE is the number of differentially methylated genes. P.DE is the p-value for overrepresentation of the GO term.

We assume that the small sample size (n = 3 per genotype) and the presence of outliers (Figure 34a) did not lead to statistical significance in the data of mean methylation differences between WT and mutant iHPCs. Therefore, to explore beyond mean methylation, we performed a comparison between each patient's mutant iHPCs and their respective WT iHPCs individually. A subsequent analysis focused on the CpGs that consistently showed differential methylation patterns, either an increase or decrease, across all patients. In order to capture even small differences, a 10 % of methylation change threshold was used. A total of 6,733 and 1,552 CpG sites were identified as 10 % hypomethylated and hypermethylated respectively in the heterozygous iHPCs compared to WT across all patients (Figure 48a and c). Similarly, 189 and 165 CpGs were 10 % hypomethylated and hypermethylated respectively in homozygous iHPCs compared to WT (Figure 48b). The higher overlap of CpGs in the heterozygous iHPCs clones could be due to the fact that all three heterozygous iHPCs were clustered together in the MDS plot, whereas this is not the case for the homozygous clones. Overall, 34 CpGs were commonly hypomethylated in both heterozygous and homozygous iHPCs compared to WT. Similarly, 35 CpGs that were commonly hypermethylated in both the heterozygous and homozygous iHPCs compared to WT. Interestingly, the hypermethylated CpGs in the heterozygous clones were not hypomethylated in the homozygous clones, and vice versa, when using the 10 % cut off.

The genomic positions of these shared hyper and hypomethylated CpGs among patients showed that the hypermethylated regions were highly significantly enriched in gene bodies, intergenic regions as well as open sea for both heterozygous and homozygous mutant clones. While hypomethylated CpGs were prominently enriched in the upstream promoter-regions (TSS1500 and TSS200) for the heterozygous mutant clones. Furthermore, it was enriched in CpG islands and the region of 2 kb flanking regions of CpG islands which are termed shore regions, and which were strongly related to gene expression. Whereas hypomethylated CpGs of homozygous mutant clones showed comparatively moderate enrichment in the 5′ untranslated regions (UTRs), gene bodies and intergenic regions (Figure 48e and f). This suggests that the mutant specific hypomethylated CpGs were located in the gene transcription sites, potentially leading to disease specific alterations. Gene ontology analysis of these differently methylated regions showed that the hypomethylated regions were associated with inflammatory responses including the production of FasL and the hypermethylated regions were associated with angiogenesis (Supplemental Figure S6).

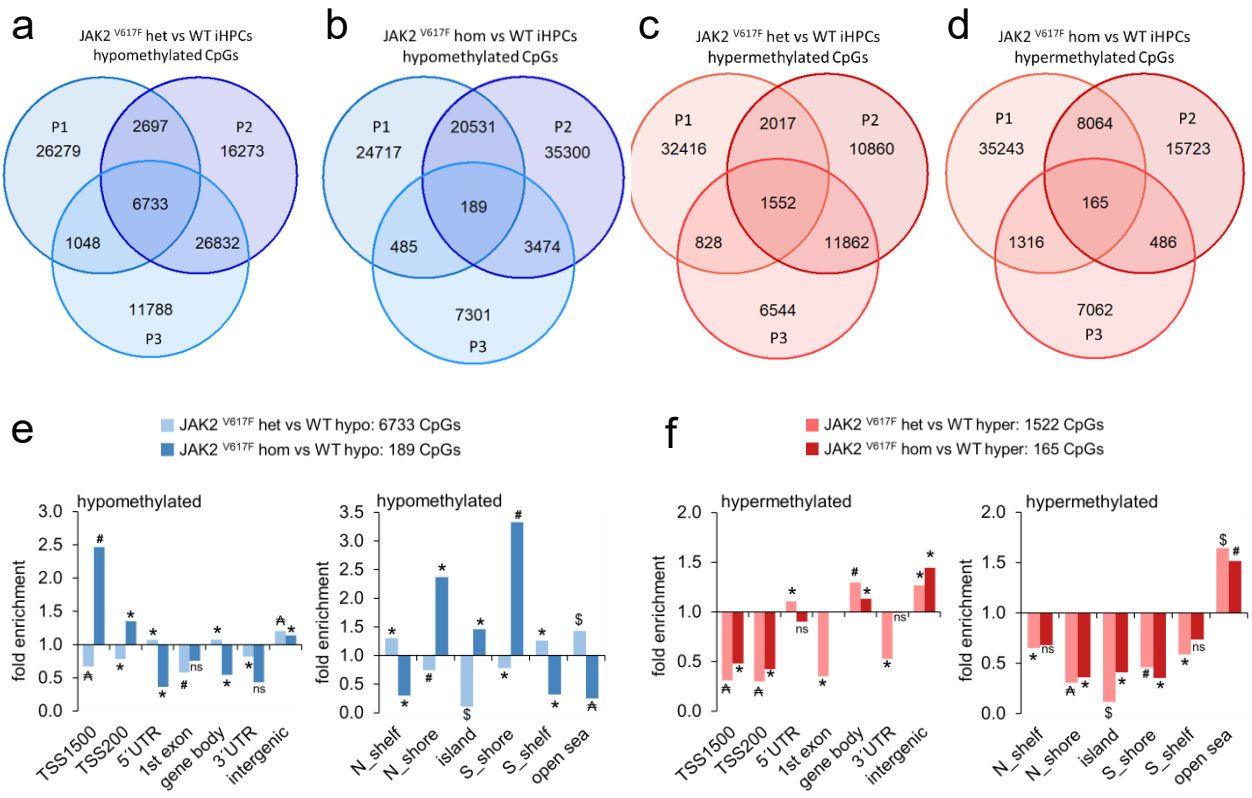

Figure 48. The common CpGs between JAK V617F heterozygous and homozygous clones compared to WT iHPCs.

Venn diagrams show the overlap of the number of CpGs that are commonly hypomethylated across all patient samples when compared to a) heterozygous vs. WT iHPCs and b) homozygous vs. WT iHPCs. Similarly, the number of CpGs that are commonly hypermethylated across all patient samples when compared to c) heterozygous vs. WT iHPCs and d) homozygous vs. WT iHPCs is shown. The methylation β-value cut off was set at < -0.1. e) Enrichment of hypomethylated CpG sites in heterozygous (from a) and homozygous clones (from b) in different genomic regions and different locations relative to CpG islands. f) Enrichment of hypermethylated CpG sites in heterozygous (from c) and homozygous clones (from d) in different genomic regions and different locations relative to CpG islands. Hypergeometric distribution: * represents $P < 0.05$, # represents $p < 10^{-10}$, ~~A~~ represents $p < 10^{-20}$, and $ represents $p < 10^{-100}$.

In addition, we looked at the epigenetic aging of these cells, based on our study we expected that the mutant cells would exhibit an increased age compared to the WT cells. However, we observed a slight tendency for age increase towards the mutant cells with hematopoietic differentiation, but not in the iPSCs (Figure 49). These predictions were overall close to 0 years, as generally observed upon reprogramming. It is important to note that these clocks developed by Horvath for whole blood and pan tissue clocks were not specifically trained for iPSCs and their differentiated cells.

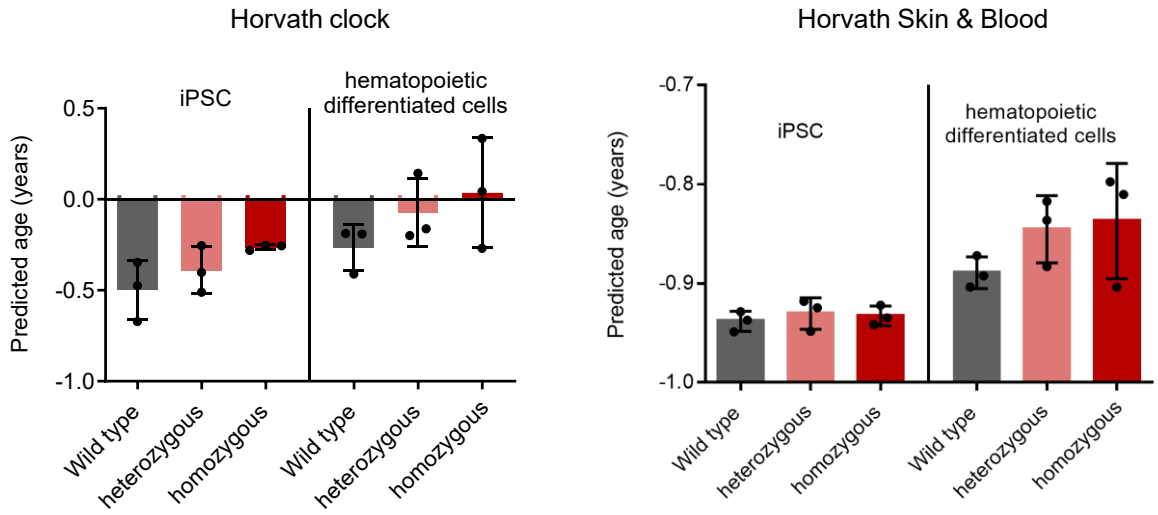

Figure 49. Epigenetic age prediction of iPSCs and their iHPCs.
Epigenetic age prediction was performed on iPSCs and iHPCs of WT, heterozygous and homozygous clones for the *JAK2* V617F mutation using the a) Horvath clock trained based on 336 CpGs in blood and the b) Horvath skin and blood clock trained on 391 CpGs in pan tissues. This figure was adapted from (Vieri et al., 2023).

3.3.5 Comparison of patient samples with *JAK2* V617F mutation to the iHPCs with *JAK2* V617F mutation

To better understand if the DNA methylation changes observed in *JAK2* V617F mutant iHPCs are comparable to those observed in MPN patients with the same *JAK2* V617F mutation, we analyzed PBMCs from 10 PMF patients carrying *JAK2* V617F mutations and 10 age matched healthy controls. The patient raw data was analyzed by Esra Dursun Torlak using a similar normalization method performed for iHPCs and iPSCs data. PMF patients showed 2198 hypermethylated CpGs and 5322 hypomethylated CpGs with more than 20 % differentially methylated and a p-value less than 0.05, in comparison to healthy controls (Supplemental Figure S7), after filtering out for the similar CpG sites in all the datasets including JAK2 patient, iHPCs, and iPSCs. These differentially methylated CpGs were further compared for the analysis of the mean methylation values in the iHPCs, where a pronounced hypomethylation was observed in the iHPCs of both heterozygous and homozygous clones in comparison to WT, but this was not prominent in hypermethylated regions (Figure 50a-b). However, these patient specific CpGs showed rather small changes in iPSCs, and they were not specific to hyper or hypomethylated regions (Figure 50c-d). Altogether, the hypomethylated DNA patterns observed in *JAK2* mutant patients are moderately recapitulated in the iHPCs, but not in iPSCs, as expected.

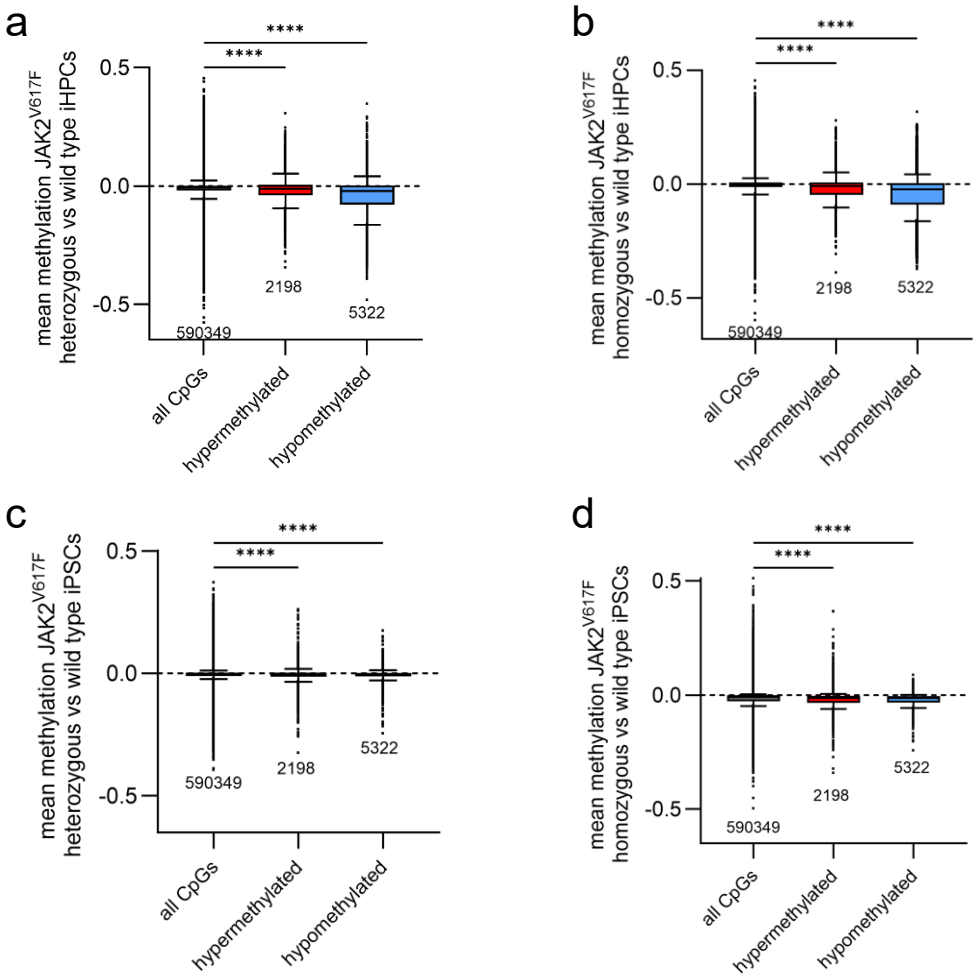

Figure 50. Average methylation difference between *JAK2* V617F iHPCs with PMF patients harboring *JAK2* V617F mutation.

CpGs that show a significant difference in mean DNA methylation for hyper- and hypomethylated CpGs between *JAK2* V617F PMF and healthy control are compared to see if the methylation changes follow a similar pattern in iHPCs from a) *JAK2* V617F heterozygous compared to their WT controls and for b) *JAK2* V617F homozygous vs. WT iHPCs. Similarly, in iPSCs from c) heterozygous vs. WT and d) homozygous clones compared to their WT controls. One-way ANOVA was performed to assess statistical significance; ** represents P ≤0.01, *** represents P ≤0.001, and **** represents P ≤0.0001.

Furthermore, we compared the significantly differentially methylated CpGs in patient samples to iHPCs with *JAK2* V617F mutation and identified that they share a significant number of hypomethylated CpGs. Specifically, heterozygous iHPCs showed 328 hypomethylated CpGs and homozygous iHPCs showed 323 hypomethylated CpGs compared to their WT control. Notably, both heterozygous and homozygous iHPCs shared 243 hypomethylated CpGs out of a total of 408 CpGs. In contrast, only a few shared hypermethylated CpGs were observed between mutant iHPCs and PMF samples (Figure 51a-b). Consistent with the previous results, iPSCs showed a very low number of shared differentially methylated CpGs compared to PMF patient samples and their respective WT controls (Figure 51c-d).

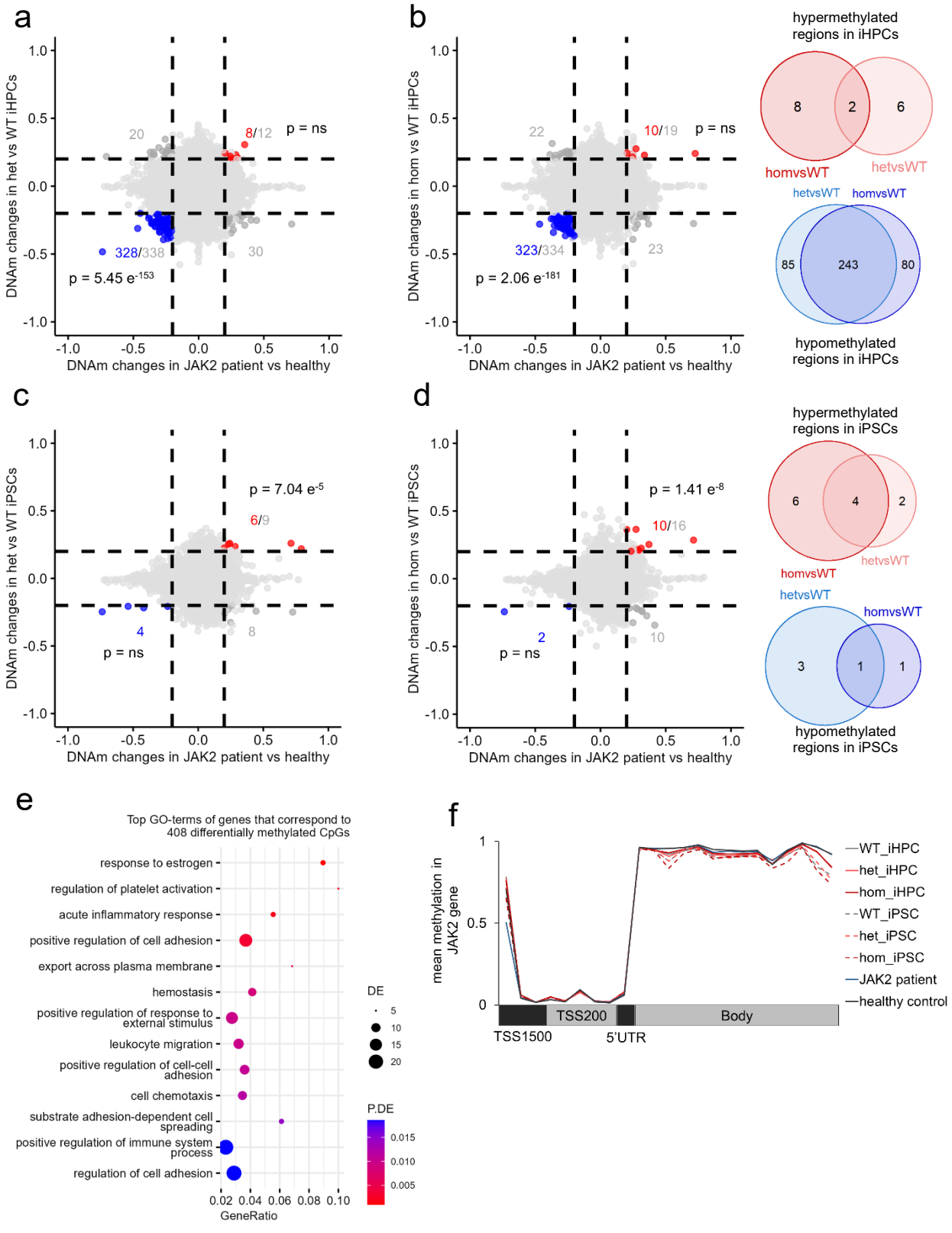
a
DNAm changes in het vs WT iHPCs
DNAm changes in JAK2 patient vs healthy
20
8/12
p = ns
328/338
30
p = 5.45 e-153
b
DNAm changes in hom vs WT iHPCs
DNAm changes in JAK2 patient vs healthy
22
10/19
p = ns
323/334
23
p = 2.06 e-181
hypermethylated regions in iHPCs
8
2
6
homvsWT
hetvsWT
hetvsWT
homvsWT
85
243
80
hypomethylated regions in iHPCs
c
DNAm changes in het vs WT iPSCs
DNAm changes in JAK2 patient vs healthy
p = 7.04 e-5
6/9
4
8
p = ns
d
DNAm changes in hom vs WT iPSCs
DNAm changes in JAK2 patient vs healthy
p = 1.41 e-8
10/16
2
10
p = ns
hypermethylated regions in iPSCs
6
4
2
homvsWT
hetvsWT
hetvsWT
homvsWT
3
1
1
hypomethylated regions in iPSCs
e
Top GO-terms of genes that correspond to 408 differentially methylated CpGs
response to estrogen
regulation of platelet activation
acute inflammatory response
positive regulation of cell adhesion
export across plasma membrane
hemostasis
positive regulation of response to external stimulus
leukocyte migration
positive regulation of cell-cell adhesion
cell chemotaxis
substrate adhesion-dependent cell spreading
positive regulation of immune system process
regulation of cell adhesion
0.02 0.04 0.06 0.08 0.10
GeneRatio
DE
5
10
15
20
P.DE
0.015
0.010
0.005
f
mean methylation in JAK2 gene
TSS1500
TSS200
5'UTR
Body
WT_iHPC
het_iHPC
hom_iHPC
WT_iPSC
het_iPSC
hom_iPSC
JAK2 patient
healthy control

Figure 51. DNA methylation changes of *JAK2* V617F iHPCs and iPSCs compared to PMF patients harboring *JAK2* V617F mutation.

Comparison of significantly differentially methylated CpGs between *JAK2* patient and healthy control with a) heterozygous iHPCs vs. WT iHPCs, b) homozygous iHPCs vs. WT iHPCs, c) heterozygous iPSCs vs. WT iPSCs, and d) homozygous iPSCs vs. WT iPSCs. Blue - hypomethylated regions, red - hypermethylated CpGs shared by both groups and the other CpGs that do not belong to these groups are shown in grey. Venn diagram represents the common CpGs between het vs. WT and hom vs. WT for hypomethylation and hypermethylation independently. Blue - hypomethylated regions and red - hypermethylated CpGs. e) Gene ontology analysis of all hypomethylated 408 CpGs shared between *JAK2* patient vs. healthy and *JAK2* mutant iHPCs vs. WT iHPCs. Biological process terms were considered and were analyzed using the R package missMethyl. GeneRatio is defined as the number of differentially expressed genes (DE genes) divided by the total number of genes in the set. DE is the number of differentially methylated genes. P.DE is the p-value for overrepresentation of the GO term. f) The mean methylation values for CpGs within the genomic location of *JAK2* gene are shown for *JAK2* V617F patient samples, healthy control, and *JAK2* V617F iHPCs and iPSCs.

Gene ontology analysis of these commonly hypomethylated CpGs showed that they were enriched in genes associated with platelet activation, blood coagulation and megakaryopoiesis (Figure 51e). This suggests that mutant iHPCs partially recapitulate the epigenetic changes observed in PMF patients with the *JAK2* V617F mutation, particularly in the hypomethylated regions. Nevertheless, no significant methylation changes were observed in the *JAK2* gene locus when comparing the *JAK2* mutant cells with the WT controls (Figure 51f).

In conclusion, the *JAK2* V617F iPSC derived hematopoietic differentiated cells showed erythrocyte bias and served as a suitable model for studying the *JAK2* mutation. However, no significant alterations in DNAm levels were observed when WT and mutant iHPC clones were compared. The hypomethylated CpGs among the iHPCs and PMF populations indicate that methylation changes do not evoke significant mutation associated epigenetic modifications, but rather contribute to play a role in the activation and regulation of the immune system and to some extent in cell lineage differentiation.

4. Discussion

4.1 Tackling healthy aging and increasing longevity

4.1.1 Cellular aging biomarkers in healthy adults

Unravelling the complex biological processes underlying cellular aging is crucial to successfully tackle age related diseases. Although there is no single gold standard for biological aging, in this thesis we compared several cellular aging factors, including epigenetic age and cellular senescence between young and old healthy blood cells. Since the first described epigenetic age predictors in 2011, numerous generations of clocks have been developed for various applications, including forensics and for particular diseases, providing information on health or disease state (Bell et al., 2019; Koch & Wagner, 2011). However, most of these clocks were based on many CpGs with the use of bead chip arrays, but use of new target assays with few CpGs are cost-effective, easier applicable and less labor intense (Han et al., 2020). To this end, we used three age-associated CpGs to predict epigenetic age in blood, selected from the 9 CpG model from a previous work (Han et al., 2020). These CpGs showed highest correlation with age, with two CpGs, in the region of *FHL2* and *PDE4C* which become hypermethylated and one CpG in *CCDC102B* which becomes hypomethylated upon aging. Our results show that the new targeted 3 CpG method can be used to predict the epigenetic age with less deviation. Yet, a few outliers were observed, which could be due to the fact that the CpGs in the model only considered a linear correlation with the chronological age, whereby age-related changes could also be accelerated in either early or late adulthood (Kananen et al., 2016). A longitudinal study of over a 12 year follow up period of young adults showed that the increase in biological age can be effectively predicted by lower physical performance and cognitive decline (Belsky et al., 2015). This underscores the importance of refining prediction models to include CpGs that correlate not only with chronological age but also with deviations in age-related changes (Bell et al., 2019). Recent advances have been employed to model the dynamic changes in methylation with the pseudotime trajectory and epigenetic state based on the similarities between the samples rather than chronological age. This model showed an association between the age associated molecular changes and mortality risk (Lapborisuth et al., 2022), highlighting the potential for more improved models to provide deeper insights into the aging process.

Age associated DNAm changes are studied using many technologies, including Illumina bead chip array, whole genome bisulfite sequencing to targeted assays using pyrosequencing, and ddPCR. Most of these are from bulk cells which only gives an overall methylation value between 0 to 1 or 0 to 100 %. This hides the changes in individual single cell or single DNA strand information. To better understand this heterogeneity, we used barcode amplicon sequencing.

This is a high-resolution method, which we used to obtain not only mean methylation values but also measure methylation levels in the neighboring CpGs on a single cell level from individual DNA strands of the target region in a window frame of about 250 bp. Using this method allowed us to predict the age for each single strand DNA as described before (Han et al., 2020). When examining the DNAm patterns of healthy individuals across distinct age groups, we observed that the DNAm patterns of specific age-related regions showed increased diversity of regional stochastic patterns with age (Figure 14). A recent study showed a nonlinear change in heterogeneity, indicating that the global heterogeneity occurs most rapidly in youth and slows down by old age (Karetnikov et al., 2024). This led us to question why DNA methylation in cells becomes more heterogeneous with age. One hypothesis is the phenomenon known as epigenetic drift. During aging, the majority of CpG islands that are initially not methylated gain methylation with time and regions with CpG sites that are initially heavily methylated lose methylation due to the disruption in the DNA methylation pattern (Issa, 2014; Teschendorff et al., 2013). In our study, we investigated this phenomenon by measuring the n-score between neighboring CpGs, which shows the increasing disorder of methylation with age. Other studies have shown that Jensen-Shannon entropy can be used to understand the heterogeneity. The increase in entropy of a CpG means that the methylation state is less predictable, and extreme methylome entropy showed a correlation with accelerated age (Hannum et al., 2013). Recent studies have shown that changes in epiallele distribution are responsible for the correlation between increased entropy and aging. As stem cell replication is the primary driver of methylation changes with age in adult tissues, this is exclusively an aging phenomenon that can be seen across different tissues (Vaidya et al., 2023). Further methods to analyze single DNA strand methylation are important in future to study if these DNAm patterns correlate with stem cell replication errors.

While cellular aging and senescence are not identical, the two processes are clearly interlinked (Wagner, 2019). To further exemplify, we compared old and young PBMC cells for senescence marker C12FDG, a β-galactosidase fluorescent substrate. We saw a trend towards high number of senescent cells in adults with progressing age in both PBMCs and lymphocytes (Figure 20). Similarly, a recent study has shown that the percentage of circulating C12FDG positive PBMCs is associated with the increase in age and serum biomarkers associated with senescence (Hambright et al., 2024). The increase in accumulation of senescent cells with age has been linked to metabolically activity, as these cells secrete senescence-associated secretory phenotype (SASP) factors leading to tissue disruption, fibrosis and inflammation (Ellison-Hughes, 2020). Senescent cells not only cause functional decline but also through their paracrine activities and long-term persistence, lead to the death of neighboring healthy cells (Overholtzer, 2019). There are substantial challenges in detecting senescent cells due to the lack of a specific marker which can be applied to a large variety of cell types and senescence

types (Suryadevara et al., 2024). Measuring the state of cellular senescence with either a single marker or at a single point in time can lead to incorrect conclusions. For example, increased senescence associated beta-galactosidase (SA-β-gal) staining may reflect a continuous increase of lysosomal mass and autophagic flux, which may also detect quiescent cells with reversible growth arrest (Ashraf et al., 2023). Recently, a machine-learning algorithms that take advantage of nuclear changes associated with senescence have been developed to quantify senescent cells (Duran et al., 2024). In addition, multiplexed cellular profiling with mass cytometry has shown promise in identifying senescent cells at single cell resolution by p16+ Ki67-BCL-2+ cells (Doolittle et al., 2023). Combination of makers, such as DNA methylation age and the apoptosis marker CD95 have also been proposed as a useful markers to study senescence in some PBMC subsets, including T, B and NK cells (Owen et al., 2023).

Blood cell composition undergoes changes as individuals age. Specifically, in mice it is shown that with age there is a bias between myeloid and lymphoid compartment (Pang et al., 2011; Tharmapalan & Wagner, 2024). Also, studies have shown that certain blood subtypes such as T cells (Jaffe & Irizarry, 2014), B cells (Frasca et al., 2011) decrease with age, while other cells as NK cells increase (Hazeldine & Lord, 2013). Our results are consistent with these findings (Figure 22a), although it should be noted that only a small number of samples were used in this study. In addition, analyzing of the different subsets within the T, B, and NK cells would be beneficial. Studies have shown that aging results in a decrease in the proliferation of T and B cells, whereas there is a decrease in naïve lymphocytes and an increase in memory cells (Nikolich-Zugich, 2018). One reason for that could be that the cells of adaptive immunity undergo dynamic epigenetic modification as they develop and during several immune responses. These accumulated alterations in DNA methylation have been hypothesized to initiate the oncogenic events in these immune cells (Kondilis-Mangum & Wade, 2013). Similarly, the function of NK cells changes with age, with an increase in the CD56dim cell population and a decrease in the CD56bright cells. CD56bright cells are potent cytokine producers, while the CD56dim NK cells are the predominant subset in the blood and are efficient effectors in immune response (Gounder et al., 2018). Further, the percentage of senescent cells in different blood subtypes are necessary, as some studies have shown that the accumulation of senescent cells during aging in mice is associated with an age-related decline in immune system capability (Ovadya et al., 2018). A recent SenMayo study explored changes in RNA expression profile associated with SASP related genes using bone marrow samples, which showed a bias of senescence towards monocyte and macrophage (Saul et al., 2022). Also, an increase number of senescent cells has been observed in PBMC sample of patients with amnestic mild cognitive impairment and Alzheimer's disease and associated with disease progression (Salech et al., 2022). Furthermore, the age range for defining young and old may also be an important aspect to consider. A recent study of plasma proteins across different age groups has shown that the proteins associated

with aging differ between men and women. Furthermore, when using a non-linear model to quantify the proteomic changes, three distinct main clusters were identified at the ages of 34, 60, and 78 (Lehallier et al., 2019). By underlying the age associated discrepancies in blood compositions, it may be foreseeable in the future to detect bias in the stem cell hierarchy and predict the perturbations in stem cell fate decisions that could eventually lead to a disease.

4.1.2 Senolytic compounds reduce epigenetic age and senescence markers

There have been several studies which utilized different methods to increase longevity in human and mice. Studies on mice with heterochronic parabiosis model showed that the systematic administration of plasma transfusions from young mice can rejuvenate aged mice by improving cognitive function and tissue regeneration (Villeda et al., 2014). Another significant discovery of the mTOR inhibitor rapamycin in 2009, which has been shown to extend the life span of mice, has opened up new opportunities to maximize the lifespan of humans (Harrison et al., 2009; Selvarani et al., 2021). In recent years, senolytic has emerged as a promising approach to eliminate senescent cells. A very small percentage of senescent cells is already enough to cause physical dysfunction in mice (Xu et al., 2018). The removal of senescent cells by the senolytic drug ABT263 has been shown to rejuvenate aged tissue stem cells in mice (Chang et al., 2016). Preclinical studies in mice and clinical studies in human showed that senolytics help to eliminate senescent cells and improve age related conditions and chronic diseases (Kirkland & Tchkonia, 2020; Rad & Grillari, 2024). In most clinical cancer trials, senolytics are used as a combination therapy that helps to counteract drug resistant cells. Most of the *in vitro* studies performed so far are based on modelling the senescence system by artificially inducing DNA damage through radiation or inflammatory cytokines to show that senolytics have the potential to eliminate these cells (Veronesi et al., 2023). There is a lack of studies to quantify and understand the senolytics treatment in primary blood samples and especially in the healthy aging humans. Therefore, we hypothesized that targeting these cells with senolytic drugs may have the potential to reduce epigenetic aging and other senescence associated markers.

For this purpose, we focused on nine senolytics drugs that have already been shown in other studies to target senescent cells and that were also chosen based on different mechanism of action that led the cells to apoptosis (as described in section 1.3.3.1). Our findings validate the accumulation of moderately higher senescence in old adults than in young adults and it can be specifically targeted by senolytics. Interestingly, we observed clearance of C12FDG positive senescent cells with some drugs and in particular a significant decrease with RG7112, nutlin-3a and JQ1 (Figure 20b). However, these results were independent of the age of the sample. Subsequently, the gene expression of CDKN2A (p16INK4a) showed a clear decrease upon treatment with all four compounds. There is increasing evidence for a correlation between p16 and chronological age (Tsygankov et al., 2009), and the elimination of p16 positive cells in mice

resulted in an expansion of lifespan (Baker et al., 2016). It was anticipated that p21 would be upregulated in senescent cells compared to those treated with senolytics. However, the observed gene expression of CDKN1A (p21) and p53 in the samples was less consistent. P21 expression has been previously discussed to be associated with a generic DNA damage response and regulated by direct transactivation via p53, which makes it difficult to use as a unique senescent marker (Hernandez-Segura et al., 2018). It is also important to better understand the relevance of cell cycle division for senescence and elimination by senolytics (Tripathi et al., 2021). The use of senolytics by removing nonfunctioning aged cells from the heterogeneous cell population and creating a microenvironment that favors the functioning cells by reducing inflammation, opens up new potentials for healthy aging and prevent the disease onset.

In addition, a striking decrease in epigenetic age was observed for some senolytic drugs in both old and young adult derived PBMCs, even with the small number of samples. We see an effect on the selected drugs, i.e., a significant decline in epigenetic age for JQ1 at high concentration, RG7112 at both concentrations and AMG232 at high concentration in PBMCs (Figure 18b). Validating our results with a substantial number of samples is required and adjusting the drug dosage for each individual would be beneficial to target them efficiently. Of the four drugs that showed an overall effect on both epigenetic age and cellular senescence, JQ1 is a potent inhibitor of the BET family that showed potential benefit in the treatment of obesity by reducing fat mass (Fornelli et al., 2024), and it also removed senescent cells in human fibroblasts induced by a related chemotherapy drug via ferroptosis, mediating an iron-dependent programmed cell death (Go et al., 2021). The other three of the four drugs, RG7112, AMG232 and nutlin-3a, belong to MDM2 inhibitors, which interfere with the interaction between p53 and MDM2 and lead to a stabilized p53 that promotes cell apoptosis. Apart from the tumor and hematological studies, RG7112 has also been shown to improve low back pain by removing senescent cells in the intervertebral disc and improving tissue homeostasis, and combination therapy with two senolytics made the effect even more pronounced (Cherif et al., 2020; Mannarino et al., 2023; Riessland & Orr, 2023). AMG232, also known as KRT 232, has not been specifically studied on aging research, even though it is currently being used in numerous clinical trials in solid tumors and hematological malignancies such as AML and myelofibrosis (Verstovsek et al., 2022). In contrast, nutlin-3a is used in many age related studies, e.g. to protect the anterior surface of the eye from SARS-CoV-2 infection by p53 activation (Zauli et al., 2022), also as a therapeutic target for age related muscular degeneration, where treatment resulted in clearance of senescent cells and improved retinal degeneration in a mouse model (Chae et al., 2021). Either way, impact of senolytic compounds on age-associated biomarkers does not reflect safety and effectiveness of senolytics on aging of the organism, which still remains to be vigorously tested *in vivo*.

Interestingly, treatment with senolytics led to a relative change within blood cell type composition. A significant decrease in NK cells upon treatment was observed. This led us to hypothesize that senolytics enhance the ability to identify and eliminate senescent cells that might be susceptible to certain cell types by altering the cytokine profiles. Recent studies have revealed that NK cells play a crucial role in immunosurveillance of senescent cells through the granule exocytosis pathway. Senescent cells upregulate the expression of the NKG2D receptor ligands MICA and ULBP2, independently of the stimuli that trigger senescence, allowing interaction with NK cells and facilitating the effective clearance of senescent cells (Sagiv et al., 2016). In addition, an age related decline in cytokine production also contributes to NK cell dysfunction (Brauning et al., 2022). The impact of senolytics on B cells is not yet fully understood but it is suggested that senolytics may help in the removal of aged B cells (Lorenzo et al., 2023). The observed relative increase in the number of T cells after senolytics treatment might be due to the removal of senescent T cells, which consequently results in the survival of functioning T cells. However, this requires further measurements. It is also possible that the increased T cell numbers might be due to the influence of the overall alteration of the lymphocyte sub compartments. It would be informative to analyze the T cell subsets such as CD8 and CD4 after the senolytics treatment, as several studies have demonstrated that CD8 T cells are responsible for the surveillance of senescent cells (Marin et al., 2023). Furthermore, it has been shown that the treatment of aged mice with senolytics restores the differentiation of CD4 T cells to a more youthful phenotype by counteracting TGF-β production by senescent cells (Lorenzo et al., 2022). Further studies are necessary to determine the effect on functioning cells after treatment and potential alterations in the stem cell population.

The elimination of senescent cells represents a promising therapeutic target for age related phenotypes and diseases. The use of senolytics has been demonstrated to have an improved effect on healthy aging, which could be employed to rejuvenate aged hematopoietic stem cells and modulate senescent immune cells. Overall, an understanding of healthy aging strategies can be used to tackle age-related diseases and to apply similar mechanisms to other diseases, including malignancies.

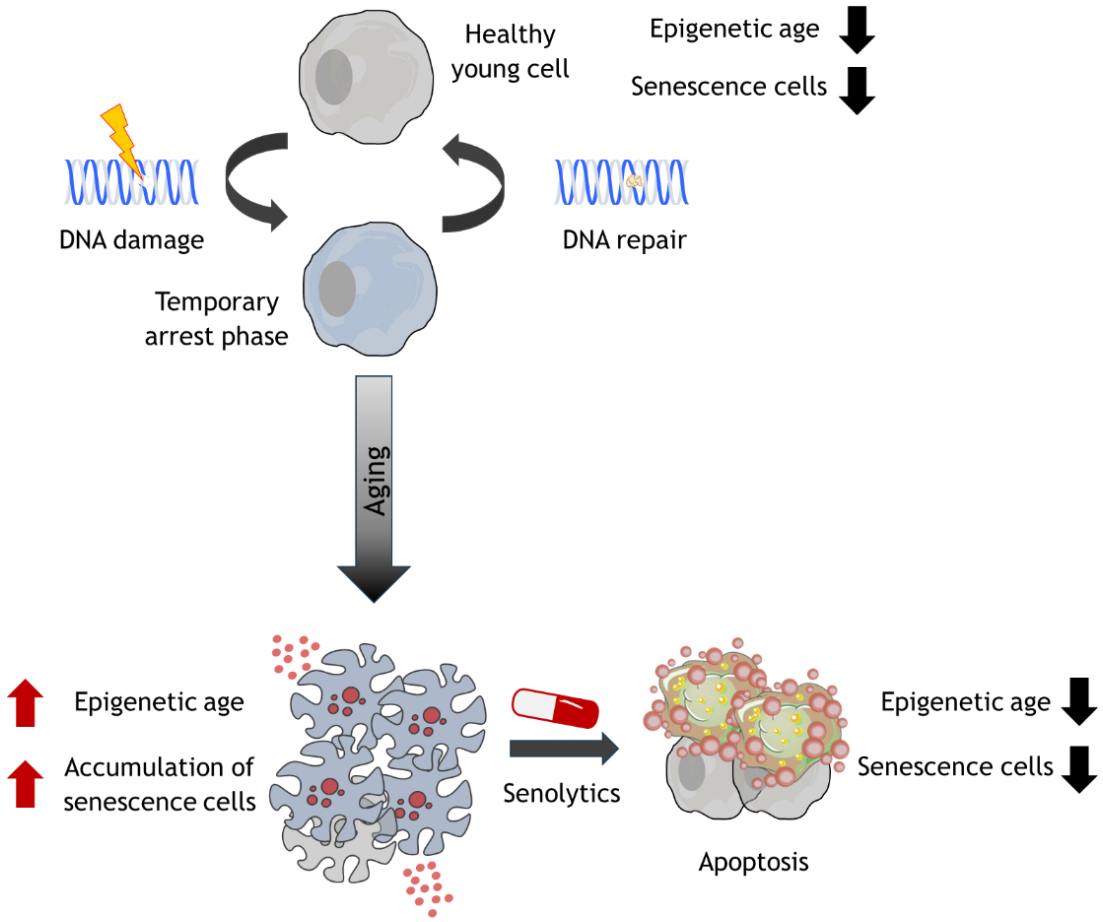

Figure 52. Graphical abstract of aging in healthy blood cells.
In the event of DNA damage, normal cells enter a transient growth arrest, thereby enabling the repair of the damaged DNA. In the event that the damage is not correctly repaired, the affected cells may undergo apoptosis or other forms of regulated cell death. Alternatively, damaged cells may undergo a process of cellular senescence and persist in the body. The accumulation of senescent cells is associated with aging, and the use of senolytics has demonstrated efficacy in removing these cells and reducing epigenetic age.

4.2 Malignant clones are prominently associated with aging and targeting them reduce mutation burden

4.2.1 Cellular aging is specifically accelerated in advanced MPN entity

The association between cancer and aging has been widely discussed, with many studies showing alterations in aging biomarkers, including epigenetic age in solid tumors or hematological malignancies (Berben et al., 2021; Horvath, 2013). Furthermore, changes in aging biomarkers have been associated with cancer incidence and mortality risk (Zheng et al., 2016). In particular, DNA methylation has been associated with disease progression, disease initiation, and the monitoring of drug responses (Nebbioso et al., 2018; Pierce, 2022). This led us to focus on the changes in cellular aging in the hematological malignancy myeloproliferative neoplasm, which is commonly diagnosed in older individuals and the severity of the disease increases with age (Baumeister, Chatain, et al., 2021).

The role of epigenetic dysregulation in the pathogenesis of MPN is widely known. Nevertheless, there are only a very few studies on epigenetic age and its relationship to MPN, which have also not yet been systematically investigated. For this purpose, we used 3 age-associated CpGs in the genes of *PDE4C*, *FHL2* and *CCDC102B* for epigenetic age prediction similar to healthy samples. Our results showed a significant acceleration in epigenetic aging across all 129 MPN samples compared to healthy samples (Figure 23b). In addition, the different MPN entities showed variances in age deviation, reflecting the severity of the disease. Compared to PMF and post-ET/PV MF, ET or PV showed a lower age deviation, and compared to PV, ET showed an even lower age deviation. In a similar study, Mc Phearson and colleagues showed an increase in epigenetic age in PV but not in ET, with methylation age predicted using the pyrosequencing method and our old 3-CpG prediction model with *ASPA*, *ITGA2B*, and *PDE4C* (Weidner et al., 2014). These findings are consistent with our study, which showed a correlation between the *JAK2* V617F mutation allele burden and epigenetic age (McPherson et al., 2019). In addition, we observed a significant increase in epigenetic age deviation among MPN patients with *JAK2* and *CALR* mutation. However, the correlation between increasing allele burden and age was only prominent in patients with *JAK2* mutation (Figure 27b), which might be attributed to the small number of samples with *CALR* mutation.

Furthermore, we observed a tendency towards higher epigenetic age in MPN samples with more than one mutation, although this needs to be proven by a large number of cohorts. Studies have shown that the association of additional mutations in MPN plays a role in clonal evolution and disease progression. Epigenetic mutations such as *DNMT3A*, *TET2*, *IDH1/2*, *EZH2* and *ASXL1* have been associated with changes in the epigenetic landscape (Szybinski & Meyer, 2021;

Vainchenker & Kralovics, 2017). The study on ASXL1 and TET2 in myelofibrosis showed that increased DNA methylation levels are associated with regulatory regions of cancer associated regions (Nielsen et al., 2017). A better understanding of the impact of these mutations on DNA methylation and epigenetic aging could provide valuable insights into the early transformation of MPN. However, there are large variances among some MPN patients who are predicted to be much younger in age. This could be due to the fact that the proportion of mutations varies across different blood compartments in an individual (Van Egeren et al., 2021), similar to DNAm varying from one cell to another (Hernando-Herraez et al., 2019). A focus on specific subsets of PBMCs for epigenetic age prediction could lead to a deeper understanding of the outliers.

Previous studies have primarily focused on identifying patient specific DNA methylation changes in MPN. A study by Perez at al. in 2013 showed comparable aberrant DNAm patterns across ET, PV and PMF subtypes of MPN when compared to healthy individuals, as well as patients with or without *JAK2* mutation (Perez et al., 2013). Similarly, ET samples with different driver mutations demonstrated that the total DNAm profiles did not show clustering based on mutation subtype (Alimam et al., 2021). However, it has been shown that these patterns were more prevalent in transformed MPNs, exhibiting increased differentially methylated regions enriched in genes associated with AML (Perez et al., 2013). Similarly, Nielsen et al. observed a distinct methylation pattern in MF patients with *ASXL1* mutation (Nielsen et al., 2017). Furthermore, a recent study showed that the DNAm profile of bone marrow derived stable and progressive PMF could distinguish fibrotic progression (Lehmann et al., 2021). Collectively, these studies indicate that DNA methylation changes are not prominently linked to MPN phenotype or mutation status. However, methylation changes are more prevalent in advanced MPNs, and the inclusion of additional mutations can influence these epigenetic changes. Interestingly, this is reflected in our epigenetic age predictions between the MPN samples. A systematic analysis of the impact of epigenetic age on the progression of fibrosis or leukemic transmission, and its relationship to driver and additional mutations, may substantiate these findings. Even though survival is a key endpoint in clinical cancer trials, lately, the use of epigenetic age has been discussed to offer a more robust measure for monitoring disease and treatment regimens (Mittal & Vaughan, 2023).

Telomere length (TL) is known as another indicator of biological age, our results on healthy individuals showed a positive correlation between TL reduction and age in granulocytes (Rufer et al., 1999). Furthermore, the differences in TL between the subpopulations of leukocytes are associated with the functionality of the cells during healthy aging. It has been hypothesized that partial telomerase deficiency may be a contributing factor in the inability to maintain telomere homeostasis, which eventually results in the loss of cell replication capacity and the onset of cellular senescence or cell death (Aubert et al., 2012; Lansdorp, 2022). The change in TL is rather disease specific. In specific malignancies, TL is shortened due to the rapid proliferation

and cycling of disease specific hematopoietic stem cells, leading to hematopoiesis exhaustion and chromosomal instability (Brummendorf et al., 2000; Ohyashiki et al., 2002). Conversely, a recent study indicates that longer telomeres and increased epigenetic aging are associated with a higher risk of developing several hematological malignancies (Y. Li et al., 2024). This suggests that increased telomerase activity, resulting in longer telomeres that enable the cells to survive longer and acquire genetic abnormalities over time, may play a role in malignancies (Hosnijeh et al., 2014; Lan et al., 2009).

To analyze the changes in telomere length in our MPN samples, we measured telomere length using Flow-FISH. PMF showed a significant reduction in telomere length in the granulocyte compartment (Figure 24b), reflecting the accelerated epigenetic age deviation. This was not observed in the lymphocyte compartment, which is consistent with the myeloid compartment restriction nature of MPN (Dahlstrom et al., 2015). PMF is considered as the most advanced subtype of MPN, associated with dysregulation of the stem cell niche and altered communication between hematopoietic stem cells and stromal cells, which maintains the neoplastic clone and leads to disruption of normal hematopoiesis (Le Bousse-Kerdiles, 2012). In another study, a few differentially methylated CpGs were found to be capable of distinguishing between stable and progressive fibrosis PMF using an EPIC array, with fibrotic progression showing accelerated epigenetic aging (Lehmann et al., 2021). Previous studies have explored the relationship between TL and MPN subtypes. One study found that TL was shorter in ET, which was also pronounced in mutations harboring *CALR*, *JAK2* and triple negative (TN) (Alimam et al., 2018). Another study found that telomere attrition was prominent in both PV and PMF (Ruella et al., 2013). These differences in reported telomere length findings across MPN studies might be attributed to differences in age ranges and allele burden, and the specific methods used to measure telomere length. In addition to MPN, other malignancies such as chronic myeloid leukemia are also associated with a significant telomere length shortening, which is correlated with the percentage of the malignant clone (Bouillon et al., 2018). The relationship between telomere length attrition and epigenetic age acceleration in hematologic diseases are widely discussed in other studies. It has been shown that both parameters clearly reflect cellular aging, but they appear to happen independently (Cypris et al., 2020).

Our results indicate a significant telomere attrition in patients with *CALR* and most prominently with *ASXL1* (Figure 29a). However, with increasing *JAK2* allele burden, the telomere attrition is rather moderate. Another study shows that telomere attrition is independent of *JAK2* positive or negative clones but rather correlates more with clonality of the malignant clone. Homozygous *JAK2* mutations have been associated with shorter telomeres compared to heterozygous clones (Bernard et al., 2009). The striking shortening of TL observed in *ASXL1* patients in the PMF and post-ET/PV-MF group confirms the association of the additional *ASXL1* mutation with a poor

clinical outcome and the likelihood of leukemic transformation (Wang et al., 2021) due to an increased replicative potential of the cells. Further study of telomerase in malignancies is necessary. The upregulation of the telomerase activity in CD34+ hematopoietic progenitor cells of Philadelphia chromosome negative MPN has been shown to result in a selective growth advantage of the malignant clone (Spanoudakis et al., 2011). This suggests that targeted inhibition of telomerase could be an effective therapeutic approach. Other studies have demonstrated that the telomerase inhibitor imetelstat is effective in patients with short TL (Frink et al., 2016) and specifically in ET patients with *ASXL1* mutation (Oppliger Leibundgut et al., 2021), supporting our findings that telomere shortening in *ASXL1* mutation may be due to replicative senescence.

This led us to question the association between senescence and MPN. Considering the clear acceleration of epigenetic aging and telomere shortening, it is expected that there would be an increased number of senescent cells. Utilizing a gene set specifically developed to identify senescence of hematopoietic and mesenchymal cells at the single cell level from SenMayo (Saul et al., 2022), we found evidence of increased gene expression signatures in all MPN sub entities. Specifically, there was a significant upregulation of interleukin-1 beta (IL-1β) in MPN groups, especially in PMF and PV. IL-1β, known as a master regulator of inflammation, controls the production of pro-inflammatory cytokines. Previous studies have shown an association between IL-1β and HSC aging, leading to reduced stem cell renewal and increased myeloid proliferation in aged and damaged mice due to increased IL-1β production (Colom Diaz et al., 2023). Its association with MPN has been well extensively studied and shown to be present in high levels in patients with advanced stages of PMF, and also correlated with MPN patients with *JAK2* V617F (Rai et al., 2022). Studies have suggested that IL-1β-mediated inflammation may promote the early clonal expansion of *JAK2* V617F clone and control the transition from CHIP to MPN (Rai et al., 2024). Another significantly upregulated gene, metalloproteinase MMP9, is evident in ET and PMF but not in PV. This is consistent with other studies that have shown an elevation in ET and PMF with an association with platelet formation and migration of megakaryocytes (Fan et al., 2023). Additionally, the matrix degrading nature of this enzyme leads to fibrotic transformation of the bone marrow by degrading the extracellular matrix components (ECM), making it a non-invasive biomarker tool for myelofibrosis (Hasselbalch et al., 2023). Lastly, a significant downregulation of AREG gene was found in all MPN subtypes, which is a ligand of the epidermal growth factor receptor (EGFR). This is consistent with previous studies on MPN (Baumeister, Maie, et al., 2021) and AML (Haouas et al., 2010). In addition, staining with senescence-associated β-galactosidase showed a tendency towards a higher level of senescence in MPN samples compared to age matched healthy samples.

4.2.2 Aberrant DNA methylation patterns are reduced in CFU colonies

The heterogeneity of cellular aging within an individual is anticipated, as each cell has its unique life history. We wanted to know whether this heterogeneity becomes more organized in the context of disease, especially when the cells sharing the same mutation undergo clonal outgrowth and potentially have the chance to share similar epigenetic patterns. Alternatively, the patterns could be much more aberrant due to the complexity of the disease and the inflammatory microenvironment. For this purpose, we compared an age matched healthy control to a PMF patient. PMF showed an aberrant methylation pattern and an increase in d-score and n-score in the age-related region of our interest, demonstrating that the heterogeneity of cells is more pronounced in the disease state than in aging due to genomic instability. Especially in the advanced MPN entity PMF there was a prominent increase compared to healthy controls, which is similar to what is known in MDS and AML (Eipel et al., 2019).

Furthermore, we analyzed the age predictions of target amplicon sequencing for each individual DNA strand, as described in a previous study (Han et al., 2020). The predicted age represents the estimated percentage of cells belonging to a specific age range, ranging between 0 to 200 years. Notably, a similar clustering of cells with a higher predicted age was observed in MPN, with a more pronounced effect than in older adults. Trapp and colleagues showed a similar prediction model for single cells, confirming our findings on epigenetic age heterogeneity among cells (Trapp et al., 2021). This could be due to the long term evolution of the disease and the differences in the clinical histories of the patient samples in our study, which may potentially lead to an increased epigenetic memory (Paska & Hudler, 2015) and epigenetic plasticity (Schoofs et al., 2014). Regardless of the MPN phenotype, malignant cells showed aberrant DNA methylation changes similar to those seen in aged cells. Thus, we hypothesized that epigenetic dysregulation may occur independently of their genetic background of a specific disease. To further elucidate this point, we performed an analysis on single cell derived CFU colonies, which were genotyped for the *JAK2* V617F mutation and used wild type as control. Interestingly, the heterogeneity in the DNAm patterns appeared to be reduced within a single CFU colony compared to the bulk PBMC samples. This supports our hypothesis, that the aberrant pattern becomes less diverse in the CFU initiating cell during the 14 days of culture expansion but becomes more diverse over the course of MPN development. A follow-up study to investigate the kinetics of this effect would be valuable. To date, there have been few studies on malignancies at the single cell level that focus on cellular aging, our findings help to narrow down the significant impact of the malignant clones. It is striking that the accelerated aging of *JAK2* mutated CFUs was observed in all MPN subtypes (Figure 28).

Nevertheless, the predicted age varies among colonies with the same genotype. Even though the mutant colonies share the same mutation status, they do not exhibit the same age difference. Furthermore, β-galactosidase staining observed a distinct morphological senescence-like phenotype within a single CFU colony. This could be due to the fact that cell differentiation is a continuous process that may not necessarily follow a uniform pattern. Even if it originates from a single cell, it can lead to different maturation states. In addition, the hierarchical and heterogeneous changes are more obscured in the context of disease (Cheng et al., 2020). Interestingly, it was found that neither the number nor the size of the colonies correlated with the replicative senescence onset (Maier et al., 2008), which further validates our finding that the observed discrepancy is not a result of the culture conditions. It would be also beneficial to find out the presence of other mutations in each colony. In future, new approaches should be developed to study disease development by examining cells at the earliest possible stage with specific CpGs associated with the disease, as opposed to merely focusing on age-related CpGs.

Regarding telomere length in CFU colonies of PV, a significantly shorter TL was observed in *JAK2*-mutated colonies compared to their WT counterparts, suggesting that accelerated aging is specifically restricted to the malignant clones. This observation is further supported by the fact that WT colonies from PV patients had a similar TL to colonies from healthy donors. Surprisingly, PMF patients showed no difference in TL between mutant and WT colonies derived from the same patient or even when compared to healthy donor derived CFUs (Figure 30b). This result was somewhat unexpected, given that, as previously discussed in our study, we observed accelerated aging in bulk PBMCs from PMF patients. This led us to question whether PMF colonies are exhausted regardless of the mutation status. This discrepancy could be due to the presence of a more primitive subset of mutant CD133+ HSPCs in PMF that exhibit multipotent cloning capacity (Triviai et al., 2015) and still exhibit normal TL. Alternatively, there may be a selective loss of these HSPC subsets with accelerated aging during the CFU assay, possibly due to hypersensitivity of progenitors to growth factors. Anyhow, it is evident that cell extrinsic factors and changes in the HSC niche affect normal hematopoiesis in PMF (Lataillade et al., 2008). To better understand the TL and telomerase activation in PMF mutant colonies, it would be ideal to study the bone marrow compartment where the neoplasm occurs.

4.2.3 Senolytic treatment targets the accelerated aged malignant clones

Treatment options for MPN primarily focus on managing symptoms and controlling complications by limiting the highly proliferating blood cell with cytoreductive agents and specifically targeting the mutant clones with JAK2 inhibitors. It is important to note that the JAK2 inhibitors primarily target the subpopulation of mature progenitor mutant cells and spare the disease initiating stem cells (Wang et al., 2014). In addition, there is a potential risk of developing mutation resistant cells, this can limit the available treatment options for patients. Furthermore, the residual cells

that are not eliminated by the immune system result in a pro inflammatory environment and cause the disease to progress to an advanced stage by acting as a tumor promoter (Zhao et al., 2021). Studies have shown that JAK inhibitors (JAKi) may contribute to ineffective targeting of MPN driving cells due to cell extrinsic mechanisms that provide cell survival signals. The combination of JAKi with MEK/ERK targeting, which is associated with MAPK signaling, has shown potential in improving the treatment outcomes of MPN patients (Stivala et al., 2019). Additionally, there are further therapeutic combinations of JAKi with BCL2, BET or PI3Kdelta inhibitors. On the other hand, senolytics, which are drugs that eliminate senescent cells, have been used in cancer clinical studies, often in combination with other cancer drugs. In cancer, cellular senescence plays a role in tumor suppression, but the accumulation of senescent cells and secretion of SASP can lead to aggressive cancer cell behavior (Demirci et al., 2021). Therefore, elimination of these cells with senolytics has been tested in different hematopoietic diseases. Recent studies have shown that combining JAKi and senolytics can effectively eliminate JAK2 inhibitor resistant cells (Jiang & Jamieson, 2018). Additionally, the targeting of senescent cells with senolytic drugs in our study has been shown to reduce the epigenetic aging of cells in old healthy adults. Therefore, we sought to study whether this approach could also be used to target malignant cells due to their accelerated cellular age.

A moderate reduction in *JAK2* V617F allele burden and an increase in average TL were observed upon treatment with JQ1 and piperlongumine. Nutlin-3a showed an increase in TL after treatment, although the mutation allele burden showed minimal change. The changes in epigenetic age were less pronounced, as there was a tendency for epigenetic age to decrease with low concentration of piperlongumine and RG7112, but this was not statistically significant. These drugs might therefore have some specificity for the malignant subset, particularly for subclones with shorter telomeres. Interestingly, this effect might be telomere biology-specific, as the expression of telomerase is exclusive to malignant cells and not observed in normal cells (Fragkiadaki et al., 2022). However, the extract mechanisms remain to be elucidated. JQ1 is a BET inhibitor that induces apoptosis in tumor cells by downregulating E2f/p21 signaling and regulating c-MYC. It has also been used in clinical trials in patients with AML and MDS (Shorstova et al., 2021). Similar to our results, Kleppe and colleagues demonstrated a reduction in the disease burden of MPN by JQ1 treatment, either alone or in combination with ruxolitinib, which was mediated by a reduction in NF-kB inflammatory changes (Kleppe et al., 2018). Other BET inhibitor proteins, such as pelabresib (CPI-0610), are used in ongoing phase 3 clinical trials in MF patients (NCT04603495). Combination with ruxolitinib has demonstrated improvement in both spleen volume and symptom score (Harrison et al., 2022). Another BET inhibitor, ABBV-744, is being tested in an ongoing clinical trial (NCT04454658). In myelofibrosis patients, ABBV-744 is used as a monotherapy and also in combination with JAKi. Another drug that showed an effect is piperlongumine, which is a potent cytotoxic component found primarily in the fruits and

roots of the plant long pepper. It selectively induces reactive oxygen species (ROS) production via inhibition of antioxidant enzymes that are important for cancer cell survival (Rawat et al., 2020). Furthermore, piperlongumine has been shown to target senescence human WI-38 fibroblasts (Wang et al., 2016) and to eliminate cancer cells by blocking the JAK2/STAT3 pathway (Chen et al., 2019).

On the other hand, navitoclax, also known as ABT263, which targets anti-apoptotic BCL-2 family proteins, has been studied in phase 2 clinical trials in patients with MF (NCT03222609). The clinical outcomes showed that the addition of a navitoclax to ruxolitinib resulted in molecular response and fibrosis reversal (Pemmaraju et al., 2022). However, our study did not reveal any effect in PV samples regarding mutation burden or cellular aging. In addition, telomerase inhibitor BIBR 1532 did not show a significant effect in the treatment for PV samples. Furthermore, the treatment of patients with PMF in CFU colonies led to cellular senescence and a reduction in the mutation burden in these patients, as discussed in our previous study (Vieri et al., 2023). The response was observed only in the patients with shorter TL and not in those with the longer TL. Telomerase activity has been associated with cancer survival, as it prevents the shortening of telomeres in cancer cells. By inhibiting telomerase, it is possible to eliminate a population of malignant cells. Another telomerase inhibitor imetelstat, has been part of the phase 2 clinical trials in MF patients (Mascarenhas et al., 2022). Taken together, these senolytic drugs may specifically target the malignant clone with a shorter TL in MPN. They can be used in a one-two punch approach, as a first step to induce cellular senescence through anticancer interventions, including telomerase inhibitors, followed by subsequent treatment with senolytics to remove those malignant cells (Wang et al., 2022). However, it must be considered that the compounds may also have non-senolytic effects, particularly at these relatively high concentrations during short-term *in vitro* treatment. Further studies at the stem cell level and in different cell compartments, as well as long-term treatments are needed to understand the mechanism behind this phenomenon. In addition, we need to keep in mind that the *in vitro* screening assays may provide a quite different outcome to *in vivo* therapy.

The decision-making process of damaged cells is critical in cancer development. If they do not undergo senescence or apoptosis, they can become cancerous. This scenario highlights a critical juncture where cells with compromised DNA integrity and inadequately replicated telomeres can evade programmed cell death or stable cell cycle arrest, allowing them to persist and proliferate abnormally and potentially resulting in tumorigenesis (Matt & Hofmann, 2016). Although temporal arrest of cell proliferation may be beneficial, the persistence of senescence cancer cells can be unfavorable. This “two-edged sword” nature of senescence needs to be further understood. The distinction between helper senescence (promotes tissue regeneration) and deleterious senescence (causes tissue damage) needs new methods to discern the early

and late phase of senescence (Tripathi et al., 2021). However, there are still challenges in senolytic treatment, as there is a potential risk for drug resistance. Different senolytics target different pathways to induce apoptosis in senescent cells, and there is no single broad range drug available to kill all senescent cells, so choosing for combination therapy is still a challenge. Additionally, genotoxic stress induced by therapy and oncogene induced senescence needs to be systematically studied to understand the mechanisms involved in senolytics. The clearance of senescent cells by senolytics may impact the immune system, as the secretion of SASP can recruit immune cells such as NK cells or cytotoxic T cells to recognize and eliminate the senescent cells (Prata et al., 2018). However, maintaining the right balance between inflammation and immune activation is important.

There are more emerging drug treatments in cancer apart from senolytics, drugs that block the DNA methylation which is known as DNA demethylating agents. Aberrant DNAm and epigenetic dysregulation have been linked with MPN pathogenesis. Inhibition of DNAm might be a potential treatment option for myeloid malignancies. This can cause cancer cells to alter genes that are silenced in normal cell development. Reactivation of these silenced genes could potentially activate the immune response against cancer, similar to how immune system recognizes viral infections (Patel et al., 2021). This led us to question the potential link between DNAm changes in MPN mutations, and further understanding of these changes could potentially uncover targets and biomarkers.

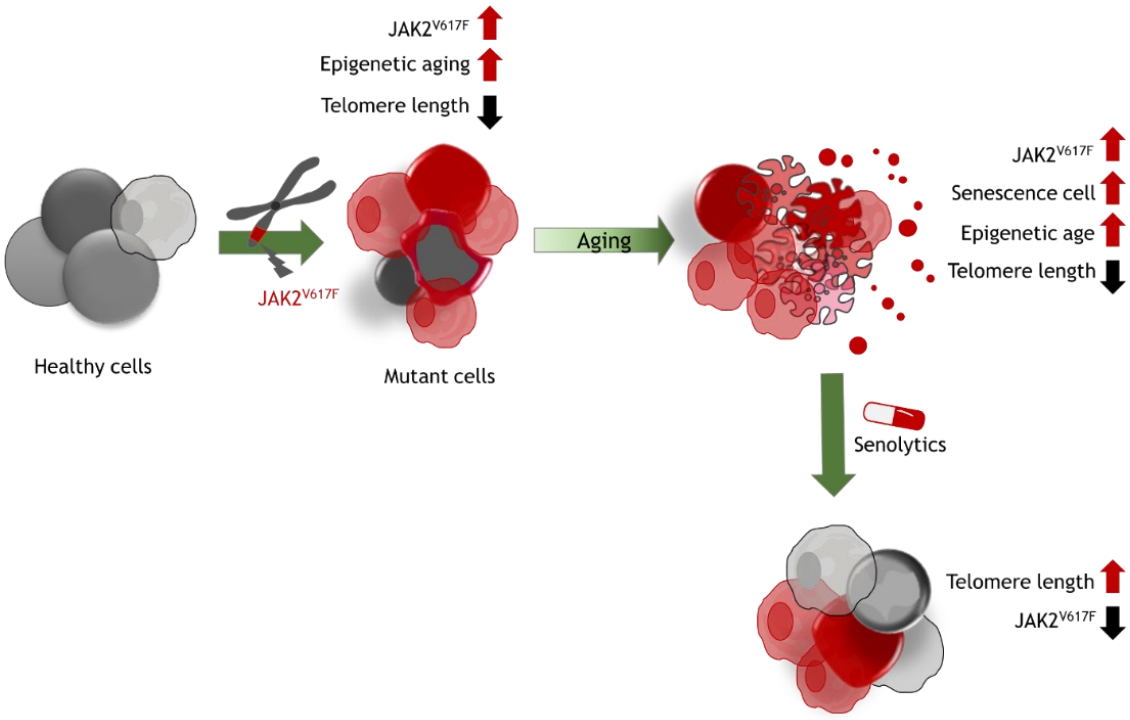

Figure 53. Graphical abstract of cellular aging which is accelerated in malignant MPN clones.
The cellular aging process is accelerated in MPN, with a correlation observed between accelerated aging and the JAK2V617F allele burden. Notably, the accelerated aging appears to be particularly prevalent in malignant clones. In polycythemia vera, the targeting of these aged cells with senolytic drugs demonstrated a reduction in allele burden, suggesting the potential for new therapeutic strategies.

4.3 *JAK2* V617F mutation alone is not enough to drive disease associated changes in DNA methylation

4.3.1 *JAK2* V617F-derived iPSC clones and their hematopoietic cells do not capture malignancy associated DNA methylation changes

JAK2 V617F gain of function mutation was first discovered in 2005 (James et al., 2005) and is known to be prominent in PV patients leading to erythrocyte bias. As JAK/STAT pathway is the one associated with BCR-ABL negative MPNs, irrespective of their driver mutations, the mutation led to constitutive activation of the signaling pathway and proliferation of the cells. Initially, it was thought that the driver mutations in MPN are the first cause of the disease and change the clonal dominance towards mutated cells. Later studies have shown that the MPN driver mutation does not necessarily have to be the first hit mutation but can also be the sequential acquisition followed by a CHIP mutation or unknown mutations. It was later found that the order of the mutation and the inclusion of the additional mutation can determine in which lineage the malignant cells want to clonally dominate (Kralovics et al., 2006). Only recently in 2022, Williams and colleagues found that the *JAK2* V617F mutation can occur very early in life, even in the embryo using a mathematical model related to hematopoietic phylogenies and clonal history (Williams et al., 2022). Studying the *JAK2* V617F mutation in an iPSC model would be a valuable method to recapitulate the early onset of the malignant phenotype and associated changes.

Our study (section 4.2) shows that indicators of cellular aging, epigenetic age and telomere length are accelerated in MPN patient samples and specifically in clones carrying the *JAK2* V617F mutation. In addition, the MPN associated mouse model including Jak2 V617F showed a clear acceleration of epigenetic aging (Figure 39b), as the mutation is induced by vav-cre and thus expressed throughout the hematopoietic system, leading to accelerated aging. Consequently, it was plausible that the *JAK2* V617F mutation has a direct impact on cellular aging. Nevertheless, neither epigenetic aging nor telomere shortening was significantly accelerated in iPSCs or iPSC-derived hematopoietic cells with the *JAK2* V617F mutation compared to their syngeneic wild-type counterparts (Figure 49). It is possible that the general resetting of age-related changes during reprogramming in iPSCs (Horvath, 2013; Weidner et al., 2014) masks some of the mutational effects that may only become apparent during prolonged differentiation. Although it was previously hypothesized that the rearrangement of chromatin during epigenetic aging could contribute to the acquisition of specific mutations (Wagner et al., 2015), this does not appear to be the case in this scenario. Nevertheless, looking not only at epigenetic aging but also at global methylation changes could shed light on whether epigenetic modifications contribute to mutation or rather to disease-related changes.

While epigenetic changes in MPN are only studied in relation to their subtypes in patient samples (McPherson et al., 2017), this led us to explore the impact of the single driver mutation *JAK2* V617F in an iPSC setup, as this may resemble the early development of disease onset. The iPSC clones used in this thesis have already been published. The isogenic controls were generated using CRISPR/Cas9 editing to achieve either a *JAK2* insertion or to repair a mutant to WT (Flosdorf et al., 2024; Satoh et al., 2021). Based on the efficiency of homology-directed repair (HDR) for these clones, both WT and heterozygous clones were obtained to generate homozygous clones. We found that iPSCs cluster according to patients rather than mutation genotype, which is expected and mirrors the patient specific genomic profile. Overall, there are very few differentially methylated CpGs between WT and mutant iPSCs, as well as between the heterozygous and homozygous *JAK2* V617F clones. This confirms that the reprogramming process resets the epigenetic landscape to establish marks of pluripotency through DNA methylation and chromatin remodeling process (Lee et al., 2014). Similar studies on mutant iPSC models have shown that there is no pronounced effect on DNAm levels while maintaining the pluripotency state. In particular, *DNMT3A* knockouts of iPSC clones, which are recurrently mutated in clonal hematopoiesis and leukemia, have shown that DNAm levels show no significant changes when comparing WT with mutant iPSC clones (Cypris et al., 2022). In addition, AML patient derived iPSCs harboring MLL rearrangements have shown that iPSCs lack leukemic potential by resetting DNA methylation and gene expression patterns, especially by erasing the epigenetic memory of the disease (Chao et al., 2017), which aligns with the findings of our study.

Hematopoietic differentiation of iPSCs is influenced by several factors such as the culture medium, cytokines, culture conditions, and plate coating. These factors collectively determine the composition of the final pool of cells (Tursky et al., 2020). Utilizing a cytokine-driven 3D differentiation protocol results in endothelial to hematopoietic transition HSCs with a distinct cobblestone-like microenvironment morphology (Ackermann et al., 2021), resembling a mixture of primitive and definitive hematopoiesis. Studies have shown that HSCs derived from primary samples more closely resemble definitive hematopoiesis (Slukvin, 2016). Analysis of surface markers and DNA methylation patterns using GO term in our study align with human hematopoietic development (Figure 44a and Figure 45e, respectively). The GO terms associated with hypermethylation are related to anatomical structures, whereas hypomethylation is more closely linked to lineage determination, immune cell regulation and activation, which is consistent with another study (Li et al., 2021). Furthermore, differentiation resulted in a heterogeneous cell population that not only consists of hematopoietic cells but also includes stromal cells, which are known to play a role in MPN (Leimkuhler et al., 2021; Ramos et al., 2017). The presence of *JAK2* mutations has been detected not only in hematopoietic cells but also in endothelial cells and their precursors (Farina et al., 2021), which led us to study the effects of *JAK2* mutation on all

cells without sorting them. In addition, the hematopoietic hierarchy is rather a continuous process and classical sorting based on surface markers would be limited as it depends on the maturity state of the cell (Ali et al., 2017; Schulte et al., 2015) and the maturation time of individual clone.

Consistent with other studies using these clones, we observed an erythrocyte bias in the *JAK2* V617F mutant clones. It is interesting that the mutation alone is sufficient to constitutively activate the JAK/STAT signaling pathway and increase the proliferation and differentiation of erythrocyte progenitors, similar to previous studies (Collins et al., 2024; Ye et al., 2014; Ye et al., 2009). The mutation has a specific affinity for promoting erythroid and megakaryocytic cell lineage differentiation and is linked with dysregulation of specific transcription factors and altered interaction with the bone marrow microenvironment (Varricchio & Hoffman, 2022). The ability to recapitulate a similar bias independent of external factors in an iPSC setting is noteworthy. Although, we saw patient-specific differences in the iHPCs, such as for patient 2, with a mutation history of 96 % *JAK2* allele burden in the primary sample, we were able to reprogram these cells into homozygous iPSCs. These homozygous clones were more likely to have a higher number of hematopoietic cells and CFU colonies than patient 1 or 3 derived homozygous iPSC clones with a 37% and 25 % *JAK2* allele burden, respectively. Overall, hematopoietic cells largely cluster according to the presence versus absence of *JAK2* mutation (Figure 47a), with some outliers in this clustering, such as patient 1 *JAK2* WT and patient 3 *JAK2* V617F homozygous. We assume that the observed differences may be attributed to the genetic editing of the clones and the mutation history of these patients from whom the cells were reprogrammed. Despite the identification of additional single nucleotide polymorphisms (SNP) in *TET2*, *CBL*, *ASXL1*, *EZH2*, *TP53*, and *SETB1* in different clones by NGS sequencing of MPN-related genes, these were classified as not pathogenic (Supplement Table S1; (Flosdorf et al., 2024)). Studies have shown an increased prevalence of the *JAK2* V617F somatic mutation in individuals with specific germline SNPs. It has been hypothesized that the predisposition of 46/1 haplotype may have contributed to the development or clonal expansion of the *JAK2* V617F positive MPNs (Hinds et al., 2016; Nielsen et al., 2013). Alternatively, DNA methylation plays an important role in SNPs, including CpG mutations, at different developmental stages and also in the context of clonal hematopoiesis of indeterminate potential, which could contribute to disease development (Silver et al., 2021; Zhou et al., 2020). The effect of these SNPs on DNA sequence variation or DNA methylation status remains unexplored.

Consequently, there are no significant differences in methylated CpGs when comparing the *JAK2* mutant to WT in iHPCs. Initially, it was assumed that the epigenetic changes in the DNAm status of the mutant iHPCs would differ from those observed in the WT. A number of different studies based on iPSC disease models have demonstrated changes in methylation patterns in comparison to their syngeneic control clones. As an example, the hematopoietic and

megakaryocytic differentiated cells of *RUNX1* mutant iPSC lines showed a distinct DNAm pattern in comparison to the WT (Tanaka et al., 2024). Similarly, the *DNMT3A* knockout iPSC clones showed considerably higher DNAm at many CpGs in wildtype iHPCs when compared to the knockout iHPC clones (Cypris et al., 2022). Additionally, *PRDM8* knockout iPSCs demonstrated methylation differences when their neuronal differentiation was compared between WT and the mutant (Cypris et al., 2020). This was not observed with *JAK2* mutant iHPCs, potentially indicating that the epigenetic alterations of *JAK2* mutations are minimal or that the inherent patient-specific variations are more pronounced than the mutation or it can also be that iHPC differentiation needs longer time to evoke such changes. Even though, the analysis of methylation changes that were not statistically significant but showed a notable trend revealed that many CpG sites in the mutant iHPCs displayed a decrease in methylation compared to the WT iHPCs. To understand this further, we employed a different approach to analyze the CpG sites that showed at least a 10 % increase or decrease in methylation in both homozygous and heterozygous iHPCs compared to their individual WT iHPCs. This approach was used to reduce the impact of donor-to-donor variability and focus more on the methylation changes that occur within each patient-derived cell. Interestingly, the differentially methylated regions showed a higher overlap in the heterozygous clone as compared to the homozygous mutant iHPCs. Furthermore, the hypomethylated regions were significantly enriched in the transcription sites of the genomic location in the mutant iHPCs, whereas the hypermethylated regions were rather in the intrinsic regions.

It is also interesting to note that the DNA methylation levels did not change in comparison between the heterozygous and homozygous *JAK2* V617F clones (Figure 47d). In the clinical setting, *JAK2* V617F heterozygous versus homozygous cells exhibit distinct biological behavior due to the gene dosage influencing the degree of enhanced *JAK2* V617F signal transduction (Moliterno et al., 2023). Furthermore, the evolution of homozygous clones, which is often caused by uniparental disomy (Li et al., 2014), is associated with disease progression and accumulation of the additional mutations (Passamonti & Rumi, 2009). The lack of DNA methylation differences between heterozygous and homozygous clones may be attributed to the fact that methylation changes require a longer period of time to acquire, while the iPSC experimental setup may not provide sufficient time for these differences to develop. In addition, the potential technical limitations associated with methylation analysis may also be a contributing factor. Although the Illumina EPIC array covers around 850,000 CpG sites, the uneven distribution of CpG probes across the genome (Moran et al., 2016) may lead to underrepresentation of certain genomic regions, and the individual CpGs on the array capture only the mean methylation levels and not the resolution of a single base. Further methods utilizing WGBS and nanopore sequencing of heterozygotes and homozygotes for each allele and allele-specific methylation remain relevant in order to make a conclusion between these clones (Ahsan et al., 2024; Do et al., 2020). Overall,

DNA methylation analysis provides insight that there are no significant methylation changes among the mutant and WT iHPCs. Even the non-significant changes in DNA methylation do not appear to drive the *JAK2* V617F mutation related pathways in the iPSCs and their differentiated iHPCs, but rather influence the cell lineage differentiation and immune response.

4.3.2 Hypomethylation is shared between *JAK2* mutation iHPCs when compared with primary patient samples carrying *JAK2* mutation

To better understand whether the DNAm changes observed in our *JAK2* V617F knockout iHPC clones are associated with aberrant DNAm patterns in patient samples, we utilized methylation profiles from PMF patients with *JAK2* V617F mutations. Although studies have shown that iHPCs from iPSCs are not identical to HSPCs from primary samples, which are more mature cells and exhibit more advanced disease progression, there were phenotypic similarities in the hematopoietic lineage cells, particularly in monocytic cells. However, it has previously been shown that DNA methylation patterns between iHPCs and HSPCs are not completely identical (Cypris et al., 2019). When comparing samples from PMF patients with *JAK2* V617F mutation to healthy individuals, it was found that the differentially methylated CpGs sites showed a predominant number of hypomethylation patterns, rather than hypermethylation (Supplemental Figure S7a). Similarly, another study observed global hypomethylation in myelofibrosis when compared to healthy controls, consistent with our data. Nevertheless, no methylation changes were observed when comparing primary and secondary myelofibrosis (Martinez-Calle et al., 2019). When comparing the methylation changes between *JAK2* patient and healthy samples, as well as between *JAK2* mutant iHPCs and WT iHPCs, *JAK2* mutant cells showed a high number of common hypomethylated CpG sites (Figure 51). While the global mean hypomethylation followed a comparable trend in both *JAK2* mutant patient and *JAK2* iHPCs, the mean methylation in hypermethylated patterns was not so pronounced (Figure 50).

Global DNA hypomethylation is a common feature in many cancers. In 1998, it was first discovered that global hypomethylation in cancer leads to the activation of oncogenes such as K-ras (Feinberg & Vogelstein, 1983). Hypomethylation at the promoter regions or transcription start sites is often associated with the increase in gene expression. The absence of methyl groups is generally associated with more open chromatin structure. This allows transcription factors and other regulatory elements to bind more easily to DNA and facilitate the initiation of transcription (Wilson et al., 2007). It has been recently hypothesized that enhancer associated DNA methylation is linked with myeloid malignancies, specifically with AML clones exhibiting hypomethylation in enhancer regions, and that the methylation levels correlate with the patient overall survival. This might potentially contribute to the gene expression in the malignant phenotype (Ordonez et al., 2019). Moreover, hypomethylation in cancer is usually located outside the promoter regions, which can lead to genomic instability and disruption of

chromosomal integrity (Ahuja & Issa, 2000; Baylin et al., 1998). Notably, the loss of methylation on repetitive elements has been associated with chromatin relaxation and unscheduled transcription in various human pathologies (Pappalardo & Barra, 2021).

With regard to the aging associated immune system impairments, which are shown to be associated with changes in DNA methylation, hypermethylation is more closely linked to regulated programmed changes, whereas hypomethylation is more related to environmental and stochastic processes (Marttila et al., 2015). One of the main aspects of cancer is DNA methylation in tumor suppressor genes, which is associated with gene silencing that is normally controlled in normal tissues (Ordonez et al., 2019). In addition, other studies have shown that hypermethylation is linked to genes associated with age related phenotypes or disease. For instance, hypermethylated differentially methylated regions in tissues overlap with stem cell bivalent chromatin markers, which is linked to stem cell aging (Cakouros & Gronthos, 2019). This further led us to the question about the association between hypomethylation in MPN disease and its impact on gene expression, including the role of abnormal DNA methylation changes and their interaction in gene silencing. This remains to be further explored.

The gene ontology (GO) term analysis of regions showing hypomethylation in mutant iHPCs compared to WT cells reveled a significant associated with immune cell signaling pathways, the activation of leukocytes, myeloid cells, and T cells, as well as genes related to IL-6 production (Figure 47e). Among the commonly methylated CpGs in both heterozygous and homozygous clones in all three donors showed that the hypermethylated genes were associated with process related to angiogenesis, while the hypomethylated genes were more related to cell lineage differentiation and inflammatory responses, including FasL ligand production (Supplemental Figure S6c-d). FasL is a member of tumor necrosis factor (TNF) cytokine family and it binds to the Fas receptor, which induces apoptosis through activation of caspases (Waring & Mullbacher, 1999). An abnormal expression of FasL/FasR has been associated with the pathogenesis of MPN and other hematological malignancies (Bar-Natan & Hoffman, 2019). Furthermore, shared hypomethylated regions between mutant iHPCs and PMFs were found to be enriched for genes involved in platelet activation, hematopoietic cell differentiation, megakaryopoiesis, blood coagulation and inflammatory responses (Figure 51e-f). Similar associations were observed when comparing *JAK2* PMF with healthy samples (Supplemental Figure S7b). These findings align with previous studies, that have shown differential methylation in genes associated with immune and inflammatory responses, cell proliferation and differentiation between transformed and chronic MPNs (Perez et al., 2013). Moreover, another study with MF patients with *ASXL1* mutation showed differentially methylated genes involved in tumor suppressor genes and inflammation (Nielsen et al., 2017).

It is hypothesized that chronic inflammation in MPN may trigger clonal evolution and contribute to complications by inducing a state of chronic oxidative stress, thereby promoting genomic instability for the acquisition of mutations (Baumeister, Chatain, et al., 2021; Hasselbalch, 2012) or giving a selective advantage to mutant *JAK2* clones in this highly inflamed environment (Fleischman, 2015). Furthermore, the activation of JAK/STAT pathway results in the production of pro inflammatory cytokines such as IL-6, leading to cell proliferation, activation, and differentiation (Cokic et al., 2015). It is important to note the limitations associated with GO terms for DNA methylation data, as it considers the number of CpG occurrences within a gene. Studies have shown that these counts can differ depending on the genes in a hyper- and hypomethylation state. Even when comparing the equal number of genes in both states, a greater number of GO terms are often observed in genes with hypermethylated CpGs (Kananen et al., 2016).

Studies have shown that inflammatory associated DNA methylation changes occur predominantly in open chromatin regions, enhancers, and other regulatory genomic loci (Wielscher et al., 2022). Additionally, the majority of differently methylated CpGs in MPN were significantly associated with enhancer regions (Martinez-Calle et al., 2019) and are consistently upregulated upon promoter hypomethylation (Alimam et al., 2021). The systemic expansion of clinical thrombotic tendency and the promotion of MPN stem cell clonal expansion are facilitated by the inflammatory state induced by *JAK2* mutant stem cells in their microenvironment. This creates a detrimental cycle that enhances the prothrombotic state in these diseases (Hasselbalch et al., 2021).

In summary, the observed changes in DNA methylation in *JAK2* V617F iHPCs and patient samples were largely associated with inflammation. No methylation changes were observed in relation to the JAK/STAT mutation pathways. This was further confirmed by analyzing the DNA methylation changes in the *JAK2* locus, where no distinction was observed between mutant and wild type cells. This suggests that the observed changes in DNA methylation do not directly contribute to the pathogenesis of the disease, but there could be a possibility that this is a result from the inflammation induced by the malignant process. In future, DNA methylation signatures may be employed to understand the impact of different degrees of inflammation (Wielscher et al., 2022). Moreover, the MPN associated complications that are driven by DNA methylation can be modified by eliminating the inflammatory environment. As in our study, treatment with senolytics may prove beneficial in removing these mutant cells. The results of the DNA methylation analysis should be interpreted with caution, as they provide only indirect evidence. To validate these findings, it is necessary to perform gene expression analysis.

4.4 Concluding remarks and outlook

Our study provides further evidence for an association between epigenetic age and cellular senescence. The removal of senescent cells using senolytic treatment was shown to reduce the epigenetic age of healthy PBMCs *in vitro*, indicating that this approach may be useful in drug screening for senolytic compounds. Furthermore, cellular aging is accelerated in MPN compared to healthy individuals based on epigenetic age, telomere length and senescence. These clones which show signs of accelerated aging can be targeted with senolytics, leading to a reduction in *JAK2* allele burden and an increase in telomere length with certain senolytics. This suggests that the senolytics may be used in MPN as a treatment option. Most drug treatment options for MPN only reduce the *JAK2* allele burden of the mature mutant progenitor cells, but do not eliminate the disease-causing mutant stem cells (Izzo et al., 2024). In the future, iPSCs could be utilized for senolytic drug screening. By utilizing the barcoded method (Cypris et al., 2022), there is a possibility to combine different types of mutant genotype and study if these drugs also eliminate the disease-causing mutant stem cells in combination with senolytics.

Accelerated epigenetic aging is prominent in cancers including MPN, however the underlying reason is not fully understood. It could result from stochastic epigenetic modifications (Meyer & Schumacher, 2024; Tong et al., 2024) or co-regulated age-associated patterns (Liesenfelder et al., 2024; Tarkhov et al., 2024). DNAm analysis of *JAK2* V617F mutant iHPCs and iPSCs showed no significant changes compared to the wild type, and not specific to the JAK/STAT mutation-pathway, suggesting that the single driver mutation is not enough to induce any DNAm alterations. It appears to be that the DNAm changes act indirectly, possibly influenced by inflammation due to increased inflammatory cytokine production (Gleitz et al., 2021; Hermouet et al., 2015). Additional mutation in the epigenetic modifiers in MPN can contribute to the DNAm aberrations (Nielsen et al., 2017; Perez et al., 2013). This could be understood by reprogramming patient samples that consist of additional MPN mutations, as this might be an exciting outlook to study the disease progression of MPN. Further investigation of the differentiation of *JAK2* V617F iPSCs into non-hematopoietic lineages would be a valuable addition to the existing work. This could provide insight into whether the mutation can give rise to normal, non-malignant cell types in the presence of the mutation. In addition, studying the interplay between epigenetic clocks, single nucleotide polymorphisms (SNP), and MPN development would be an interesting aspect, as SNPs are associated with epigenetic changes which could influence the epigenetic clocks while that can also influence the acquisition of somatic mutations through a shared heritable factor (Morales Berstein et al., 2022).

Our study provides evidence that DNAm changes occur in the MPN patient samples, and the stochasticity reduced in colony forming unit derived mutant cells. However, in early disease

onset by utilizing the iPSC derived hematopoietic cells models, it appears that the mutation alone is not enough for the DNAm acquisition. Either these alterations may appear later through the clonal evolution via inflammation, or the proliferation of cell phenotypical differences, or affect other epigenetic modifications. This work highlights the interplay between cancer and aging and offers novel therapeutic targets for malignancies by focusing on aged cells. In addition, it opens avenues for studying the relevance of DNAm in cancer beyond being a biomarker.

References

Ackermann, M., Haake, K., Kempf, H., Kaschutnig, P., Weiss, A. C., Nguyen, A. H. H., Abeln, M., Merkert, S., Kuhnel, M. P., Hartmann, D., Jonigk, D., Thum, T., Kispert, A., Milsom, M. D., & Lachmann, N. (2021). A 3D iPSC-differentiation model identifies interleukin-3 as a regulator of early human hematopoietic specification. *Haematologica*, *106*(5), 1354-1367. https://doi.org/10.3324/haematol.2019.228064

Ackermann, M., Liebhaber, S., Klusmann, J. H., & Lachmann, N. (2015). Lost in translation: pluripotent stem cell-derived hematopoiesis. *EMBO Mol Med*, *7*(11), 1388-1402. https://doi.org/10.15252/emmm.201505301

Ahmad, H., Jahn, N., & Jaiswal, S. (2023). Clonal Hematopoiesis and Its Impact on Human Health. *Annu Rev Med*, *74*, 249-260. https://doi.org/10.1146/annurev-med-042921-112347

Ahsan, M. U., Gouru, A., Chan, J., Zhou, W., & Wang, K. (2024). A signal processing and deep learning framework for methylation detection using Oxford Nanopore sequencing. *Nat Commun*, *15*(1), 1448. https://doi.org/10.1038/s41467-024-45778-y

Ahuja, N., & Issa, J. P. (2000). Aging, methylation and cancer. *Histol Histopathol*, *15*(3), 835-842. https://doi.org/10.14670/HH-15.835

Alberts, B., Johnson, A., Lewis, J., Raff, M., Roberts, K., & Walter, P. (2002). *Molecular Biology of the Cell, 4th edition* (4th ed.). Garland Science.

Ali, M. A. E., Fuse, K., Tadokoro, Y., Hoshii, T., Ueno, M., Kobayashi, M., Nomura, N., Vu, H. T., Peng, H., Hegazy, A. M., Masuko, M., Sone, H., Arai, F., Tajima, A., & Hirao, A. (2017). Functional dissection of hematopoietic stem cell populations with a stemness-monitoring system based on NS-GFP transgene expression. *Sci Rep*, *7*(1), 11442. https://doi.org/10.1038/s41598-017-11909-3

Alimam, S., McLornan, D. P., Jiang, J., Radia, D., Mufti, G. J., & Harrison, C. N. (2018). Shortened telomeres in essential thrombocythemia: clinicopathological and treatment correlations. *Haematologica*, *103*(6), e234-e236. https://doi.org/10.3324/haematol.2017.180851

Alimam, S., Villiers, W., Dillon, R., Simpson, M., Runglall, M., Smith, A., Chatzikyriakou, P., Lavender, P., Kanda, A., Mills, K., Bellosillo Paricio, B., Kaufman-Cook, J., Ord, S., Kordasti, S., Radia, D., Woodley, C., Francis, Y., Mufti, G., McLornan, D. P., & Harrison, C. N. (2021). Patients with triple-negative, JAK2V617F- and CALR-mutated essential thrombocythemia share a unique gene expression signature. *Blood Adv*, *5*(4), 1059-1068. https://doi.org/10.1182/bloodadvances.2020003172

Alle, Q., Le Borgne, E., Milhavet, O., & Lemaitre, J. M. (2021). Reprogramming: Emerging Strategies to Rejuvenate Aging Cells and Tissues. *Int J Mol Sci*, *22*(8). https://doi.org/10.3390/ijms22083990

Alsayegh, K., Cortes-Medina, L. V., Ramos-Mandujano, G., Badraiq, H., & Li, M. (2019). Hematopoietic Differentiation of Human Pluripotent Stem Cells: HOX and GATA Transcription Factors as Master Regulators. *Curr Genomics*, *20*(6), 438-452. https://doi.org/10.2174/1389202920666191017163837

Amaya-Montoya, M., Perez-Londono, A., Guatibonza-Garcia, V., Vargas-Villanueva, A., & Mendivil, C. O. (2020). Cellular Senescence as a Therapeutic Target for Age-Related Diseases: A Review. *Adv Ther*, *37*(4), 1407-1424. https://doi.org/10.1007/s12325-020-01287-0

Anderson, N. M., & Simon, M. C. (2020). The tumor microenvironment. *Curr Biol*, *30*(16), R921-R925. https://doi.org/10.1016/j.cub.2020.06.081

Arber, D. A., Orazi, A., Hasserjian, R., Thiele, J., Borowitz, M. J., Le Beau, M. M., Bloomfield, C. D., Cazzola, M., & Vardiman, J. W. (2016). The 2016 revision to the World Health Organization classification of myeloid neoplasms and acute leukemia. *Blood*, *127*(20), 2391-2405. https://doi.org/10.1182/blood-2016-03-643544

Arnold, K. R., & Rose, M. R. (2023). *Conceptual Breakthroughs in The Evolutionary Biology of Aging*. Academic Press.

Arora, S., Thompson, P. J., Wang, Y., Bhattacharyya, A., Apostolopoulou, H., Hatano, R., Naikawadi, R. P., Shah, A., Wolters, P. J., Koliwad, S., Bhattacharya, M., & Bhushan, A. (2021). Invariant Natural Killer T cells coordinate removal of senescent cells. *Med*, *2*(8), 938-950. https://doi.org/10.1016/j.medj.2021.04.014

Ashraf, H. M., Fernandez, B., & Spencer, S. L. (2023). The intensities of canonical senescence biomarkers integrate the duration of cell-cycle withdrawal. *Nat Commun*, *14*(1), 4527. https://doi.org/10.1038/s41467-023-40132-0

Aubert, G., Baerlocher, G. M., Vulto, I., Poon, S. S., & Lansdorp, P. M. (2012). Collapse of telomere homeostasis in hematopoietic cells caused by heterozygous mutations in telomerase genes. *PLoS Genet*, *8*(5), e1002696. https://doi.org/10.1371/journal.pgen.1002696

Bader, M. S., & Meyer, S. C. (2022). JAK2 in Myeloproliferative Neoplasms: Still a Protagonist. *Pharmaceuticals (Basel)*, *15*(2). https://doi.org/10.3390/ph15020160

Baker, D. J., Childs, B. G., Durik, M., Wijers, M. E., Sieben, C. J., Zhong, J., Saltness, R. A., Jeganathan, K. B., Verzosa, G. C., Pezeshki, A., Khazaie, K., Miller, J. D., & van Deursen, J. M. (2016). Naturally occurring p16(Ink4a)-positive cells shorten healthy lifespan. *Nature*, *530*(7589), 184-189. https://doi.org/10.1038/nature16932

Bar-Natan, M., & Hoffman, R. (2019). New insights into the causes of thrombotic events in patients with myeloproliferative neoplasms raise the possibility of novel therapeutic approaches. *Haematologica*, *104*(1), 3-6. https://doi.org/10.3324/haematol.2018.205989

Barbui, T., Tefferi, A., Vannucchi, A. M., Passamonti, F., Silver, R. T., Hoffman, R., Verstovsek, S., Mesa, R., Kiladjian, J. J., Hehlmann, R., Reiter, A., Cervantes, F., Harrison, C., Mc Mullin, M. F., Hasselbalch, H. C., Koschmieder, S., Marchetti, M., Bacigalupo, A., Finazzi, G., . . . Barosi, G. (2018). Philadelphia chromosome-negative classical myeloproliferative neoplasms: revised management recommendations from European LeukemiaNet. *Leukemia*, *32*(5), 1057-1069. https://doi.org/10.1038/s41375-018-0077-1

Barres, R., & Zierath, J. R. (2016). The role of diet and exercise in the transgenerational epigenetic landscape of T2DM. *Nat Rev Endocrinol*, *12*(8), 441-451. https://doi.org/10.1038/nrendo.2016.87

Bartels, S., Faisal, M., Busche, G., Schlue, J., Hasemeier, B., Schipper, E., Vogtmann, J., Westphal, L., Lehmann, U., & Kreipe, H. (2020). Mutations associated with age-related clonal hematopoiesis in PMF patients with rapid progression to myelofibrosis. *Leukemia*, *34*(5), 1364-1372. https://doi.org/10.1038/s41375-019-0668-5

Baumeister, J., Chatain, N., Sofias, A. M., Lammers, T., & Koschmieder, S. (2021). Progression of Myeloproliferative Neoplasms (MPN): Diagnostic and Therapeutic Perspectives. *Cells*, *10*(12). https://doi.org/10.3390/cells10123551

Baumeister, J., Maie, T., Chatain, N., Gan, L., Weinbergerova, B., de Toledo, M. A. S., Eschweiler, J., Maurer, A., Mayer, J., Kubesova, B., Racil, Z., Schuppert, A., Costa, I., Koschmieder, S., Brummendorf, T. H., & Gezer, D. (2021). Early and late stage MPN patients show distinct gene expression profiles in CD34(+) cells. *Ann Hematol*, *100*(12), 2943-2956. https://doi.org/10.1007/s00277-021-04615-8

Baxter, E. J., Scott, L. M., Campbell, P. J., East, C., Fourouclas, N., Swanton, S., Vassiliou, G. S., Bench, A. J., Boyd, E. M., Curtin, N., Scott, M. A., Erber, W. N., Green, A. R., & Cancer Genome, P. (2005). Acquired mutation of the tyrosine kinase JAK2 in human myeloproliferative disorders. *Lancet*, *365*(9464), 1054-1061. https://doi.org/10.1016/S0140-6736(05)71142-9

Baylin, S. B., Herman, J. G., Graff, J. R., Vertino, P. M., & Issa, J. P. (1998). Alterations in DNA methylation: a fundamental aspect of neoplasia. *Adv Cancer Res*, *72*, 141-196. https://www.ncbi.nlm.nih.gov/pubmed/9338076

Baylis, D., Bartlett, D. B., Patel, H. P., & Roberts, H. C. (2013). Understanding how we age: insights into inflammaging. *Longev Healthspan*, *2*(1), 8. https://doi.org/10.1186/2046-2395-2-8

Becker, K. A., Ghule, P. N., Therrien, J. A., Lian, J. B., Stein, J. L., van Wijnen, A. J., & Stein, G. S. (2006). Self-renewal of human embryonic stem cells is supported by a shortened G1 cell cycle phase. *J Cell Physiol*, *209*(3), 883-893. https://doi.org/10.1002/jcp.20776

Bell, C. G., Lowe, R., Adams, P. D., Baccarelli, A. A., Beck, S., Bell, J. T., Christensen, B. C., Gladyshev, V. N., Heijmans, B. T., Horvath, S., Ideker, T., Issa, J. J., Kelsey, K. T., Marioni, R. E., Reik, W., Relton, C. L., Schalkwyk, L. C., Teschendorff, A. E., Wagner, W., . . . Rakyan, V. K. (2019). DNA methylation aging clocks: challenges and recommendations. *Genome Biol*, *20*(1), 249. https://doi.org/10.1186/s13059-019-1824-y

Belsky, D. W., Caspi, A., Houts, R., Cohen, H. J., Corcoran, D. L., Danese, A., Harrington, H., Israel, S., Levine, M. E., Schaefer, J. D., Sugden, K., Williams, B., Yashin, A. I., Poulton, R., & Moffitt, T. E. (2015). Quantification of biological aging in young adults. *Proc Natl Acad Sci U S A*, *112*(30), E4104-4110. https://doi.org/10.1073/pnas.1506264112

Belyavsky, A., Petinati, N., & Drize, N. (2021). Hematopoiesis during Ontogenesis, Adult Life, and Aging. *Int J Mol Sci*, *22*(17). https://doi.org/10.3390/ijms22179231

Berben, L., Floris, G., Wildiers, H., & Hatse, S. (2021). Cancer and Aging: Two Tightly Interconnected Biological Processes. *Cancers (Basel)*, *13*(6). https://doi.org/10.3390/cancers13061400

Bernard, L., Belisle, C., Mollica, L., Provost, S., Roy, D. C., Gilliland, D. G., Levine, R. L., & Busque, L. (2009). Telomere length is severely and similarly reduced in JAK2V617F-positive and -negative myeloproliferative neoplasms. *Leukemia*, *23*(2), 287-291. https://doi.org/10.1038/leu.2008.319

Blackburn, E. H. (2001). Switching and signaling at the telomere. *Cell*, *106*(6), 661-673. https://doi.org/10.1016/s0092-8674(01)00492-5

Blagosklonny, M. V. (2022). Hallmarks of cancer and hallmarks of aging. *Aging (Albany NY)*, *14*(9), 4176-4187. https://doi.org/10.18632/aging.204082

Blasco, M. A. (2005). Telomeres and human disease: ageing, cancer and beyond. *Nat Rev Genet*, *6*(8), 611-622. https://doi.org/10.1038/nrg1656

Bocklandt, S., Lin, W., Sehl, M. E., Sanchez, F. J., Sinsheimer, J. S., Horvath, S., & Vilain, E. (2011). Epigenetic predictor of age. *PLoS One*, *6*(6), e14821. https://doi.org/10.1371/journal.pone.0014821

Bodnar, A. G., Ouellette, M., Frolkis, M., Holt, S. E., Chiu, C. P., Morin, G. B., Harley, C. B., Shay, J. W., Lichtsteiner, S., & Wright, W. E. (1998). Extension of life-span by introduction of telomerase into normal human cells. *Science*, *279*(5349), 349-352. https://doi.org/10.1126/science.279.5349.349

Boehnke, J., Atakhanov, S., Toledo, M. A. S., Schuler, H. M., Sontag, S., Chatain, N., Koschmieder, S., Brummendorf, T. H., Kramann, R., & Zenke, M. (2021). CRISPR/Cas9 mediated CXCL4 knockout in human iPS cells of polycythemia vera patient with JAK2 V617F mutation. *Stem Cell Res*, *55*, 102490. https://doi.org/10.1016/j.scr.2021.102490

Bouillon, A. S., Ventura Ferreira, M. S., Awad, S. A., Richter, J., Hochhaus, A., Kunzmann, V., Dengler, J., Janssen, J., Ossenkoppele, G., Westerweel, P. E., Te Boekhorst, P. A. W., Mahon, F. X., Hjorth-Hansen, H., Isfort, S., Fioretos, T., Hummel, S., Schemionek, M., Wilop, S., Koschmieder, S., . . . Brummendorf, T. H. (2018). Telomere shortening correlates with leukemic stem cell burden at diagnosis of chronic myeloid leukemia. *Blood Adv*, *2*(13), 1572-1579. https://doi.org/10.1182/bloodadvances.2018017772

Boyle, C., Lansdorp, P. M., & Edelstein-Keshet, L. (2023). Predicting the number of lifetime divisions for hematopoietic stem cells from telomere length measurements. *iScience*, *26*(7), 107053. https://doi.org/10.1016/j.isci.2023.107053

Brauning, A., Rae, M., Zhu, G., Fulton, E., Admasu, T. D., Stolzing, A., & Sharma, A. (2022). Aging of the Immune System: Focus on Natural Killer Cells Phenotype and Functions. *Cells*, *11*(6). https://doi.org/10.3390/cells11061017

Brummendorf, T. H., Holyoake, T. L., Rufer, N., Barnett, M. J., Schulzer, M., Eaves, C. J., Eaves, A. C., & Lansdorp, P. M. (2000). Prognostic implications of differences in telomere length between normal and malignant cells from patients with chronic myeloid leukemia measured by flow cytometry. *Blood*, *95*(6), 1883-1890. https://www.ncbi.nlm.nih.gov/pubmed/10706851

Buganim, Y., Faddah, D. A., & Jaenisch, R. (2013). Mechanisms and models of somatic cell reprogramming. *Nat Rev Genet*, *14*(6), 427-439. https://doi.org/10.1038/nrg3473

Buhl, E. M., Djudjaj, S., Klinkhammer, B. M., Ermert, K., Puelles, V. G., Lindenmeyer, M. T., Cohen, C. D., He, C., Borkham-Kamphorst, E., Weiskirchen, R., Denecke, B.,

Trairatphisan, P., Saez-Rodriguez, J., Huber, T. B., Olson, L. E., Floege, J., & Boor, P. (2020). Dysregulated mesenchymal PDGFR-beta drives kidney fibrosis. *EMBO Mol Med*, *12*(3), e11021. https://doi.org/10.15252/emmm.201911021

Buscarlet, M., Provost, S., Zada, Y. F., Barhdadi, A., Bourgoin, V., Lepine, G., Mollica, L., Szuber, N., Dube, M. P., & Busque, L. (2017). DNMT3A and TET2 dominate clonal hematopoiesis and demonstrate benign phenotypes and different genetic predispositions. *Blood*, *130*(6), 753-762. https://doi.org/10.1182/blood-2017-04-777029

Cakouros, D., & Gronthos, S. (2019). Epigenetic Regulation of Bone Marrow Stem Cell Aging: Revealing Epigenetic Signatures associated with Hematopoietic and Mesenchymal Stem Cell Aging. *Aging Dis*, *10*(1), 174-189. https://doi.org/10.14336/AD.2017.1213

Calado, R. T., & Dumitriu, B. (2013). Telomere dynamics in mice and humans. *Semin Hematol*, *50*(2), 165-174. https://doi.org/10.1053/j.seminhematol.2013.03.030

Calado, R. T., & Young, N. S. (2009). Telomere diseases. *N Engl J Med*, *361*(24), 2353-2365. https://doi.org/10.1056/NEJMra0903373

Calvi, L. M., & Link, D. C. (2015). The hematopoietic stem cell niche in homeostasis and disease. *Blood*, *126*(22), 2443-2451. https://doi.org/10.1182/blood-2015-07-533588

Canu, G., & Ruhrberg, C. (2021). First blood: the endothelial origins of hematopoietic progenitors. *Angiogenesis*, *24*(2), 199-211. https://doi.org/10.1007/s10456-021-09783-9

Carmona, J. J., & Michan, S. (2016). Biology of Healthy Aging and Longevity. *Rev Invest Clin*, *68*(1), 7-16. https://www.ncbi.nlm.nih.gov/pubmed/27028172

Carobbio, A., Vannucchi, A. M., Rumi, E., De Stefano, V., Rambaldi, A., Carli, G., Randi, M. L., Gisslinger, H., Passamonti, F., Thiele, J., Gangat, N., Tefferi, A., & Barbui, T. (2023). Survival expectation after thrombosis and overt-myelofibrosis in essential thrombocythemia and prefibrotic myelofibrosis: a multistate model approach. *Blood Cancer J*, *13*(1), 115. https://doi.org/10.1038/s41408-023-00887-7

Cerneckis, J., Cai, H., & Shi, Y. (2024). Induced pluripotent stem cells (iPSCs): molecular mechanisms of induction and applications. *Signal Transduct Target Ther*, *9*(1), 112. https://doi.org/10.1038/s41392-024-01809-0

Chae, J. B., Jang, H., Son, C., Park, C. W., Choi, H., Jin, S., Lee, H. Y., Lee, H., Ryu, J. H., Kim, N., Kim, C., & Chung, H. (2021). Targeting senescent retinal pigment epithelial cells facilitates retinal regeneration in mouse models of age-related macular degeneration. *Geroscience*, *43*(6), 2809-2833. https://doi.org/10.1007/s11357-021-00457-4

Chaib, S., Tchkonia, T., & Kirkland, J. L. (2022). Cellular senescence and senolytics: the path to the clinic. *Nat Med*, *28*(8), 1556-1568. https://doi.org/10.1038/s41591-022-01923-y

Chan, S. R., & Blackburn, E. H. (2004). Telomeres and telomerase. *Philos Trans R Soc Lond B Biol Sci*, *359*(1441), 109-121. https://doi.org/10.1098/rstb.2003.1370

Chang, J., Wang, Y., Shao, L., Laberge, R. M., Demaria, M., Campisi, J., Janakiraman, K., Sharpless, N. E., Ding, S., Feng, W., Luo, Y., Wang, X., Aykin-Burns, N., Krager, K., Ponnappan, U., Hauer-Jensen, M., Meng, A., & Zhou, D. (2016). Clearance of senescent cells by ABT263 rejuvenates aged hematopoietic stem cells in mice. *Nat Med*, *22*(1), 78-83. https://doi.org/10.1038/nm.4010

Chao, M. P., Gentles, A. J., Chatterjee, S., Lan, F., Reinisch, A., Corces, M. R., Xavy, S., Shen, J., Haag, D., Chanda, S., Sinha, R., Morganti, R. M., Nishimura, T., Ameen, M., Wu, H., Wernig, M., Wu, J. C., & Majeti, R. (2017). Human AML-iPSCs Reacquire Leukemic Properties after Differentiation and Model Clonal Variation of Disease. *Cell Stem Cell*, *20*(3), 329-344 e327. https://doi.org/10.1016/j.stem.2016.11.018

Chen, D., Ma, Y., Li, P., Liu, M., Fang, Y., Zhang, J., Zhang, B., Hui, Y., & Yin, Y. (2019). Piperlongumine Induces Apoptosis and Synergizes with Doxorubicin by Inhibiting the JAK2-STAT3 Pathway in Triple-Negative Breast Cancer. *Molecules*, *24*(12). https://doi.org/10.3390/molecules24122338

Chen, Q., Song, S., Wei, S., Liu, B., Honjo, S., Scott, A., Jin, J., Ma, L., Zhu, H., Skinner, H. D., Johnson, R. L., & Ajani, J. A. (2015). ABT-263 induces apoptosis and synergizes with chemotherapy by targeting stemness pathways in esophageal cancer. *Oncotarget*, *6*(28), 25883-25896. https://doi.org/10.18632/oncotarget.4540

Chen, Y. C., Gotea, V., Margolin, G., & Elnitski, L. (2017). Significant associations between driver gene mutations and DNA methylation alterations across many cancer types. *PLoS Comput Biol*, *13*(11), e1005840. https://doi.org/10.1371/journal.pcbi.1005840

Cheng, H., Zheng, Z., & Cheng, T. (2020). New paradigms on hematopoietic stem cell differentiation. *Protein Cell*, *11*(1), 34-44. https://doi.org/10.1007/s13238-019-0633-0

Cherif, H., Bisson, D. G., Mannarino, M., Rabau, O., Ouellet, J. A., & Haglund, L. (2020). Senotherapeutic drugs for human intervertebral disc degeneration and low back pain. *Elife*, *9*. https://doi.org/10.7554/eLife.54693

Cimmino, L., Dolgalev, I., Wang, Y., Yoshimi, A., Martin, G. H., Wang, J., Ng, V., Xia, B., Witkowski, M. T., Mitchell-Flack, M., Grillo, I., Bakogianni, S., Ndiaye-Lobry, D., Martin, M. T., Guillamot, M., Banh, R. S., Xu, M., Figueroa, M. E., Dickins, R. A., . . . Aifantis, I. (2017). Restoration of TET2 Function Blocks Aberrant Self-Renewal and Leukemia Progression. *Cell*, *170*(6), 1079-1095 e1020. https://doi.org/10.1016/j.cell.2017.07.032

Cokic, V. P., Mitrovic-Ajtic, O., Beleslin-Cokic, B. B., Markovic, D., Buac, M., Diklic, M., Kraguljac-Kurtovic, N., Damjanovic, S., Milenkovic, P., Gotic, M., & Raj, P. K. (2015). Proinflammatory Cytokine IL-6 and JAK-STAT Signaling Pathway in Myeloproliferative Neoplasms. *Mediators Inflamm*, *2015*, 453020. https://doi.org/10.1155/2015/453020

Collins, T. B., Laranjeira, A. B. A., Kong, T., Fulbright, M. C., Fisher, D. A. C., Sturgeon, C. M., Batista, L. F. Z., & Oh, S. T. (2024). Altered erythropoiesis via JAK2 and ASXL1 mutations in myeloproliferative neoplasms. *Exp Hematol*, *132*, 104178. https://doi.org/10.1016/j.exphem.2024.104178

Colom Diaz, P. A., Mistry, J. J., & Trowbridge, J. J. (2023). Hematopoietic stem cell aging and leukemia transformation. *Blood*, *142*(6), 533-542. https://doi.org/10.1182/blood.2022017933

Constantinescu, S. N., Vainchenker, W., Levy, G., & Papadopoulos, N. (2021). Functional Consequences of Mutations in Myeloproliferative Neoplasms. *Hemasphere*, *5*(6), e578. https://doi.org/10.1097/HS9.0000000000000578

Cross, N. C. P., Ernst, T., Branford, S., Cayuela, J. M., Deininger, M., Fabarius, A., Kim, D. D. H., Machova Polakova, K., Radich, J. P., Hehlmann, R., Hochhaus, A., Apperley, J. F., & Soverini, S. (2023). European LeukemiaNet laboratory recommendations for the diagnosis and management of chronic myeloid leukemia. *Leukemia*, *37*(11), 2150-2167. https://doi.org/10.1038/s41375-023-02048-y

Cuollo, L., Antonangeli, F., Santoni, A., & Soriani, A. (2020). The Senescence-Associated Secretory Phenotype (SASP) in the Challenging Future of Cancer Therapy and Age-Related Diseases. *Biology (Basel)*, *9*(12). https://doi.org/10.3390/biology9120485

Cypris, O., Eipel, M., Franzen, J., Rosseler, C., Tharmapalan, V., Kuo, C. C., Vieri, M., Nikolic, M., Kirschner, M., Brummendorf, T. H., Zenke, M., Lampert, A., Beier, F., & Wagner, W. (2020). PRDM8 reveals aberrant DNA methylation in aging syndromes and is relevant for hematopoietic and neuronal differentiation. *Clin Epigenetics*, *12*(1), 125. https://doi.org/10.1186/s13148-020-00914-5

Cypris, O., Franzen, J., Frobel, J., Gluck, P., Kuo, C. C., Schmitz, S., Nuchtern, S., Zenke, M., & Wagner, W. (2022). Hematopoietic differentiation persists in human iPSCs defective in de novo DNA methylation. *BMC Biol*, *20*(1), 141. https://doi.org/10.1186/s12915-022-01343-x

Cypris, O., Frobel, J., Rai, S., Franzen, J., Sontag, S., Goetzke, R., Szymanski de Toledo, M. A., Zenke, M., & Wagner, W. (2019). Tracking of epigenetic changes during hematopoietic differentiation of induced pluripotent stem cells. *Clin Epigenetics*, *11*(1), 19. https://doi.org/10.1186/s13148-019-0617-1

Dagher, T., Maslah, N., Edmond, V., Cassinat, B., Vainchenker, W., Giraudier, S., Pasquier, F., Verger, E., Niwa-Kawakita, M., Lallemand-Breitenbach, V., Plo, I., Kiladjian, J. J., Villeval, J. L., & de The, H. (2021). JAK2V617F myeloproliferative neoplasm eradication by a novel interferon/arsenic therapy involves PML. *J Exp Med*, *218*(2). https://doi.org/10.1084/jem.20201268

Dahlstrom, J., Zhang, X., Ghaderi, M., Hultcrantz, M., Bjorkholm, M., & Xu, D. (2015). Dysregulation of shelterin factors coupled with telomere shortening in Philadelphia

chromosome negative myeloproliferative neoplasms. *Haematologica*, *100*(10), e402-405. https://doi.org/10.3324/haematol.2015.125765

de Boni, L., Gasparoni, G., Haubenreich, C., Tierling, S., Schmitt, I., Peitz, M., Koch, P., Walter, J., Wullner, U., & Brustle, O. (2018). DNA methylation alterations in iPSC- and hESC-derived neurons: potential implications for neurological disease modeling. *Clin Epigenetics*, *10*, 13. https://doi.org/10.1186/s13148-018-0440-0

Deaton, A. M., & Bird, A. (2011). CpG islands and the regulation of transcription. *Genes Dev*, *25*(10), 1010-1022. https://doi.org/10.1101/gad.2037511

Debacq-Chainiaux, F., Erusalimsky, J. D., Campisi, J., & Toussaint, O. (2009). Protocols to detect senescence-associated beta-galactosidase (SA-betagal) activity, a biomarker of senescent cells in culture and in vivo. *Nat Protoc*, *4*(12), 1798-1806. https://doi.org/10.1038/nprot.2009.191

Demirci, D., Dayanc, B., Mazi, F. A., & Senturk, S. (2021). The Jekyll and Hyde of Cellular Senescence in Cancer. *Cells*, *10*(2). https://doi.org/10.3390/cells10020208

Di Giacomo, D., Quintini, M., Pierini, V., Pellanera, F., La Starza, R., Gorello, P., Matteucci, C., Crescenzi, B., Fiumara, P. F., Veltroni, M., Borlenghi, E., Albano, F., Forghieri, F., Maccaferri, M., Bettelli, F., Luppi, M., Cuneo, A., Rossi, G., & Mecucci, C. (2022). Genomic and clinical findings in myeloid neoplasms with PDGFRB rearrangement. *Ann Hematol*, *101*(2), 297-307. https://doi.org/10.1007/s00277-021-04712-8

Di Micco, R., Krizhanovsky, V., Baker, D., & d'Adda di Fagagna, F. (2021). Cellular senescence in ageing: from mechanisms to therapeutic opportunities. *Nat Rev Mol Cell Biol*, *22*(2), 75-95. https://doi.org/10.1038/s41580-020-00314-w

Do, C., Dumont, E. L. P., Salas, M., Castano, A., Mujahed, H., Maldonado, L., Singh, A., DaSilva-Arnold, S. C., Bhagat, G., Lehman, S., Christiano, A. M., Madhavan, S., Nagy, P. L., Green, P. H. R., Feinman, R., Trimble, C., Illsley, N. P., Marder, K., Honig, L., . . . Tycko, B. (2020). Allele-specific DNA methylation is increased in cancers and its dense mapping in normal plus neoplastic cells increases the yield of disease-associated regulatory SNPs. *Genome Biol*, *21*(1), 153. https://doi.org/10.1186/s13059-020-02059-3

Doolittle, M. L., Saul, D., Kaur, J., Rowsey, J. L., Vos, S. J., Pavelko, K. D., Farr, J. N., Monroe, D. G., & Khosla, S. (2023). Multiparametric senescent cell phenotyping reveals targets of senolytic therapy in the aged murine skeleton. *Nat Commun*, *14*(1), 4587. https://doi.org/10.1038/s41467-023-40393-9

Doss, M. X., & Sachinidis, A. (2019). Current Challenges of iPSC-Based Disease Modeling and Therapeutic Implications. *Cells*, *8*(5). https://doi.org/10.3390/cells8050403

Duran, I., Pombo, J., Sun, B., Gallage, S., Kudo, H., McHugh, D., Bousset, L., Barragan Avila, J. E., Forlano, R., Manousou, P., Heikenwalder, M., Withers, D. J., Vernia, S., Goldin, R. D., & Gil, J. (2024). Detection of senescence using machine learning algorithms based on nuclear features. *Nat Commun*, *15*(1), 1041. https://doi.org/10.1038/s41467-024-45421-w

Eipel, M., Bozic, T., Mies, A., Beier, F., Jost, E., Brummendorf, T. H., Platzbecker, U., & Wagner, W. (2019). Tracking myeloid malignancies by targeted analysis of successive DNA methylation at neighboring CG dinucleotides. *Haematologica*, *104*(8), e349-e351. https://doi.org/10.3324/haematol.2018.209734

El-Daly, H., Kull, M., Zimmermann, S., Pantic, M., Waller, C. F., & Martens, U. M. (2005). Selective cytotoxicity and telomere damage in leukemia cells using the telomerase inhibitor BIBR1532. *Blood*, *105*(4), 1742-1749. https://doi.org/10.1182/blood-2003-12-4322

Ellison-Hughes, G. M. (2020). First evidence that senolytics are effective at decreasing senescent cells in humans. *EBioMedicine*, *56*, 102473. https://doi.org/10.1016/j.ebiom.2019.09.053

Elsafi Mabrouk, M. H., Goetzke, R., Abagnale, G., Yesilyurt, B., Salz, L., Cypris, O., Gluck, P., Liesenfelder, S., Zeevaert, K., Ma, Z., Toledo, M. A. S., Li, R., Costa, I. G., Lampert, A., Pachauri, V., Schnakenberg, U., Zenke, M., & Wagner, W. (2022). The spatial self-organization within pluripotent stem cell colonies is continued in detaching aggregates. *Biomaterials*, *282*, 121389. https://doi.org/10.1016/j.biomaterials.2022.121389

Esteller, M. (2005). Aberrant DNA methylation as a cancer-inducing mechanism. *Annu Rev Pharmacol Toxicol*, *45*, 629-656. https://doi.org/10.1146/annurev.pharmtox.45.120403.095832

Ewald, L., Dittmann, J., Vogler, M., & Fulda, S. (2019). Side-by-side comparison of BH3-mimetics identifies MCL-1 as a key therapeutic target in AML. *Cell Death Dis*, *10*(12), 917. https://doi.org/10.1038/s41419-019-2156-2

Fabris, F., & Randi, M. L. (2009). Essential thrombocythemia: past and present. *Intern Emerg Med*, *4*(5), 381-388. https://doi.org/10.1007/s11739-009-0284-x

Falandry, C., Bonnefoy, M., Freyer, G., & Gilson, E. (2014). Biology of cancer and aging: a complex association with cellular senescence. *J Clin Oncol*, *32*(24), 2604-2610. https://doi.org/10.1200/JCO.2014.55.1432

Fan, W., Cao, W., Shi, J., Gao, F., Wang, M., Xu, L., Wang, F., Li, Y., Guo, R., Bian, Z., Li, W., Jiang, Z., & Ma, W. (2023). Contributions of bone marrow monocytes/macrophages in myeloproliferative neoplasms with JAK2(V617F) mutation. *Ann Hematol*, *102*(7), 1745-1759. https://doi.org/10.1007/s00277-023-05284-5

Farina, M., Russo, D., & Hoffman, R. (2021). The possible role of mutated endothelial cells in myeloproliferative neoplasms. *Haematologica*, *106*(11), 2813-2823. https://doi.org/10.3324/haematol.2021.278499

Feinberg, A. P., & Vogelstein, B. (1983). Hypomethylation of ras oncogenes in primary human cancers. *Biochem Biophys Res Commun*, *111*(1), 47-54. https://doi.org/10.1016/s0006-291x(83)80115-6

Ferreira, M. S. V., Kirschner, M., Halfmeyer, I., Estrada, N., Xicoy, B., Isfort, S., Vieri, M., Zamora, L., Abels, A., Bouillon, A. S., Begemann, M., Schemionek, M., Maurer, A., Koschmieder, S., Wilop, S., Panse, J., Brummendorf, T. H., & Beier, F. (2020). Comparison of flow-FISH and MM-qPCR telomere length assessment techniques for the screening of telomeropathies. *Ann N Y Acad Sci*, *1466*(1), 93-103. https://doi.org/10.1111/nyas.14248

Feusier, J. E., Arunachalam, S., Tashi, T., Baker, M. J., VanSant-Webb, C., Ferdig, A., Welm, B. E., Rodriguez-Flores, J. L., Ours, C., Jorde, L. B., Prchal, J. T., & Mason, C. C. (2021). Large-Scale Identification of Clonal Hematopoiesis and Mutations Recurrent in Blood Cancers. *Blood Cancer Discov*, *2*(3), 226-237. https://doi.org/10.1158/2643-3230.BCD-20-0094

Fleischman, A. G. (2015). Inflammation as a Driver of Clonal Evolution in Myeloproliferative Neoplasm. *Mediators Inflamm*, *2015*, 606819. https://doi.org/10.1155/2015/606819

Flosdorf, N., Bohnke, J., de Toledo, M. A. S., Lutterbach, N., Lerma, V. G., Grasshoff, M., Olschok, K., Gupta, S., Tharmapalan, V., Schmitz, S., Gotz, K., Schuler, H. M., Maurer, A., Sontag, S., Kustermann, C., Sere, K., Wagner, W., Costa, I. G., Brummendorf, T. H., . . . Zenke, M. (2024). Proinflammatory phenotype of iPS cell-derived JAK2 V617F megakaryocytes induces fibrosis in 3D in vitro bone marrow niche. *Stem Cell Reports*. https://doi.org/10.1016/j.stemcr.2023.12.011

Fornelli, C., Sofia Cento, A., Nevi, L., Mastrocola, R., Ferreira Alves, G., Caretti, G., Collino, M., & Penna, F. (2024). The BET inhibitor JQ1 targets fat metabolism and counteracts obesity. *J Adv Res*. https://doi.org/10.1016/j.jare.2024.02.001

Fragkiadaki, P., Renieri, E., Kalliantasi, K., Kouvidi, E., Apalaki, E., Vakonaki, E., Mamoulakis, C., Spandidos, D. A., & Tsatsakis, A. (2022). Tauelomerase inhibitors and activators in aging and cancer: A systematic review. *Mol Med Rep*, *25*(5). https://doi.org/10.3892/mmr.2022.12674

Fransquet, P. D., Wrigglesworth, J., Woods, R. L., Ernst, M. E., & Ryan, J. (2019). The epigenetic clock as a predictor of disease and mortality risk: a systematic review and meta-analysis. *Clin Epigenetics*, *11*(1), 62. https://doi.org/10.1186/s13148-019-0656-7

Frasca, D., Diaz, A., Romero, M., Landin, A. M., & Blomberg, B. B. (2011). Age effects on B cells and humoral immunity in humans. *Ageing Res Rev*, *10*(3), 330-335. https://doi.org/10.1016/j.arr.2010.08.004

Frink, R. E., Peyton, M., Schiller, J. H., Gazdar, A. F., Shay, J. W., & Minna, J. D. (2016). Telomerase inhibitor imetelstat has preclinical activity across the spectrum of non-small cell lung cancer oncogenotypes in a telomere length dependent manner. *Oncotarget*, *7*(22), 31639-31651. https://doi.org/10.18632/oncotarget.9335

Fusaki, N., Ban, H., Nishiyama, A., Saeki, K., & Hasegawa, M. (2009). Efficient induction of transgene-free human pluripotent stem cells using a vector based on Sendai virus, an RNA virus that does not integrate into the host genome. *Proc Jpn Acad Ser B Phys Biol Sci*, *85*(8), 348-362. https://doi.org/10.2183/pjab.85.348

Gaj, T., Gersbach, C. A., & Barbas, C. F., 3rd. (2013). ZFN, TALEN, and CRISPR/Cas-based methods for genome engineering. *Trends Biotechnol*, *31*(7), 397-405. https://doi.org/10.1016/j.tibtech.2013.04.004

Gangat, N., Karrar, O., Al-Kali, A., Begna, K. H., Elliott, M. A., Wolanskyj-Spinner, A. P., Pardanani, A., Hanson, C. A., Ketterling, R. P., & Tefferi, A. (2024). One thousand patients with essential thrombocythemia: the Mayo Clinic experience. *Blood Cancer J*, *14*(1), 11. https://doi.org/10.1038/s41408-023-00972-x

Gao, X., Xu, C., Asada, N., & Frenette, P. S. (2018). The hematopoietic stem cell niche: from embryo to adult. *Development*, *145*(2). https://doi.org/10.1242/dev.139691

Gems, D., & de Magalhaes, J. P. (2021). The hoverfly and the wasp: A critique of the hallmarks of aging as a paradigm. *Ageing Res Rev*, *70*, 101407. https://doi.org/10.1016/j.arr.2021.101407

Genovese, G., Kahler, A. K., Handsaker, R. E., Lindberg, J., Rose, S. A., Bakhoum, S. F., Chambert, K., Mick, E., Neale, B. M., Fromer, M., Purcell, S. M., Svantesson, O., Landen, M., Hoglund, M., Lehmann, S., Gabriel, S. B., Moran, J. L., Lander, E. S., Sullivan, P. F., . . . McCarroll, S. A. (2014). Clonal hematopoiesis and blood-cancer risk inferred from blood DNA sequence. *N Engl J Med*, *371*(26), 2477-2487. https://doi.org/10.1056/NEJMoa1409405

Ghosh, J., Koussa, R. E., Mohamad, S. F., Liu, J., Kacena, M. A., & Srour, E. F. (2021). Cellular components of the hematopoietic niche and their regulation of hematopoietic stem cell function. *Curr Opin Hematol*, *28*(4), 243-250. https://doi.org/10.1097/MOH.0000000000000656

Gil, J. (2023). The challenge of identifying senescent cells. *Nat Cell Biol*, *25*(11), 1554-1556. https://doi.org/10.1038/s41556-023-01267-w

Gleitz, H. F. E., Benabid, A., & Schneider, R. K. (2021). Still a burning question: the interplay between inflammation and fibrosis in myeloproliferative neoplasms. *Curr Opin Hematol*, *28*(5), 364-371. https://doi.org/10.1097/MOH.0000000000000669

Go, S., Kang, M., Kwon, S. P., Jung, M., Jeon, O. H., & Kim, B. S. (2021). The Senolytic Drug JQ1 Removes Senescent Cells via Ferroptosis. *Tissue Eng Regen Med*, *18*(5), 841-850. https://doi.org/10.1007/s13770-021-00346-z

Goldman, E. A., Spellman, P. T., & Agarwal, A. (2023). Defining clonal hematopoiesis of indeterminate potential: evolutionary dynamics and detection under aging and inflammation. *Cold Spring Harb Mol Case Stud*, *9*(2). https://doi.org/10.1101/mcs.a006251

Gounder, S. S., Abdullah, B. J. J., Radzuanb, N., Zain, F., Sait, N. B. M., Chua, C., & Subramani, B. (2018). Effect of Aging on NK Cell Population and Their Proliferation at Ex Vivo Culture Condition. *Anal Cell Pathol (Amst)*, *2018*, 7871814. https://doi.org/10.1155/2018/7871814

Goyal, Y., Busch, G. T., Pillai, M., Li, J., Boe, R. H., Grody, E. I., Chelvanambi, M., Dardani, I. P., Emert, B., Bodkin, N., Braun, J., Fingerman, D., Kaur, A., Jain, N., Ravindran, P. T., Mellis, I. A., Kiani, K., Alicea, G. M., Fane, M. E., . . . Raj, A. (2023). Diverse clonal fates emerge upon drug treatment of homogeneous cancer cells. *Nature*, *620*(7974), 651-659. https://doi.org/10.1038/s41586-023-06342-8

Greenfield, G., McMullin, M. F., & Mills, K. (2021). Molecular pathogenesis of the myeloproliferative neoplasms. *J Hematol Oncol*, *14*(1), 103. https://doi.org/10.1186/s13045-021-01116-z

Greider, C. W. (1996). Telomere length regulation. *Annu Rev Biochem*, *65*, 337-365. https://doi.org/10.1146/annurev.bi.65.070196.002005

Haas, S., Trumpp, A., & Milsom, M. D. (2018). Causes and Consequences of Hematopoietic Stem Cell Heterogeneity. *Cell Stem Cell*, *22*(5), 627-638. https://doi.org/10.1016/j.stem.2018.04.003

Hambright, W. S., Duke, V. R., Goff, A. D., Goff, A. W., Minas, L. T., Kloser, H., Gao, X., Huard, C., Guo, P., Lu, A., Mitchell, J., Mullen, M., Su, C., Tchkonia, T., Espindola Netto, J. M., Robbins, P. D., Niedernhofer, L. J., Kirkland, J. L., Bahney, C. S., . . . Huard, J. (2024). Clinical validation of C(12)FDG as a marker associated with senescence and osteoarthritic phenotypes. *Aging Cell*, *23*(5), e14113. https://doi.org/10.1111/acel.14113

Han, Y., Eipel, M., Franzen, J., Sakk, V., Dethmers-Ausema, B., Yndriago, L., Izeta, A., de Haan, G., Geiger, H., & Wagner, W. (2018). Epigenetic age-predictor for mice based on three CpG sites. *Elife*, *7*. https://doi.org/10.7554/eLife.37462

Han, Y., Franzen, J., Stiehl, T., Gobs, M., Kuo, C. C., Nikolic, M., Hapala, J., Koop, B. E., Strathmann, K., Ritz-Timme, S., & Wagner, W. (2020). New targeted approaches for epigenetic age predictions. *BMC Biol*, *18*(1), 71. https://doi.org/10.1186/s12915-020-00807-2

Hanahan, D., & Weinberg, R. A. (2000). The hallmarks of cancer. *Cell*, *100*(1), 57-70. https://doi.org/10.1016/s0092-8674(00)81683-9

Hanahan, D., & Weinberg, R. A. (2011). Hallmarks of cancer: the next generation. *Cell*, *144*(5), 646-674. https://doi.org/10.1016/j.cell.2011.02.013

Hannum, G., Guinney, J., Zhao, L., Zhang, L., Hughes, G., Sadda, S., Klotzle, B., Bibikova, M., Fan, J. B., Gao, Y., Deconde, R., Chen, M., Rajapakse, I., Friend, S., Ideker, T., & Zhang, K. (2013). Genome-wide methylation profiles reveal quantitative views of human aging rates. *Mol Cell*, *49*(2), 359-367. https://doi.org/10.1016/j.molcel.2012.10.016

Haouas, H., Haouas, S., Uzan, G., & Hafsia, A. (2010). Identification of new markers discriminating between myeloid and lymphoid acute leukemia. *Hematology*, *15*(4), 193-203. https://doi.org/10.1179/102453310X12647083620769

Harrison, C. N., Gupta, V. K., Gerds, A. T., Rampal, R., Verstovsek, S., Talpaz, M., Kiladjian, J. J., Mesa, R., Kuykendall, A. T., Vannucchi, A. M., Palandri, F., Grosicki, S., Devos, T., Jourdan, E., Wondergem, M. J., Al-Ali, H. K., Buxhofer-Ausch, V., Alvarez-Larran, A., Patriarca, A., . . . Mascarenhas, J. (2022). Phase III MANIFEST-2: pelabresib + ruxolitinib vs placebo + ruxolitinib in JAK inhibitor treatment-naive myelofibrosis. *Future Oncol*, *18*(27), 2987-2997. https://doi.org/10.2217/fon-2022-0484

Harrison, D. E., Strong, R., Sharp, Z. D., Nelson, J. F., Astle, C. M., Flurkey, K., Nadon, N. L., Wilkinson, J. E., Frenkel, K., Carter, C. S., Pahor, M., Javors, M. A., Fernandez, E., & Miller, R. A. (2009). Rapamycin fed late in life extends lifespan in genetically heterogeneous mice. *Nature*, *460*(7253), 392-395. https://doi.org/10.1038/nature08221

Hasegawa, H., Yamada, Y., Iha, H., Tsukasaki, K., Nagai, K., Atogami, S., Sugahara, K., Tsuruda, K., Ishizaki, A., & Kamihira, S. (2009). Activation of p53 by Nutlin-3a, an antagonist of MDM2, induces apoptosis and cellular senescence in adult T-cell leukemia cells. *Leukemia*, *23*(11), 2090-2101. https://doi.org/10.1038/leu.2009.171

Hassani, S. N., Moradi, S., Taleahmad, S., Braun, T., & Baharvand, H. (2019). Transition of inner cell mass to embryonic stem cells: mechanisms, facts, and hypotheses. *Cell Mol Life Sci*, *76*(5), 873-892. https://doi.org/10.1007/s00018-018-2965-y

Hasselbalch, H. C. (2012). Perspectives on chronic inflammation in essential thrombocythemia, polycythemia vera, and myelofibrosis: is chronic inflammation a trigger and driver of clonal evolution and development of accelerated atherosclerosis and second cancer? *Blood*, *119*(14), 3219-3225. https://doi.org/10.1182/blood-2011-11-394775

Hasselbalch, H. C., Elvers, M., & Schafer, A. I. (2021). The pathobiology of thrombosis, microvascular disease, and hemorrhage in the myeloproliferative neoplasms. *Blood*, *137*(16), 2152-2160. https://doi.org/10.1182/blood.2020008109

Hasselbalch, H. C., Junker, P., Skov, V., Kjaer, L., Knudsen, T. A., Larsen, M. K., Holmstrom, M. O., Andersen, M. H., Jensen, C., Karsdal, M. A., & Willumsen, N. (2023). Revisiting Circulating Extracellular Matrix Fragments as Disease Markers in Myelofibrosis and Related Neoplasms. *Cancers (Basel)*, *15*(17). https://doi.org/10.3390/cancers15174323

Hayflick, L., & Moorhead, P. S. (1961). The serial cultivation of human diploid cell strains. *Exp Cell Res*, *25*, 585-621. https://doi.org/10.1016/0014-4827(61)90192-6

Hazeldine, J., & Lord, J. M. (2013). The impact of ageing on natural killer cell function and potential consequences for health in older adults. *Ageing Res Rev*, *12*(4), 1069-1078. https://doi.org/10.1016/j.arr.2013.04.003

He, Y., & Ecker, J. R. (2015). Non-CG Methylation in the Human Genome. *Annu Rev Genomics Hum Genet*, *16*, 55-77. https://doi.org/10.1146/annurev-genom-090413-025437
Hermouet, S., Bigot-Corbel, E., & Gardie, B. (2015). Pathogenesis of Myeloproliferative Neoplasms: Role and Mechanisms of Chronic Inflammation. *Mediators Inflamm*, *2015*, 145293. https://doi.org/10.1155/2015/145293
Hernandez-Segura, A., Nehme, J., & Demaria, M. (2018). Hallmarks of Cellular Senescence. *Trends Cell Biol*, *28*(6), 436-453. https://doi.org/10.1016/j.tcb.2018.02.001
Hernando-Herraez, I., Evano, B., Stubbs, T., Commere, P. H., Jan Bonder, M., Clark, S., Andrews, S., Tajbakhsh, S., & Reik, W. (2019). Ageing affects DNA methylation drift and transcriptional cell-to-cell variability in mouse muscle stem cells. *Nat Commun*, *10*(1), 4361. https://doi.org/10.1038/s41467-019-12293-4
Herranz, N., & Gil, J. (2018). Mechanisms and functions of cellular senescence. *J Clin Invest*, *128*(4), 1238-1246. https://doi.org/10.1172/JCI95148
Hickson, L. J., Langhi Prata, L. G. P., Bobart, S. A., Evans, T. K., Giorgadze, N., Hashmi, S. K., Herrmann, S. M., Jensen, M. D., Jia, Q., Jordan, K. L., Kellogg, T. A., Khosla, S., Koerber, D. M., Lagnado, A. B., Lawson, D. K., LeBrasseur, N. K., Lerman, L. O., McDonald, K. M., McKenzie, T. J., . . . Kirkland, J. L. (2019). Senolytics decrease senescent cells in humans: Preliminary report from a clinical trial of Dasatinib plus Quercetin in individuals with diabetic kidney disease. *EBioMedicine*, *47*, 446-456. https://doi.org/10.1016/j.ebiom.2019.08.069
Hinds, D. A., Barnholt, K. E., Mesa, R. A., Kiefer, A. K., Do, C. B., Eriksson, N., Mountain, J. L., Francke, U., Tung, J. Y., Nguyen, H. M., Zhang, H., Gojenola, L., Zehnder, J. L., & Gotlib, J. (2016). Germ line variants predispose to both JAK2 V617F clonal hematopoiesis and myeloproliferative neoplasms. *Blood*, *128*(8), 1121-1128. https://doi.org/10.1182/blood-2015-06-652941
Horvath, S. (2013). DNA methylation age of human tissues and cell types. *Genome Biol*, *14*(10), R115. https://doi.org/10.1186/gb-2013-14-10-r115
Horvath, S., & Raj, K. (2018). DNA methylation-based biomarkers and the epigenetic clock theory of ageing. *Nat Rev Genet*, *19*(6), 371-384. https://doi.org/10.1038/s41576-018-0004-3
Hosnijeh, F. S., Matullo, G., Russo, A., Guarrera, S., Modica, F., Nieters, A., Overvad, K., Guldberg, P., Tjonneland, A., Canzian, F., Boeing, H., Aleksandrova, K., Trichopoulou, A., Lagiou, P., Trichopoulos, D., Tagliabue, G., Tumino, R., Panico, S., Palli, D., . . . Vermeulen, R. (2014). Prediagnostic telomere length and risk of B-cell lymphoma-Results from the EPIC cohort study. *Int J Cancer*, *135*(12), 2910-2917. https://doi.org/10.1002/ijc.28934
How, J., Garcia, J. S., & Mullally, A. (2023). Biology and therapeutic targeting of molecular mechanisms in MPNs. *Blood*, *141*(16), 1922-1933. https://doi.org/10.1182/blood.2022017416
Huang, W., Hickson, L. J., Eirin, A., Kirkland, J. L., & Lerman, L. O. (2022). Cellular senescence: the good, the bad and the unknown. *Nat Rev Nephrol*, *18*(10), 611-627. https://doi.org/10.1038/s41581-022-00601-z
Issa, J. P. (2014). Aging and epigenetic drift: a vicious cycle. *J Clin Invest*, *124*(1), 24-29. https://doi.org/10.1172/JCI69735
Ivancich, M., Schrank, Z., Wojdyla, L., Leviskas, B., Kuckovic, A., Sanjali, A., & Puri, N. (2017). Treating Cancer by Targeting Telomeres and Telomerase. *Antioxidants (Basel)*, *6*(1). https://doi.org/10.3390/antiox6010015
Ivanovs, A., Rybtsov, S., Ng, E. S., Stanley, E. G., Elefanty, A. G., & Medvinsky, A. (2017). Human haematopoietic stem cell development: from the embryo to the dish. *Development*, *144*(13), 2323-2337. https://doi.org/10.1242/dev.134866
Izzo, F., Myers, R. M., Ganesan, S., Mekerishvili, L., Kottapalli, S., Prieto, T., Eton, E. O., Botella, T., Dunbar, A. J., Bowman, R. L., Sotelo, J., Potenski, C., Mimitou, E. P., Stahl, M., El Ghaity-Beckley, S., Arandela, J., Raviram, R., Choi, D. C., Hoffman, R., . . . Landau, D. A. (2024). Mapping genotypes to chromatin accessibility profiles in single cells. *Nature*, *629*(8014), 1149-1157. https://doi.org/10.1038/s41586-024-07388-y

Jaffe, A. E., & Irizarry, R. A. (2014). Accounting for cellular heterogeneity is critical in epigenome-wide association studies. *Genome Biol*, *15*(2), R31. https://doi.org/10.1186/gb-2014-15-2-r31
Jaiswal, S. (2020). Clonal hematopoiesis and nonhematologic disorders. *Blood*, *136*(14), 1606-1614. https://doi.org/10.1182/blood.2019000989
Jaiswal, S., & Ebert, B. L. (2019). Clonal hematopoiesis in human aging and disease. *Science*, *366*(6465). https://doi.org/10.1126/science.aan4673
Jaiswal, S., Fontanillas, P., Flannick, J., Manning, A., Grauman, P. V., Mar, B. G., Lindsley, R. C., Mermel, C. H., Burtt, N., Chavez, A., Higgins, J. M., Moltchanov, V., Kuo, F. C., Kluk, M. J., Henderson, B., Kinnunen, L., Koistinen, H. A., Ladenvall, C., Getz, G., . . . Ebert, B. L. (2014). Age-related clonal hematopoiesis associated with adverse outcomes. *N Engl J Med*, *371*(26), 2488-2498. https://doi.org/10.1056/NEJMoa1408617
James, C., Ugo, V., Le Couedic, J. P., Staerk, J., Delhommeau, F., Lacout, C., Garcon, L., Raslova, H., Berger, R., Bennaceur-Griscelli, A., Villeval, J. L., Constantinescu, S. N., Casadevall, N., & Vainchenker, W. (2005). A unique clonal JAK2 mutation leading to constitutive signalling causes polycythaemia vera. *Nature*, *434*(7037), 1144-1148. https://doi.org/10.1038/nature03546
Jaskelioff, M., Muller, F. L., Paik, J. H., Thomas, E., Jiang, S., Adams, A. C., Sahin, E., Kost-Alimova, M., Protopopov, A., Cadinanos, J., Horner, J. W., Maratos-Flier, E., & Depinho, R. A. (2011). Telomerase reactivation reverses tissue degeneration in aged telomerase-deficient mice. *Nature*, *469*(7328), 102-106. https://doi.org/10.1038/nature09603
Jiang, Q., & Jamieson, C. (2018). BET'ing on Dual JAK/BET Inhibition as a Therapeutic Strategy for Myeloproliferative Neoplasms. *Cancer Cell*, *33*(1), 3-5. https://doi.org/10.1016/j.ccell.2017.12.007
Jinek, M., Chylinski, K., Fonfara, I., Hauer, M., Doudna, J. A., & Charpentier, E. (2012). A programmable dual-RNA-guided DNA endonuclease in adaptive bacterial immunity. *Science*, *337*(6096), 816-821. https://doi.org/10.1126/science.1225829
Justice, J. N., Nambiar, A. M., Tchkonia, T., LeBrasseur, N. K., Pascual, R., Hashmi, S. K., Prata, L., Masternak, M. M., Kritchevsky, S. B., Musi, N., & Kirkland, J. L. (2019). Senolytics in idiopathic pulmonary fibrosis: Results from a first-in-human, open-label, pilot study. *EBioMedicine*, *40*, 554-563. https://doi.org/10.1016/j.ebiom.2018.12.052
Jylhava, J., Pedersen, N. L., & Hagg, S. (2017). Biological Age Predictors. *EBioMedicine*, *21*, 29-36. https://doi.org/10.1016/j.ebiom.2017.03.046
Kalmer, M., Pannen, K., Lemanzyk, R., Wirths, C., Baumeister, J., Maurer, A., Kricheldorf, K., Schifflers, J., Gezer, D., Isfort, S., Brummendorf, T. H., Koschmieder, S., & Chatain, N. (2022). Clonogenic assays improve determination of variant allele frequency of driver mutations in myeloproliferative neoplasms. *Ann Hematol*, *101*(12), 2655-2663. https://doi.org/10.1007/s00277-022-05000-9
Kananen, L., Marttila, S., Nevalainen, T., Jylhava, J., Mononen, N., Kahonen, M., Raitakari, O. T., Lehtimaki, T., & Hurme, M. (2016). Aging-associated DNA methylation changes in middle-aged individuals: the Young Finns study. *BMC Genomics*, *17*, 103. https://doi.org/10.1186/s12864-016-2421-z
Kapetanos, K., Asimakopoulos, D., Christodoulou, N., Vogt, A., & Khan, W. (2021). Chronological Age Affects MSC Senescence In Vitro-A Systematic Review. *Int J Mol Sci*, *22*(15). https://doi.org/10.3390/ijms22157945
Karetnikov, D. I., Romanov, S. E., Baklaushev, V. P., & Laktionov, P. P. (2024). Age Prediction Using DNA Methylation Heterogeneity Metrics. *Int J Mol Sci*, *25*(9). https://doi.org/10.3390/ijms25094967
Karin, O., Agrawal, A., Porat, Z., Krizhanovsky, V., & Alon, U. (2019). Senescent cell turnover slows with age providing an explanation for the Gompertz law. *Nat Commun*, *10*(1), 5495. https://doi.org/10.1038/s41467-019-13192-4
Kim, K., Doi, A., Wen, B., Ng, K., Zhao, R., Cahan, P., Kim, J., Aryee, M. J., Ji, H., Ehrlich, L. I., Yabuuchi, A., Takeuchi, A., Cunniff, K. C., Hongguang, H., McKinney-Freeman, S., Naveiras, O., Yoon, T. J., Irizarry, R. A., Jung, N., . . . Daley, G. Q. (2010). Epigenetic memory in induced pluripotent stem cells. *Nature*, *467*(7313), 285-290. https://doi.org/10.1038/nature09342

Kim Sh, S. H., Kaminker, P., & Campisi, J. (2002). Telomeres, aging and cancer: in search of a happy ending. *Oncogene*, *21*(4), 503-511. https://doi.org/10.1038/sj.onc.1205077
Kirkland, J. L., & Tchkonia, T. (2020). Senolytic drugs: from discovery to translation. *J Intern Med*, *288*(5), 518-536. https://doi.org/10.1111/joim.13141
Kirschner, M., Maurer, A., Wlodarski, M. W., Ventura Ferreira, M. S., Bouillon, A. S., Halfmeyer, I., Blau, W., Kreuter, M., Rosewich, M., Corbacioglu, S., Beck, J., Schwarz, M., Bittenbring, J., Radsak, M. P., Wilk, C. M., Koschmieder, S., Begemann, M., Kurth, I., Schemionek, M., . . . Beier, F. (2018). Recurrent somatic mutations are rare in patients with cryptic dyskeratosis congenita. *Leukemia*, *32*(8), 1762-1767. https://doi.org/10.1038/s41375-018-0125-x
Klampfl, T., Gisslinger, H., Harutyunyan, A. S., Nivarthi, H., Rumi, E., Milosevic, J. D., Them, N. C., Berg, T., Gisslinger, B., Pietra, D., Chen, D., Vladimer, G. I., Bagienski, K., Milanesi, C., Casetti, I. C., Sant'Antonio, E., Ferretti, V., Elena, C., Schischlik, F., . . . Kralovics, R. (2013). Somatic mutations of calreticulin in myeloproliferative neoplasms. *N Engl J Med*, *369*(25), 2379-2390. https://doi.org/10.1056/NEJMoa1311347
Kleppe, M., Koche, R., Zou, L., van Galen, P., Hill, C. E., Dong, L., De Groote, S., Papalexi, E., Hanasoge Somasundara, A. V., Cordner, K., Keller, M., Farnoud, N., Medina, J., McGovern, E., Reyes, J., Roberts, J., Witkin, M., Rapaport, F., Teruya-Feldstein, J., . . . Levine, R. L. (2018). Dual Targeting of Oncogenic Activation and Inflammatory Signaling Increases Therapeutic Efficacy in Myeloproliferative Neoplasms. *Cancer Cell*, *33*(1), 29-43 e27. https://doi.org/10.1016/j.ccell.2017.11.009
Klutstein, M., Nejman, D., Greenfield, R., & Cedar, H. (2016). DNA Methylation in Cancer and Aging. *Cancer Res*, *76*(12), 3446-3450. https://doi.org/10.1158/0008-5472.CAN-15-3278
Koch, C. M., & Wagner, W. (2011). Epigenetic-aging-signature to determine age in different tissues. *Aging (Albany NY)*, *3*(10), 1018-1027. https://doi.org/10.18632/aging.100395
Kondilis-Mangum, H. D., & Wade, P. A. (2013). Epigenetics and the adaptive immune response. *Mol Aspects Med*, *34*(4), 813-825. https://doi.org/10.1016/j.mam.2012.06.008
Konopleva, M., Martinelli, G., Daver, N., Papayannidis, C., Wei, A., Higgins, B., Ott, M., Mascarenhas, J., & Andreeff, M. (2020). MDM2 inhibition: an important step forward in cancer therapy. *Leukemia*, *34*(11), 2858-2874. https://doi.org/10.1038/s41375-020-0949-z
Koschmieder, S., Gottgens, B., Zhang, P., Iwasaki-Arai, J., Akashi, K., Kutok, J. L., Dayaram, T., Geary, K., Green, A. R., Tenen, D. G., & Huettner, C. S. (2005). Inducible chronic phase of myeloid leukemia with expansion of hematopoietic stem cells in a transgenic model of BCR-ABL leukemogenesis. *Blood*, *105*(1), 324-334. https://doi.org/10.1182/blood-2003-12-4369
Kovtonyuk, L. V., Fritsch, K., Feng, X., Manz, M. G., & Takizawa, H. (2016). Inflamm-Aging of Hematopoiesis, Hematopoietic Stem Cells, and the Bone Marrow Microenvironment. *Front Immunol*, *7*, 502. https://doi.org/10.3389/fimmu.2016.00502
Kralovics, R. (2008). Genetic complexity of myeloproliferative neoplasms. *Leukemia*, *22*(10), 1841-1848. https://doi.org/10.1038/leu.2008.233
Kralovics, R., Passamonti, F., Buser, A. S., Teo, S. S., Tiedt, R., Passweg, J. R., Tichelli, A., Cazzola, M., & Skoda, R. C. (2005). A gain-of-function mutation of JAK2 in myeloproliferative disorders. *N Engl J Med*, *352*(17), 1779-1790. https://doi.org/10.1056/NEJMoa051113
Kralovics, R., Teo, S. S., Li, S., Theocharides, A., Buser, A. S., Tichelli, A., & Skoda, R. C. (2006). Acquisition of the V617F mutation of JAK2 is a late genetic event in a subset of patients with myeloproliferative disorders. *Blood*, *108*(4), 1377-1380. https://doi.org/10.1182/blood-2005-11-009605
Kramer, F., & Mullally, A. (2023). Antibody targeting of mutant calreticulin in myeloproliferative neoplasms. *J Cell Mol Med*, *28*(5), e17896. https://doi.org/10.1111/jcmm.17896
Krueger, F., & Andrews, S. R. (2011). Bismark: a flexible aligner and methylation caller for Bisulfite-Seq applications. *Bioinformatics*, *27*(11), 1571-1572. https://doi.org/10.1093/bioinformatics/btr167

Kumari, R., & Jat, P. (2021). Mechanisms of Cellular Senescence: Cell Cycle Arrest and Senescence Associated Secretory Phenotype. *Front Cell Dev Biol*, *9*, 645593. https://doi.org/10.3389/fcell.2021.645593

Kuykendall, A. T., Horvat, N. P., Pandey, G., Komrokji, R., & Reuther, G. W. (2020). Finding a Jill for JAK: Assessing Past, Present, and Future JAK Inhibitor Combination Approaches in Myelofibrosis. *Cancers (Basel)*, *12*(8). https://doi.org/10.3390/cancers12082278

Lan, Q., Cawthon, R., Shen, M., Weinstein, S. J., Virtamo, J., Lim, U., Hosgood, H. D., 3rd, Albanes, D., & Rothman, N. (2009). A prospective study of telomere length measured by monochrome multiplex quantitative PCR and risk of non-Hodgkin lymphoma. *Clin Cancer Res*, *15*(23), 7429-7433. https://doi.org/10.1158/1078-0432.CCR-09-0845

Lange, L., Morgan, M., & Schambach, A. (2021). The hemogenic endothelium: a critical source for the generation of PSC-derived hematopoietic stem and progenitor cells. *Cell Mol Life Sci*, *78*(9), 4143-4160. https://doi.org/10.1007/s00018-021-03777-y

Lanikova, L., Babosova, O., & Prchal, J. T. (2019). Experimental Modeling of Myeloproliferative Neoplasms. *Genes (Basel)*, *10*(10). https://doi.org/10.3390/genes10100813

Lansdorp, P. M. (2022). Telomeres, aging, and cancer: the big picture. *Blood*, *139*(6), 813-821. https://doi.org/10.1182/blood.2021014299

Lapborisuth, K., Farrell, C., & Pellegrini, M. (2022). Pseudotime Analysis Reveals Exponential Trends in DNA Methylation Aging with Mortality Associated Timescales. *Cells*, *11*(5). https://doi.org/10.3390/cells11050767

Lataillade, J. J., Pierre-Louis, O., Hasselbalch, H. C., Uzan, G., Jasmin, C., Martyre, M. C., Le Bousse-Kerdiles, M. C., French, I., & the European, E. N. o. M. (2008). Does primary myelofibrosis involve a defective stem cell niche? From concept to evidence. *Blood*, *112*(8), 3026-3035. https://doi.org/10.1182/blood-2008-06-158386

Law, J. A., & Jacobsen, S. E. (2010). Establishing, maintaining and modifying DNA methylation patterns in plants and animals. *Nat Rev Genet*, *11*(3), 204-220. https://doi.org/10.1038/nrg2719

Le Bousse-Kerdiles, M. C. (2012). Primary myelofibrosis and the "bad seeds in bad soil" concept. *Fibrogenesis Tissue Repair*, *5*(Suppl 1), S20. https://doi.org/10.1186/1755-1536-5-S1-S20

Lee, D. S., Shin, J. Y., Tonge, P. D., Puri, M. C., Lee, S., Park, H., Lee, W. C., Hussein, S. M., Bleazard, T., Yun, J. Y., Kim, J., Li, M., Cloonan, N., Wood, D., Clancy, J. L., Mosbergen, R., Yi, J. H., Yang, K. S., Kim, H., . . . Seo, J. S. (2014). An epigenomic roadmap to induced pluripotency reveals DNA methylation as a reprogramming modulator. *Nat Commun*, *5*, 5619. https://doi.org/10.1038/ncomms6619

Lee, S., Yu, Y., Trimpert, J., Benthani, F., Mairhofer, M., Richter-Pechanska, P., Wyler, E., Belenki, D., Kaltenbrunner, S., Pammer, M., Kausche, L., Firsching, T. C., Dietert, K., Schotsaert, M., Martinez-Romero, C., Singh, G., Kunz, S., Niemeyer, D., Ghanem, R., . . . Schmitt, C. A. (2021). Virus-induced senescence is a driver and therapeutic target in COVID-19. *Nature*, *599*(7884), 283-289. https://doi.org/10.1038/s41586-021-03995-1

Lee, S. J., Jung, C., Oh, J. E., Kim, S., Lee, S., Lee, J. Y., & Yoon, Y. S. (2023). Generation of Red Blood Cells from Human Pluripotent Stem Cells-An Update. *Cells*, *12*(11). https://doi.org/10.3390/cells12111554

Lehallier, B., Gate, D., Schaum, N., Nanasi, T., Lee, S. E., Yousef, H., Moran Losada, P., Berdnik, D., Keller, A., Verghese, J., Sathyan, S., Franceschi, C., Milman, S., Barzilai, N., & Wyss-Coray, T. (2019). Undulating changes in human plasma proteome profiles across the lifespan. *Nat Med*, *25*(12), 1843-1850. https://doi.org/10.1038/s41591-019-0673-2

Lehmann, U., Stark, H., Bartels, S., Schlue, J., Busche, G., & Kreipe, H. (2021). Genome-wide DNA methylation profiling is able to identify prefibrotic PMF cases at risk for progression to myelofibrosis. *Clin Epigenetics*, *13*(1), 28. https://doi.org/10.1186/s13148-021-01010-y

Leimkuhler, N. B., Gleitz, H. F. E., Ronghui, L., Snoeren, I. A. M., Fuchs, S. N. R., Nagai, J. S., Banjanin, B., Lam, K. H., Vogl, T., Kuppe, C., Stalmann, U. S. A., Busche, G., Kreipe, H., Gutgemann, I., Krebs, P., Banz, Y., Boor, P., Tai, E. W., Brummendorf, T. H., . . . Schneider, R. K. (2021). Heterogeneous bone-marrow stromal progenitors drive

myelofibrosis via a druggable alarmin axis. *Cell Stem Cell*, *28*(4), 637-652 e638. https://doi.org/10.1016/j.stem.2020.11.004
Lelarge, V., Capelle, R., Oger, F., Mathieu, T., & Le Calve, B. (2024). Senolytics: from pharmacological inhibitors to immunotherapies, a promising future for patients' treatment. *NPJ Aging*, *10*(1), 12. https://doi.org/10.1038/s41514-024-00138-4
Lenz, M., Goetzke, R., Schenk, A., Schubert, C., Veeck, J., Hemeda, H., Koschmieder, S., Zenke, M., Schuppert, A., & Wagner, W. (2015). Epigenetic biomarker to support classification into pluripotent and non-pluripotent cells. *Sci Rep*, *5*, 8973. https://doi.org/10.1038/srep08973
Levine, R. L., Wadleigh, M., Cools, J., Ebert, B. L., Wernig, G., Huntly, B. J., Boggon, T. J., Wlodarska, I., Clark, J. J., Moore, S., Adelsperger, J., Koo, S., Lee, J. C., Gabriel, S., Mercher, T., D'Andrea, A., Frohling, S., Dohner, K., Marynen, P., . . . Gilliland, D. G. (2005). Activating mutation in the tyrosine kinase JAK2 in polycythemia vera, essential thrombocythemia, and myeloid metaplasia with myelofibrosis. *Cancer Cell*, *7*(4), 387-397. https://doi.org/10.1016/j.ccr.2005.03.023
Li, J., Kent, D. G., Godfrey, A. L., Manning, H., Nangalia, J., Aziz, A., Chen, E., Saeb-Parsy, K., Fink, J., Sneade, R., Hamilton, T. L., Pask, D. C., Silber, Y., Zhao, X., Ghevaert, C., Liu, P., & Green, A. R. (2014). JAK2V617F homozygosity drives a phenotypic switch in myeloproliferative neoplasms, but is insufficient to sustain disease. *Blood*, *123*(20), 3139-3151. https://doi.org/10.1182/blood-2013-06-510222
Li, N., Nguyen, B. T., Zhang, Z., & Zhang, Y. (2024). Visualization of DNA Methylation in Cell Cycle Genes during iPSC Cardiac Differentiation. *bioRxiv*. https://doi.org/10.1101/2024.01.17.575536
Li, X., Liu, D., Zhang, L., Wang, H., Li, Y., Li, Z., He, A., Liu, B., Zhou, J., Tang, F., & Lan, Y. (2021). The comprehensive DNA methylation landscape of hematopoietic stem cell development. *Cell Discov*, *7*(1), 86. https://doi.org/10.1038/s41421-021-00298-7
Li, X., Zeng, X., Xu, Y., Wang, B., Zhao, Y., Lai, X., Qian, P., & Huang, H. (2020). Mechanisms and rejuvenation strategies for aged hematopoietic stem cells. *J Hematol Oncol*, *13*(1), 31. https://doi.org/10.1186/s13045-020-00864-8
Li, Y., Chen, J., Sun, T., Chen, Y., Fu, R., Liu, X., Xue, F., Liu, W., Ju, M., Dai, X., Dong, H., Li, H., Wang, W., Chi, Y., & Zhang, L. (2024). Genetically determined telomere length and risk for haematologic diseases: results from large prospective cohorts and Mendelian Randomization analysis. *Blood Cancer J*, *14*(1), 48. https://doi.org/10.1038/s41408-024-01035-5
Li, Y., Tang, C., Liu, F., Zhu, C., Liu, F., Zhu, P., & Wang, L. (2022). DNA methylation safeguards the generation of hematopoietic stem and progenitor cells by repression of Notch signaling. *Development*, *149*(10). https://doi.org/10.1242/dev.200390
Li, Z., He, S., & Look, A. T. (2019). The MCL1-specific inhibitor S63845 acts synergistically with venetoclax/ABT-199 to induce apoptosis in T-cell acute lymphoblastic leukemia cells. *Leukemia*, *33*(1), 262-266. https://doi.org/10.1038/s41375-018-0201-2
Liesenfelder, S., Elsafi Mabrouk, M. H., Illiescu, J., Varona Baranda, M., Mizi, A., Wessiepe, M., Papantonis, A., & Wagner, W. (2024). Epigenetic editing at individual age-associated CpGs affects the genome-wide epigenetic aging landscape. *Biorxiv*, *https://doi.org/10.1101/2024.06.04.597161*.
Liggett, L. A., & Sankaran, V. G. (2020). Unraveling Hematopoiesis through the Lens of Genomics. *Cell*, *182*(6), 1384-1400. https://doi.org/10.1016/j.cell.2020.08.030
Lin, Q., & Wagner, W. (2015). Epigenetic Aging Signatures Are Coherently Modified in Cancer. *PLoS Genet*, *11*(6), e1005334. https://doi.org/10.1371/journal.pgen.1005334
Liu, X., Wang, Y., Zhang, X., Gao, Z., Zhang, S., Shi, P., Zhang, X., Song, L., Hendrickson, H., Zhou, D., & Zheng, G. (2018). Senolytic activity of piperlongumine analogues: Synthesis and biological evaluation. *Bioorg Med Chem*, *26*(14), 3925-3938. https://doi.org/10.1016/j.bmc.2018.06.013
Liu, X. L., Ding, J., & Meng, L. H. (2018). Oncogene-induced senescence: a double edged sword in cancer. *Acta Pharmacol Sin*, *39*(10), 1553-1558. https://doi.org/10.1038/aps.2017.198
Lomonosova, E., & Chinnadurai, G. (2008). BH3-only proteins in apoptosis and beyond: an overview. *Oncogene*, *27 Suppl 1*(Suppl 1), S2-19. https://doi.org/10.1038/onc.2009.39

Lopez-Otin, C., Blasco, M. A., Partridge, L., Serrano, M., & Kroemer, G. (2013). The hallmarks of aging. *Cell*, *153*(6), 1194-1217. https://doi.org/10.1016/j.cell.2013.05.039
Lopez-Otin, C., Blasco, M. A., Partridge, L., Serrano, M., & Kroemer, G. (2023). Hallmarks of aging: An expanding universe. *Cell*, *186*(2), 243-278. https://doi.org/10.1016/j.cell.2022.11.001
Lopez-Otin, C., Pietrocola, F., Roiz-Valle, D., Galluzzi, L., & Kroemer, G. (2023). Meta-hallmarks of aging and cancer. *Cell Metab*, *35*(1), 12-35. https://doi.org/10.1016/j.cmet.2022.11.001
Lorenzo, E. C., Torrance, B. L., & Haynes, L. (2023). Impact of senolytic treatment on immunity, aging, and disease. *Front Aging*, *4*, 1161799. https://doi.org/10.3389/fragi.2023.1161799
Lorenzo, E. C., Torrance, B. L., Keilich, S. R., Al-Naggar, I., Harrison, A., Xu, M., Bartley, J. M., & Haynes, L. (2022). Senescence-induced changes in CD4 T cell differentiation can be alleviated by treatment with senolytics. *Aging Cell*, *21*(1), e13525. https://doi.org/10.1111/acel.13525
Lu, M., Wang, X., Li, Y., Tripodi, J., Mosoyan, G., Mascarenhas, J., Kremyanskaya, M., Najfeld, V., & Hoffman, R. (2012). Combination treatment in vitro with Nutlin, a small-molecule antagonist of MDM2, and pegylated interferon-alpha 2a specifically targets JAK2V617F-positive polycythemia vera cells. *Blood*, *120*(15), 3098-3105. https://doi.org/10.1182/blood-2012-02-410712
Luo, C., Hajkova, P., & Ecker, J. R. (2018). Dynamic DNA methylation: In the right place at the right time. *Science*, *361*(6409), 1336-1340. https://doi.org/10.1126/science.aat6806
Maier, A. B., Maier, I. L., van Heemst, D., & Westendorp, R. G. (2008). Colony formation and colony size do not reflect the onset of replicative senescence in human fibroblasts. *J Gerontol A Biol Sci Med Sci*, *63*(7), 655-659. https://doi.org/10.1093/gerona/63.7.655
Makii, C., Oda, K., Ikeda, Y., Sone, K., Hasegawa, K., Uehara, Y., Nishijima, A., Asada, K., Koso, T., Fukuda, T., Inaba, K., Oki, S., Machino, H., Kojima, M., Kashiyama, T., Mori-Uchino, M., Arimoto, T., Wada-Hiraike, O., Kawana, K., . . . Fujii, T. (2016). MDM2 is a potential therapeutic target and prognostic factor for ovarian clear cell carcinomas with wild type TP53. *Oncotarget*, *7*(46), 75328-75338. https://doi.org/10.18632/oncotarget.12175
Manghwar, H., Li, B., Ding, X., Hussain, A., Lindsey, K., Zhang, X., & Jin, S. (2020). CRISPR/Cas Systems in Genome Editing: Methodologies and Tools for sgRNA Design, Off-Target Evaluation, and Strategies to Mitigate Off-Target Effects. *Adv Sci (Weinh)*, *7*(6), 1902312. https://doi.org/10.1002/advs.201902312
Mannarino, M., Wu-Martinez, O., Sheng, K., Li, L., Navarro-Ramirez, R., Jarzem, P., Ouellet, J. A., Cherif, H., & Haglund, L. (2023). Senolytic Combination Treatment Is More Potent Than Single Drugs in Reducing Inflammatory and Senescence Burden in Cells from Painful Degenerating IVDs. *Biomolecules*, *13*(8). https://doi.org/10.3390/biom13081257
Marin, I., Serrano, M., & Pietrocola, F. (2023). Recent insights into the crosstalk between senescent cells and CD8 T lymphocytes. *NPJ Aging*, *9*(1), 8. https://doi.org/10.1038/s41514-023-00105-5
Martinez-Calle, N., Pascual, M., Ordonez, R., Eneriz, E. S. J., Kulis, M., Miranda, E., Guruceaga, E., Segura, V., Larrayoz, M. J., Bellosillo, B., Calasanz, M. J., Besses, C., Rifon, J., Martin-Subero, J. I., Agirre, X., & Prosper, F. (2019). Epigenomic profiling of myelofibrosis reveals widespread DNA methylation changes in enhancer elements and ZFP36L1 as a potential tumor suppressor gene that is epigenetically regulated. *Haematologica*, *104*(8), 1572-1579. https://doi.org/10.3324/haematol.2018.204917
Mascarenhas, J., Harrison, C. N., Kiladjian, J. J., Komrokji, R. S., Koschmieder, S., Vannucchi, A. M., Berry, T., Redding, D., Sherman, L., Dougherty, S., Peng, L., Sun, L., Huang, F., Wan, Y., Feller, F. M., Rizo, A., & Verstovsek, S. (2022). Imetelstat in intermediate-2 or high-risk myelofibrosis refractory to JAK inhibitor: IMpactMF phase III study design. *Future Oncol*, *18*(22), 2393-2402. https://doi.org/10.2217/fon-2022-0235
Maslah, N., Benajiba, L., Giraudier, S., Kiladjian, J. J., & Cassinat, B. (2023). Clonal architecture evolution in Myeloproliferative Neoplasms: from a driver mutation to a complex heterogeneous mutational and phenotypic landscape. *Leukemia*, *37*(5), 957-963. https://doi.org/10.1038/s41375-023-01886-0

Maslah, N., Verger, E., Giraudier, S., Chea, M., Hoffman, R., Mascarenhas, J., Cassinat, B., & Kiladjian, J. J. (2022). Single-cell analysis reveals selection of TP53-mutated clones after MDM2 inhibition. *Blood Adv*, *6*(9), 2813-2823. https://doi.org/10.1182/bloodadvances.2021005867

Matsunaga, T., Iske, J., Schroeter, A., Azuma, H., Zhou, H., & Tullius, S. G. (2021). The potential of Senolytics in transplantation. *Mech Ageing Dev*, *200*, 111582. https://doi.org/10.1016/j.mad.2021.111582

Matt, S., & Hofmann, T. G. (2016). The DNA damage-induced cell death response: a roadmap to kill cancer cells. *Cell Mol Life Sci*, *73*(15), 2829-2850. https://doi.org/10.1007/s00018-016-2130-4

Mattei, A. L., Bailly, N., & Meissner, A. (2022). DNA methylation: a historical perspective. *Trends Genet*, *38*(7), 676-707. https://doi.org/10.1016/j.tig.2022.03.010

McPherson, S., Greenfield, G., Andersen, C., Grinfeld, J., Hasselbalch, H. C., Nangalia, J., Mills, K. I., & McMullin, M. F. (2019). Methylation age as a correlate for allele burden, disease status, and clinical response in myeloproliferative neoplasm patients treated with vorinostat. *Exp Hematol*, *79*, 26-34. https://doi.org/10.1016/j.exphem.2019.09.025

McPherson, S., McMullin, M. F., & Mills, K. (2017). Epigenetics in Myeloproliferative Neoplasms. *J Cell Mol Med*, *21*(9), 1660-1667. https://doi.org/10.1111/jcmm.13095

Melo, J. V., Gordon, D. E., Cross, N. C., & Goldman, J. M. (1993). The ABL-BCR fusion gene is expressed in chronic myeloid leukemia. *Blood*, *81*(1), 158-165. https://www.ncbi.nlm.nih.gov/pubmed/8417787

Merlinsky, T. R., Levine, R. L., & Pronier, E. (2019). Unfolding the Role of Calreticulin in Myeloproliferative Neoplasm Pathogenesis. *Clin Cancer Res*, *25*(10), 2956-2962. https://doi.org/10.1158/1078-0432.CCR-18-3777

Mesnieres, M., Bohm, A. M., Peredo, N., Trompet, D., Valle-Tenney, R., Bajaj, M., Corthout, N., Nefyodova, E., Cardoen, R., Baatsen, P., Munck, S., Nagy, A., Haigh, J. J., Khurana, S., Verfaillie, C. M., & Maes, C. (2021). Fetal hematopoietic stem cell homing is controlled by VEGF regulating the integrity and oxidative status of the stromal-vascular bone marrow niches. *Cell Rep*, *36*(8), 109618. https://doi.org/10.1016/j.celrep.2021.109618

Meyer, D. H., & Schumacher, B. (2024). Aging clocks based on accumulating stochastic variation. *Nat Aging*, *4*(6), 871-885. https://doi.org/10.1038/s43587-024-00619-x

Michael Waskom, O. B., drewokane, Paul Hobson, Yaroslav Halchenko, Saulius Lukauskas. (2016). *seaborn: v0.7.0 (January 2016)*. In

Milanovic, M., Fan, D. N. Y., Belenki, D., Dabritz, J. H. M., Zhao, Z., Yu, Y., Dorr, J. R., Dimitrova, L., Lenze, D., Monteiro Barbosa, I. A., Mendoza-Parra, M. A., Kanashova, T., Metzner, M., Pardon, K., Reimann, M., Trumpp, A., Dorken, B., Zuber, J., Gronemeyer, H., . . . Schmitt, C. A. (2018). Senescence-associated reprogramming promotes cancer stemness. *Nature*, *553*(7686), 96-100. https://doi.org/10.1038/nature25167

Miller, A. L., Fehling, S. C., Garcia, P. L., Gamblin, T. L., Council, L. N., van Waardenburg, R., Yang, E. S., Bradner, J. E., & Yoon, K. J. (2019). The BET inhibitor JQ1 attenuates double-strand break repair and sensitizes models of pancreatic ductal adenocarcinoma to PARP inhibitors. *EBioMedicine*, *44*, 419-430. https://doi.org/10.1016/j.ebiom.2019.05.035

Mittal, B. B., & Vaughan, D. E. (2023). Inclusion of epigenetic age acceleration in oncological trials. *Lancet Healthy Longev*, *4*(5), e185-e186. https://doi.org/10.1016/S2666-7568(23)00034-X

Moliterno, A. R., Kaizer, H., & Reeves, B. N. (2023). JAK2 V617F allele burden in polycythemia vera: burden of proof. *Blood*, *141*(16), 1934-1942. https://doi.org/10.1182/blood.2022017697

Moore, L. D., Le, T., & Fan, G. (2013). DNA methylation and its basic function. *Neuropsychopharmacology*, *38*(1), 23-38. https://doi.org/10.1038/npp.2012.112

Morales Berstein, F., McCartney, D. L., Lu, A. T., Tsilidis, K. K., Bouras, E., Haycock, P., Burrows, K., Phipps, A. I., Buchanan, D. D., Cheng, I., consortium, P., Martin, R. M., Davey Smith, G., Relton, C. L., Horvath, S., Marioni, R. E., Richardson, T. G., & Richmond, R. C. (2022). Assessing the causal role of epigenetic clocks in the

development of multiple cancers: a Mendelian randomization study. *Elife*, *11*. https://doi.org/10.7554/eLife.75374
Moran, S., Arribas, C., & Esteller, M. (2016). Validation of a DNA methylation microarray for 850,000 CpG sites of the human genome enriched in enhancer sequences. *Epigenomics*, *8*(3), 389-399. https://doi.org/10.2217/epi.15.114
Morrison, S. J., & Scadden, D. T. (2014). The bone marrow niche for haematopoietic stem cells. *Nature*, *505*(7483), 327-334. https://doi.org/10.1038/nature12984
Morrison, S. J., Wandycz, A. M., Hemmati, H. D., Wright, D. E., & Weissman, I. L. (1997). Identification of a lineage of multipotent hematopoietic progenitors. *Development*, *124*(10), 1929-1939. https://doi.org/10.1242/dev.124.10.1929
Mossahebi-Mohammadi, M., Quan, M., Zhang, J. S., & Li, X. (2020). FGF Signaling Pathway: A Key Regulator of Stem Cell Pluripotency. *Front Cell Dev Biol*, *8*, 79. https://doi.org/10.3389/fcell.2020.00079
Moulard, O., Mehta, J., Fryzek, J., Olivares, R., Iqbal, U., & Mesa, R. A. (2014). Epidemiology of myelofibrosis, essential thrombocythemia, and polycythemia vera in the European Union. *Eur J Haematol*, *92*(4), 289-297. https://doi.org/10.1111/ejh.12256
Munoz-Espin, D., Canamero, M., Maraver, A., Gomez-Lopez, G., Contreras, J., Murillo-Cuesta, S., Rodriguez-Baeza, A., Varela-Nieto, I., Ruberte, J., Collado, M., & Serrano, M. (2013). Programmed cell senescence during mammalian embryonic development. *Cell*, *155*(5), 1104-1118. https://doi.org/10.1016/j.cell.2013.10.019
Munoz-Espin, D., & Serrano, M. (2014). Cellular senescence: from physiology to pathology. *Nat Rev Mol Cell Biol*, *15*(7), 482-496. https://doi.org/10.1038/nrm3823
Nangalia, J., Massie, C. E., Baxter, E. J., Nice, F. L., Gundem, G., Wedge, D. C., Avezov, E., Li, J., Kollmann, K., Kent, D. G., Aziz, A., Godfrey, A. L., Hinton, J., Martincorena, I., Van Loo, P., Jones, A. V., Guglielmelli, P., Tarpey, P., Harding, H. P., . . . Green, A. R. (2013). Somatic CALR mutations in myeloproliferative neoplasms with nonmutated JAK2. *N Engl J Med*, *369*(25), 2391-2405. https://doi.org/10.1056/NEJMoa1312542
Nebbioso, A., Tambaro, F. P., Dell'Aversana, C., & Altucci, L. (2018). Cancer epigenetics: Moving forward. *PLoS Genet*, *14*(6), e1007362. https://doi.org/10.1371/journal.pgen.1007362
Neo, W. H., Lie, A. L. M., Fadlullah, M. Z. H., & Lacaud, G. (2021). Contributions of Embryonic HSC-Independent Hematopoiesis to Organogenesis and the Adult Hematopoietic System. *Front Cell Dev Biol*, *9*, 631699. https://doi.org/10.3389/fcell.2021.631699
Nielsen, C., Birgens, H. S., Nordestgaard, B. G., & Bojesen, S. E. (2013). Diagnostic value of JAK2 V617F somatic mutation for myeloproliferative cancer in 49 488 individuals from the general population. *Br J Haematol*, *160*(1), 70-79. https://doi.org/10.1111/bjh.12099
Nielsen, H. M., Andersen, C. L., Westman, M., Kristensen, L. S., Asmar, F., Kruse, T. A., Thomassen, M., Larsen, T. S., Skov, V., Hansen, L. L., Bjerrum, O. W., Hasselbalch, H. C., Punj, V., & Gronbaek, K. (2017). Epigenetic changes in myelofibrosis: Distinct methylation changes in the myeloid compartments and in cases with ASXL1 mutations. *Sci Rep*, *7*(1), 6774. https://doi.org/10.1038/s41598-017-07057-3
Nikolich-Zugich, J. (2018). The twilight of immunity: emerging concepts in aging of the immune system. *Nat Immunol*, *19*(1), 10-19. https://doi.org/10.1038/s41590-017-0006-x
Nishino, K., Toyoda, M., Yamazaki-Inoue, M., Fukawatase, Y., Chikazawa, E., Sakaguchi, H., Akutsu, H., & Umezawa, A. (2011). DNA methylation dynamics in human induced pluripotent stem cells over time. *PLoS Genet*, *7*(5), e1002085. https://doi.org/10.1371/journal.pgen.1002085
Nothof, S. A., Magdinier, F., & Van-Gils, J. (2022). Chromatin Structure and Dynamics: Focus on Neuronal Differentiation and Pathological Implication. *Genes (Basel)*, *13*(4). https://doi.org/10.3390/genes13040639
Ohi, Y., Qin, H., Hong, C., Blouin, L., Polo, J. M., Guo, T., Qi, Z., Downey, S. L., Manos, P. D., Rossi, D. J., Yu, J., Hebrok, M., Hochedlinger, K., Costello, J. F., Song, J. S., & Ramalho-Santos, M. (2011). Incomplete DNA methylation underlies a transcriptional memory of somatic cells in human iPS cells. *Nat Cell Biol*, *13*(5), 541-549. https://doi.org/10.1038/ncb2239

Ohyashiki, J. H., Sashida, G., Tauchi, T., & Ohyashiki, K. (2002). Telomeres and telomerase in hematologic neoplasia. *Oncogene*, *21*(4), 680-687. https://doi.org/10.1038/sj.onc.1205075

Olschok, K., Han, L., de Toledo, M. A. S., Bohnke, J., Grasshoff, M., Costa, I. G., Theocharides, A., Maurer, A., Schuler, H. M., Buhl, E. M., Pannen, K., Baumeister, J., Kalmer, M., Gupta, S., Boor, P., Gezer, D., Brummendorf, T. H., Zenke, M., Chatain, N., & Koschmieder, S. (2021). CALR frameshift mutations in MPN patient-derived iPSCs accelerate maturation of megakaryocytes. *Stem Cell Reports*, *16*(11), 2768-2783. https://doi.org/10.1016/j.stemcr.2021.09.019

Oppliger Leibundgut, E., Haubitz, M., Burington, B., Ottmann, O. G., Spitzer, G., Odenike, O., McDevitt, M. A., Roth, A., Snyder, D. S., & Baerlocher, G. M. (2021). Dynamics of mutations in patients with essential thrombocythemia treated with imetelstat. *Haematologica*, *106*(9), 2397-2404. https://doi.org/10.3324/haematol.2020.252817

Orkin, S. H., & Zon, L. I. (2008). Hematopoiesis: an evolving paradigm for stem cell biology. *Cell*, *132*(4), 631-644. https://doi.org/10.1016/j.cell.2008.01.025

Ortmann, C. A., Kent, D. G., Nangalia, J., Silber, Y., Wedge, D. C., Grinfeld, J., Baxter, E. J., Massie, C. E., Papaemmanuil, E., Menon, S., Godfrey, A. L., Dimitropoulou, D., Guglielmelli, P., Bellosillo, B., Besses, C., Dohner, K., Harrison, C. N., Vassiliou, G. S., Vannucchi, A., . . . Green, A. R. (2015). Effect of mutation order on myeloproliferative neoplasms. *N Engl J Med*, *372*(7), 601-612. https://doi.org/10.1056/NEJMoa1412098

Ovadya, Y., Landsberger, T., Leins, H., Vadai, E., Gal, H., Biran, A., Yosef, R., Sagiv, A., Agrawal, A., Shapira, A., Windheim, J., Tsoory, M., Schirmbeck, R., Amit, I., Geiger, H., & Krizhanovsky, V. (2018). Impaired immune surveillance accelerates accumulation of senescent cells and aging. *Nat Commun*, *9*(1), 5435. https://doi.org/10.1038/s41467-018-07825-3

Overholtzer, M. (2019). Senescent cells feed on their neighbours. *Nature*, *574*(7780), 635-636. https://doi.org/10.1038/d41586-019-03271-3

Owen, B. M., Phie, J., Huynh, J., Needham, S., & Fraser, C. (2023). Evaluation of quantitative biomarkers of aging in human PBMCs. *Front Aging*, *4*, 1260502. https://doi.org/10.3389/fragi.2023.1260502

Padgett, J., & Santos, S. D. M. (2020). From clocks to dominoes: lessons on cell cycle remodelling from embryonic stem cells. *FEBS Lett*. https://doi.org/10.1002/1873-3468.13862

Palm, W., & de Lange, T. (2008). How shelterin protects mammalian telomeres. *Annu Rev Genet*, *42*, 301-334. https://doi.org/10.1146/annurev.genet.41.110306.130350

Pandey, G., Kuykendall, A. T., & Reuther, G. W. (2022). JAK2 inhibitor persistence in MPN: uncovering a central role of ERK activation. *Blood Cancer J*, *12*(1), 13. https://doi.org/10.1038/s41408-022-00609-5

Pang, W. W., Price, E. A., Sahoo, D., Beerman, I., Maloney, W. J., Rossi, D. J., Schrier, S. L., & Weissman, I. L. (2011). Human bone marrow hematopoietic stem cells are increased in frequency and myeloid-biased with age. *Proc Natl Acad Sci U S A*, *108*(50), 20012-20017. https://doi.org/10.1073/pnas.1116110108

Papapetrou, E. P. (2019). Modeling myeloid malignancies with patient-derived iPSCs. *Exp Hematol*, *71*, 77-84. https://doi.org/10.1016/j.exphem.2018.11.006

Papp, B., & Plath, K. (2011). Reprogramming to pluripotency: stepwise resetting of the epigenetic landscape. *Cell Res*, *21*(3), 486-501. https://doi.org/10.1038/cr.2011.28

Pappalardo, X. G., & Barra, V. (2021). Losing DNA methylation at repetitive elements and breaking bad. *Epigenetics Chromatin*, *14*(1), 25. https://doi.org/10.1186/s13072-021-00400-z

Paramos-de-Carvalho, D., Jacinto, A., & Saude, L. (2021). The right time for senescence. *Elife*, *10*. https://doi.org/10.7554/eLife.72449

Paska, A. V., & Hudler, P. (2015). Aberrant methylation patterns in cancer: a clinical view. *Biochem Med (Zagreb)*, *25*(2), 161-176. https://doi.org/10.11613/BM.2015.017

Passamonti, F., & Mora, B. (2023). Myelofibrosis. *Blood*, *141*(16), 1954-1970. https://doi.org/10.1182/blood.2022017423

Passamonti, F., & Rumi, E. (2009). Clinical relevance of JAK2 (V617F) mutant allele burden. *Haematologica*, *94*(1), 7-10. https://doi.org/10.3324/haematol.2008.001271

Patel, A. A., Cahill, K., Saygin, C., & Odenike, O. (2021). Cedazuridine/decitabine: from preclinical to clinical development in myeloid malignancies. *Blood Adv*, *5*(8), 2264-2271. https://doi.org/10.1182/bloodadvances.2020002929

Pecquet, C., Chachoua, I., Roy, A., Balligand, T., Vertenoeil, G., Leroy, E., Albu, R. I., Defour, J. P., Nivarthi, H., Hug, E., Xu, E., Ould-Amer, Y., Mouton, C., Colau, D., Vertommen, D., Shwe, M. M., Marty, C., Plo, I., Vainchenker, W., . . . Constantinescu, S. N. (2019). Calreticulin mutants as oncogenic rogue chaperones for TpoR and traffic-defective pathogenic TpoR mutants. *Blood*, *133*(25), 2669-2681. https://doi.org/10.1182/blood-2018-09-874578

Pemmaraju, N., Garcia, J. S., Potluri, J., Harb, J. G., Sun, Y., Jung, P., Qin, Q. Q., Tantravahi, S. K., Verstovsek, S., & Harrison, C. (2022). Addition of navitoclax to ongoing ruxolitinib treatment in patients with myelofibrosis (REFINE): a post-hoc analysis of molecular biomarkers in a phase 2 study. *Lancet Haematol*, *9*(6), e434-e444. https://doi.org/10.1016/S2352-3026(22)00116-8

Pereira, B., Correia, F. P., Alves, I. A., Costa, M., Gameiro, M., Martins, A. P., & Saraiva, J. A. (2024). Epigenetic reprogramming as a key to reverse ageing and increase longevity. *Ageing Res Rev*, *95*, 102204. https://doi.org/10.1016/j.arr.2024.102204

Perez, C., Pascual, M., Martin-Subero, J. I., Bellosillo, B., Segura, V., Delabesse, E., Alvarez, S., Larrayoz, M. J., Rifon, J., Cigudosa, J. C., Besses, C., Calasanz, M. J., Cross, N. C., Prosper, F., & Agirre, X. (2013). Aberrant DNA methylation profile of chronic and transformed classic Philadelphia-negative myeloproliferative neoplasms. *Haematologica*, *98*(9), 1414-1420. https://doi.org/10.3324/haematol.2013.084160

Perna, L., Zhang, Y., Mons, U., Holleczek, B., Saum, K. U., & Brenner, H. (2016). Epigenetic age acceleration predicts cancer, cardiovascular, and all-cause mortality in a German case cohort. *Clin Epigenetics*, *8*, 64. https://doi.org/10.1186/s13148-016-0228-z

Phetfong, J., Supokawej, A., Wattanapanitch, M., Kheolamai, P., Y, U. P., & Issaragrisil, S. (2016). Cell type of origin influences iPSC generation and differentiation to cells of the hematoendothelial lineage. *Cell Tissue Res*, *365*(1), 101-112. https://doi.org/10.1007/s00441-016-2369-y

Pierce, B. L. (2022). The aging epigenome. *Elife*, *11*. https://doi.org/10.7554/eLife.78693

Pietra, D., Rumi, E., Ferretti, V. V., Di Buduo, C. A., Milanesi, C., Cavalloni, C., Sant'Antonio, E., Abbonante, V., Moccia, F., Casetti, I. C., Bellini, M., Renna, M. C., Roncoroni, E., Fugazza, E., Astori, C., Boveri, E., Rosti, V., Barosi, G., Balduini, A., & Cazzola, M. (2016). Differential clinical effects of different mutation subtypes in CALR-mutant myeloproliferative neoplasms. *Leukemia*, *30*(2), 431-438. https://doi.org/10.1038/leu.2015.277

Pikman, Y., Lee, B. H., Mercher, T., McDowell, E., Ebert, B. L., Gozo, M., Cuker, A., Wernig, G., Moore, S., Galinsky, I., DeAngelo, D. J., Clark, J. J., Lee, S. J., Golub, T. R., Wadleigh, M., Gilliland, D. G., & Levine, R. L. (2006). MPLW515L is a novel somatic activating mutation in myelofibrosis with myeloid metaplasia. *PLoS Med*, *3*(7), e270. https://doi.org/10.1371/journal.pmed.0030270

Pinho, S., & Frenette, P. S. (2019). Haematopoietic stem cell activity and interactions with the niche. *Nat Rev Mol Cell Biol*, *20*(5), 303-320. https://doi.org/10.1038/s41580-019-0103-9

Pinjala, P., Tryphena, K. P., Prasad, R., Khatri, D. K., Sun, W., Singh, S. B., Gugulothu, D., Srivastava, S., & Vora, L. (2023). CRISPR/Cas9 assisted stem cell therapy in Parkinson's disease. *Biomater Res*, *27*(1), 46. https://doi.org/10.1186/s40824-023-00381-y

Plo, I., Bellanne-Chantelot, C., Mosca, M., Mazzi, S., Marty, C., & Vainchenker, W. (2017). Genetic Alterations of the Thrombopoietin/MPL/JAK2 Axis Impacting Megakaryopoiesis. *Front Endocrinol (Lausanne)*, *8*, 234. https://doi.org/10.3389/fendo.2017.00234

Prata, L., Ovsyannikova, I. G., Tchkonia, T., & Kirkland, J. L. (2018). Senescent cell clearance by the immune system: Emerging therapeutic opportunities. *Semin Immunol*, *40*, 101275. https://doi.org/10.1016/j.smim.2019.04.003

Puri, D., & Wagner, W. (2023). Epigenetic rejuvenation by partial reprogramming. *Bioessays*, *45*(4), e2200208. https://doi.org/10.1002/bies.202200208
R Core Team. (2022). *R: A language and environment for statistical computing.* . In R Foundation for Statistical Computing. https://www.R-project.org/
Rad, A. N., & Grillari, J. (2024). Current senolytics: Mode of action, efficacy and limitations, and their future. *Mech Ageing Dev*, *217*, 111888. https://doi.org/10.1016/j.mad.2023.111888
Radke, K., Beug, H., Kornfeld, S., & Graf, T. (1982). Transformation of both erythroid and myeloid cells by E26, an avian leukemia virus that contains the myb gene. *Cell*, *31*(3 Pt 2), 643-653. https://doi.org/10.1016/0092-8674(82)90320-8
Rai, S., Grockowiak, E., Hansen, N., Luque Paz, D., Stoll, C. B., Hao-Shen, H., Mild-Schneider, G., Dirnhofer, S., Farady, C. J., Mendez-Ferrer, S., & Skoda, R. C. (2022). Inhibition of interleukin-1beta reduces myelofibrosis and osteosclerosis in mice with JAK2-V617F driven myeloproliferative neoplasm. *Nat Commun*, *13*(1), 5346. https://doi.org/10.1038/s41467-022-32927-4
Rai, S., Zhang, Y., Grockowiak, E., Kimmerlin, Q., Hansen, N., Stoll, C. B., Usart, M., Luque Paz, D., Hao-Shen, H., Zhu, Y., Roux, J., Bader, M. S., Dirnhofer, S., Farady, C. J., Schroeder, T., Mendez-Ferrer, S., & Skoda, R. C. (2024). IL-1beta promotes MPN disease initiation by favoring early clonal expansion of JAK2-mutant hematopoietic stem cells. *Blood Adv*, *8*(5), 1234-1249. https://doi.org/10.1182/bloodadvances.2023011338
Ramos, T. L., Sanchez-Abarca, L. I., Roson-Burgo, B., Redondo, A., Rico, A., Preciado, S., Ortega, R., Rodriguez, C., Muntion, S., Hernandez-Hernandez, A., De Las Rivas, J., Gonzalez, M., Gonzalez Porras, J. R., Del Canizo, C., & Sanchez-Guijo, F. (2017). Mesenchymal stromal cells (MSC) from JAK2+ myeloproliferative neoplasms differ from normal MSC and contribute to the maintenance of neoplastic hematopoiesis. *PLoS One*, *12*(8), e0182470. https://doi.org/10.1371/journal.pone.0182470
Rao, I., Crisafulli, L., Paulis, M., & Ficara, F. (2022). Hematopoietic Cells from Pluripotent Stem Cells: Hope and Promise for the Treatment of Inherited Blood Disorders. *Cells*, *11*(3). https://doi.org/10.3390/cells11030557
Rawat, L., Hegde, H., Hoti, S. L., & Nayak, V. (2020). Piperlongumine induces ROS mediated cell death and synergizes paclitaxel in human intestinal cancer cells. *Biomed Pharmacother*, *128*, 110243. https://doi.org/10.1016/j.biopha.2020.110243
Razgonova, M. P., Zakharenko, A. M., Golokhvast, K. S., Thanasoula, M., Sarandi, E., Nikolouzakis, K., Fragkiadaki, P., Tsoukalas, D., Spandidos, D. A., & Tsatsakis, A. (2020). Telomerase and telomeres in aging theory and chronographic aging theory (Review). *Mol Med Rep*, *22*(3), 1679-1694. https://doi.org/10.3892/mmr.2020.11274
Reimann, M., Lee, S., & Schmitt, C. A. (2024). Cellular senescence: Neither irreversible nor reversible. *J Exp Med*, *221*(4). https://doi.org/10.1084/jem.20232136
Riessland, M., & Orr, M. E. (2023). Translating the Biology of Aging into New Therapeutics for Alzheimer's Disease: Senolytics. *J Prev Alzheimers Dis*, *10*(4), 633-646. https://doi.org/10.14283/jpad.2023.104
Rolles, B., Gorgulho, J., Tometten, M., Roderburg, C., Vieri, M., Abels, A., Vucur, M., Heymann, F., Tacke, F., Brummendorf, T. H., Luedde, T., Beier, F., & Loosen, S. H. (2021). Telomere Shortening in Peripheral Leukocytes Is Associated With Poor Survival in Cancer Patients Treated With Immune Checkpoint Inhibitor Therapy. *Front Oncol*, *11*, 729207. https://doi.org/10.3389/fonc.2021.729207
Rowe, R. G., & Daley, G. Q. (2019). Induced pluripotent stem cells in disease modelling and drug discovery. *Nat Rev Genet*, *20*(7), 377-388. https://doi.org/10.1038/s41576-019-0100-z
Ruella, M., Salmoiraghi, S., Risso, A., Carobbio, A., Buttiglieri, S., Spatola, T., Sivera, P., Ricca, I., Barbui, T., Tarella, C., & Rambaldi, A. (2013). Telomere shortening in Ph-negative chronic myeloproliferative neoplasms: a biological marker of polycythemia vera and myelofibrosis, regardless of hydroxycarbamide therapy. *Exp Hematol*, *41*(7), 627-634. https://doi.org/10.1016/j.exphem.2013.03.007
Rufer, N., Brummendorf, T. H., Kolvraa, S., Bischoff, C., Christensen, K., Wadsworth, L., Schulzer, M., & Lansdorp, P. M. (1999). Telomere fluorescence measurements in granulocytes and T lymphocyte subsets point to a high turnover of hematopoietic stem

cells and memory T cells in early childhood. *J Exp Med*, *190*(2), 157-167. https://doi.org/10.1084/jem.190.2.157

Rumi, E., Pietra, D., Ferretti, V., Klampfl, T., Harutyunyan, A. S., Milosevic, J. D., Them, N. C., Berg, T., Elena, C., Casetti, I. C., Milanesi, C., Sant'antonio, E., Bellini, M., Fugazza, E., Renna, M. C., Boveri, E., Astori, C., Pascutto, C., Kralovics, R., . . . Associazione Italiana per la Ricerca sul Cancro Gruppo Italiano Malattie Mieloproliferative, I. (2014). JAK2 or CALR mutation status defines subtypes of essential thrombocythemia with substantially different clinical course and outcomes. *Blood*, *123*(10), 1544-1551. https://doi.org/10.1182/blood-2013-11-539098

Sadighi Akha, A. A. (2018). Aging and the immune system: An overview. *J Immunol Methods*, *463*, 21-26. https://doi.org/10.1016/j.jim.2018.08.005

Saez-Atienzar, S., & Masliah, E. (2020). Cellular senescence and Alzheimer disease: the egg and the chicken scenario. *Nat Rev Neurosci*, *21*(8), 433-444. https://doi.org/10.1038/s41583-020-0325-z

Sagiv, A., Burton, D. G., Moshayev, Z., Vadai, E., Wensveen, F., Ben-Dor, S., Golani, O., Polic, B., & Krizhanovsky, V. (2016). NKG2D ligands mediate immunosurveillance of senescent cells. *Aging (Albany NY)*, *8*(2), 328-344. https://doi.org/10.18632/aging.100897

Sahin, I., Zhang, S., Navaraj, A., Zhou, L., Dizon, D., Safran, H., & El-Deiry, W. S. (2020). AMG-232 sensitizes high MDM2-expressing tumor cells to T-cell-mediated killing. *Cell Death Discov*, *6*, 57. https://doi.org/10.1038/s41420-020-0292-1

Salech, F., SanMartin, C. D., Concha-Cerda, J., Romero-Hernandez, E., Ponce, D. P., Liabeuf, G., Rogers, N. K., Murgas, P., Bruna, B., More, J., & Behrens, M. I. (2022). Senescence Markers in Peripheral Blood Mononuclear Cells in Amnestic Mild Cognitive Impairment and Alzheimer's Disease. *Int J Mol Sci*, *23*(16). https://doi.org/10.3390/ijms23169387

Sander, J. D., & Joung, J. K. (2014). CRISPR-Cas systems for editing, regulating and targeting genomes. *Nat Biotechnol*, *32*(4), 347-355. https://doi.org/10.1038/nbt.2842

Sangkhae, V., Etheridge, S. L., Kaushansky, K., & Hitchcock, I. S. (2014). The thrombopoietin receptor, MPL, is critical for development of a JAK2V617F-induced myeloproliferative neoplasm. *Blood*, *124*(26), 3956-3963. https://doi.org/10.1182/blood-2014-07-587238

Satoh, T., Toledo, M. A. S., Boehnke, J., Olschok, K., Flosdorf, N., Gotz, K., Kustermann, C., Sontag, S., Sere, K., Koschmieder, S., Brummendorf, T. H., Chatain, N., Tagawa, Y. I., & Zenke, M. (2021). Human DC3 Antigen Presenting Dendritic Cells From Induced Pluripotent Stem Cells. *Front Cell Dev Biol*, *9*, 667304. https://doi.org/10.3389/fcell.2021.667304

Saul, D., Kosinsky, R. L., Atkinson, E. J., Doolittle, M. L., Zhang, X., LeBrasseur, N. K., Pignolo, R. J., Robbins, P. D., Niedernhofer, L. J., Ikeno, Y., Jurk, D., Passos, J. F., Hickson, L. J., Xue, A., Monroe, D. G., Tchkonia, T., Kirkland, J. L., Farr, J. N., & Khosla, S. (2022). A new gene set identifies senescent cells and predicts senescence-associated pathways across tissues. *Nat Commun*, *13*(1), 4827. https://doi.org/10.1038/s41467-022-32552-1

Schafer, M. J., White, T. A., Iijima, K., Haak, A. J., Ligresti, G., Atkinson, E. J., Oberg, A. L., Birch, J., Salmonowicz, H., Zhu, Y., Mazula, D. L., Brooks, R. W., Fuhrmann-Stroissnigg, H., Pirtskhalava, T., Prakash, Y. S., Tchkonia, T., Robbins, P. D., Aubry, M. C., Passos, J. F., . . . LeBrasseur, N. K. (2017). Cellular senescence mediates fibrotic pulmonary disease. *Nat Commun*, *8*, 14532. https://doi.org/10.1038/ncomms14532

Schmidt, M., Zeevaert, K., Elsafi Mabrouk, M. H., Goetzke, R., & Wagner, W. (2023). Epigenetic biomarkers to track differentiation of pluripotent stem cells. *Stem Cell Reports*, *18*(1), 145-158. https://doi.org/10.1016/j.stemcr.2022.11.001

Schofield, R. (1978). The relationship between the spleen colony-forming cell and the haemopoietic stem cell. *Blood Cells*, *4*(1-2), 7-25. https://www.ncbi.nlm.nih.gov/pubmed/747780

Schoofs, T., Berdel, W. E., & Muller-Tidow, C. (2014). Origins of aberrant DNA methylation in acute myeloid leukemia. *Leukemia*, *28*(1), 1-14. https://doi.org/10.1038/leu.2013.242

Schulte, R., Wilson, N. K., Prick, J. C., Cossetti, C., Maj, M. K., Gottgens, B., & Kent, D. G. (2015). Index sorting resolves heterogeneous murine hematopoietic stem cell populations. *Exp Hematol*, *43*(9), 803-811. https://doi.org/10.1016/j.exphem.2015.05.006

Selvarani, R., Mohammed, S., & Richardson, A. (2021). Effect of rapamycin on aging and age-related diseases-past and future. *Geroscience*, *43*(3), 1135-1158. https://doi.org/10.1007/s11357-020-00274-1

Shammas, M. A. (2011). Telomeres, lifestyle, cancer, and aging. *Curr Opin Clin Nutr Metab Care*, *14*(1), 28-34. https://doi.org/10.1097/MCO.0b013e32834121b1

Shamsian, A., Sahebnasagh, R., Norouzy, A., Hussein, S. H., Ghahremani, M. H., & Azizi, Z. (2022). Cancer cells as a new source of induced pluripotent stem cells. *Stem Cell Res Ther*, *13*(1), 459. https://doi.org/10.1186/s13287-022-03145-y

Shay, J. W. (2016). Role of Telomeres and Telomerase in Aging and Cancer. *Cancer Discov*, *6*(6), 584-593. https://doi.org/10.1158/2159-8290.CD-16-0062

Shay, J. W., & Roninson, I. B. (2004). Hallmarks of senescence in carcinogenesis and cancer therapy. *Oncogene*, *23*(16), 2919-2933. https://doi.org/10.1038/sj.onc.1207518

Shen, J., Lyu, C., Zhu, Y., Feng, Z., Zhang, S., Hoyle, D. L., Ji, G., Brodsky, R. A., Cheng, T., & Wang, Z. Z. (2019). Defining early hematopoietic-fated primitive streak specification of human pluripotent stem cells by the orchestrated balance of Wnt, activin, and BMP signaling. *J Cell Physiol*, *234*(9), 16136-16147. https://doi.org/10.1002/jcp.28272

Shibuya, M. (2011). Vascular Endothelial Growth Factor (VEGF) and Its Receptor (VEGFR) Signaling in Angiogenesis: A Crucial Target for Anti- and Pro-Angiogenic Therapies. *Genes Cancer*, *2*(12), 1097-1105. https://doi.org/10.1177/1947601911423031

Shimizu, T., Kubovcakova, L., Nienhold, R., Zmajkovic, J., Meyer, S. C., Hao-Shen, H., Geier, F., Dirnhofer, S., Guglielmelli, P., Vannucchi, A. M., Feenstra, J. D., Kralovics, R., Orkin, S. H., & Skoda, R. C. (2016). Loss of Ezh2 synergizes with JAK2-V617F in initiating myeloproliferative neoplasms and promoting myelofibrosis. *J Exp Med*, *213*(8), 1479-1496. https://doi.org/10.1084/jem.20151136

Shorstova, T., Foulkes, W. D., & Witcher, M. (2021). Achieving clinical success with BET inhibitors as anti-cancer agents. *Br J Cancer*, *124*(9), 1478-1490. https://doi.org/10.1038/s41416-021-01321-0

Silver, A. J., Bick, A. G., & Savona, M. R. (2021). Germline risk of clonal haematopoiesis. *Nat Rev Genet*, *22*(9), 603-617. https://doi.org/10.1038/s41576-021-00356-6

Slukvin, II. (2016). Generating human hematopoietic stem cells in vitro -exploring endothelial to hematopoietic transition as a portal for stemness acquisition. *FEBS Lett*, *590*(22), 4126-4143. https://doi.org/10.1002/1873-3468.12283

Spanoudakis, E., Bazdiara, I., Pantelidou, D., Kotsianidis, I., Papadopoulos, V., Margaritis, D., Xanthopoulidis, G., Moustakidis, E., Mantzourani, S., Bourikas, G., & Tsatalas, C. (2011). Dynamics of telomere's length and telomerase activity in Philadelphia chromosome negative myeloproliferative neoplasms. *Leuk Res*, *35*(4), 459-464. https://doi.org/10.1016/j.leukres.2010.07.042

St Sauver, J. L., Weston, S. A., Atkinson, E. J., Mc Gree, M. E., Mielke, M. M., White, T. A., Heeren, A. A., Olson, J. E., Rocca, W. A., Palmer, A. K., Cummings, S. R., Fielding, R. A., Bielinski, S. J., & LeBrasseur, N. K. (2023). Biomarkers of cellular senescence and risk of death in humans. *Aging Cell*, *22*(12), e14006. https://doi.org/10.1111/acel.14006

Stivala, S., Codilupi, T., Brkic, S., Baerenwaldt, A., Ghosh, N., Hao-Shen, H., Dirnhofer, S., Dettmer, M. S., Simillion, C., Kaufmann, B. A., Chiu, S., Keller, M., Kleppe, M., Hilpert, M., Buser, A. S., Passweg, J. R., Radimerski, T., Skoda, R. C., Levine, R. L., & Meyer, S. C. (2019). Targeting compensatory MEK/ERK activation increases JAK inhibitor efficacy in myeloproliferative neoplasms. *J Clin Invest*, *129*(4), 1596-1611. https://doi.org/10.1172/JCI98785

Storer, M., Mas, A., Robert-Moreno, A., Pecoraro, M., Ortells, M. C., Di Giacomo, V., Yosef, R., Pilpel, N., Krizhanovsky, V., Sharpe, J., & Keyes, W. M. (2013). Senescence is a developmental mechanism that contributes to embryonic growth and patterning. *Cell*, *155*(5), 1119-1130. https://doi.org/10.1016/j.cell.2013.10.041

Suryadevara, V., Hudgins, A. D., Rajesh, A., Pappalardo, A., Karpova, A., Dey, A. K., Hertzel, A., Agudelo, A., Rocha, A., Soygur, B., Schilling, B., Carver, C. M., Aguayo-Mazzucato, C., Baker, D. J., Bernlohr, D. A., Jurk, D., Mangarova, D. B., Quardokus, E. M., Enninga, E. A. L., . . . Neretti, N. (2024). SenNet recommendations for detecting senescent cells in different tissues. *Nat Rev Mol Cell Biol*. https://doi.org/10.1038/s41580-024-00738-8

Swartjes, T., Staals, R. H. J., & van der Oost, J. (2020). Editor's cut: DNA cleavage by CRISPR RNA-guided nucleases Cas9 and Cas12a. *Biochem Soc Trans*, *48*(1), 207-219. https://doi.org/10.1042/BST20190563

Szuber, N., Mudireddy, M., Nicolosi, M., Penna, D., Vallapureddy, R. R., Lasho, T. L., Finke, C., Begna, K. H., Elliott, M. A., Hook, C. C., Wolanskyj, A. P., Patnaik, M. M., Hanson, C. A., Ketterling, R. P., Sirhan, S., Pardanani, A., Gangat, N., Busque, L., & Tefferi, A. (2019). 3023 Mayo Clinic Patients With Myeloproliferative Neoplasms: Risk-Stratified Comparison of Survival and Outcomes Data Among Disease Subgroups. *Mayo Clin Proc*, *94*(4), 599-610. https://doi.org/10.1016/j.mayocp.2018.08.022

Szybinski, J., & Meyer, S. C. (2021). Genetics of Myeloproliferative Neoplasms. *Hematol Oncol Clin North Am*, *35*(2), 217-236. https://doi.org/10.1016/j.hoc.2020.12.002

Tada, M., Morizane, A., Kimura, H., Kawasaki, H., Ainscough, J. F., Sasai, Y., Nakatsuji, N., & Tada, T. (2003). Pluripotency of reprogrammed somatic genomes in embryonic stem hybrid cells. *Dev Dyn*, *227*(4), 504-510. https://doi.org/10.1002/dvdy.10337

Tada, M., Takahama, Y., Abe, K., Nakatsuji, N., & Tada, T. (2001). Nuclear reprogramming of somatic cells by in vitro hybridization with ES cells. *Curr Biol*, *11*(19), 1553-1558. https://doi.org/10.1016/s0960-9822(01)00459-6

Takahashi, K., Tanabe, K., Ohnuki, M., Narita, M., Ichisaka, T., Tomoda, K., & Yamanaka, S. (2007). Induction of pluripotent stem cells from adult human fibroblasts by defined factors. *Cell*, *131*(5), 861-872. https://doi.org/10.1016/j.cell.2007.11.019

Takahashi, K., & Yamanaka, S. (2006). Induction of pluripotent stem cells from mouse embryonic and adult fibroblast cultures by defined factors. *Cell*, *126*(4), 663-676. https://doi.org/10.1016/j.cell.2006.07.024

Takahashi, K., & Yamanaka, S. (2016). A decade of transcription factor-mediated reprogramming to pluripotency. *Nat Rev Mol Cell Biol*, *17*(3), 183-193. https://doi.org/10.1038/nrm.2016.8

Tanaka, Y., Nakanishi, Y., Furuhata, E., Nakada, K. I., Maruyama, R., Suzuki, H., & Suzuki, T. (2024). FLI1 is associated with regulation of DNA methylation and megakaryocytic differentiation in FPDMM caused by a RUNX1 transactivation domain mutation. *Sci Rep*, *14*(1), 14080. https://doi.org/10.1038/s41598-024-64829-4

Tarkhov, A. E., Lindstrom-Vautrin, T., Zhang, S., Ying, K., Moqri, M., Zhang, B., Tyshkovskiy, A., Levy, O., & Gladyshev, V. N. (2024). Nature of epigenetic aging from a single-cell perspective. *Nat Aging*, *4*(6), 854-870. https://doi.org/10.1038/s43587-024-00616-0

Tefferi, A. (2011). How I treat myelofibrosis. *Blood*, *117*(13), 3494-3504. https://doi.org/10.1182/blood-2010-11-315614

Tefferi, A. (2023). Primary myelofibrosis: 2023 update on diagnosis, risk-stratification, and management. *Am J Hematol*, *98*(5), 801-821. https://doi.org/10.1002/ajh.26857

Tefferi, A., Alkhateeb, H., & Gangat, N. (2023). Blast phase myeloproliferative neoplasm: contemporary review and 2024 treatment algorithm. *Blood Cancer J*, *13*(1), 108. https://doi.org/10.1038/s41408-023-00878-8

Tefferi, A., & Barbui, T. (2023). Polycythemia vera: 2024 update on diagnosis, risk-stratification, and management. *Am J Hematol*, *98*(9), 1465-1487. https://doi.org/10.1002/ajh.27002

Tefferi, A., Lasho, T. L., Begna, K. H., Patnaik, M. M., Zblewski, D. L., Finke, C. M., Laborde, R. R., Wassie, E., Schimek, L., Hanson, C. A., Gangat, N., Wang, X., & Pardanani, A. (2015). A Pilot Study of the Telomerase Inhibitor Imetelstat for Myelofibrosis. *N Engl J Med*, *373*(10), 908-919. https://doi.org/10.1056/NEJMoa1310523

Tefferi, A., Vannucchi, A. M., & Barbui, T. (2021). Polycythemia vera: historical oversights, diagnostic details, and therapeutic views. *Leukemia*, *35*(12), 3339-3351. https://doi.org/10.1038/s41375-021-01401-3

Teschendorff, A. E., West, J., & Beck, S. (2013). Age-associated epigenetic drift: implications, and a case of epigenetic thrift? *Hum Mol Genet*, *22*(R1), R7-R15. https://doi.org/10.1093/hmg/ddt375

Tharmapalan, V., & Wagner, W. (2024). Biomarkers for aging of blood - how transferable are they between mice and humans? *Exp Hematol*, 104600. https://doi.org/10.1016/j.exphem.2024.104600

Thiele, J., Kvasnicka, H. M., Orazi, A., Gianelli, U., Gangat, N., Vannucchi, A. M., Barbui, T., Arber, D. A., & Tefferi, A. (2023). The international consensus classification of myeloid neoplasms and acute Leukemias: myeloproliferative neoplasms. *Am J Hematol*, *98*(1), 166-179. https://doi.org/10.1002/ajh.26751

Tong, H., Dwaraka, V. B., Chen, Q., Luo, Q., Lasky-Su, J. A., Smith, R., & Teschendorff, A. E. (2024). Quantifying the stochastic component of epigenetic aging. *Nat Aging*, *4*(6), 886-901. https://doi.org/10.1038/s43587-024-00600-8

Trapp, A., Kerepesi, C., & Gladyshev, V. N. (2021). Profiling epigenetic age in single cells. *Nat Aging*, *1*(12), 1189-1201. https://doi.org/10.1038/s43587-021-00134-3

Tripathi, U., Misra, A., Tchkonia, T., & Kirkland, J. L. (2021). Impact of Senescent Cell Subtypes on Tissue Dysfunction and Repair: Importance and Research Questions. *Mech Ageing Dev*, *198*, 111548. https://doi.org/10.1016/j.mad.2021.111548

Triviai, I., Stubig, T., Niebuhr, B., Hussein, K., Tsiftsoglou, A., Fehse, B., Stocking, C., & Kroger, N. (2015). CD133 marks a stem cell population that drives human primary myelofibrosis. *Haematologica*, *100*(6), 768-779. https://doi.org/10.3324/haematol.2014.118463

Trybek, T., Kowalik, A., Gozdz, S., & Kowalska, A. (2020). Telomeres and telomerase in oncogenesis. *Oncol Lett*, *20*(2), 1015-1027. https://doi.org/10.3892/ol.2020.11659

Tsygankov, D., Liu, Y., Sanoff, H. K., Sharpless, N. E., & Elston, T. C. (2009). A quantitative model for age-dependent expression of the p16INK4a tumor suppressor. *Proc Natl Acad Sci U S A*, *106*(39), 16562-16567. https://doi.org/10.1073/pnas.0904405106

Tursky, M. L., Loi, T. H., Artuz, C. M., Alateeq, S., Wolvetang, E. J., Tao, H., Ma, D. D., & Molloy, T. J. (2020). Direct Comparison of Four Hematopoietic Differentiation Methods from Human Induced Pluripotent Stem Cells. *Stem Cell Reports*, *15*(3), 735-748. https://doi.org/10.1016/j.stemcr.2020.07.009

Usart, M., Stetka, J., Luque Paz, D., Hansen, N., Kimmerlin, Q., Almeida Fonseca, T., Lock, M., Kubovcakova, L., Karjalainen, R., Hao-Shen, H., Borsch, A., El Taher, A., Schulz, J., Leroux, J. C., Dirnhofer, S., & Skoda, R. C. (2024). Loss of Dnmt3a increased self-renewal and resistance to pegIFNalpha in JAK2-V617F-positive myeloproliferative neoplasms. *Blood*. https://doi.org/10.1182/blood.2023020270

Vaidya, H., Jeong, H. S., Keith, K., Maegawa, S., Calendo, G., Madzo, J., Jelinek, J., & Issa, J. J. (2023). DNA methylation entropy as a measure of stem cell replication and aging. *Genome Biol*, *24*(1), 27. https://doi.org/10.1186/s13059-023-02866-4

Vainchenker, W., & Kralovics, R. (2017). Genetic basis and molecular pathophysiology of classical myeloproliferative neoplasms. *Blood*, *129*(6), 667-679. https://doi.org/10.1182/blood-2016-10-695940

Van Egeren, D., Escabi, J., Nguyen, M., Liu, S., Reilly, C. R., Patel, S., Kamaz, B., Kalyva, M., DeAngelo, D. J., Galinsky, I., Wadleigh, M., Winer, E. S., Luskin, M. R., Stone, R. M., Garcia, J. S., Hobbs, G. S., Camargo, F. D., Michor, F., Mullally, A., . . . Hormoz, S. (2021). Reconstructing the Lineage Histories and Differentiation Trajectories of Individual Cancer Cells in Myeloproliferative Neoplasms. *Cell Stem Cell*, *28*(3), 514-523 e519. https://doi.org/10.1016/j.stem.2021.02.001

Vannucchi, A. M., Antonioli, E., Guglielmelli, P., Pardanani, A., & Tefferi, A. (2008). Clinical correlates of JAK2V617F presence or allele burden in myeloproliferative neoplasms: a critical reappraisal. *Leukemia*, *22*(7), 1299-1307. https://doi.org/10.1038/leu.2008.113

Vannucchi, A. M., Verstovsek, S., Guglielmelli, P., Griesshammer, M., Burn, T. C., Naim, A., Paranagama, D., Marker, M., Gadbaw, B., & Kiladjian, J. J. (2017). Ruxolitinib reduces JAK2 p.V617F allele burden in patients with polycythemia vera enrolled in the RESPONSE study. *Ann Hematol*, *96*(7), 1113-1120. https://doi.org/10.1007/s00277-017-2994-x

Varricchio, L., & Hoffman, R. (2022). Megakaryocytes Are Regulators of the Tumor Microenvironment and Malignant Hematopoietic Progenitor Cells in Myelofibrosis. *Front Oncol*, *12*, 906698. https://doi.org/10.3389/fonc.2022.906698

Veland, N., & Chen, T. (2017). *Chapter 2 - Mechanisms of DNA Methylation and Demethylation During Mammalian Development* (2nd ed.). Academic Press. https://doi.org/10.1016/B978-0-12-805388-1.00002-X

Velten, L., Haas, S. F., Raffel, S., Blaszkiewicz, S., Islam, S., Hennig, B. P., Hirche, C., Lutz, C., Buss, E. C., Nowak, D., Boch, T., Hofmann, W. K., Ho, A. D., Huber, W., Trumpp, A., Essers, M. A., & Steinmetz, L. M. (2017). Human haematopoietic stem cell lineage commitment is a continuous process. *Nat Cell Biol*, *19*(4), 271-281. https://doi.org/10.1038/ncb3493

Veronesi, F., Contartese, D., Di Sarno, L., Borsari, V., Fini, M., & Giavaresi, G. (2023). In Vitro Models of Cell Senescence: A Systematic Review on Musculoskeletal Tissues and Cells. *Int J Mol Sci*, *24*(21). https://doi.org/10.3390/ijms242115617

Verstovsek, S., Al-Ali, H. K., Mascarenhas, J., Perkins, A., Vannucchi, A. M., Mohan, S. R., Scott, B. L., Woszczyk, D., Koschmieder, S., Garcia-Delgado, R., Laszlo, R., McGreivy, J. S., Rothbaum, W. P., & Kiladjian, J. J. (2022). BOREAS: a global, phase III study of the MDM2 inhibitor navtemadlin (KRT-232) in relapsed/refractory myelofibrosis. *Future Oncol*. https://doi.org/10.2217/fon-2022-0901

Vieri, M., Brummendorf, T. H., & Beier, F. (2021). Treatment of telomeropathies. *Best Pract Res Clin Haematol*, *34*(2), 101282. https://doi.org/10.1016/j.beha.2021.101282

Vieri, M., Tharmapalan, V., Kalmer, M., Baumeister, J., Nikolic, M., Schnitker, M., Kirschner, M., Flosdorf, N., de Toledo, M. A. S., Zenke, M., Koschmieder, S., Brummendorf, T. H., Beier, F., & Wagner, W. (2023). Cellular aging is accelerated in the malignant clone of myeloproliferative neoplasms. *Blood Cancer J*, *13*(1), 164. https://doi.org/10.1038/s41408-023-00936-1

Villeda, S. A., Plambeck, K. E., Middeldorp, J., Castellano, J. M., Mosher, K. I., Luo, J., Smith, L. K., Bieri, G., Lin, K., Berdnik, D., Wabl, R., Udeochu, J., Wheatley, E. G., Zou, B., Simmons, D. A., Xie, X. S., Longo, F. M., & Wyss-Coray, T. (2014). Young blood reverses age-related impairments in cognitive function and synaptic plasticity in mice. *Nat Med*, *20*(6), 659-663. https://doi.org/10.1038/nm.3569

Wagner, W. (2019). The Link Between Epigenetic Clocks for Aging and Senescence. *Front Genet*, *10*, 303. https://doi.org/10.3389/fgene.2019.00303

Wagner, W., Weidner, C. I., & Lin, Q. (2015). Do age-associated DNA methylation changes increase the risk of malignant transformation? *Bioessays*, *37*(1), 20-24. https://doi.org/10.1002/bies.201400063

Wakita, M., Takahashi, A., Sano, O., Loo, T. M., Imai, Y., Narukawa, M., Iwata, H., Matsudaira, T., Kawamoto, S., Ohtani, N., Yoshimori, T., & Hara, E. (2020). A BET family protein degrader provokes senolysis by targeting NHEJ and autophagy in senescent cells. *Nat Commun*, *11*(1), 1935. https://doi.org/10.1038/s41467-020-15719-6

Wang, L., Lankhorst, L., & Bernards, R. (2022). Exploiting senescence for the treatment of cancer. *Nat Rev Cancer*, *22*(6), 340-355. https://doi.org/10.1038/s41568-022-00450-9

Wang, X., Ye, F., Tripodi, J., Hu, C. S., Qiu, J., Najfeld, V., Novak, J., Li, Y., Rampal, R., & Hoffman, R. (2014). JAK2 inhibitors do not affect stem cells present in the spleens of patients with myelofibrosis. *Blood*, *124*(19), 2987-2995. https://doi.org/10.1182/blood-2014-02-558015

Wang, Y., Chang, J., Liu, X., Zhang, X., Zhang, S., Zhang, X., Zhou, D., & Zheng, G. (2016). Discovery of piperlongumine as a potential novel lead for the development of senolytic agents. *Aging (Albany NY)*, *8*(11), 2915-2926. https://doi.org/10.18632/aging.101100

Wang, Z., Liu, W., Wang, M., Li, Y., Wang, X., Yang, E., Ming, J., Quan, R., & Hu, X. (2021). Prognostic value of ASXL1 mutations in patients with primary myelofibrosis and its relationship with clinical features: a meta-analysis. *Ann Hematol*, *100*(2), 465-479. https://doi.org/10.1007/s00277-020-04387-7

Waring, P., & Mullbacher, A. (1999). Cell death induced by the Fas/Fas ligand pathway and its role in pathology. *Immunol Cell Biol*, *77*(4), 312-317. https://doi.org/10.1046/j.1440-1711.1999.00837.x

Weidner, C. I., Lin, Q., Koch, C. M., Eisele, L., Beier, F., Ziegler, P., Bauerschlag, D. O., Jockel, K. H., Erbel, R., Muhleisen, T. W., Zenke, M., Brummendorf, T. H., & Wagner, W. (2014). Aging of blood can be tracked by DNA methylation changes at just three CpG sites. *Genome Biol*, *15*(2), R24. https://doi.org/10.1186/gb-2014-15-2-r24

Werner, B., Beier, F., Hummel, S., Balabanov, S., Lassay, L., Orlikowsky, T., Dingli, D., Brummendorf, T. H., & Traulsen, A. (2015). Reconstructing the in vivo dynamics of

hematopoietic stem cells from telomere length distributions. *Elife*, *4*. https://doi.org/10.7554/eLife.08687

Wielscher, M., Mandaviya, P. R., Kuehnel, B., Joehanes, R., Mustafa, R., Robinson, O., Zhang, Y., Bodinier, B., Walton, E., Mishra, P. P., Schlosser, P., Wilson, R., Tsai, P. C., Palaniswamy, S., Marioni, R. E., Fiorito, G., Cugliari, G., Karhunen, V., Ghanbari, M., . . . Jarvelin, M. R. (2022). DNA methylation signature of chronic low-grade inflammation and its role in cardio-respiratory diseases. *Nat Commun*, *13*(1), 2408. https://doi.org/10.1038/s41467-022-29792-6

Williams, N., Lee, J., Mitchell, E., Moore, L., Baxter, E. J., Hewinson, J., Dawson, K. J., Menzies, A., Godfrey, A. L., Green, A. R., Campbell, P. J., & Nangalia, J. (2022). Life histories of myeloproliferative neoplasms inferred from phylogenies. *Nature*, *602*(7895), 162-168. https://doi.org/10.1038/s41586-021-04312-6

Wilson, A. S., Power, B. E., & Molloy, P. L. (2007). DNA hypomethylation and human diseases. *Biochim Biophys Acta*, *1775*(1), 138-162. https://doi.org/10.1016/j.bbcan.2006.08.007

Wyles, S. P., Tchkonia, T., & Kirkland, J. L. (2022). Targeting Cellular Senescence for Age-Related Diseases: Path to Clinical Translation. *Plast Reconstr Surg*, *150*, 20S-26S. https://doi.org/10.1097/PRS.0000000000009669

Xie, M., Lu, C., Wang, J., McLellan, M. D., Johnson, K. J., Wendl, M. C., McMichael, J. F., Schmidt, H. K., Yellapantula, V., Miller, C. A., Ozenberger, B. A., Welch, J. S., Link, D. C., Walter, M. J., Mardis, E. R., Dipersio, J. F., Chen, F., Wilson, R. K., Ley, T. J., & Ding, L. (2014). Age-related mutations associated with clonal hematopoietic expansion and malignancies. *Nat Med*, *20*(12), 1472-1478. https://doi.org/10.1038/nm.3733

Xu, J., & Liu, Y. (2021). Probing Chromatin Compaction and Its Epigenetic States in situ With Single-Molecule Localization-Based Super-Resolution Microscopy [Review]. *Frontiers in Cell and Developmental Biology*, *9*. https://doi.org/10.3389/fcell.2021.653077

Xu, M., Pirtskhalava, T., Farr, J. N., Weigand, B. M., Palmer, A. K., Weivoda, M. M., Inman, C. L., Ogrodnik, M. B., Hachfeld, C. M., Fraser, D. G., Onken, J. L., Johnson, K. O., Verzosa, G. C., Langhi, L. G. P., Weigl, M., Giorgadze, N., LeBrasseur, N. K., Miller, J. D., Jurk, D., . . . Kirkland, J. L. (2018). Senolytics improve physical function and increase lifespan in old age. *Nat Med*, *24*(8), 1246-1256. https://doi.org/10.1038/s41591-018-0092-9

Yan, X., Xu, Z., Zhang, P., Sun, Q., Jia, Y., Qin, T., Qu, S., Pan, L., Li, Z., Liu, J., Song, Z., Gao, Q., Jiao, M., Gong, J., Wang, H., Li, B., & Xiao, Z. (2023). Non-driver mutations landscape in different stages of primary myelofibrosis determined ASXL1 mutations play a critical role in disease progression. *Blood Cancer J*, *13*(1), 56. https://doi.org/10.1038/s41408-023-00829-3

Ye, Z., Liu, C. F., Lanikova, L., Dowey, S. N., He, C., Huang, X., Brodsky, R. A., Spivak, J. L., Prchal, J. T., & Cheng, L. (2014). Differential sensitivity to JAK inhibitory drugs by isogenic human erythroblasts and hematopoietic progenitors generated from patient-specific induced pluripotent stem cells. *Stem Cells*, *32*(1), 269-278. https://doi.org/10.1002/stem.1545

Ye, Z., Zhan, H., Mali, P., Dowey, S., Williams, D. M., Jang, Y. Y., Dang, C. V., Spivak, J. L., Moliterno, A. R., & Cheng, L. (2009). Human-induced pluripotent stem cells from blood cells of healthy donors and patients with acquired blood disorders. *Blood*, *114*(27), 5473-5480. https://doi.org/10.1182/blood-2009-04-217406

Yin, X., Hu, L., Zhang, Y., Zhu, C., Cheng, H., Xie, X., Shi, M., Zhu, P., Zhao, X., Chen, W., Zhang, L., Arakaki, C., Hao, S., Wang, M., Cao, W., Ma, S., Zhang, X. B., & Cheng, T. (2020). PDGFB-expressing mesenchymal stem cells improve human hematopoietic stem cell engraftment in immunodeficient mice. *Bone Marrow Transplant*, *55*(6), 1029-1040. https://doi.org/10.1038/s41409-019-0766-z

Yu, J., Vodyanik, M. A., Smuga-Otto, K., Antosiewicz-Bourget, J., Frane, J. L., Tian, S., Nie, J., Jonsdottir, G. A., Ruotti, V., Stewart, R., Slukvin, II, & Thomson, J. A. (2007). Induced pluripotent stem cell lines derived from human somatic cells. *Science*, *318*(5858), 1917-1920. https://doi.org/10.1126/science.1151526

Yvernogeau, L., Gautier, R., Petit, L., Khoury, H., Relaix, F., Ribes, V., Sang, H., Charbord, P., Souyri, M., Robin, C., & Jaffredo, T. (2019). In vivo generation of haematopoietic

stem/progenitor cells from bone marrow-derived haemogenic endothelium. *Nat Cell Biol*, *21*(11), 1334-1345. https://doi.org/10.1038/s41556-019-0410-6

Zauli, G., AlHilali, S., Al-Swailem, S., Secchiero, P., & Voltan, R. (2022). Therapeutic potential of the MDM2 inhibitor Nutlin-3 in counteracting SARS-CoV-2 infection of the eye through p53 activation. *Front Med (Lausanne)*, *9*, 902713. https://doi.org/10.3389/fmed.2022.902713

Zeineddine, D., Hammoud, A. A., Mortada, M., & Boeuf, H. (2014). The Oct4 protein: more than a magic stemness marker. *Am J Stem Cells*, *3*(2), 74-82. https://www.ncbi.nlm.nih.gov/pubmed/25232507

Zhang, L., Mack, R., Breslin, P., & Zhang, J. (2020). Molecular and cellular mechanisms of aging in hematopoietic stem cells and their niches. *J Hematol Oncol*, *13*(1), 157. https://doi.org/10.1186/s13045-020-00994-z

Zhao, H., Wu, L., Yan, G., Chen, Y., Zhou, M., Wu, Y., & Li, Y. (2021). Inflammation and tumor progression: signaling pathways and targeted intervention. *Signal Transduct Target Ther*, *6*(1), 263. https://doi.org/10.1038/s41392-021-00658-5

Zheng, Y., Joyce, B. T., Colicino, E., Liu, L., Zhang, W., Dai, Q., Shrubsole, M. J., Kibbe, W. A., Gao, T., Zhang, Z., Jafari, N., Vokonas, P., Schwartz, J., Baccarelli, A. A., & Hou, L. (2016). Blood Epigenetic Age may Predict Cancer Incidence and Mortality. *EBioMedicine*, *5*, 68-73. https://doi.org/10.1016/j.ebiom.2016.02.008

Zhou, W., Triche, T. J., Jr., Laird, P. W., & Shen, H. (2018). SeSAMe: reducing artifactual detection of DNA methylation by Infinium BeadChips in genomic deletions. *Nucleic Acids Res*, *46*(20), e123. https://doi.org/10.1093/nar/gky691

Zhou, Y., He, F., Pu, W., Gu, X., Wang, J., & Su, Z. (2020). The Impact of DNA Methylation Dynamics on the Mutation Rate During Human Germline Development. *G3 (Bethesda)*, *10*(9), 3337-3346. https://doi.org/10.1534/g3.120.401511

Zhu, Y., Tchkonia, T., Pirtskhalava, T., Gower, A. C., Ding, H., Giorgadze, N., Palmer, A. K., Ikeno, Y., Hubbard, G. B., Lenburg, M., O'Hara, S. P., LaRusso, N. F., Miller, J. D., Roos, C. M., Verzosa, G. C., LeBrasseur, N. K., Wren, J. D., Farr, J. N., Khosla, S., . . . Kirkland, J. L. (2015). The Achilles' heel of senescent cells: from transcriptome to senolytic drugs. *Aging Cell*, *14*(4), 644-658. https://doi.org/10.1111/acel.12344

Zoico, E., Nori, N., Darra, E., Tebon, M., Rizzatti, V., Policastro, G., De Caro, A., Rossi, A. P., Fantin, F., & Zamboni, M. (2021). Senolytic effects of quercetin in an in vitro model of pre-adipocytes and adipocytes induced senescence. *Sci Rep*, *11*(1), 23237. https://doi.org/10.1038/s41598-021-02544-0

Zvereva, M. I., Shcherbakova, D. M., & Dontsova, O. A. (2010). Telomerase: structure, functions, and activity regulation. *Biochemistry (Mosc)*, *75*(13), 1563-1583. https://doi.org/10.1134/s0006297910130055

Supplemental Materials

Supplement Table S1. Overview of patient samples used for iPSC reprogramming.

Patient	Age	Gender	Patient JAK2^{V617F}	Clone name	hPSC registry ID	Genotype	Clone JAK2^{V617F}	Additional single nucleotide polymorphism (SNPs)	Generation	References
Patient 1	43	f	37%	PV007	UKAi002-A	Wild type		39% CBL	Reprogramming	(Satoh et al., 2021)
				PV009	UKAi002-B	Heterozygous	48%	25% CBL, 27% TET2	Reprogramming	(Satoh et al., 2021)
				PV012	UKAi002-B3	Homozygous	100%	100% ASXL1, 42% CBL, 49% DNMT3A, 51% EZH2, 48% MPL, 100% SETPB1, 50% SH2B3, 52% TET2, 51% TP53	CRISPR/Cas9	(Flosdorf et al., 2024)
Patient 2	47	m	96%	PV2072	UKAi003-A1	Wild type		100% ASXL1, 49% DNMT3A, 53% EZH2, 100% TP53	CRISPR/Cas9 repair	(Flosdorf et al., 2024)
				PV2070	UKAi003-A2	Heterozygous	52%	100% ASXL1, 51% DNMT3A, 51% EZH2, 100% TP53	CRISPR/Cas9 repair	(Flosdorf et al., 2024)
				PV2021	UKAi003-A	Homozygous	99%	100% ASXL1, 51% EZH2, 99% TP53	Reprogramming	(Satoh et al., 2021)
Patient 3	38	m	25%	PV3026	UKAi013-A	Wild type		100% ASXL1, 46% TET2, 56% TP53	Reprogramming	(Flosdorf et al., 2024)
				PV3006	UKAi013-B	Heterozygous	39%	100% ASXL1, 51% SETPB1, 50% TET2, 52% TP53	Reprogramming	(Flosdorf et al., 2024)
				PV3007	UKAi013-B1	Homozygous	100%	100% ASXL1, 51% DNMT3A, 49% EZH2, 50% SETPB1, 50% TET2, 50% TP53	CRISPR/Cas9	(Flosdorf et al., 2024)

List of all iPSC clones used in this study, their genotype, how the respective clones were generated and the references.

Supplemental Figure

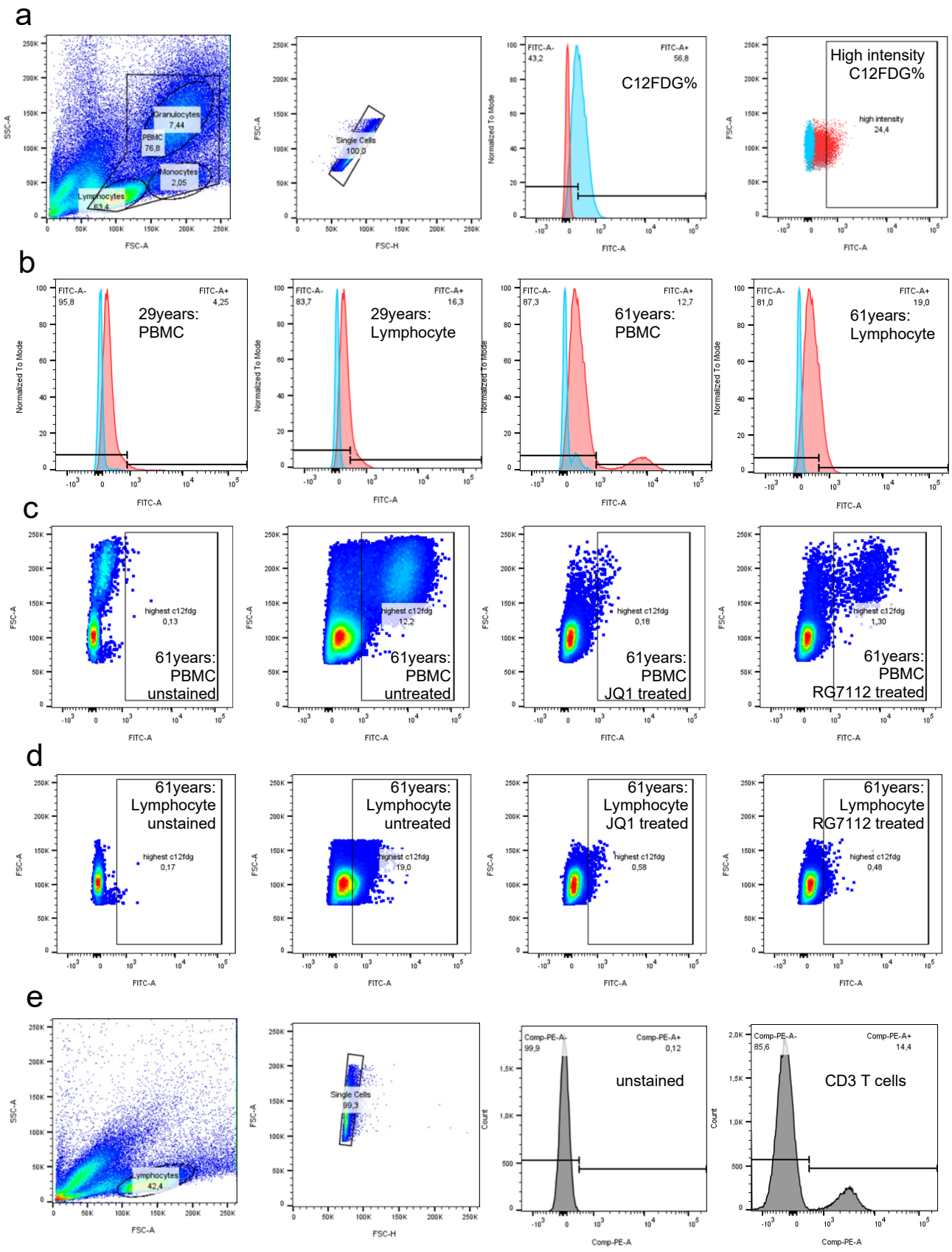

Supplemental Figure S1. Gating strategy for the flow cytometry data with the healthy senolytics treated PBMCs.

a) Gating for strategy for the selection of C12FDG cells is as follows: FSC vs. SSC (forward scatter, FSC, size vs. side scatter, SSC, granularity) for PBMS including monocytes, granulocytes and lymphocytes. FSC-A vs. FSC-H for doublets exclusion. FITC gating in relation to the autofluorescence control. FSC-A vs. FITC for the selection of high intensity C12FDG staining. b) C12FDG-FITC positive cells was shown at 29 and 61 years of age, in the PBMC and lymphocyte population with background autofluorescence control. c) High intensity C12FDG-FITC positive cells of a 61-year-old PBMC sample is shown in the following order: autofluorescence control (unstained), untreated, after the treatment with JQ1 and RG7112 (from left to right). d) As shown in (c), but in lymphocyte population. e) Gating strategy for lymphocyte compartment exemplarily shown for T-cell analysis in the following order: FSC vs. SSC for lymphocyte selection, FSC-A vs. FSC-H for doublets exclusion, gating at autofluorescence control, and the implication of this gating for the CD3 marker, as an example.

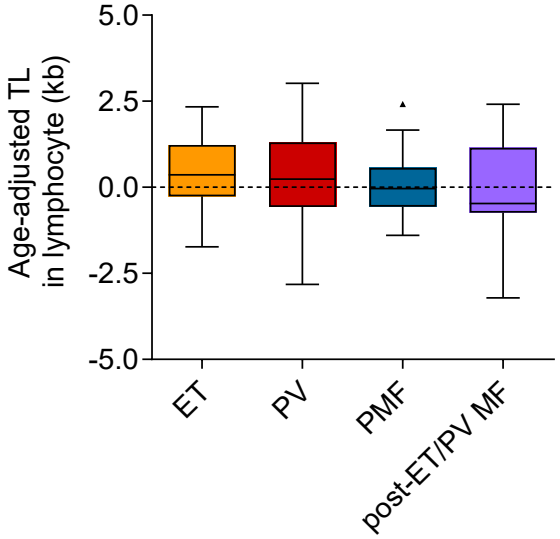

Supplemental Figure S2. Age-adjusted telomere length in lymphocytes in different MPN entities.

Telomere length (TL, in kb) was measured in lymphocytes via flow-FISH in blood of MPN patients (n = 129). One-sample t-test was used to calculate statistical significance. There is no significant reduction in telomere length is observed in lymphocyte compartment in any MPN entities.

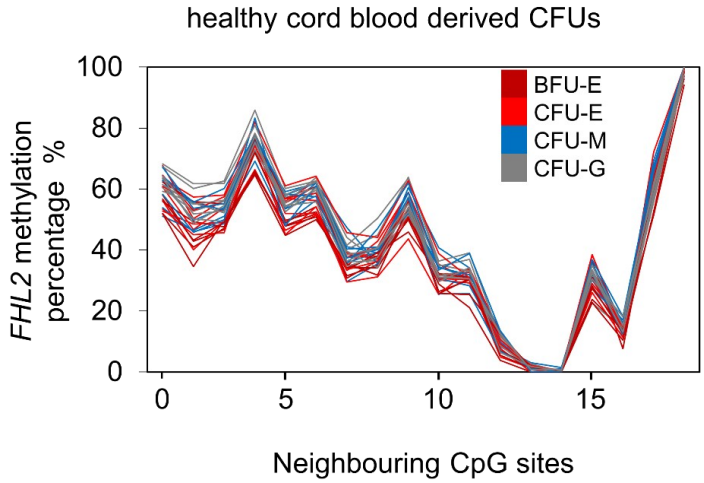

Supplemental Figure S3. Exemplarily for one age-associated region, *FHL2* methylation percentage differences between different CFU subtypes.

CFU-E = CFU erythrocyte; BFU-E = CFU burst forming unit erythrocyte; CFU-M = CFU macrophage; CFU-G = CFU granulocyte.

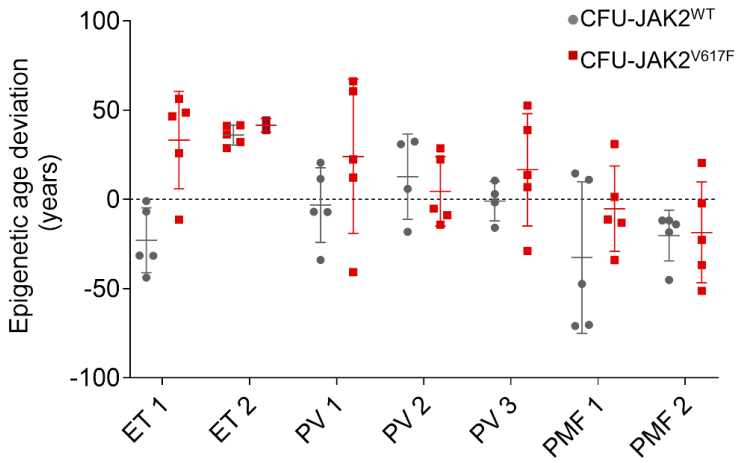

Supplemental Figure S4. Cellular aging is accelerated in colony forming units with *JAK2* V617F using 2 CpG prediction, *PDE4C* and *FHL2*.

Epigenetic age predictions were performed in CFUs without (n = 5) and with *JAK2* V617F (n = 5) in patients affected by either ET, PV, or PMF.

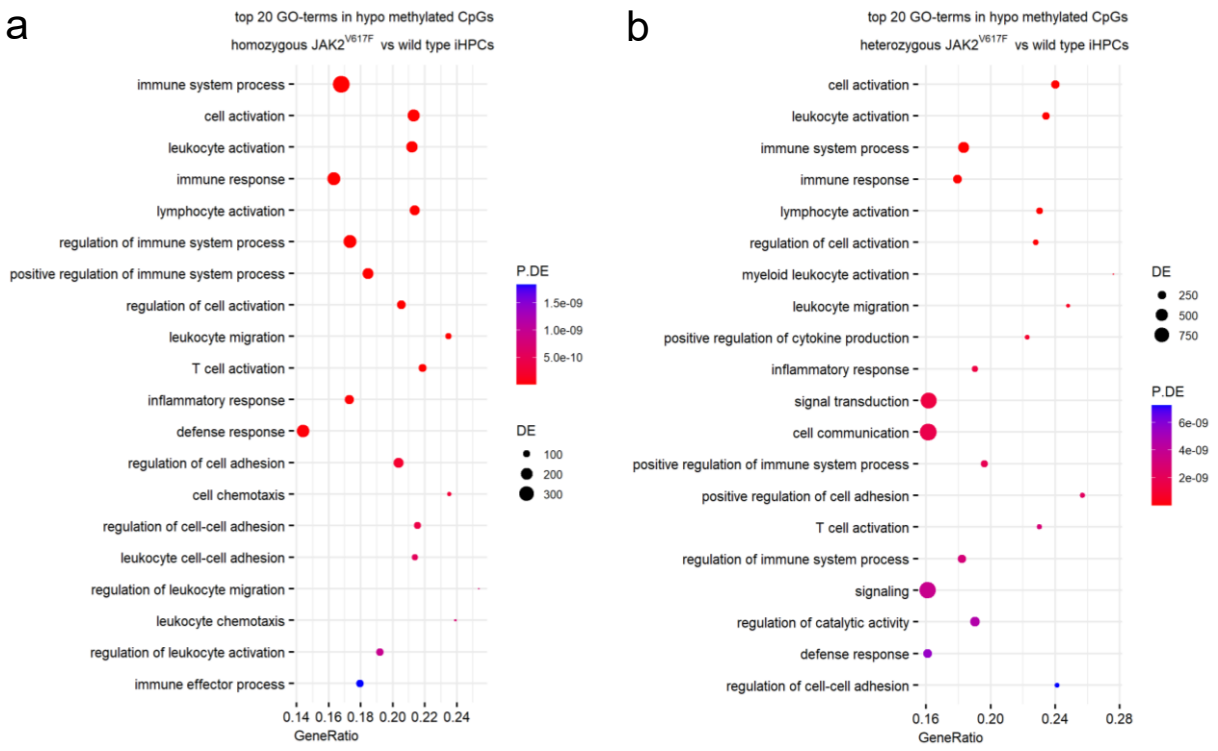

Supplemental Figure S5. Gene ontology term analysis of hypomethylated CpGs between mutant iHPCs and WT iHPCs.

GO term analysis of the top hypomethylated CpGs associated with genes, when comparing a) homozygous iHPCs with WT iHPCs and b) heterozygous iHPCs with WT iHPCs. Biological process terms were considered, and terms with a false discovery rate (FDR) of less than 0.1 were analyzed using the R package missMethyl. GeneRatio is defined as the number of differentially expressed genes (DE genes) divided by the total number of genes in the set. DE is the number of differentially methylated genes. P.DE is the p-value for overrepresentation of the GO term.

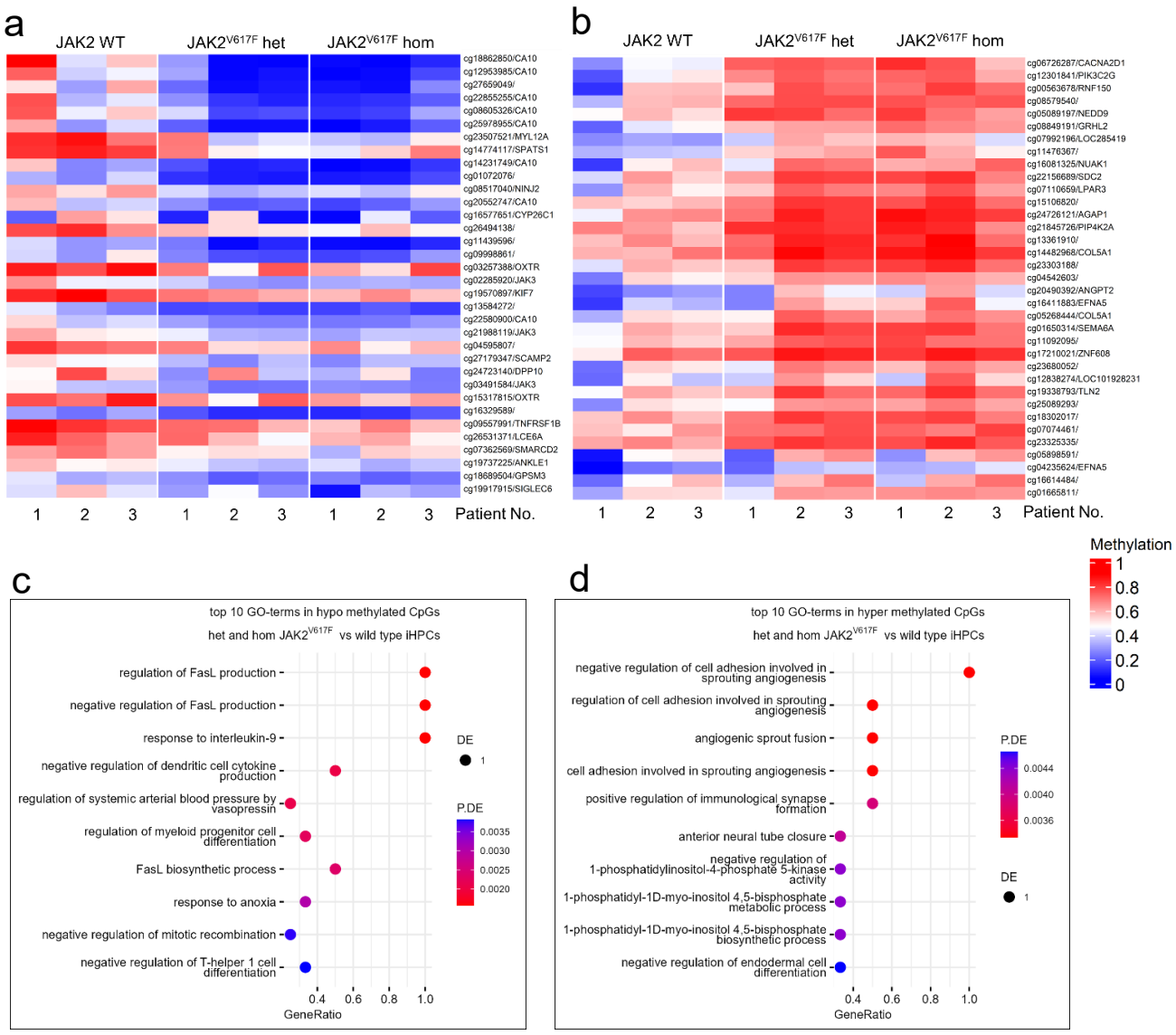

Supplemental Figure S6. Methylation changes in the heterozygous and homozygous iHPCs compared to WT across all patients.

Heatmaps for top 20 differentially methylated CpGs across all patients, where a) Top 20 hypomethylated CpGs and b) hypermethylated CpGs are common in both heterozygous and homozygous clones compared to WT iHPCs. GO term analysis of the commonly CpGs that were differentially methylated in both heterozygous and homozygous iHPCs compared to WT showing genes associated with c) hypomethylation and d) hypermethylation.

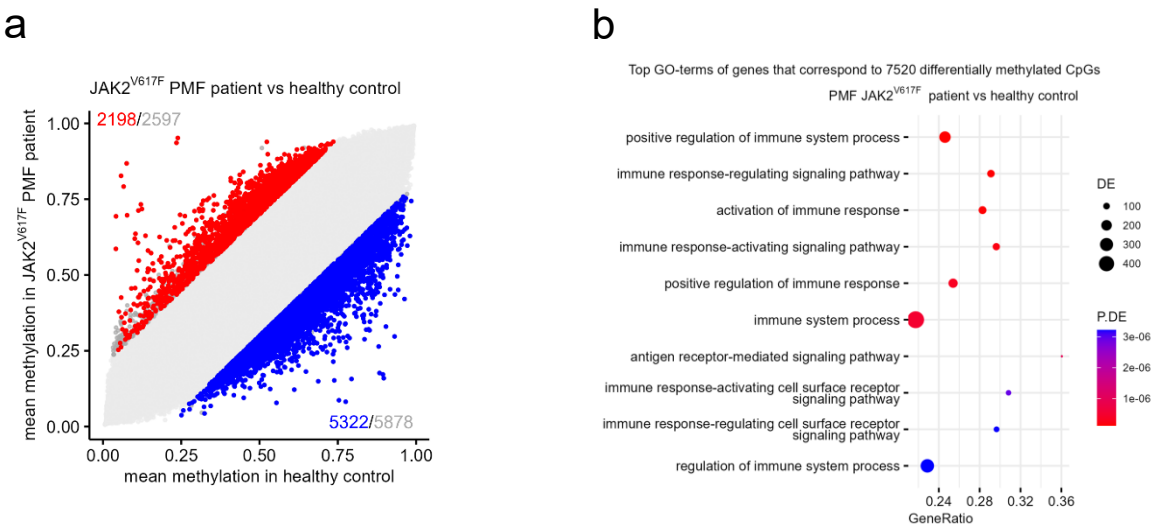

Supplemental Figure S7. DNA methylation changes in PMF patients with *JAK2* V617F mutation compared to healthy controls.

a) Scatter plots show DNA methylation levels primary myelofibrosis (PMF) with *JAK2* V617F mutation (n = 10) in comparison to data of healthy donors (n = 10). The numbers indicate the difference in mean methylation of cut-off 0.2 in grey and those that are significant in color, with blue indicating hypomethylation and red indicating hypermethylation. b) GO term analysis of the top statistically significant CpGs that were differentially methylated in both hypo- and hypermethylated genes when comparing PMF with healthy.

List of Figures

List of Supplemental Figures

List of Tables

List of Supplemental Tables

List of Abbreviations

°C	degrees Celsius
µl	microliter
µM	micromolar
5hmC	5-hydroxymethylcytosine
ABL	Abelson murine leukemia
AML	acute myeloid leukemia
ANOVA	analysis of variance
APC	allophycocyanin
ASXL1	additional sex combs–like transcriptional regulator 1
BBA-Seq	barcoded bisulfite amplicon sequencing
BCR	breakpoint cluster region
BER	base excision repair
bFGF	basic Fibroblast Growth Factor
BFU-E	burst forming unit – erythroid
BMP4	bone morphogenetic protein 4
bp	base pair
C12FDG	5-dodecanoylaminofluorescein di-β-D-galactopyranoside
CALR	calreticulin
CAR-T	chimeric antigen receptor T-cell
CCDC102B	coiled-coil domain-containing protein 102B

CDK	cyclin-dependent kinase
CFU	colony forming unit
CFU-E	colony forming unit erythroid
CFU-G	colony forming unit granulocyte
CFU-GEMM	colony forming unit granulocyte, erythrocyte, macrophage, megakaryocyte
CFU-GM	colony forming unit granulocyte, macrophage
CFU-M	colony forming unit macrophage
CHIP	clonal hematopoiesis of intermediate potential
CML	chronic myeloid leukemia
C-MYC	cellular myelocytomatosis oncogene
CpG	cytosine guanine dinucleotide
CRISPR/Cas 9	clustered regularly interspaced short palindromic repeats guided Cas9 nucleases
D+Q	dasatinib in combination with quercetin
ddPCR	digital droplet PCR
DDR	DNA damage response
DE	differentially expressed
DMSO	dimethyl sulfoxide
DNAm	DNA methylation
DNMT3A	DNA (cytosine-5-)-methyltransferase 3α
DNMTs	DNA methyltransferases
DSB	double stranded breaks
EB	embryoid body
ECM	extracellular matrix components
EGFR	epidermal growth factor receptor
EHT	endothelial-to-hematopoietic transition
EMP	erythromyeloid progenitor cell
EMT	epithelial-mesenchymal transition
EPIC	Illumina Methylation EPIC BeadChip
ESC	embryonic stem cells
ET	essential thrombocythemia
FACS	Fluorescence-activated cell sorting
FDR	false discovery rate
FGF2	fibroblast growth factor 2
FHL2	four and a half LIM domains protein 2
FITC	Fluorescein isothiocyanate
FSC	forward scatter
GEO	Gene Expression Omnibus
GM-CSF	granulocyte-macrophage colony-stimulating factor
GO	gene ontology
HDR	homology directed repair
HE	hemogenic endothelium
het	heterozygous
hom	homozygous

HSC	hematopoietic stem cell
Hsf4	heat shock transcription factor 4
HSPCs	hematopoietic stem/progenitor cells
HUVEC	human umbilical cord vein endothelial cells
IC50	half-maximal inhibitory concentration
IFN-alpha	interferon-alpha
iHPC	iPSC-derived hematopoietic progenitor cell
IL	interleukin
iPSC	induced pluripotent stem cell
JAK	Janus Kinase
JAKi	JAK inhibitors
Kcns1	potassium voltage-gated channel modifier subfamily S member 1
KLF4	Kruppel-like factor 4
LIN28	cell lineage abnormal 28
LOH	loss of heterogeneity
MACS	magnetic assisted cell sorting
MAD	mean age deviation
MAPK	mitogen-activated protein kinase
MDS	myelodysplastic syndrome
MDS plot	multidimensional scaling plot
MF	myelofibrosis
MgCl2	magnesium chloride
ml	milliliters
MPL	myeloproliferative leukemia protein
MPN	myeloproliferative neoplasms
MSC	mesenchymal stem cell
NF-kB	nuclear factor-kappa B
ng	nanogram
NGS	next-generation sequencing
NHEJ	non-homologous end joining
NK cells	natural killer cells
OCT	octamer binding transcription factor
OOB	out-of-band
p-adj	adjusted p-value
PAM	protospacer adjacent motif
PBMC	peripheral blood mononuclear cell
PBS	phosphate-buffered saline
PC	principal component
PCR	polymerase chain reaction
PDE4C	phosphodiesterase 4C
PDGFRB	platelet-derived growth factor receptor beta
PDMS	polydimethylsiloxane
PI	propidium Iodide
PI3K	phosphoinositide 3-kinase

PMF	primary myelofibrosis
Prima1	proline rich membrane anchor 1
PRPF8	pre-mRNA processing factor 8
PV	polycythemia vera
R^2	coefficient of Determination
ROS	reactive oxygen species
SAM	S-adenyl methionine
SASP	senescence-associated secretory phenotype
SA-β-gal	SA-β-galactosidase
SCF	stem cell factor
SF3B1	splicing factor 3b, subunit 1
SNP	single nucleotide polymorphisms
SOX2	sex-determining region y-box 2 transcription factor
SRSF2	serine and arginine rich splicing factor 2
SSC	side scatter
STAT	signal transducer and activator of transcription
TALENs	transcription activator like effector nucleases
TERC	telomerase RNA component
TERT	telomerase reverse transcriptase
TET2	tet methylcytosine dioxygenase 2
TL	telomere length
TP53	tumor protein p53
TSS	transcription start sites
TSS1500	1500 bp upstream of TSS
TSS200	200 bp upstream of TSS
U2AF1	U2 small nuclear RNA auxiliary factor 1
UPD	uniparental disomy
VAF	variant allele frequency
VEGF	vascular endothelial growth factor A
VEGF	vascular endothelial growth factor
WT	wildtype
β	beta value

Declaration of Authorship

Eidesstattliche Erklärung

I, Vithurithra Tharmapalan

declare that this thesis and the work presented in it are my own and has been generated by me as the result of my own original research.

Hiermit erkläre ich an Eides statt / I do solemnely swear that:

1. This work was done wholly or mainly while in candidature for the doctoral degree at this faculty and university;
2. Where any part of this thesis has previously been submitted for a degree or any other qualification at this university or any other institution, this has been clearly stated;
3. Where I have consulted the published work of others or myself, this is always clearly attributed;
4. Where I have quoted from the work of others or myself, the source is always given. This thesis is entirely my own work, with the exception of such quotations;
5. I have acknowledged all major sources of assistance;
6. Where the thesis is based on work done by myself jointly with others, I have made clear exactly what was done by others and what I have contributed myself;
7. Parts of this work have been published before as:

   Vieri M*, Tharmapalan V* et al. (2023), Blood Cancer J.

   Tharmapalan V et al. (2025) NPJ Aging.

Aachen,

_____

Vithurithra Tharmapalan

Publications

- Vieri M *, **Tharmapalan V *,** Kalmer M, Baumeister J, Nikolić M, Schnitker M, Kirschner M, Flosdorf N, de Toledo MAS, Zenke M, Koschmieder S, Brümmendorf TH *, Beier F *, Wagner W *. Cellular aging is accelerated in the malignant clone of myeloproliferative neoplasms. Blood Cancer J. 2023 Nov 6;13(1):164. doi: 10.1038/s41408-023-00936-1. PMID: 37926720; PMCID: PMC10625927. (*equal contribution).

  Contribution VT: contributed to experimental design, performed cell culture, senolytic drug testing, senescence staining, targeted bisulfite amplicon sequencing, and analyzed the results from pyrosequencing, Miseq, microarray and methylation data; wrote the first draft of manuscript with MV and WW.

- **Tharmapalan V**, Du Marchie Sarvaas M, Bleichert M, Wessiepe M, Wagner W. Senolytic compounds reduce epigenetic age of blood samples *in vitro*. NPJ Aging. 2025 Feb 4;11(1):6. doi: 10.1038/s41514-025-00199-z. PMID: 39905063; PMCID: PMC11794651.

  Contribution VT: involved in conceptualization of research; carried out the experiments; analyzed the data; and wrote the first draft of manuscript with WW.

- **Tharmapalan V**, Wagner W. Biomarkers for aging of blood – how transferable are they between mice and humans? Exp Hematol. 2024 Aug 9:104600. doi: 10.1016/j.exphem.2024.104600.

  Contribution VT: wrote the first draft of manuscript with WW.

- Flosdorf N, Böhnke J, de Toledo MAS, Lutterbach N, Lerma VG, Graßhoff M, Olschok K, Gupta S, **Tharmapalan V**, Schmitz S, Götz K, Schüler HM, Maurer A, Sontag S, Küstermann C, Seré K, Wagner W, Costa IG, Brümmendorf TH, Koschmieder S, Chatain N, Castilho M, Schneider RK, Zenke M. Proinflammatory phenotype of iPS cell-derived JAK2 V617F megakaryocytes induces fibrosis in 3D *in vitro* bone marrow niche. Stem Cell Reports. 2024 Feb 13;19(2):224-238. doi: 10.1016/j.stemcr.2023.12.011. Epub 2024 Jan 25. PMID: 38278152; PMCID: PMC10874863.

  Contribution VT: performed bioinformatic analysis of DNA methylation for Epi-Pluri-Score; edited and approved the final manuscript.

- Dursun Torlak E, **Tharmapalan V**, Kricheldorf K, Schifflers J, Caduc M, Zenke M, Koschmieder S, Wagner W. DNA methylation in primary myelofibrosis is partly associated

with driver mutations and distinct from other myeloid malignancies. MedRxiv; revised manuscript submitted.

Contribution VT: performed iPSC experiments and supported analysis of DNAm data and wrote the first draft of manuscript with EDT and WW.

- Perez-Correa JF, **Tharmapalan V**, Geiger H, Wagner W. Epigenetic Clocks for Mice Based on Age-Associated Regions That are Conserved Between Mouse Strains and Human. Front Cell Dev Biol. 2022 Jun 3;10:902857. doi: 10.3389/fcell.2022.902857. PMID: 35721486; PMCID: PMC9204067.

  Contribution VT: supported the study design and analysis; edited and approved the final manuscript. (The results of this publication are not part of this thesis)

- Franzen J, Nüchtern S, **Tharmapalan V**, Vieri M, Nikolić M, Han Y, Balfanz P, Marx N, Dreher M, Brümmendorf TH, Dahl E, Beier F, Wagner W. Epigenetic Clocks Are Not Accelerated in COVID-19 Patients. Int J Mol Sci. 2021 Aug 27;22(17):9306. doi: 10.3390/ijms22179306. PMID: 34502212; PMCID: PMC8431654.

  Contribution VT: performed MiSeq experiments; edited and approved the final manuscript. (The results of this publication are not part of this thesis)

- Cypris O, Eipel M, Franzen J, Rösseler C, **Tharmapalan V**, Kuo CC, Vieri M, Nikolić M, Kirschner M, Brümmendorf TH, Zenke M, Lampert A, Beier F, Wagner W. PRDM8 reveals aberrant DNA methylation in aging syndromes and is relevant for hematopoietic and neuronal differentiation. Clin Epigenetics. 2020 Aug 20;12(1):125. doi: 10.1186/s13148-020-00914-5. PMID: 32819411; PMCID: PMC7439574.

  Contribution VT: performed and analyzed BBA-seq experiments; edited and approved the final manuscript. (The results of this publication are not part of this thesis)

- Sontag S, Bocova L, Hubens WHG, Nüchtern S, Schnitker M, Look T, Schröder KM, Plümäkers B, **Tharmapalan V**, Wessiepe M, Kraus T, Kramer J, Rink L, Koschmieder S, Wagner W. Toward Clinical Application of Leukocyte Counts Based on Targeted DNA Methylation Analysis. Clin Chem. 2022 May 18;68(5):646-656. doi: 10.1093/clinchem/hvac006. PMID: 35157041.

  Contribution VT: designed the ddPCR assay for absolute quantification; edited and approved the final manuscript. (The results of this publication are not part of this thesis).

Conference attendance

Talk and Poster presentation:

Tharmapalan V, Vieri M, Kalmer M, Nikolić M, Schnitker M, Kirschner M, Koschmieder S, Brümmendorf T, Beier F, Wagner W. Cellular age is accelerated in myeloproliferative neoplasms (2022). 10th International Annual Conference of the GSCN, Münster, Germany.

Pitch talk presentation:

Tharmapalan V, Nikolić M, Kalmer M, Vieri M, Koschmieder S, Franzen J, Brümmendorf T, Beier F, Wagner W. Epigenetic Age is Accelerated in Myeloproliferative Neoplasms (2021). 10th International Meeting of the Stem Cell Network NRW, virtual conference.

Poster presentation:

Tharmapalan V, Vieri M, Kalmer M, Nikolić M, Kirschner M, Koschmieder S, Brümmendorf T, Beier F, Wagner W. Cellular age is accelerated in myeloproliferative neoplasms (2022). 13th Internal Meeting of the Stem Cell Network NRW, Herne, Germany.

Acknowledgement

"The noblest pleasure is the joy of understanding." da Vinci

I truly believe that science is a collaborative work where you are inspired by each other. I am grateful that I have the opportunity to work with really talented people who are motivated and curious to find things out, while being kind to one another.

Firstly, I would like to thank my supervisor Prof. Wolfgang Wagner for giving me the opportunity to pursue an important step in my career. Thank you for all the discussions, encouragement, and opportunities to explore science. I thank you for your patience and time in letting me learn new things, giving me time to discuss new ideas and for your willingness to collaborate. I have really learned to articulate, write, review and discuss science, and I thank you for creating a comfortable working atmosphere to make this possible.

I would further like to thank my second supervisor Prof. Steffen Koschmieder, for accepting to review my thesis and your valuable insights and time for this project. Thank you for all the discussions during the MPN meetings and the opportunity to be part of the CRU344 consortium, which truly made all the collaboration projects possible. I thank Prof. Martin Zenke for providing the valuable iPSC clones to work on this project. More than that, thank you for always finding time for discussions when I had questions. You truly inspire a whole new generation of students with your infectious interest in science. I would also like to thank Prof. Tim Brümmendorf for asking the critical questions to drive this project forward. I would like to extend my thanks to Fabian Beier for backing the MPN collaborative project. Furthermore, I would like to thank Dr. Jacopo Di Russo for taking the time to review my thesis and for being a member of my thesis committee. Martina Wessiepe and Biobank for providing the samples, and the people who kindly donated their samples for experiments.

I give a big gratitude to Margherita Vieri, this project would not have been successful and so engaging and collaborative, if it’s not you. You truly enriched this project, and always been helpful and been my next to call person. Now I have a friend, thank you Marghe for everything. I remember the first time asking you to look at your CFUs together and showing me to how to pick the colonies, and now we have come a long way from bouldering to being there for each other, thanks Milena Kalmer (Mile :D). The plan for all three of us working in different places and collaborating with one another is still in the plan. I am looking forward to this part of the future.

I would like to thank Olivia Cypris for introducing me to iPSCs, Marco Schmidt for helping me with R programming and Marcelo Szymanski de Toledo for always there to answer the questions. Further I wanted to thank Miriam and Matthis for doing the DNA work that I almost dodged to do. Thank you, Milos, for all the Miseq analysis, I truly appreciate the time you took to analyze the data. We actually did 10 Miseqs together in less than 6 months’ time, thank you for always finding time for me. Thanks, Esra for the analysis of EPIC array patient data and I am really happy that now you are part of the MPN project.

Further I would like to thank Juan, an awesome master student I had, now a PhD student, for bringing smile and happiness around. Michael, thank you for doing a good job in the limited time you had for your master internship.

I wanted to thank all my former and current office mates, Lucia, Olivia, Syeda, Alex, Sven, and Erik, there was never a dull moment in the office. From sharing food to exploring weird ideas to endless things we talked about that need to be censored: D It was such fun with you all! Lucia, we had a very good time from baking to pottery to discussing lives, I will always cherish the memory. Olivia, thank you for spending a remarkable time together during covid office times going for walks and playing board games. I wanted to give my gratitude to Ian, even for knowing for a shorter time you became the cool part of the group, further to Roman, Marghe, Mile, Deepika, Wouter and especially to Wolfgang for taking your time to correct my thesis, I truly appreciate your inputs despite the amount of work you had and still managed to find time. Further, I wanted to thank all the members of the group, including Juan, Giulia, Esra, Rim, Deepika, Ian, Kira, Martina, Miriam, Wouter, Moni, Martina, Ledio, Mohamed, Selina, Desiree, Katharina, Vera and Anna for always bringing a nice friendly atmosphere to make work a bit of fun.

Work can also give friends to cherish in the lifetime, I thank Roman, Alina, Julia, Tiago, Giulia and Juan. I thank each individual of you for motivating me when I had bad days, always been empathetical and listening to my endless philosophical thoughts, you people are awesome, I truly value you in my life. I thank all my friends for being supportive and loving in all these years. My school friends, thank you for being understanding and finding time to always keep in touch and always making me part in your life. It's exciting but similarly scary when you move countries, I thank all my roommates, people I got to know from studies for making the time rememberable even in the exam periods. Further people I got to know in Aachen, all the bouldering friends, my saxophone teacher, and friends of friends, you all made this city a happy place even in the incredible stressful working hours. Last but not least, my family, thank you for being an incredible part of my life. My parents, Appa, you wanted me to be a doctor when I was 10 and I learned the work ethics from you, and Amma, for being a person for always choosing kindness and being understanding. My brothers, Vichu Anna, you are the most intelligent person I know, thank you for inspiring me to push my limits, Jana, for helping me to do the things on my own. You both make me humble and thrive to be a better person. Anni, thank you for always being warm and understanding and Athira, you inspire me, and I love you the most. My aunt and uncle for welcoming us and giving us a place in your life and making sure that we don't miss home. I thank all the incredible people in my life for being kind, respectful, supportive and motivating. This life would be meaningless without you all.